



UNIwersytet Jagielloński  
w Krakowie

Faculty of Chemistry  
Jagiellonian University

**Design, synthesis, and activity evaluation of small-molecule  
inhibitors of PD-1/PD-L1 interaction**

Magdalena Żarnik

Dissertation prepared under the supervision of  
prof. dr Tadeusz Holak  
Chemical Biology and Drug Design Group

Kraków 2023

The research was carried out in the Chemical Biology and Drug Design Group at the Faculty of Chemistry of the Jagiellonian University and was financed by the FNP as part of the TEAM program with the project:

**'Development of small molecule chemical compounds for cancer immunotherapy'**

Part of the research was carried out thanks to funds obtained from the National Science Center as part of the PRELUDIUM 20 competition for the project entitled:

**'SAR analysis and synthesis of complex, small-molecule PD-1/PD-L1 interaction antagonists'**



## Acknowledgements

*I would like to express my thanks to my supervisor, prof. dr Tadeusz Holak for providing me with the opportunity to conduct very interesting research as well as for the supervision during my PhD studies.*

*I also thank dr Jacek Plewka for providing HTRF analyses of prepared compounds and for his valuable guidance during compounds' activity analyses.*

*I would also like to thank dr Ewa Surmiak for the HTRF measurements.*

*Special thanks also to dr Bogdan Musielak, dr Damian Muszak, dr Mirosław Nawój, and mgr Marcin Pustuła for NMR measurements.*

*I would also like to thank dr hab. Lukasz Skalniak and mgr Justyna Kocik-Król for the performance of cell line tests for compounds' activity assessment.*

*I am also grateful to dr Katarzyna Magiera, mgr Ismael Rodriguez, and mgr Dominik Sala for protein preparation, crystallization of protein-inhibitor complexes, X-ray data collection, and structure refinement.*

*I would like to give my special thanks to mgr Magdalena Karpa, lic. Magdalena Michalska and lic. Izabela Lyko, who were the students involved in my research.*

*I would also like to thank all lab colleagues for their cooperation and atmosphere during everyday work.*

*Special gratitude to my husband, Bartłomiej Żarnik, and my Parents for being always at my side.*

## Academic Achievements

### Publications:

- 1) Guzik K., Tomala M., Muszak D., Konieczny M., Hec A., Błaszkiwicz U., Pustuła M., Butera R. Dömling A., Holak T.A. (2019). Development of the Inhibitors that Target the PD-1/PD-L1 Interaction-A Brief Look at Progress on Small Molecules, Peptides, and Macrocycles, *Molecules*, 24, 2071–2100. doi:10.3390/molecules24112071.
- 2) Konieczny M., Musielak B., Kocik J., Skalniak L, Sala D., Czub M., Magiera-Mularz K., Rodriguez I., Myrcha M., Stec M., Siedlar M., Holak T.A., Plewka J. (2020). Di-bromo-Based Small- Molecule Inhibitors of the PD-1/PD-L1 Immune Checkpoint, *Journal of Medicinal Chemistry*, 63, 11271–11285. doi: 10.1021/acs.jmedchem.0c01260.
- 3) Janczy- Cempa E., Mazuryk O., Sirbu D., Chopin N., Żarnik M., Zastawna M., Colas C., Hiebel M.A., Suzenet F., Brindell M. (2021). Nitro-Pyrazinotriazapentalene scaffolds- nitroreductase quantification and in vitro fluorescence imaging of hypoxia. *Sens. Actuators B Chem.*, 346, 130504. doi: 10.1016/j.snb.2021.130504.
- 4) Kiteł R., Rodríguez I., del Corte X., Atmaj J, Żarnik M., Surmiak E., Muszak D., Magiera-Mularz K., Popowicz G., Holak T., Musielak B. (2022). Exploring the Surface of the Ectodomain of the PD-L1 Immune Checkpoint with Small-Molecule Fragments, *ACS Chem. Biol.*, 17, 2655–2663. doi: 10.1021/acscchembio.2c00583.

### Participation in grants:

- 1) Scholarship holder of the TEAM /2017-4/35 project "Development of small molecule chemical compounds for cancer immunotherapy" financed by the FNP.

### Project management:

- 1) "SAR analysis and synthesis of complex, small-molecule PD-1/PD-L1 interaction antagonists" (PSP no.: K/PBM/000808) as part of Preludium 20 financed by the National Science Centre.

## Table of Contents

Acknowledgements .....	3
Academic Achievements .....	4
Streszczenie .....	7
Summary .....	9
1. Literature Introduction .....	11
1.1. Immunotherapy as New Release in Cancer Treatment .....	11
1.2. PD-1 and PD-L1- Proteins Structure and Functions .....	12
1.3. Mechanisms of Expression of Checkpoint Ligands in the Tumor Microenvironment (TME).....	13
1.4. Inhibition of Immunocheckpoint (ICI) as Strategy to Restore Immune System .....	15
1.5. The Use of Monoclonal Antibodies for PD-1/PD-L1 Blockage .....	16
1.6. Peptidic and Peptidomimetical PD-1/PD-L1 Inhibitors .....	17
1.7. Nonpeptidic Small-Molecule Inhibitors- Development Based on Structural Analysis of hPD-1/hPD-L1 Complex.....	22
1.8. Nonpeptidic, Small Molecule Inhibitors Development – Examples of Already Known Inhibitors.....	25
1.8.1. Non-dimeric Small Molecule Inhibitors .....	25
1.8.2. Elongated Type of Small Molecule Inhibitors .....	38
2. Performed Research .....	45
2.1. 2H-benzo[b][1,4]oxazin-3(4H)-one's Derivatives as Potential PD-1/PD-L1 Immunomodulators .....	48
2.1.1. 2 Synthesis of 2H-benzo[b][1,4]oxazin-3(4H)-one's Derivative.....	48
2.1.2. Activity Evaluation of 2H-benzo[b][1,4]oxazin-3(4H)-one Derivatives .....	51
2.2. Synthesis of Biphenyl Based Small-molecule Inhibitors of the PD-1/PD-L1 Immune Checkpoint .....	54
2.2.1. Identification of the Short Fragments That Bind to PD-L1 .....	54
2.2.2. Development of the 2-Bromo-1,1'-Biphenyl-Based Antagonists of PD-L1 – Synthesis and Activity Determination.....	58
2.2.3. Modeling the Interactions with Dimeric PD-L1 .....	63
2.3. Preparation of 2-Substituted 1,1'-Biphenyl Derivatives .....	64
2.3.1. Optimisation of the 1,1'-Biphenyl Fragment.....	64
2.3.2. Synthesis of the PD-1/PD-L1 Inhibitors 3.46-3.60 .....	65
2.3.3. Activity Evaluation of 1,1'-Biphenyl Fragment Based Inhibitors.....	67
2.4. 2,3-dihydro-1H-indene Derivative as the Elongated Potential PD-L1 Antagonists..	73
2.4.1. Synthesis of Potential 2,3-dihydro-1H-indene Based Derivative .....	73
2.4.2. The Study of Geometric Isomerism of the Products of the Wittig Reaction .....	76
2.4 Assessment of <i>in vitro</i> Activity of 2,3-Dihydro-1H-Indene Derivative Towards PD-1/PD-L1 .....	78

2.5.	Preparation of ARB272542 Derivatives as Potential PD-1/PD-L1 Inhibitors – Synthesis and Activity Determination.....	80
2.6.	3,4-dihydro-2H-benzo[b][1,4]oxazine Derivatives as Potential PD-1/PD-L1 Antagonists.....	83
2.6.1.	3,4-Dihydro-2H-Benzo[b][1,4]Oxazine - Fragment Identification.....	83
2.6.2.	Synthesis of 3,4-Dihydro-2H-Benzo[b][1,4]Oxazine Derivatives.....	83
2.6.3.	Assessment of Biochemical Activity of 3,4-Dihydro-2H-Benzo[b][1,4]Oxazine Derivatives towards PD-1/PD-L1 .....	84
2.7.	Elongated <i>Pseudo</i> C <sub>2</sub> - PD-1/PD-L1 Inhibitors.....	86
2.7.1.	Elongated <i>Pseudo</i> C <sub>2</sub> -Symmetric PD-1/PD-L1 Inhibitors – Evolution .....	86
2.7.2.	Synthesis and Activity Determination of Elongated <i>Pseudo</i> C <sub>2</sub> -symmetric PD-1/PD-L1 inhibitors.....	87
3.	Conclusions and Perspectives .....	95
4.	Materials and Methods .....	99
4.1.	General Information – Organic Synthesis .....	99
4.2.	Synthetic Protocols.....	99
4.2.1.	Synthesis of 2H-benzo[b][1,4]oxazin-3(4H)-one’s Derivative.....	99
4.2.2.	Synthesis of Biphenyl Based Small-molecule Inhibitors of the PD-1/PD-L1 Immune Checkpoint .....	103
4.2.3.	Preparation of 2-substituted 1,1'-biphenyl Derivatives .....	121
4.2.4.	2,3-dihydro-1H-indene Derivative as Elongated Potential PD-L1 Antagonists ..	135
4.2.5.	Preparation of ARB272542 Derivatives as Potential PD-1/PD-L1 Derivatives – Synthesis and Activity Determination.....	141
4.2.6.	3,4-dihydro-2H-benzo[b][1,4]oxazine Derivatives as Potential PD-1/PD-L1 Antagonists.....	145
4.2.7.	Elongated <i>Pseudo</i> C <sub>2</sub> -symmetric PD-1/PD-L1 Inhibitors.....	156
4.3.	Protein Expression and Purification .....	178
4.4.	<i>weak</i> -Antagonist-Induced Dissociation Assay ( <i>w</i> -AIDA-NMR) .....	178
4.5.	Homogeneous Time-Resolved Fluorescence (HTRF) .....	178
4.6.	Cell Culture.....	179
4.7.	hPD-1/hPD-L1 Immune Checkpoint Blockade Assay .....	179
4.8.	Cytotoxicity Assay .....	180
4.9.	Crystallization and the Crystal Structure Determination.....	180
	Literature .....	181
	List of Abbreviations.....	190

## Streszczenie

Wiązanie liganda programowanej śmierci 1 (PD-L1, ang. Programmed Death Ligand 1) z jego docelowym receptorem PD-1 (ang. Programmed Death 1) ma znaczący wpływ na tłumienie odpowiedzi immunologicznej organizmu i jest związane z hamowaniem proliferacji limfocytów T, uwalnianiem cytokin oraz cytotoksycznością, co powoduje apoptozę T specyficznych limfocytów. Wprowadzenie inhibitorów, celujących w interakcje PD-1/PD-L1, jest obecnie stosowane w immunoterapii wielu typów nowotworów i wypiera stopniowo bardziej tradycyjne sposoby leczenia raka, takie jak chemioterapia, czy radioterapia. Wdrożenie tej strategii poprzez zaangażowanie przeciwciał monoklonalnych (mAbs) dowiodło bezpośrednio, że modulacja odpowiedzi immunologicznej może doprowadzić do przywrócenia funkcji specyficznych limfocytów T oraz do normalizacji odpowiedzi przeciwnowotworowych, będąc tym samym skuteczną strategią w leczeniu raka.

Poza wymienionymi zaletami, zastosowanie przeciwciał monoklonalnych w terapii wiąże się niestety z pewnymi niedogodnościami, takimi jak słaby profil farmakokinetyczny przy podawaniu doustnym, niepożądane skutki uboczne pochodzenia immunologicznego (ang. irAE) i słaba penetracja guza, spowodowana znacznymi rozmiarami (150 kDa) przeciwciała. Ponadto terapie oparte na mAbs są skorelowane z wysokimi kosztami, co ogranicza uniwersalność stosowania tej metody immunoterapeutycznej. Spektakularne wyniki badań klinicznych uzyskane przy stosowaniu przeciwciał monoklonalnych skierowanych na oddziaływanie PD-1/PD-L1 sprawiły, że niskocząsteczkowe inhibitory celujące w punkt kontroli PD-1/PD-L1 są intensywnie poszukiwane. Zastosowanie małowcząsteczkowych antagonistów oddziaływania PD-1/PD-L1 mogłoby pozwolić obejść niedogodności związane ze stosowaniem mAbs i zarazem stworzyć alternatywę wśród immunoterapeutycznych metod leczenia. Dlatego też poszukiwanie niskocząsteczkowych inhibitorów punktu kontroli immunologicznej PD-1/PDL1 jest intensywnie rozwijającym się tematem badawczym, a optymalizacja struktury potencjalnych antagonistów stała się również przedmiotem moich zainteresowań.

Głównym celem moich badań była optymalizacja struktury, przeprowadzenie syntezy organicznej wybranych grup inhibitorów oraz analiza właściwości otrzymanych związków pod względem ich zastosowania jako antagonistów białka PD-L1. Początkowo w ramach prowadzonych badań dokonano syntezy immunomodulatorów PD-1/PD-L1 jako pochodnych 1,1'-biphenylu. Fragmenty stanowiące rdzenie poszczególnych grup cząsteczek były optymalizowane przy użyciu metod takich jak modelowanie molekularne, spektroskopia

jądrowego rezonansu magnetycznego połączona z testem dysocjacji indukowanej słabym antagonistą (*w*-AIDA NMR, ang. *weak*-Antagonist Induced Dissociation Assay Nuclear Magnetic Resonance), pomiary fluorescencji czasowo rozdzielczej (HTRF, ang. Homogenous Time Resolved Fluorescence) a także wzorując się znanymi dotychczas w literaturze strukturami antagonistów białka PD-L1. Przy użyciu syntezy zbieżnej i liniowej, pomyślnie zsyntezowano inhibitory będące pochodnymi 2H-benzo[b][1,4]oksazyn-3(4H)-onu, 2-bromo-1,1'-bifenylu, 1,1':2',1''-terfenylu, 2-fluoro-1,1'-bifenylu, 2-chloro-1,1'-bifenylu, 2-iodo-1,1'-bifenylu. Powinowactwo otrzymanych związków determinowano przy użyciu techniki HTRF oraz badając zdolność otrzymanych cząsteczek do aktywacji limfocytów T w komórkowym teście blokady punktu kontroli immunologicznej. Spośród otrzymanych związków inhibitor **3.17** jako pochodna 2-bromo-1,1'-bifenylu okazał się przynieść najbardziej satysfakcjonujące wyniki, charakteryzując się  $IC_{50}$  równym  $15.0 \pm 0.2$  nM,  $EC_{50}$  wynoszącym  $6.6 \pm 0.8$   $\mu$ M oraz brakiem cytotoksyczności w zakresie aż do 100  $\mu$ M stężenia związku. Dla innej pochodnej 2-fluoro-1,1'-bifenylu otrzymano wysokorozdzielczą strukturę krystaliczną związku **3.54** z białkiem PD-L1. Analiza struktury krystalicznej pozwoliła na dogłębną analizę interakcji związku **3.54** z miejscem wiążącym w obrębie dimerycznego PD-L1.

Jako kontynuację badań podjęto próbę otrzymania grupy rozbudowanych, małowcząsteczkowych antagonistów punktu kontroli immunologicznej PD-1/PD-L1. Zsyntezowano związki będące pochodnymi ugrupowań takich jak 2,3-dihydro-1H-inden, 2,2'-dimetylo-1,1'-bifenyl, 2-fluoro-2'-metylo-1,1'-bifenyl oraz grupę pochodnych 3,4-dihydro-2H-benzo[b][1,4]oksazyny. Wśród wskazanych, pseudo  $C_2$ -symetryczne pochodne 2-fluoro-2'-metylo-1,1'-bifenylu oraz 2,2'-dimetylo-1,1'-bifenyl wykazały najlepsze właściwości, charakteryzując się  $IC_{50}$  w zakresie do 1 nM dla pięciu pochodnych - **7.31**- **7.33**, **7.35** i **7.37** oraz  $EC_{50}$  w zakresie do 500 nM dla sześciu spośród otrzymanych związków - **7.31** - **7.36**. Zastosowana modyfikacja małych cząsteczek związana z ich wydłużeniem i powiększeniem ich struktury, przyczyniła się do wzmocnienia wiązania inhibitorów poprzez zwiększenie ilości jego interakcji z białkiem PD-L1.

Podsumowując, prezentowana rozprawa doktorska przedstawia zarówno syntezę 59 finalnych cząsteczek jak i charakterystykę powinowactwa otrzymanych cząsteczek w stosunku do białka PD-L1. Wyniki przeprowadzonych przeze mnie badań, związanych z przeprowadzeniem analizy zależności struktura-aktywność (SAR, ang. Structure-Activity Relationship) i otrzymaniem związków na drodze syntezy organicznej, mogą przyczynić się do stworzenia nowej klasy potencjalnych inhibitorów punktu kontrolni immunologicznej PD-1/PD-L1.



## Summary

Binding of programmed death ligand 1 (PD-L1) to its target receptor PD-1 has a major impact on the suppression of the body's immune response and is associated with inhibition of T-cell proliferation, cytokine release and cytotoxicity leading to apoptosis of specific T lymphocytes. The introduction of inhibitors that disrupt the PD-1/PD-L1 interaction is currently being used in the immunotherapy of many types of cancer and is gradually replacing more traditional methods of cancer treatment such as chemotherapy and radiotherapy. The implementation of this strategy through the use of monoclonal antibodies (mAbs) in therapy has directly demonstrated that modulation of the immune response can restore the function of specific T lymphocytes and normalize the anti-tumor response, making it an effective strategy in the treatment of cancer.

In addition to these advantages, the use of monoclonal antibodies in therapy is unfortunately associated with some disadvantages, such as a poor pharmacokinetic profile when administered orally, adverse immune-related side effects (irAE), and poor tumor penetration due to the large size (150 kDa) of the antibody. Furthermore, mAbs-based treatments have been associated with high costs, limiting the versatility of this immunotherapeutic approach. The spectacular results obtained in clinical trials with monoclonal antibodies targeting the PD-1/PD-L1 interaction have led to an intense search for small molecule inhibitors targeting the PD-1/PD-L1 checkpoint. The use of small molecule antagonists of the PD-1/PD-L1 interaction could overcome the drawbacks associated with the use of mAbs while providing an alternative immunotherapeutic treatment modality. Therefore, the search for small molecule inhibitors of the PD-1/PD-L1 immune checkpoint is an intensively developing research topic, and the optimization of the structure of potential antagonists has also become the subject of my interest.

The main objective of my research was to optimize the structure, perform the organic synthesis and analyze the biochemical activity of the obtained compounds in terms of their use as PD-L1 antagonists. The first step of the research was the synthesis of PD-1/PD-L1 immunomodulators as 1,1'-biphenyl derivatives. Fragments constituting the nuclei of individual molecule groups were optimized using methods such as molecular modeling, nuclear magnetic resonance (NMR) spectroscopy combined with weak-Antagonist Induced Dissociation Assay (w-AIDA), time-resolved fluorescence measurements (HTRF, Homogeneous Time-Resolved Fluorescence), as well as by following the known structures of PD-L1 protein antagonists published so far in the literature.

Using convergent and linear synthesis, inhibitors derived from 2H-benzo[b][1,4]oxazin-3(4H)-one, 2-bromo-1,1'-biphenyl, 1,1':2', 1''-terphenyl, 2-fluoro-1,1'-biphenyl, 2-chloro-1,1'-biphenyl, 2-iodo-1,1'-biphenyl were successfully synthesized. The affinity of the obtained compounds was determined using the HTRF technique and by studying the ability of the obtained molecules to activate T lymphocytes in a cellular immune checkpoint blockade assay. Among the obtained compounds, **3.17** inhibitor as a 2-bromo-1,1'-biphenyl derivative gave the most satisfactory results, being characterized by an  $IC_{50}$  of  $15.0 \pm 0.2$  nM and  $EC_{50}$  of  $6.6 \pm 0.8$   $\mu$ M and lack of cytotoxicity up to 100  $\mu$ M concentration of the compound. For another 2-fluoro-1,1'-biphenyl derivative, a high-resolution co-crystal structure of compound **3.54** with PD-L1 protein was obtained. Analysis of the crystal structure allowed for an in-depth insight into the binding mode of compound **3.54** within dimeric PD-L1.

As a continuation of the research, an attempt was made to synthesize a group of extended, small-molecule PD-1/PD-L1 immune checkpoint antagonists. Compounds derived from groups such as 2,3-dihydro-1H-indene, 2,2'-dimethyl-1,1'-biphenyl, 2-fluoro-2'-methyl-1,1'-biphenyl, and 3,4-dihydro-2H-benzo[b][1,4]oxazine were obtained. Among the indicated, pseudo- $C_2$ -symmetric derivatives of 2-fluoro-2'-methyl-1,1'-biphenyl and 2,2'-dimethyl-1,1'-biphenyl showed the best properties, characterized by  $IC_{50}$  in the range of up to 1 nM for five derivatives - **7.31-7.33**, **7.35** and **7.37**, and  $EC_{50}$  in the range up to 500 nM for six of the obtained compounds - **7.31 - 7.36**. The applied modification of small molecules related to their elongation and enlargement of their structure contributed to strengthening the binding of inhibitors by increasing the number of its interactions with the PD-L1 protein.

In summary, the presented herein doctoral dissertation provided both the synthetic description of 59 final molecules and the characteristics of the affinity of the obtained molecules in relation to the PD-L1 protein. In conclusion, the results of my research, related to both structure-activity relationship (SAR) analysis and the preparation of compounds by organic synthesis manners, may contribute to the formulation of a new class of potential inhibitors of the PD-1/PD-L1 immune checkpoint.

# 1. Literature Introduction

## 1.1. Immunotherapy as New Release in Cancer Treatment

Traditional therapeutic approaches to cancer treatment are gradually being replaced by the use of agents that provide amplification of immune effector mechanisms, broadly referred to as "immunotherapy" (Kazemi *et al.*, 2016). Immunotherapeutic methods have been shown to have unparalleled advantages over conventional treatments such as radiotherapy and chemotherapy, prolonging progression-free survival (PFS) and overall survival (OS) (Tan *et al.*, 2020). In contrast to traditional cancer treatment methods, immunotherapy dynamically modulates the immune system by regulating the immune microenvironment, allowing immune cells to attack and eliminate tumor cells (Couzin-Frankel, 2013).

Among immunotherapeutic methods, active and passive types of immunotherapy techniques can be distinguished. Active immunotherapy consists of stimulating effector functions *in vivo* and aims to achieve a therapeutic effect by increasing the patient's immune response, for example by administering tumor cell antigens (specific active immunotherapy) or immuno-stimulating preparations such as cytokines (non-specific active immunotherapy) (Papaioannou *et al.*, 2016). Passive immunotherapy compensates for the deficient immune functions by using *ex vivo* activated cells or molecules and is mainly used in patients with low responsible immune status. In this category, we can mention methods such as infusion of tumor-specific antibodies, systemic administration of recombinant cytokines and adoptive transfer of immune cells preactivated to lyse tumors *in vivo* (Papaioannou *et al.*, 2016).

Moreover, some studies revealed information, that combination of immunotherapeutic techniques with traditional antitumor methods, or multiple immuncheckpoint inhibitor (ICI)-based therapy could significantly enhance most of the effects of treatment, but further research on that topic is required (Tan *et al.*, 2020). The advantages associated with application of immunotherapeutic techniques induced gradual deepening of the research related to antitumor drugs and generated the the increase in the demand for immunotherapeutic drugs in the market. The importance of research related to immune checkpoint inhibition was emphasized by the Nobel Prize in Medicine awarded to James P. Allison and Tasuku Honjo in 2018 (Ledford, *et al.*, 2018), who proved that inhibition of negative immune checkpoint regulators can be a successful way to prevent tumor immunosuppressive mechanisms (Dunn *et al.*, 2002). Allison found that cytotoxic T lymphocyte antigen 4 (CTLA-4) - a protein receptor expressed on the surface of the T cell - is able to inhibit the activity of T cells, preventing them from mounting

a full-scale immune attack. In his research, he suggested that blockade of the checkpoint receptor, CTLA-4, would set the immune system free from inspecting cancer cells, which he proved by showing that antibodies against CTLA-4 erased tumors in mice (Leach *et al.*, 1996). In 2010, Bristol-Myers Squibb company, tested CTLA-4 antibody on metastatic melanoma patients and showed that this treatment resulted in the prolongation of life from 6 months without antibody treatment to an average of 10 months after treatment (Couzin-Frankel Jennifer, 2013). The early 1990s also saw the discovery of another T-lymphocyte receptor, programmed death 1 (PD-1), whose blockade was thought to overcome immune resistance. Trials of anti-PD-1 antibodies in humans began in 2006, reporting significantly better effects and milder side effects of therapy. Clinical trials have shown that the use of anti-PD-1 antibodies leads to objective responses in approximately one in four to one in five patients with non-small cell lung cancer, melanoma, or renal cell cancer. In addition, the side effect profile does not appear to preclude its use. (Sponsored by Bristol-Myers Squibb and others; ClinicalTrials.gov number, NCT00730639) (Topalian *et al.*, 2012). More recently, protein death 1 (PD-1)/protein death ligand 1 (PD-L1) has emerged as one of the most important immune checkpoint (ICP) targets for cancer immunotherapy (Topalian *et al.*, 2015).

## **1.2. PD-1 and PD-L1- Proteins Structure and Functions**

Programmed cell death protein 1 (PD-1) has been shown to play an essential role in the regulation of autoimmunity, including both induction and maintenance of peripheral tolerance. PD-1 protein is encoded by the PDCD1 gene and belongs to the CD28/CTLA-4 immunoglobulin family, sharing 23% amino acid sequence homology with cytotoxic T-lymphocyte-associated antigen 4 (CTLA-4) (Okazaki *et al.*, 2006).

The extracellular region of PD-1 contains a single IgV-like domain and its cytoplasmic region consists of an immunoreceptor tyrosine-based inhibitory motif (ITIM) and an immunoreceptor tyrosine-based switch motif (ITSM) (Okazaki *et al.*, 2006). PD-1 was isolated by subtractive hybridization as a molecule whose expression in a thymic T-cell line was enhanced by apoptotic stimuli (Ishida *et al.*, 1992). Furthermore, it was found to be expressed not only on the surface of T cells, but also on B cells, natural killer T (NKT) cells, killer cells (KT), activated monocytes and dendritic cells, suggesting a broader role in immune regulation. Upon stimulation of PD-1 by antigen, PD-1 recruits the protein tyrosine phosphatase src homology 2 domain-containing tyrosine phosphatase 2 (SHP-2) to ITSM and dephosphorylates effector molecules downstream of the antigen receptor (Okazaki *et al.*, 2002).

The ligands for PD-1 (PD-Ls) are PD-L1 (also known as B7-H1) and PD-L2 (B7-DC). Both proteins are type I transmembrane proteins with IgV- and IgC-like domains in the extracellular region. (Freeman et al., 2000). The PD-L1 protein is expressed on antigen-presenting cells and has shown the ability to turn off autoreactive T cells and induce peripheral tolerance, whereas PD-L1 presented on parenchymal cells prevents tissue destruction by suppressing effector T cells to maintain tolerance. In contrast to PD-L1, which is constitutively expressed on T cells, B cells, macrophages and dendritic cells (DCs), PD-L2 expression is more tightly regulated and is observed on activated macrophages and DCs (Okazaki *et al.*, 2006). PD-L1 is abundant in lymphoid and non-lymphoid tissues and various tumor cells, especially in melanoma, lung cancer, pancreatic cancer, kidney cancer, bladder cancer and many others (Dong *et al.*, 2002).

PD-L1 exposed on the surface of tumor cells interacts with PD-1 expressed by T cells, resulting in the induction of inhibitory signals, which is related to the immune evasion mechanism of tumors (Pardoll, 2012). PD-1 is thought to be involved in the engagement with its ligand PD-L1 or PD-L2, which results in the delivery of a negative signal by recruitment of Src homology 2 domain-containing tyrosine phosphatase 2 (SHP-2) to the phosphorylated tyrosine residue in the cytoplasmic region (Okazaki *et al.*, 2006). Surprisingly, several groups have also reported positive effects of PD-L1 and PD-L2 on T cells, such as an increase in T cell proliferation as a result of inhibition of interferon (IFN)  $\gamma$ -induced nitric oxide production (Yamazaki *et al.*, 2005). However, the negative effects associated with the presence of PD-L1/PD-L2 ligands due to inhibition of the immune response are significantly more dominant and important.

### **1.3. Mechanisms of Expression of Checkpoint Ligands in the Tumor Microenvironment (TME)**

The PD-1/PD-L1 pathway has been postulated to regulate immune responses and control the induction and maintenance of immune tolerance in the tumor microenvironment. Two different mechanisms of PD-L1 overexpression relevant to innate and adaptive resistance, which can coexist in the TME, are known in the literature (Topalian *et al.*, 2015). Intrinsic resistance results from the activation of some signal transduction pathways (AKT pathway, STAT 3 pathway) or genetic alterations and causes constitutive expression of PD-L1 by tumor cells (Parsa *et al.*, 2007). In contrast to intrinsic resistance, adaptive overexpression of PD-L1 is related to the release of cytokines, particularly IFN- $\gamma$ . Activated Th1-type helper CD4 cells,

stimulated CD8 cells and NK cells produce IFN- $\gamma$ , and the resulting inflammatory immune microenvironment "threatens" the tumor (Taube *et al.*, 2013). As a result of tumor cells sensing the inflammatory immune microenvironment, adaptive resistance alerts the cancer cell, leading to PD-L1 overexpression, which can help cancer cells evade immune surveillance. The described mechanisms are visualized in Figure 1.

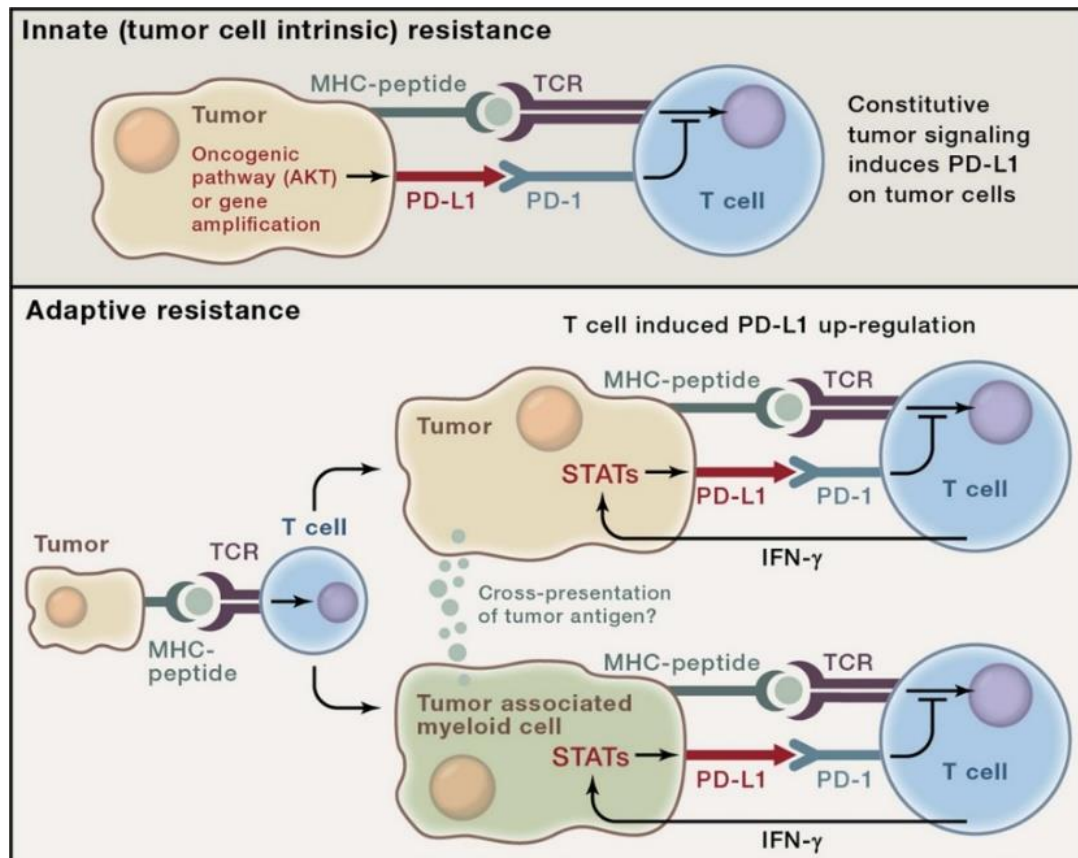


Figure 1. The mechanisms of expression immune checkpoint related ligands in tumor microenvironment. (Topalian *et al.*, 2015).

Early studies reported that the concept of adaptive resistance is not only consistent with the expression of PD-L1 on cancer cells, but can also apply to the induction of PD-L1 on myeloid cells, including dendritic cells, which can significantly suppress T-cell activation. In addition to tumor cells, PD-L1+ suppressive myeloid cells or DC in the TME or tumor-draining lymph nodes can also cause T-cell exhaustion. Llosa *et al.* (2014) showed that myeloid cells predominate over cancer cells in PD-L1 expression, which was observed in MSI colon cancer.

## 1.4. Inhibition of Immunecheckpoint (ICI) as Strategy to Restore Immune System

Based on the assumptions of immunotherapy, functional exhaustion, and anergy can be controlled by immune checkpoint blockade (Baumeister *et al.*, 2016). Under normal conditions, the role of inhibitory checkpoint protein is to prevent autoimmune disease damage. The presence of TME has a negative influence on T cells and prevents T cells from approaching the tumor, weakening the ability of the immune system to recognize and fight tumor cells (Ramsay, 2013). In the TME, cancer cells, and other immune cells are able to release cytokines such as CSF-1, and TGF- $\beta$ , which are recognized by dendritic cells (DCs) and antigen-presenting cells (APCs). This process brings DCs/APCs and T cells into close proximity and the B7 ligand identified by the DC/APC recognizes the CD28 receptor on the T cell.

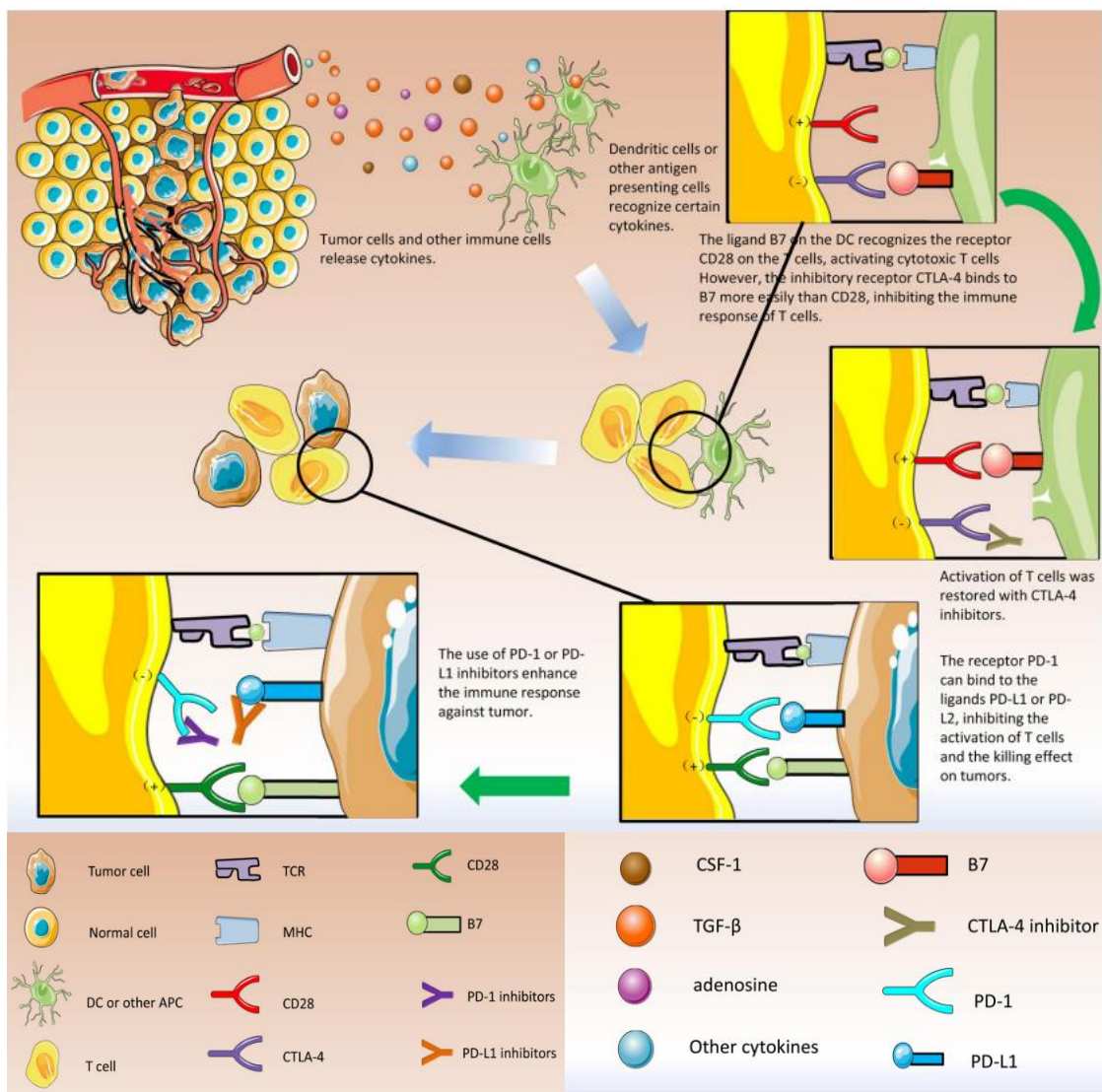


Figure 2. The impact of ICIs on immune resistance to cancer (Tan *et al.*, 2020).

As a result, cytotoxic T cells are activated and proliferation and migration of T cells to the tumor occurs. However, on activated T cells, the inhibitory receptor CTLA-4 binds more readily to B7 than to CD28, leading to exhaustion of the antitumor T-cell response. In parallel, activated T cells act on tumor cells. On the activated T-cell expression of PD-1 and engagement of the overexpressed protein in the binding with PD-L1 or PD-L2 respectively occurs, inhibiting the activation of T-cells (Ohaegbulam *et al.*, 2015). The use of CTLA-4 inhibitors or PD-1/PD-L1 inhibitors *in vivo* can enhance the immune response of T cells against tumors and inhibit tumor proliferation. The described process is shown in Figure 2 (Tan *et al.*, 2020).

### **1.5. The Use of Monoclonal Antibodies for PD-1/PD-L1 Blockage**

The induction of antitumor responses can be achieved by targeting the PD-1/PD-L1 pathway. The implementation of this strategy using monoclonal antibodies (mAbs) has directly demonstrated that modulation of immunity can be an effective strategy in cancer treatment (Ohaegbulam *et al.*, 2015). However, from the wide range of monoclonal antibodies clinically tested, only six have been approved by the US Food and Drug Administration and the European Medicines Agency (Wolchok *et al.*, 2013, Mahoney *et al.*, 2015). Three of them pembrolizumab, nivolumab, cemiplimab are registered as PD-1 inhibitors and another three avelumab, atezolizumab and durvalumab were accepted as PD-L1 inhibitors, providing the improvement in various type of cancer therapy such as metastatic melanoma, non-small cell lung cancer (NSCLC) and renal cell carcinoma (Hoos, 2016; Khalil *et al.*, 2016).

Undeniably, immunotherapeutic methods show significantly higher efficacy than traditional methods of cancer treatment, although it is still difficult to increase response rates above 20-50% in curing solid tumors (Garon *et al.*, 2015; Balar *et al.*, 2017; Basu *et al.*, 2019). The intermediate response rate of the therapy influenced by the presence of several activated alternative immune escape mechanisms could be overcome by the application of combination therapies (Kim *et al.*, 2016). Since 2015, the FDA accepted the combination therapy of combined anti-PD-1 and anti-CTLA-4 mAbs for the treatment of BRAF V600 wild-type, unresectable and metastatic melanoma (Farkona *et al.*, 2016). Apart from the mentioned advantages, the application of mAbs-based therapy is unfortunately associated with some drawbacks, such as poor pharmacokinetic profile for oral administration, immune-related adverse events (irAEs), and poor tumor penetration identification with large size (150 kDa) of antibodies. In addition, mAbs-based therapy involves high manufacturing and health care costs, which limits the universality of this method (Baldo, 2013). Therefore, another method to disrupt



immune checkpoint PD-1/PD-L1 proteins is highly desired. The solution to this problem could be the design of alternative ICIs, such as macrocyclic peptide inhibitors or small molecule inhibitors, which are currently under intense investigation.

## 1.6. Peptidic and Peptidomimetical PD-1/PD-L1 Inhibitors

One of the first concepts of an alternative to monoclonal antibodies was the construction of peptides and peptidomimetics, which can be considered as a compromise between a monoclonal antibody and a small molecule type inhibitor. Aurigene Discovery Technologies, in collaboration with Laboratories Pierre Fabre, focused on the development of peptides that have a strong anticancer activity with improved tumor penetration ability, are associated with lower molecular masses and show fewer side effects compared to the already used monoclonal antibodies (Liu *et al.*, 2019). One of the compounds they proposed was AUNP-12 (Figure 3, **1.1**), a 29-mer peptide that contains the elements of human PD-1 in its structure. The high affinity of **1.1** to block the PD-1/PD-L1 and PD-1/PD-L2 pathways was demonstrated on the HEK293 cell lines expressing hPD-L2 and on the MDA-MB-231 cells expressing hPD-L1. The EC<sub>50</sub> values determined from the proliferation-based experiments are 0.72 nM and 0.41 nM, respectively. In preclinical studies, **1.1** inhibited the growth of B16F10 murine melanoma cells and reduced the number of neoplastic cells in a mouse model of breast cancer (Sasikumar *et al.*, 2013, Wang, T. *et al.*, 2019).

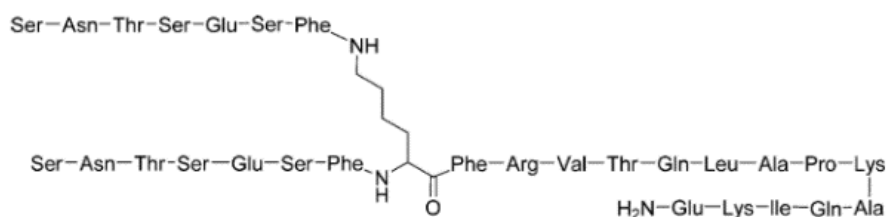


Figure 3. The structure of **1.1** (AUNP12).

Bristol-Myers-Squibb (BMS) has patented another group of peptide inhibitors as macrocyclic peptides (MCPs) containing from 13 to 15 residues involved in the PD-1/PD-L1 interaction. Magiera-Mularz and collaborators from Jagiellonian University have characterized the examples of macrocyclic-peptide PD-1/PD-L1 antagonists developed by Bristol-Myers Squibb (Figure 4, **1.2.**, **1.3**, **1.4**) (Magiera K. *et al.*, 2017). The observed restoration of the TCR-responsive promoter under the control of the NFAT promoter overexpressing PD-1 was demonstrated for three of the presented macrocyclic peptides (Figure 4, **1.2.**, **1.3**, **1.4**). The EC<sub>50</sub> values determined for molecules **1.2** (BMS-57), **1.3** (BMS-71), and **1.4** (BMS-99) were 556

nM, 293 nM, and 6300 nM respectively when the value obtained for anti-PD-1 antibody durvalumab was calculated for 0.20 nM. X-ray crystallography provided structural insight into the interactions of **1.2** (BMS-57) and **1.3** (BMS-71) with PD-L1. The results of the obtained co-crystal structures of **1.2** (BMS-57) or **1.3** (BMS-71) with PD-L1 show that no significant structural changes are induced within the PD-L1 receptor upon ligand binding and the observed interactions mimic about 37% of the PD-L1/mAbs interaction observed in avelumab and PD-L1 binding.

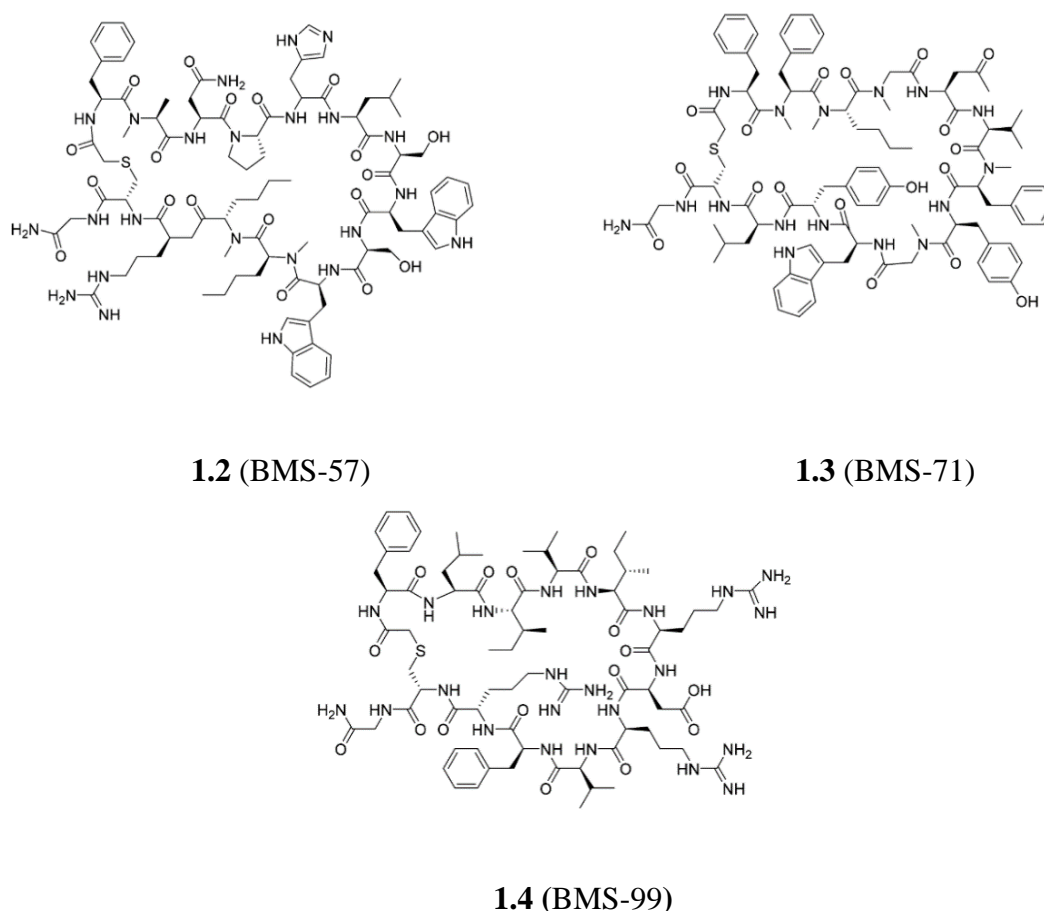


Figure 4. The examples of MCPs: **1.2** (BMS-57), **1.3** (BMS-71) and **1.4** (BMS-99) developed by BMS company and characterized by Magiera K. *et al.*, 2017.

Moreover, among macrocyclic peptides we can distinguish **1.5** (BMS-986189) (structure not fully disclosed), consisting of a 45-residue N- methylated backbone with 14 amide bonds and 1 thioether bond has successfully entered a Phase I clinical trial. Starting in 2016, **1.5** (BMS-986189) is tested for the treatment of severe sepsis (Wang, T. *et al.*, 2019).

Interesting derivatization of the MCPs as potential inhibitors of PD-L1 was proposed by Aurigene and resulted in the construction of tripeptide peptidomimetics with hydrazine and urea linkers shown in Figure 5.

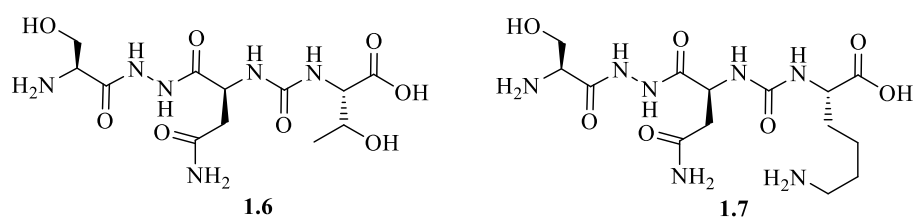


Figure 5. Peptidomimetics proposed by Aurigene.

The potency of the compounds against PD-L1 was checked in murine splenocyte proliferation assay (MSPA), where the best MSPA results at the level of 68% and MSPA up to 87% at 100 nM concentration were obtained for **1.6** and **1.7** respectively. The structure-activity relationship proved that the best results were obtained after methylation of the C-terminal carboxyl group and after the introduction of lysine in the side chain (Guzik *et al.*, 2019). Compound **1.6** was also subjected to a cell-based PD-1/PD-L1 and PD-1/PD-L2 blockade bioassay, yielding results with EC<sub>50</sub> values in the nanomolar range (EC<sub>50</sub> = 30 nM for PD-L1 and EC<sub>50</sub> = 40 nM for PD-L2). Further determination of biological activity of **1.6** involved the *in vivo* studies using the CT-26 colon cancer mouse model (3 mg/kg, 25 days) and *Pseudomonas aeruginosa* in a lung infection mice model (10 mg/kg, three times daily, 11 days), where molecule **1.6** was able to reduce tumor growth by up to 46% (Sasikumar *et al.*, 2013, Sasikumar *et al.*, 2015).

Further modifications of the peptidomimetics structure, proved that the introduction of a glycol-derived linker to the molecule can provide the improvement of MSPA results even to 95% splenocyte proliferation rates for compound **1.8** (Figure 6). Another idea to evaluate the activity of potential inhibitors was to incorporate 1,2,4-oxadiazole and 1,2,4-thiadiazole, as well as 1,3,4-oxadiazole (**1.9**, **1.10**) and 1,3,4-thiadiazole (**1.11**) rings in amino acid side chains as the scaffolds for these compounds (Sasikumar *et al.*, 2015, Sasikumar *et al.*, 2018a, Sasikumar *et al.*, 2018b, Sasikumar *et al.*, 2019). However, the results of MSPA show the preference of the oxadiazole ring over the thiadiazole moiety in the inhibitor's structure (Figure 6). Additionally, the SAR analysis proved the improvement of compound activity due to the introduction of pyridine, piperidine, or morpholine moiety into the compound structure. The greater results up to 92% splenocyte proliferation rates in MSPA were obtained for compound

**1.10** containing primary amines and urea moieties in its structure and molecule **1.9** with pyridine substituent attached (Sasikumar *et al.*, 2018a, Shaabani *et al.*, 2018b).

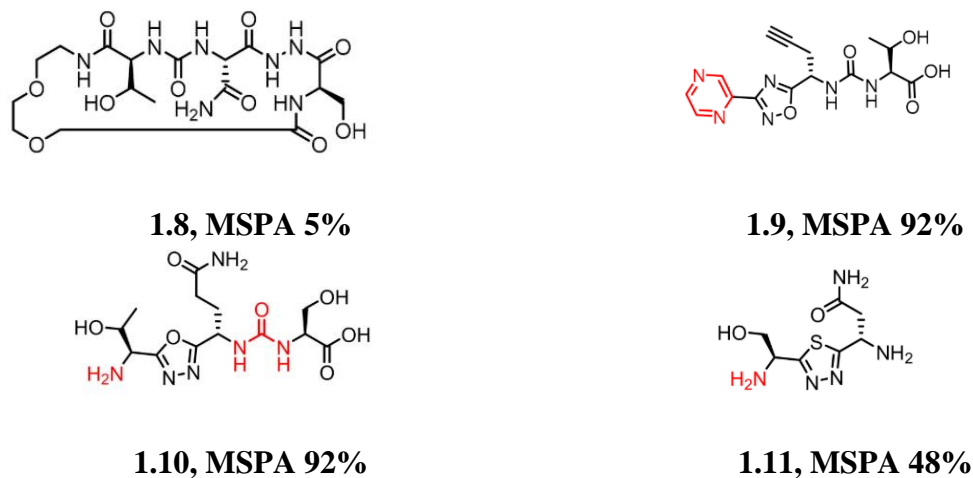


Figure 6. Evaluated peptidic inhibitors **1.8-1.11** (Sasikumar *et al.*, 2018a, Sasikumar *et al.*, 2018b).

Among a wide range of peptidomimetics, we can highlight the compound **1.12 - CA-170**, disclosed by the companies Aurigene and Curis, which is currently an oral immune checkpoint inhibitor showing preclinical anti-tumor efficacy (Lazorchak *et al.*, 2016, Sasikumar *et al.*, 2016, Sasikumar *et al.*, 2021). The proposed structure (Figure 7) of the compound is derived from identified high-affinity peptide from the receptor-ligand interface sequence. The minimal pharmacophore within the peptide was then converted into the heterocyclic amino-derived compound containing a 1,2,4-oxadiazole ring and expanded with amino acid groups as in the pharmacophore (Sasikumar *et al.*, 2021). These modifications result in the formation of **1.12 - CA-170** with improved functional activity, metabolic stability, and oral bioavailability.

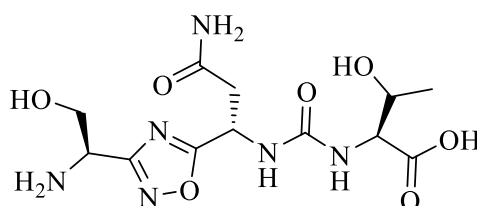


Figure 7. The structure of **1.12 CA-170** (Sasikumar *et al.*, 2021).

Dose-response analyses of **1.12 - CA-170** demonstrated the similar potencies of **1.12 - CA-170** and commercial antibodies to rescue IFN $\gamma$  release inhibited by PD-L1, PD-L2, and VISTA. In addition, the mode of interaction between **1.12 - CA-170** and PD-L1 was investigated. According to previous results, direct binding of **1.12 - CA-170** to PD-L1 has not been demonstrated by techniques such as SPR and solution NMR using recombinant proteins containing extracellular domains (Musielak *et al.*, 2019). Nevertheless, Sasikumar and co-

workers further studied the interaction between the ligand and PD-L1 using NMR spectroscopy in the native environment. In this case, CHO-K1 cells overexpressing PD-L1 were used. This interaction was monitored by the difference in the nuclear spin relaxation or transverse relaxation ( $T_2$ ) rates of a small ligand in the presence and the absence of the macromolecular targets such as cells and demonstrated the specific interaction of **1.12 - CA-170** to PD-L1 overexpressed in the cellular context. A dose-dependent increase in  $T_2$  values of **1.12 - CA-170** in the presence of PD-L1 overexpressed CHO-K1 cells in comparison to parental CHO-K1 was observed. The lower  $T_2$  values that raise upon increasing the **1.12 - CA-170** concentration demonstrates the binding of **1.12 - CA-170** to cellular PD-L1 under physiological conditions. Furthermore, in a widely used TR-FRET assay **1.12 - CA-170** was not found to possess the ability to disturb PD-1/PD-L1 complex formation, what is consistent with previous data (Musielak *et al.*, 2019). **1.12 - CA-170**, interacting with PD-L1 is expected to bind to a relatively small solvent-exposed hotspot, within the binding interface of PD1: PD-L1. The studies mentioned above led to the finding that **1.12 - CA-170** binds to PD-L1, resulting in the formation of a functionally inactive ternary complex, but without disrupting the PD-1/PD-L1 pathway (Sasikumar *et al.*, 2021).

**1.12 - CA-170** is also the first small molecule, which is able to target two checkpoint proteins PD-L1 and VISTA. This can be explained by the structural similarity of belonging to the B7 class proteins. Possibly, the structure of **1.12 - CA-170**, forming minimal pharmacophore derived from PD-1/PD-L1 interaction, recognizes the binding pockets or grooves in VISTA. The evaluation of the functional activity of **1.12 - CA-170** showed, that the compound enables the rescue of the splenocytes/PBMC proliferation and IFN- $\gamma$  release using mouse splenocytes and non-human primate PBMCs in the presence of PD-L1. The efficacy of **1.12 - CA-170** was evaluated in three immunocompetent tumor mouse models: CT26 and MC38 (colon cancer) and B16F10 (melanoma lung metastasis model). Analyses of the immunopharmacodynamic modulation induced by **1.12 - CA-170** administration showed an increase in CD8 T-cells, CD4 T-cells proliferation, and escalated expression of OX-40 on CD4 and CD8 T cells. Moreover, **1.12 - CA-170** induced an increase in the intracellular levels of granzyme B in CD8 T cells and prolonged intracellular IFN- $\gamma$  levels of CD8 T cells in the blood. *In vivo*, studies proved tumor growth inhibition (43% for MC38) and metastasis reduction (73% for B16F10) **1.12 - CA-170** doses. Additionally, **1.12 - CA-170** combined with docetaxel led to a synergistic effect providing 68% of TGI (43% TGI for docetaxel alone in the CT26 colon carcinoma model). In conclusion, **1.12 - CA-170** was found to have potent activity and low toxicity profile in animal studies in rodents and mammals (Sasikumar *et al.*, 2018, Sasikumar

*et al.*, 2021). Compound **1.12 - CA-170**, exhibiting promising activity for the treatment of advanced solid tumors and lymphomas, successfully overcame Phase I trials, as a small-molecule inhibitor of PD-L1/L2 and VISTA (NCT02812875, clinicaltrials.gov). Completing Phase 1, **1.12 - CA-170** demonstrated dose-proportional plasma exposure with a  $T_{1/2}$  of ~4–9.5 h with the acceptable profile of safety. Peripheral T-cells activation was associated with an increased proportion of circulating CD8+ and CD4+ T cells expressing the activation markers CD69, Granzyme B, and OX-40 (CD134). Currently, **1.12 - CA-170** is undergoing Phase II clinical trials in lung cancer, head and neck/oral cavity cancer, MSI-H positive cancers, and Hodgkin lymphoma in India (CTRI/2017/12/011026, ctri.nic.in).

The results obtained for **1.12 - CA-170** encourage the development of small molecule inhibitors as a promising alternative to mAbs, with could possess the convenience of oral dosing, shorter half-life, and better management of adverse events.

### **1.7. Nonpeptidic Small-Molecule Inhibitors- Development Based on Structural Analysis of hPD-1/hPD-L1 Complex**

The development of small molecule inhibitors of protein death 1/protein death ligand 1 is primarily based on the knowledge of the PD-1/PD-L1 immune checkpoint crystal structure. The structural basis of the discussed crystal structure was first published in 2008 and revealed the structural interactions of the murine PD-1 and human PD-L1 proteins (PDB 3SBW, 3BIK) (Lin *et al.*, 2008). The extracellular structure of human PD-1 has also been solved (PDB 3RRQ). Despite this state of knowledge, the fact of modest human and murine PD-1 sequence identity (64% of identity) and substantial differences in murine and human PD-1 bindings modes made the determination of the crystal structure of the human PD-1/PD-L1 complex indispensable.

In 2015, the hard work of researchers from Holak's group resulted in the successful resolution of the crystal structure of the hPD-1/PD-L1 complex (Zak, *et al.*, 2015, PDB: 4Z18) (Figure 8). More detailed analyses of the complex structure show that the structural rearrangement of hPD-1 is induced by the formation of the bond with hPD-L1. The significant structural flexibility of hPD-1 involves the changes in the range of 62-82 hPD-1 residues, which includes the reorganization of the CC' loop (Figure 8). This characteristic rearrangement is only representative of hPD-1 upon complex formation with hPD-L1. In contrast to hPD-1, the rearrangement of hPD-L1 involves only minor adjustments in the arrangement of side chains without significant changes within the backbone.

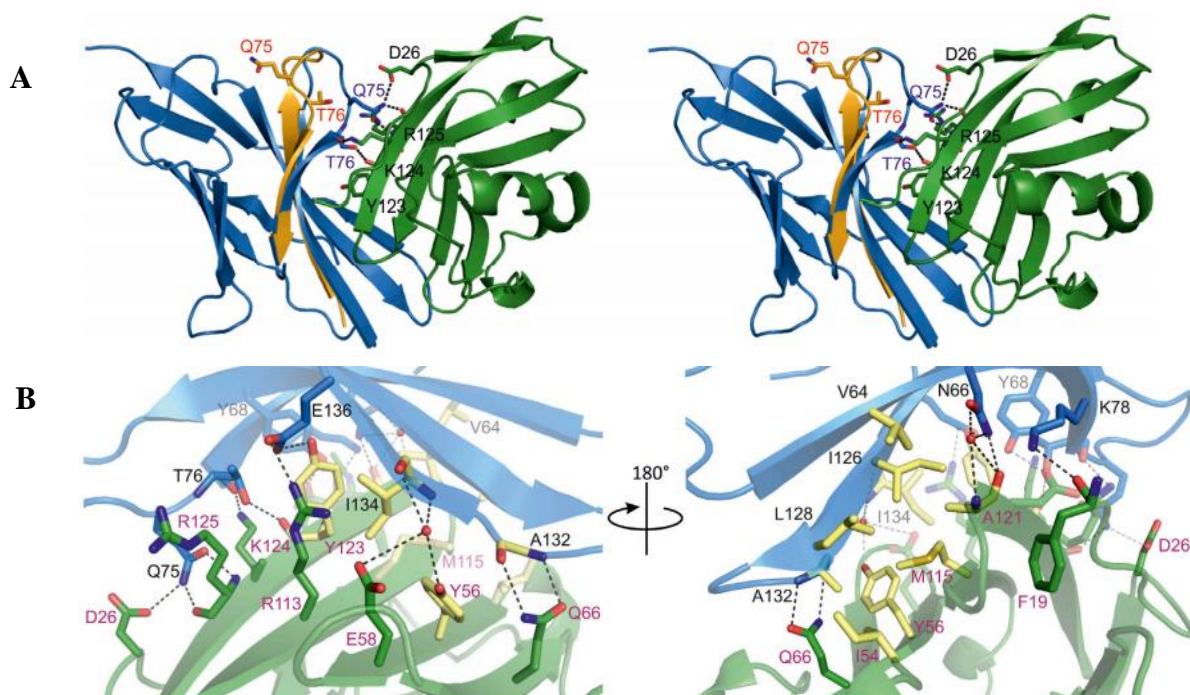


Figure 8. Ribbon representation the human PD-1/PD-L1 complex. Presentation of hPD-1 in blue and hPD-L1 in green colours. A. The structural rearrangement of hPD-1 induced by formation of the bond with hPD-L1. Residues 62-82 of apo-hPD-1 (PDB: 3RRQ) are shown in yellow colours to visualised differences upon complex formation. B. Close-up views of the hPD-1/hPD-L1 interface with highlight of important residues as sticks. Additional colours where used to indicate hydrophobic interactions (yellow), water molecules (red spheres) and hydrogen bonding (black dash lines) (Zak, *et al.*, 2015).

Analyzing the changes we can observe, that in the apo PD-1 structure, the loop retains an open conformation with Met70 and Ser71 forming part of a C $\beta$  strand within an antiparallel CF  $\beta$  sheet, and all the side chains within the loop point away from the ligand binding site. Complex formation induces loop rearrangement in a form of a 90° twist and associated ~5 Å displacement of C $\alpha$  carbons and also the displacement of other side chain atoms. The rearrangement is stabilized by four hydrogen bonds between the side chains of Gln75 and  $^L$ Arg125 (L means that amino acid is from hPD-L1), the side chains of Gln75 and  $^L$ Asp26, the side chain hydroxyl oxygen of Thr76 and the backbone carbonyl oxygen of  $^L$ Tyr123, and between the backbone carbonyl oxygen of Thr76 and the side-chain amine of  $^L$ Lys124 from PD-L1. In addition, the hydrophobic core of the complex is stabilized by another hydrogen bond formed between the hydroxyl group of Tyr68 and the carboxylic group of  $^L$ Asp122, the carbonyl group of Glu136 with the hydroxyl group of  $^L$ Tyr123, and between the side chain of Asn66 and the main-chain oxygen of  $^L$ Ala121. Moreover,  $\pi$ - $\pi$  stacking of Tyr68 and  $^L$ Tyr123 can be observed. Additionally, amino acids from the protein interface are involved in several polar interactions including salts bridges between Glu136 and  $^L$ Arg113, water-mediated interactions of Ile134,

L Tyr56 and L Glu58 as well as hydrogen bonding between the backbone amide of Ala132 and the side-chain carbonyl group of L Gln66.

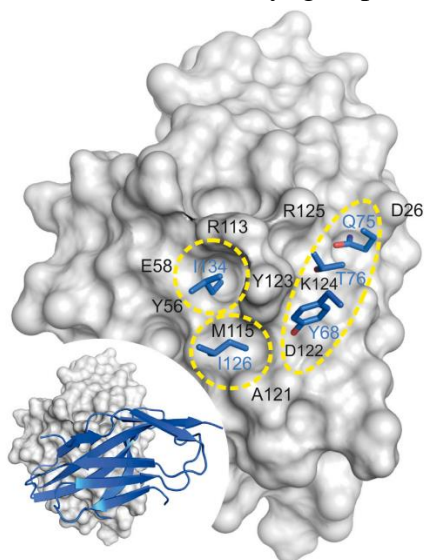


Figure 9. The visualisation of the main ‘hot spots’ (marked in yellow circles) on the PD-L1 surface. hPD-1 was represented in blue and hPD-L1 in grey colours.

To date, many examples of crystal structures of hPD-L1 or hPD-1 bound to multiple antibodies directed on “hot spots” on the protein surface were obtained. The prime example here shows clinically approved pembrolizumab and nivolumab, whose Fab fragments were complexed with hPD-1 (PDB: 5GGS, 5GGR) (Lee *et al.*, 2016). From the examples of hPD-L1/antibody crystal structures we can distinguished structures of BMS-936559 Fab (5GGT) or the single chain Fv fragment (scFv) of avelumab (PDB 5GRJ) complexed with PD-L1 (Liu *et al.*, 2016). The presented scientific background opens a way for development of small molecules can potentially mimic an effect of hPD-1 to h-PD-L1 binding. Prior to the resolution of the hPD-1/hPD-L1 crystal structure, the design of small molecule inhibitors was quite challenging. This was due to the significantly different interaction surface within the hPD-1/PD-L1 complex compared to the previously published m/h complex and the plasticity of the PD-1 receptor during complex formation. However, the data provided by the analysis of structural changes upon h-PD-1/hPD-L1 formation opened a way for determine the “hot spots” that could be targeted by small-molecule inhibitors. The hPD-1 hot spots are mostly hydrophobic and consist of Asn66, Tyr68, Gly124, Ile126, Leu128, Ile134, and Glu136 located in the anterior leaflet of hPD-1. Three main “hot spots” on the PD-L1 surface where identified, providing molecular insights into development of more efficient therapeutics (Figure 9). The first “hot spot” accommodates Ile 134 and comprises the side chains of L Tyr56, L Glu58, L Arg113, L Met115, and L Tyr123. Ile 126 is accommodated by second pocket, composed by L Met115, L Ala121, and L Tyr123. The third “hot spot” is comprised of L Asp122 to L Arg126 main and side chains. As a extended corrugation it can accommodate Tyr68, Gln75, and Thr76. The analyses of druggable surface of h-PD-L1 leads to the conclusion that the size and structure of the first “hot spot” is ideal for the incorporation of six-membered aromatic ring, since it consist of the aromatic ring of Tyr68 on one side and the backbone of Glu136 on the other side of the groove. The properties of the second “hot spot” are perfect for accommodating a branched aliphatic moiety that could anchor with a terminal hydrogen bond donor group at carbonyl oxygen of L Ala121. In summary, the defined “hot spots” provide the structural basis for the



rational design of small-molecule antagonists capable of dissociating the PD-1/PD-L1 complex (Zak *et al.*, 2015).

## 1.8. Nonpeptidic, Small Molecule Inhibitors Development – Examples of Already Known Inhibitors

### 1.8.1. Non-dimeric Small Molecule Inhibitors

Examination of the interactions described above clearly demonstrated that the human PD-1/PD-L1 immune checkpoint pathway can be targeted by small molecule inhibitors, prompting the development of small molecule PD-1/PD-L1 inhibitors. A recent review article confirms that the rate of new small molecules targeting PD-1/PD-L1 production is still increasing rapidly, and the development of inhibitors is expanding (Pan *et al.*, 2021).

However, even before the elucidation of the structure of the hPD-1/PD-L1 complex, the first patents for small molecule inhibitors blocking the PD-1/PD-L1 interaction were disclosed. In 2011, Sharpe *et al.* in the patent application (WO2011082400 A2) proposed PD-1/PD-L1 pathway inhibitors as derivatives of antibiotics such as sulfamonomethoxines (**1.13**) and sulfamethizoles (**1.14**) (Figure 10). The patented molecules were effective *in vivo*, with the wild-type PD-1C T cells and PD-1<sup>-/-</sup> cells showing their inhibitory activities at the compound concentration range of 0-10  $\mu$ M, with low cytotoxicity of the tested compounds. Furthermore,  $\mu$ M concentrations of **1.13** and **1.14**, tested in the INF $\gamma$  release assay in transgenic mouse T cells expressing PD-1 were able to rescue PD-1-mediated inhibition of INF $\gamma$  secretion.

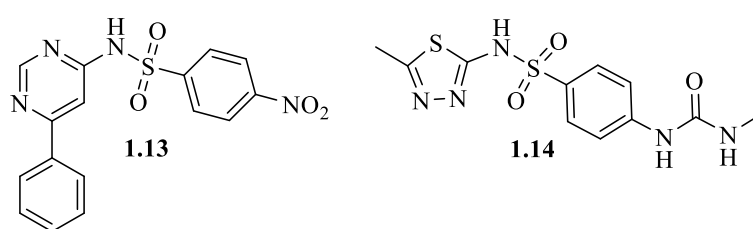


Figure 10. Examples of the PD-1/PD-L1 sulfamonomethoxine **1.13** and sulfamethizole **1.14** inhibitors.

In 2015, another group of small molecule inhibitors was unveiled by the company Bristol-Myer Squibb (BMS) (Chupak *et al.*, 2015a). The general structure of the inhibitors proposed by BMS consists of a scaffold based on a substituted biphenyl group, which is linked to another aromatic ring by a benzyl ether bond (Figure 11). To determine the binding affinities of the compounds proposed in the first patent, homogeneous time-resolved fluorescence (HTRF) assay was applied, resulting in the determination of IC<sub>50</sub> values from 0.6 nM to 20  $\mu$ M (Chupak

*et al.*, 2015a). The modified general structure proposed not much later included the introduction of the 2,3-dihydrobenzo[*b*][1,4]dioxine moiety instead of the distal phenyl ring and the addition of cyanopyridine or benzonitrile to the central phenyl. The applied modifications resulted in significant improvement of the activity of the compounds, even to 0.6-10 nM  $IC_{50}$  values by HTRF assay (Chupak *et al.*, 2015b). The further modification of the general structure of BMS-type compounds includes the extension of the distal phenyl ring with hydrophilic substituents attached *via* an ether bond, and (pseudo)symmetrisation of the compound. These adjustments provided positive effects on the activity of the compounds, resulting in the decrease of  $IC_{50}$  even to the value of 0.04 nM (Yeung *et al.*, 2017, Yeung *et al.*, 2018a, Yeung *et al.*, 2018b).

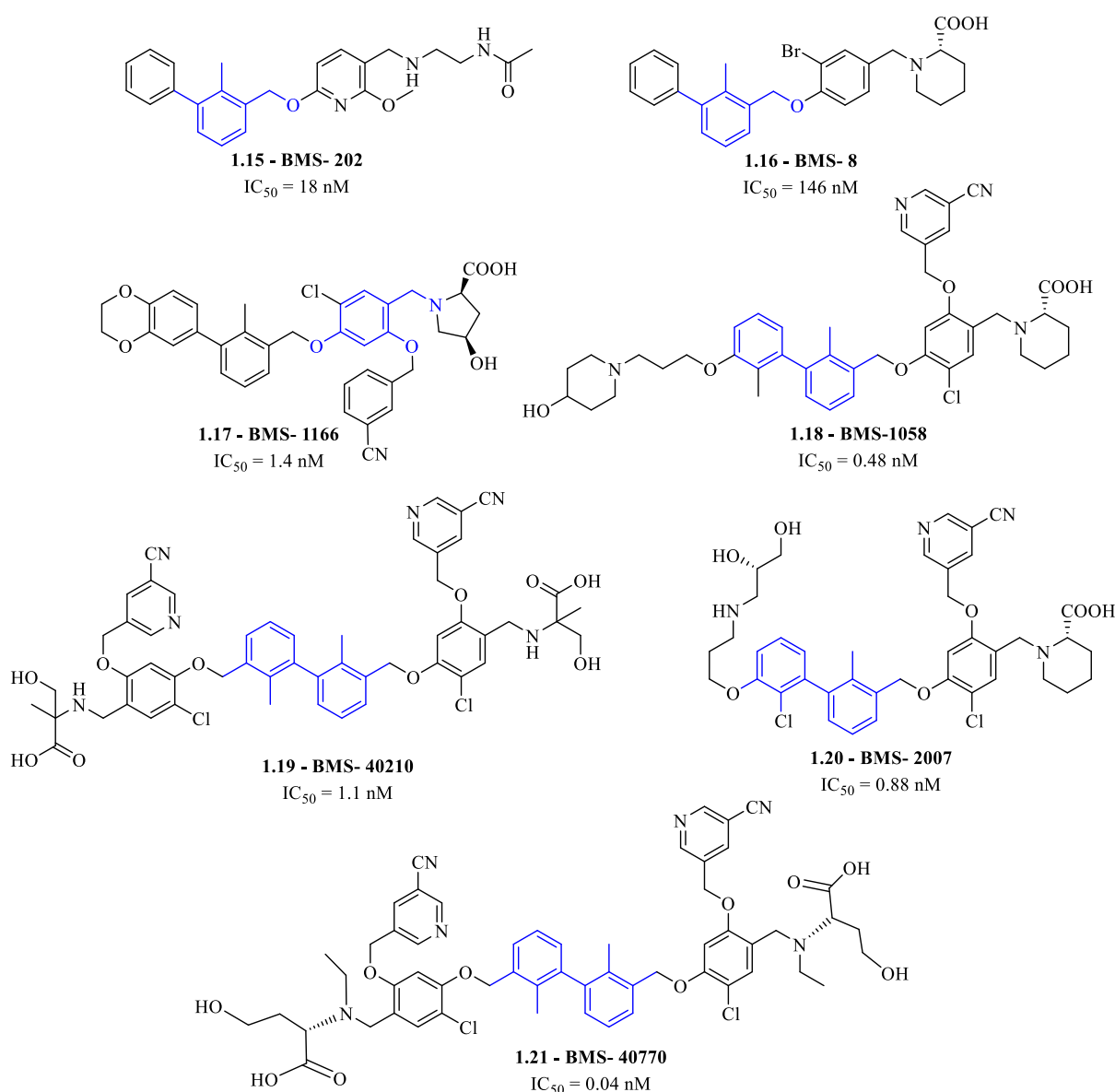


Figure 11. The examples of patented by BMS company small molecule inhibitors of PD-1/PD-L1 pathway, **1.15-1.21** (Chupak *et al.*, 2015a, Chupak *et al.*, 2015b, Yeung *et al.*, 2017, Yeung *et al.*, 2018a, Yeung *et al.*, 2018b).

The knowledge of the human PD-1/PD-L1 binding mode led to the report of the first co-crystal structures of hPD-L1 complexed with small molecule inhibitors (PDB: 5J89, 5J8O) (Zak *et al.*, 2016). The small molecules co-crystallized with hPD-L1 represent the representative examples of the scaffold patented by the company Bristol-Myers-Squibb based on the 2-methyl-3-biphenyl-methanol core. In addition, X-ray crystal studies have shown that the small molecules studied not only induce specific binding to hPD-L1 but also cause dimerization of the protein upon ligand binding (Zak *et al.*, 2016; Guzik *et al.*, 2017). In contrast to antibodies that bind to PD-L1 in a 1:1 ratio, **1.22 - BMS-202** was found to form a complex with PD-L1 in a 1:2 stoichiometry. Therefore, the assembled asymmetric unit consists of four protein molecules organized in two dimers with an inhibitor molecule located at the interface of each dimer, which is visualized in Figure 12 (Zak *et al.*, 2016).

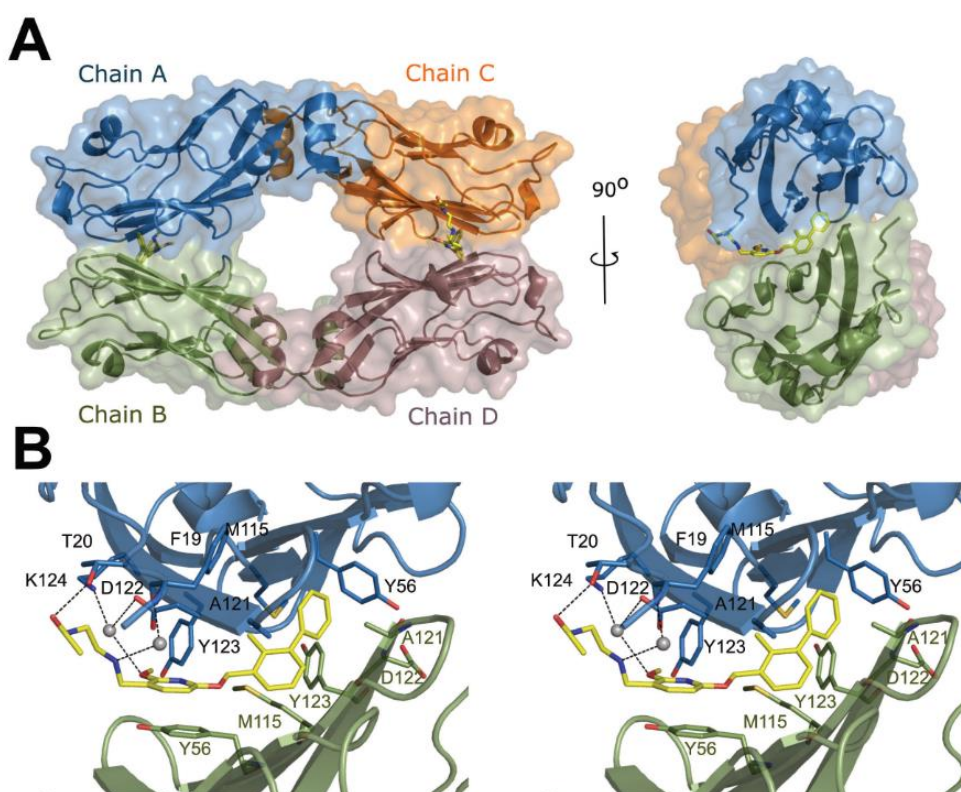


Figure 12. (A). Tetramer is composed by four molecules of PD-L1 (mixed ribbon/ surface representation) organized into two dimers (green and blue, and orange and brown) with one inhibitor molecule of **1.22 - BMS-202** (yellow) located at the interface of each dimer. (B) **1.22 - BMS-202** binding to the of PD-L1 dimer – detailed interaction (water molecules are represented by grey spheres and hydrogen bonding by black dotted lines) (Zak *et al.*, 2016).

The binding part of the ligand with the dimer requires the PD-1 interaction region of PD-L1, which prevents PD-1 from forming the complex with PD-L1. The introduced antagonist is located in a cylindrical, hydrophobic pocket formed between two monomeric PD-L1 proteins within the dimer. The observed interactions include  $\pi$ - $\pi$  stacking between the distal phenyl ring

within the biphenyl moiety of the compound and Tyr56<sub>A</sub> and  $\pi$ -alkyl interaction with Met115<sub>A</sub> and Ala121<sub>B</sub>. In addition, the central ring of methoxy-pyridine is strongly involved in the interaction by providing the water-mediated single pair  $\pi$ -interaction with Phe19<sub>B</sub> and the water-mediated interactions of the methoxyl group with the side chains of Asp122<sub>A</sub>, Lys124<sub>A</sub>, and with the carbonyl group of Tyr123<sub>A</sub>. In addition, N-(2-aminoethyl)acetamide provides the electrostatic interactions. The rationalization of human PD-1/PD-L1 disruption upon ligand (1.22 - BMS-202) incorporation is shown in Figure 13 (Zak *et al.*, 2016).

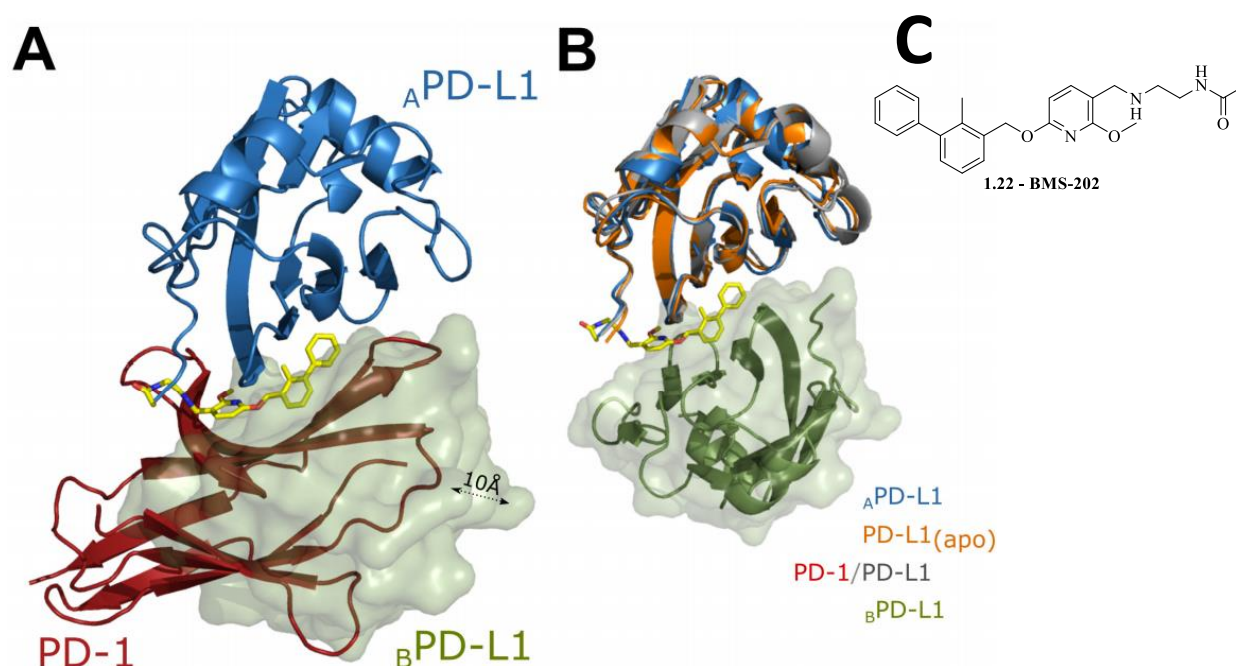


Figure 13. Visualisation of human PD-1/PD-L1 complex inhibition upon BMS-202 incorporation. (A) The superimposition of **1.22 - BMS-202** induced PD-L1 dimer and PD-1/PD-L1 complex. A single molecule of PD-L1<sub>A</sub> within the **1.22 - BMS-202** (yellow) induced dimer PD-L1<sub>B</sub> (blue ribbon- model A, green surface – model B). **1.22 - BMS-202** induced dimerization of PD-L1 masks almost the entire PD-1 (red ribbon) interaction surface thereby preventing PD-1/PD-L1 interaction.(B) Superposition of the PD-L1 molecules: apo-PD-L1 (orange ribbon; PDB 5C3T), PD-L1 from the PD-1/PD-L1 complex (PDB 4ZQK; PD-L1 presented as grey ribbon; PD-1 is not shown) and PD-L1 from PD-L1/**1.22 - BMS-202** complex (PD-L1<sub>A</sub> shown as blue ribbon; **1.22 - BMS-202** shown in yellow) structures demonstrates that PD-L1 does not undergo significant structural rearrangement upon interaction with **1.22 - BMS-202**. Model B of PD-L1/**1.22 - BMS-202** dimer is shown as green ribbon and surface. (C) **1.22 - BMS-202** structure. (Zak *et al.*, 2016).

Skalniak and co-workers also evaluated the biological activity of some BMS-type inhibitors and showed that **1.17 - BMS-1166** has low toxicity to Jurkat T cells and is able to restore effector Jurkat T cells with EC<sub>50</sub> values of 276 ± 29 nM (Skalniak, *et al.*, 2017), however, this value is significantly different from that obtained for mAbs.

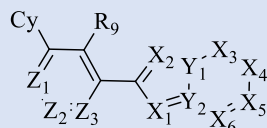
In addition, recent research by Chen and co-workers provided information on the mechanism of **1.17 - BMS-1166** and PD-L1 interaction (Chen *et al.*, 2020). Chen proposed that

**1.17 - BMS-1166** specifically affects PD-L1 glycosylation and thus prevents the transport of under-glycosylated PD-L1 to the Golgi apparatus. Therefore, this process led to accumulation of PD-L1 in endoplasmic reticulum (ER) and subsequently provide the blockade of PD-1/PD-L1 signalling and recovery of T-cell activity. However, it was discovered that the glycosylation inhibition was related to blocking the partially glycosylated 43-kDa form of PD-L1 from further glycosylation to the ~55-kDa form. Thus, a 43-kDa form of PD-L1 with a different glycan structure was generated. Furthermore, analysis of the co-crystal structure of **1.17 - BMS-1166/PD-L1** described by Skalniak *et al.* and the dimerization of the protein upon **1.17 - BMS-1166** binding suggests that PD-L1 dimer may block its ER export. It is conceivable that dimer formation blocks further glycosylation and may lead to misfolding and subsequent degradation of PD-L1 (Skalniak *et al.*, 2017, Chen *et al.*, 2020).

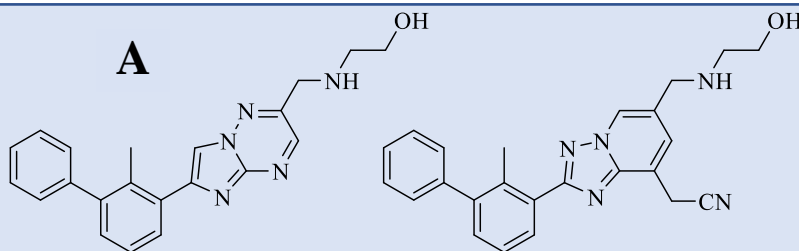
The interesting results on BMS-like small molecules described above have suggested that most of the presented PD-1 / PD-L1 antagonists produced by pharmaceutical companies and academic research groups are based on the biphenyl core and patterned on BMS-like compounds (Guzik *et al.*, 2017; Liu *et al.*, 2021; Pan *et al.*, 2021). This is rationalized on awareness of the co-crystal structure of hPD-L1 and its ligand, for example **1.22 - BMS-202**, where the antagonist accommodates the hydrophobic cleft between two PD-L1 proteins within the dimer.

Next generations of PD-1/PD-L1 small molecule inhibitors have been proposed by Incyte Corporation. Below are some of the general structures disclosed by Incyte Corporation and examples of the most prominent compounds. The core of the compounds derived from General Structure I is based on biphenyl derivative and consists of a heteroaromatic ring attached to the central ring of the biphenyl core (Figure 14A). This modification led to the generation of the fused system containing from 1 to 4 nitrogen atoms. The preliminary activity of the compounds towards PD-1/PD-L1 dissociation was determined by homogeneous time-resolved fluorescence (HTRF) assay. The best described compounds **1.23** and **1.24** were able to disrupt PD-1/PD-L1 complex formation with IC<sub>50</sub> values below 100 nM. Analysing the activities of other of the obtained compounds, the best results were presented for the structures containing 4 nitrogen atoms within the heteroaromatic ring and possessing an attached solubilizing agent at the X<sub>4</sub> position on the heteroaromatic moiety (Wu *et al.*, 2017a).

general structure I



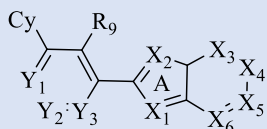
where, Z<sub>1</sub>, Z<sub>2</sub>, Z<sub>3</sub> are N or CR  
 Cy and R are cycloalkyl, aryl,  
 heteroaryl, heterocycloaryl or H  
 X<sub>1</sub>-X<sub>6</sub> are N or CR  
 Y<sub>1</sub>, Y<sub>2</sub> are C or N



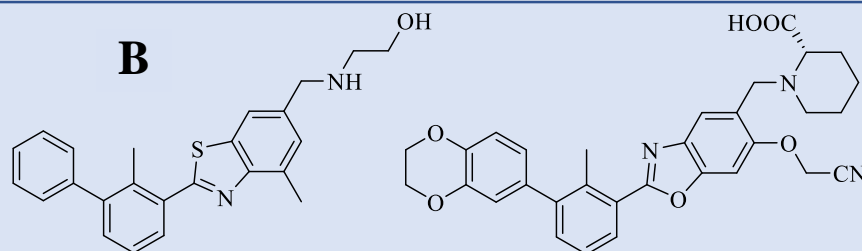
**1.23** - IC<sub>50</sub> <100 nM

**1.24** - IC<sub>50</sub> <100 nM

general structure II



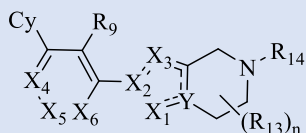
where, Cy and R are cycloalkyl, aryl,  
 heteroaryl, heterocycloaryl or H  
 X<sub>1</sub> and X<sub>2</sub> are O or S/CR and N  
 X<sub>3</sub>-X<sub>6</sub> are CR or N  
 Y<sub>1</sub>-Y<sub>3</sub> are CR or N



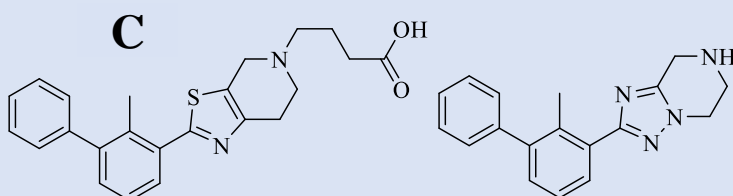
**1.25** - 100 nM < IC<sub>50</sub> <1000 nM

**1.26** - 10 nM > IC<sub>50</sub>

general structure III



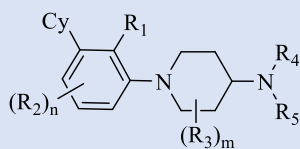
where, Cy and R are cycloalkyl, aryl,  
 heteroaryl, heterocycloaryl or H  
 X<sub>1</sub> and X<sub>2</sub> are O, S, N, NR, CR  
 X<sub>2</sub> is N or C  
 X<sub>3</sub>-X<sub>6</sub> are CR or N  
 Y is CR or N



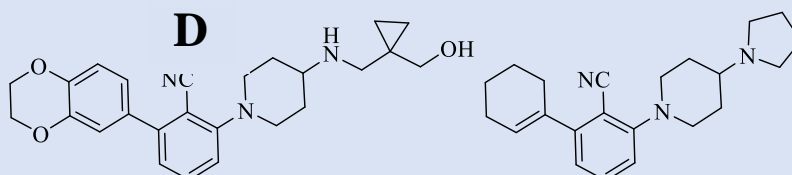
**1.27** - 100 nM < IC<sub>50</sub>

**1.28** - 500 nM < IC<sub>50</sub> <10000 nM

general structure IV



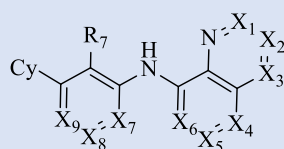
where,  
 Cy and R are cycloalkyl, aryl,  
 heteroaryl, heterocycloaryl or H



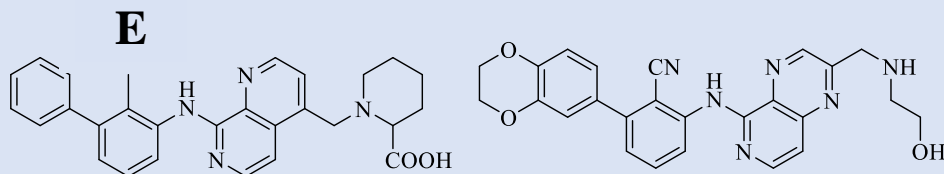
**1.29** - IC<sub>50</sub> <100 nM

**1.30** - 100 nM < IC<sub>50</sub> <500 nM

general structure V



where, X<sub>1</sub>-X are N or CN  
 wherein X<sub>1</sub>, X<sub>2</sub> and X<sub>3</sub> are not all  
 simultaneously N  
 Cy and R are cycloalkyl, aryl,  
 heteroaryl, heterocycloaryl or H



**1.31** - IC<sub>50</sub> <10 nM

**1.32** - IC<sub>50</sub> <10 nM

Figure 14. The general structures I-V and most prominent examples of derivatives of each of general structure disclosed by Incyte Corporation, **1.23 – 1.32** (Wu *et al.*, 2017a, Li *et al.*, 2017a, Li *et al.*, 2017b, Lu *et al.*, 2017, Lajkiewicz *et al.*, 2017).

The second generation of compounds disclosed by Incyte Corporation includes some changes in the position and type of heteroatoms within the heterocyclic ring system (general structure **II**, Figure 14B). Patent application WO2017087777 A1 includes small molecules such as benzoxazole, furo[2,3-b]pyridine, furo[2,3-b]pyrazine and benzothiazole derivatives - **1.25** - **1.26** (Li *et al.*, 2017a) and shows that the presence of benzoxazole within the compound structure is beneficial for the potency of the compounds. In addition, it has been demonstrated that introduction of substituent *via* ether linkage at X<sub>5</sub> position (**1.26**) improves the potency of compounds. This strategy was used for the generation of compound **1.26** and resulted in a promising IC<sub>50</sub> value of less than 10 nM determined by HTRF assay (Li *et al.*, 2017a).

Further research on small molecule design led to the introduction of a five-membered heteroaromatic ring fused to a piperidine moiety into the inhibitor structure (general structure **III**, Figure 14C, **1.27** – **1.28**). Most of the disclosed compounds show the IC<sub>50</sub> value in the micromolar range, except for molecule **1.27**, which IC<sub>50</sub> is estimated to be below the 100 nM value (Li *et al.*, 2017).

Another Incyte scaffold is an N-arylated-4-amino piperidine fragment. (general structure **IV**). The potency of the molecules presented by Lu and co-workers (**1.29**, **1.30**) were in a similar range to those presented in the previous patents. The work suggests that the exchange of the distal aryl ring from the biphenyl core and the incorporation of cyclohexene in molecule **1.30** negatively affected the activity of the compounds (Figure 14D) (Lu *et al.*, 2017).

The next modifications of the scaffold led to the development of a new group of inhibitors with general structure **V** shown in Figure 14E (**1.31**, **1.32**). The modifications included insertion of an amine bond, which allowed linking the biphenyl scaffold to a heteroaromatic ring system containing up to three nitrogen atoms. These modifications resulted in a significant decrease of the IC<sub>50</sub> value below 10 nM (Lajkiewicz *et al.*, 2017). Analysis of the molecular structures of this group of inhibitors led to the observation that the affinity of the compound strongly depends on the position of the nitrogen atom. In annellated heteroatomic ring system, the preferred position of nitrogen atom is position X<sub>6</sub> (in general structure **V**).

Other potential inhibitors proposed by Incyte Corporation comprise a group of picolinamide derivatives with general structure **VI** (Figure 15A, **1.33**). The structures of the molecules contain the six-membered ring of heteroatom linked *via* amide bond to the proximal phenyl ring of biphenyl scaffold. Introduction of amide implements the possibility of rotation of heteroaryl during the interaction of the molecule with the target, what could provide the enhancement in the small molecule's activity. Moreover, when analysing the patent results, it was easy to observe that the incorporation of the second nitrogen atom into the heteroaromatic

ring, as well as the introduction of the bulky substituent at the X<sub>2</sub> position, does not provide a positive influence on the molecule's potency (Wu *et al.*, 2017b).

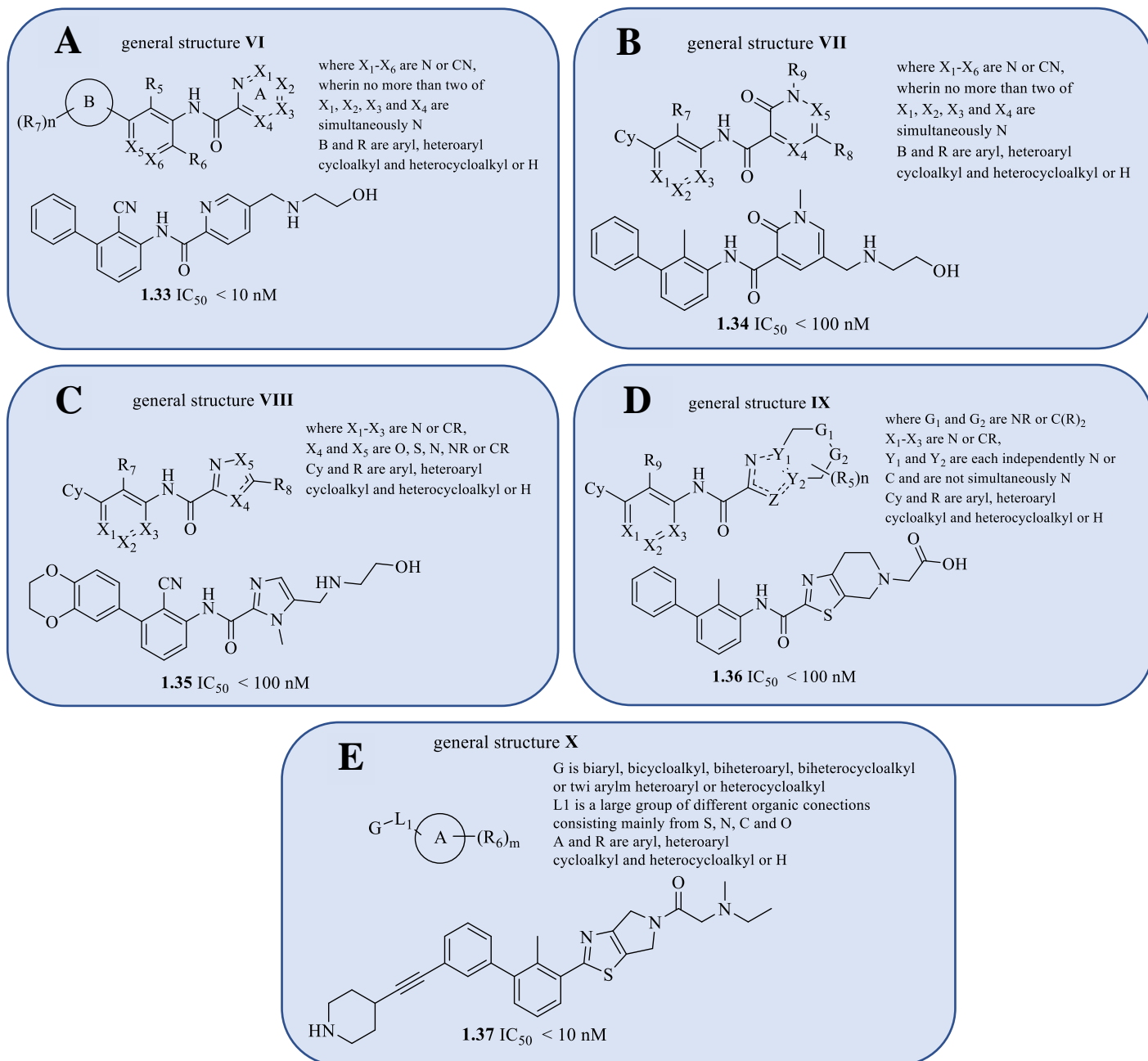


Figure 15. The general structures **VI-X** and the most representative examples (**1.33 – 1.37**) of inhibitors related to each of general structure for compounds disclosed by Incyte Corporation (Wu *et al.*, 2017b, Yu *et al.*, 2018, Wu *et al.*, 2018a, Xiao *et al.*, 2017, Wu *et al.*, 2018b).

Subsequently, the next scaffold involving the N-methyl-2-pyridone-6-carboxamide derivatives was proposed (General Structure **VII**, Figure 15B). However, when analysing the influence of carbonyl group introduction, a negative effect of this modification was observed (**1.34**). Furthermore, during the optimization of the solubilizing group, it was investigated that



ethyl N-substitution of the amine group led to a significant decrease in inhibitor activity (Yu *et al.*, 2018).

Further modification of the scaffold provided the construction of the group of compounds within the biphenyl core linked by amide bond with diheterocyclic five-membered aromatic ring (**1.35**, general structure **VIII**, Figure 15C) or with diheterocyclic five-membered aromatic ring fused with piperidine (**1.36**, general structure **IX**, Figure 15D). The SAR analysis presents the advantageous accommodation of imidazole, pyrazole or thiazole as pyrrole and oxazole in the structure of immunomodulator. The best from this series of compounds molecules **1.35**, **1.36** possess  $IC_{50}$  values below 100 nM by HTRF assay (Wu *et al.*, 2018a, Xiao *et al.*, 2017).

The last of the general structures presented herein general structure **X** combines the rigid scaffolds containing the biphenyl core fused with a phenyl or heterocyclic ring, directly or through an amide/amine bond (Figure 15E). Interestingly, promising results were obtained for the extended compounds where a 4-piperidineethynyl substituent was attached at the 3' position of the biphenyl (**1.37**). The  $IC_{50}$  value of this immunomodulator **1.37** was found to remain below 10 nM (Wu *et al.*, 2018b).

Another large pharmaceutical company with a strong interest in the production of small molecule PD-1/PD-L1 inhibitors is ChemoCentryx. The compounds described in the disclosed patents are based on 4-phenyl-2,3-dihydro-1H-inden-1-ol (Figure 16, **1.38**, **1.39**).

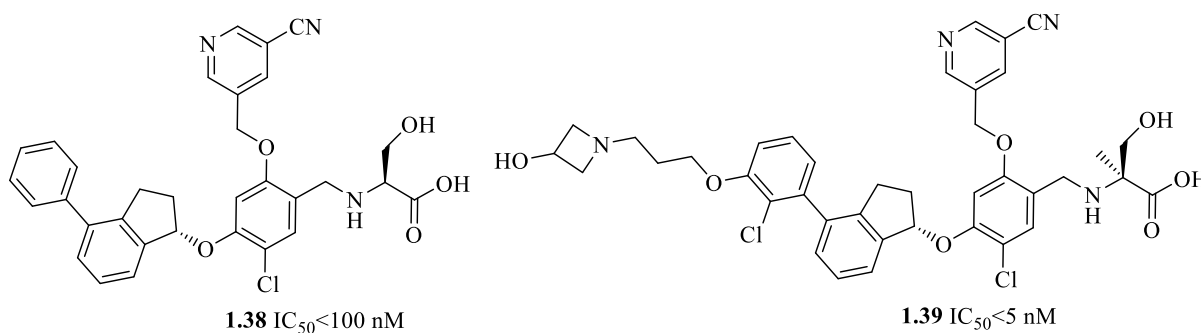


Figure 16. The representative examples of immunomodulators (**1.38**, **1.39**) published by ChemoCentryx company.

The design strategy of the immunomodulators is based on scaffold rigidification through the incorporation of an ether linker, which couples the substituted indenyl group with the central aromatic ring of the compound. SAR studies also revealed that factors such as attachment of cyanopyridine substituent to the central aromatic ring, presence of additional solubilizing group linked to the 3'-position of the phenyl ring distal from the biphenyl core, and S-configuration of the inhibitor are favored. Application of these operations allowed to obtain compound **1.39** which presents half inhibitory concentration value below 5 nM. The potency of compound **1.39**

to target the PD-1/PD-L1 pathway was also determined by enzyme-linked immunosorbent ELISA, cell-based reporter, and mixed lymphocyte reaction (MLR) assays. In addition, excellent results were obtained in *in vivo* assays where the A375 human melanoma cells were co-implanted with human peripheral blood mononuclear cells (PBMCs) into immunodeficient NOD/SCID mice. As a result, the lead structure CCX4503 was found to inhibit tumor growth with efficacy comparable to the anti-human PD-L1 antibody (Lange *et al.*, 2018, Lange *et al.*, 2019, Vilalta Colomel *et al.*, 2018).

Small molecule antagonists of the PD-1/PD-L1 immune checkpoint also became the subject of interest of Guangzhou Maxinovel Pharmaceuticals. The novelty of the structures of the disclosed compounds is related to the proposed connection between the biphenyl scaffold and the third aromatic moiety through ethenyl or ethynyl moieties (Figure 17).

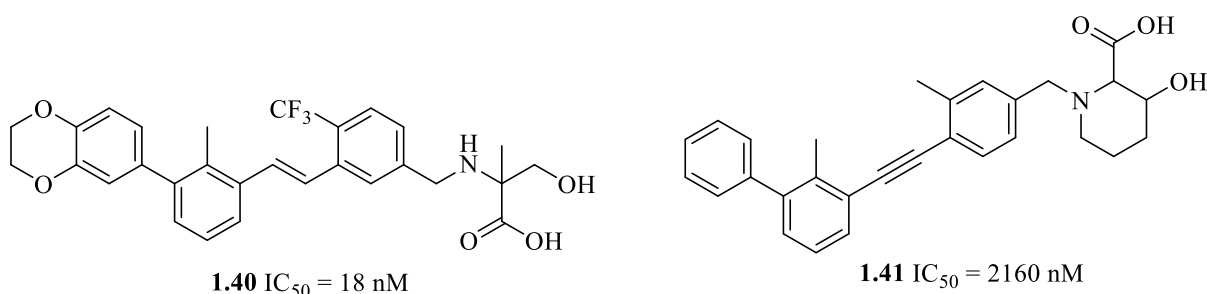


Figure 17. The structures of compounds **1.40**, **1.41** proposed by Maxinovel Corporation (Wang, Y. *et al.*, 2018a).

Surprisingly, the activities of ethenyl and ethynyl based antagonists were determined to be in the same range, despite different geometry of the linkers. It was also observed that the introduction of  $-CF_3$  substituent (**1.40**) provides the significant increase of the compound's potency towards PD-L1 binding. As a result, the half inhibitory value determined for **1.40** was calculated to be 18 nM for the compound. Among the compounds patented by Maxinovel Corporation, **1.42 - MAX-10129** with not fully disclosed structure showed significant oral bioavailability as well as high tolerability and dose-dependent inhibition of tumor progression in MC-38 mice model of colorectal cancer. **1.42 - MAX-10129** was reported to have synergistic antitumor activity in combination therapy with CTLA-4 antibody, epacadostat (IDO inhibitor), Celebrex (COX-2 inhibitor) and cisplatin (Wang *et al.*, 2018a, Wang *et al.*, 2018b).

Feng's team at the Chinese Academy of Medical Science reported a series of bromo benzyl phenyl ether derivatives substituted with a methylene pyridine moiety. The representative examples of the compounds we were able to dissociate PD-1/PD-L1 checkpoint with extremely low, even picomolar ranges (Figure 18, **1.43**, **1.44**).

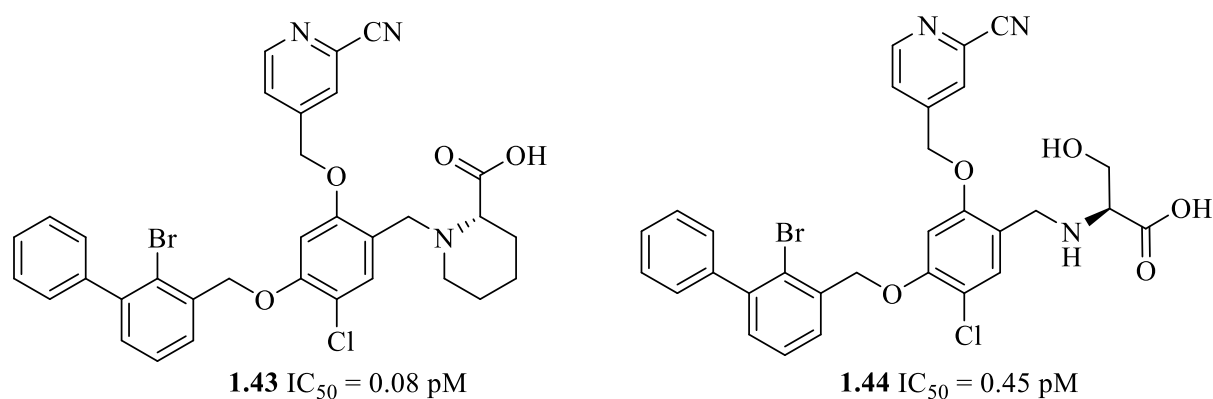


Figure 18. The examples of the most representative inhibitors – **1.43**, **1.44**- form bromo benzyl phenyl ether derivatives patented by Chinese Academy of Medical Sciences (Feng *et al.*, 2017a, Feng *et al.*, 2017b, Feng *et al.*, 2017c).

Some of the compounds described in the patent were also able to release IFN- $\gamma$  in PBMCs expressing PD-1 and to abolish the inhibitory effect of PD-L1 on IFN- $\gamma$  at 10 nM. In addition, some of the disclosed immunomodulators were tested in the subcutaneously transplanted mouse B16F10 tumor model. It was found that the proposed inhibitors were able to significantly inhibit the growth of tumor volume and its weight at the dose of 15 mg/kg. The inhibition rate of tumor weight reached 64.11% (Feng *et al.*, 2017a, Feng *et al.*, 2017b, Feng *et al.*, 2017c).

The teams of Ping Gong and Xiaobo Wang from Shenyang Pharmaceutical University recently published two groups of compounds, [1,2,4]triazolo[4,3-a]pyridine derivatives and indoline-bearing compounds, as potential PD-1/PD-L1 immunomodulators (Figure 19) (Qin *et al.*, 2019, Qin *et al.*, 2020).

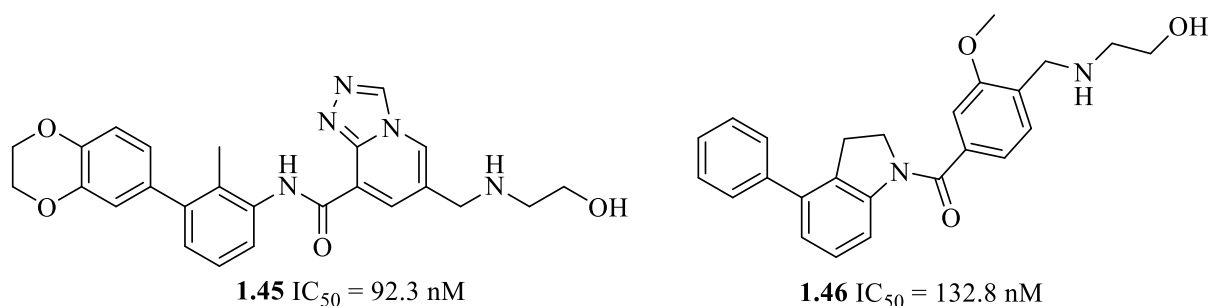


Figure 19. The examples of compounds **1.45**, **1.46** disclosed by Shenyang Pharmaceutical University (Qin *et al.*, 2019, Qin *et al.*, 2020).

The structure of the first group of compounds is rationalized by SAR analyses, which indicated that the fusion of an additional heteroaromatic ring with pyridine could help fill the space and provide additional interactions during binding to PD-L1. In addition, the solubilizing group was attached at the 6-position of the [1,2,4]triazolo[4,3-a]pyridine core. Analysing the indoline fragment bearing compounds, the ring fusion strategy was also used to attach additional five-membered ring. Among the presented group of inhibitors, compounds 1.45 and 1.46 provided the best IC<sub>50</sub> values of 92.3 nM and 132.8 nM by HTRF assay, respectively. Moreover, both presented compounds caused the dose-dependent secretion of INF- $\gamma$  in a co-culture model of Hep3B/OS-8/hPD-L1 and CD3 T cells (Qin *et al.*, 2019, Qin *et al.*, 2020).

The development of BMS-type compounds has progressively expanded. Below are two more examples of immunomodulators disclosed by Cheng and co-workers and Wang Y. and co-workers (Figure 20, **1.47**, **1.48**). Compound **1.47** is a quinazoline derivative formed by the fusion of the pyrimidine ring to the 2- and 3-positions of the biphenyl core. The analysis of the binding mode between the inhibitor and target protein shows that the strategy of additional heteroatomic ring introduction allows the  $\pi$ -alkyl interactions with Ala121 and Met115, which lead to the improvement of the binding mode. In the *in vitro* assay, compound **1.47** showed potency to reach the PD-1/PD-L1 pathway with an IC<sub>50</sub> value of 1.57 nM. Moreover, **1.47** was not only able to release EC in the cell-based PD-1/PD-L1 blockade bioassay but also presented an acceptable toxicity profile on PBMCs with IC<sub>50</sub> value of 12.42 mM (Wang, Y. *et al.*, 2022).

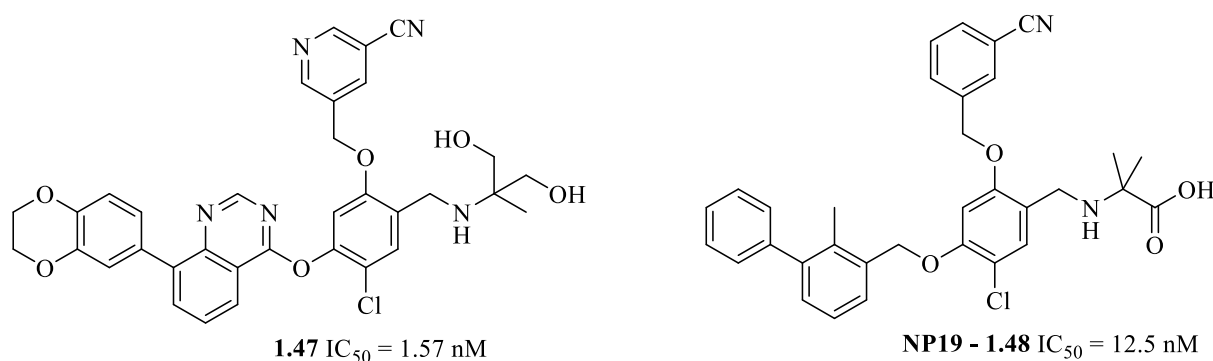


Figure 20. BMS-type inspired PD-1/PD-L1 immunomodulators **1.47** and **1.48** proposed by Cheng and co-workers and by Wang Y. and his team (Cheng *et al.*, 2020, Wang, Y. *et al.*, 2022).

Cheng *et al.* in the 2020 paper present compound **1.48 - NP19**, which inhibits human PD-1/PD-L1 interaction with IC<sub>50</sub> values of 12.5 nM in HTRF binding assays (Figure 20, **1.48**). In addition, compound **1.48 - NP19** was shown to dose-dependently produce IFN- $\gamma$  in a co-culture model of Hep3B/OS-8/hPD-L1 and CD3 T cells. **1.48 - NP19** also exhibits significant *in vivo*

antitumor efficacy in a B16-F10 melanoma and H22 hepatoma mouse tumor model (Cheng *et al.*, 2020).

Muszak and co-workers proposed the group of small molecule PD-1/PD-L1 inhibitors based on a terphenyl scaffold, which is derived from the rigidified biphenyl-inspired structure (Figure 21, **1.49**, **1.50**) (Muszak *et al.*, 2021).

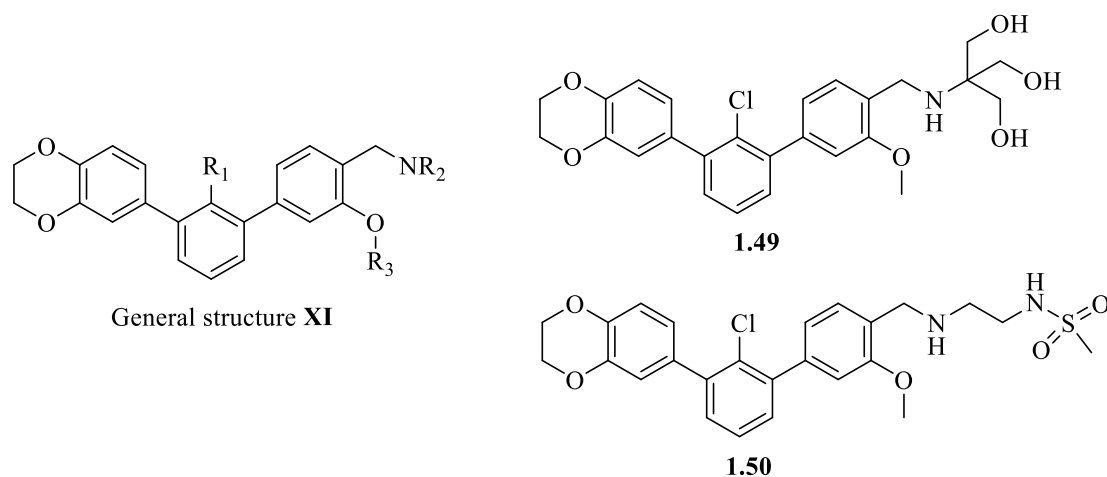


Figure 21. (A) The general structure **XI** of terphenyl based small molecules. (B) The examples of most prominent terphenyl based small molecule inhibitors, **1.49** and **1.50**.

The SAR analysis on the general structure resulted in the selection of the best set of substituents and provided the molecule **1.49** which exhibits enhanced potency towards the target proved due to HTRF, NMR, and cell-based assay. The half inhibitory concentration value determined due to HTRF assay was below 1 nM, while EC<sub>50</sub> calculated due to ICB assay was estimated at ca. 1 μM. The best of the obtained compound also allowed the activation of Jurkat effector cells to levels comparable to those obtained with the use of antibodies. In addition, compound **1.49** showed efficacy to activate the antitumor response using primary human immune cells from healthy donors, inducing PD-1 expression and increasing the number of CD25-positive and HLA-DR-positive T cells in PBMCs and CHO/TCRAct/PD-L1 cell system. The presence of molecule **1.49** also provided an enhanced level of immune-related cytokines release, underlining its good properties towards primary human T cells. Moreover, the cross-reactivity studies of **1.49** between murine and human PD-L1 proved that no cross-reactivity was observed, providing specificity for the human protein analog. The binding mode of the terphenyl-based molecule was studied using **1.50** as an example by X-ray crystallography. The analyses of the co-crystal structure of **1.50** and PD-L1 showed a similar to other anti-PD-L1 inhibitors' interaction with protein involving dimerization of target protein (Muszak *et al.*, 2021).

In 2022, Wang, T. *et al.*, proposed the group of small-molecule PD-1/PD-L1 antagonists as biphenyl derivatives, where the biphenyl core is directly attached to the 1,3,4-oxadiazole moiety. The best of these molecules (structure **1.51** in Figure 22) shows the ability not only to inhibit PD-1/PD-L1 but also to promote dimerization, followed by PD-L1 internalization into the cytosol, to finally induce the degradation of PD-L1 in tumor cells through a lysosome-dependent pathway. In addition, **1.51** also shows promising *in vivo* anticancer activity by decreasing the level of PD-L1 expression in tumor tissues in two different murine tumor models (the B16-F10 and the CT26 murine melanoma model in BALB/c mice). Wang, T. *et al.* claim that the application of **1.51** at a dose of 160 mg/kg provides better results in terms of tumor growth reduction efficacy than the PD-L1 antibody tested. Compound **1.51** was also subjected to combination therapy with PD-L1 antibody in the B16-F10 tumor model, with even better results. The effect of combining **1.51** (80 mg/kg) with the PD-L1 antibody was also significantly better than the effect of **1.51** (160 mg/kg) monotherapy (Wang, T. *et al.*, 2022).

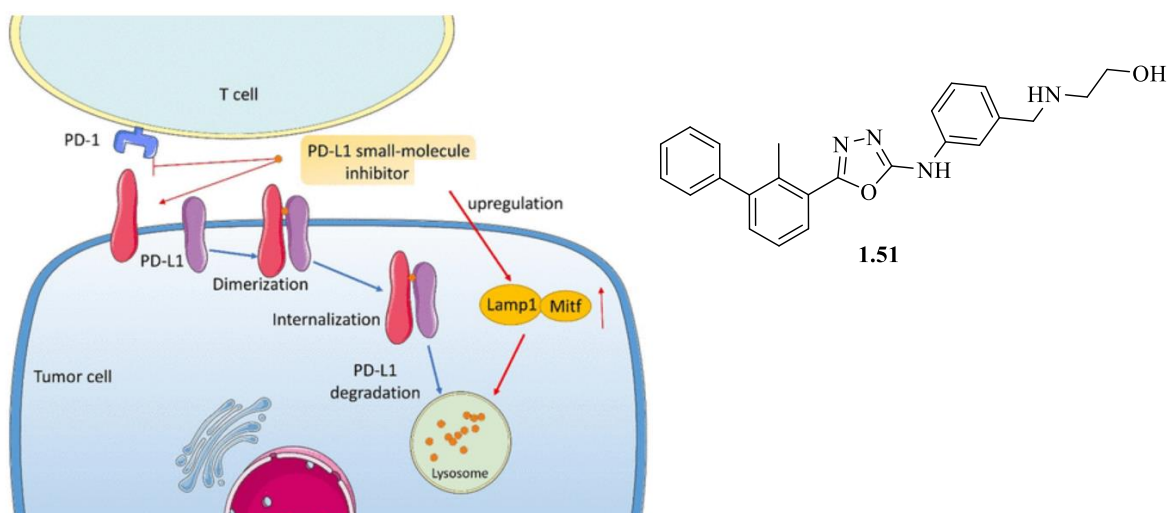


Figure 22. The visualisation of internalisation and degradation of PD-L1 due to introduction of **1.51** (Wang, T. *et al.*, 2022).

### 1.8.2. Elongated Type of Small Molecule Inhibitors

More recently, an elongated generation of biphenyl core-based small molecules develops progressively. The elongation, or in some cases, dimerization of the compounds could provide the enhancement in binding potency by an increase of the surface of interactions.

One of the first elongated compounds was the group of (pseudo)symmetric immunomodulators reported by Arising International LLC as inhibitors of both PD-1/PD-L1 and CD80/PD-L1. Utilizing the HTRF assay, the estimated IC<sub>50</sub> value of molecule **1.52** was below 0.1 μM. Also, the other derivatives of this scaffold present *in vitro* activity in a similar, low micromolar range. This not fully satisfying potency can be justified, by poor solubility is a result of the highly hydrophobic core of compounds (**1.52**) (Figure 23) (Wang, M. *et al.*, 2019).

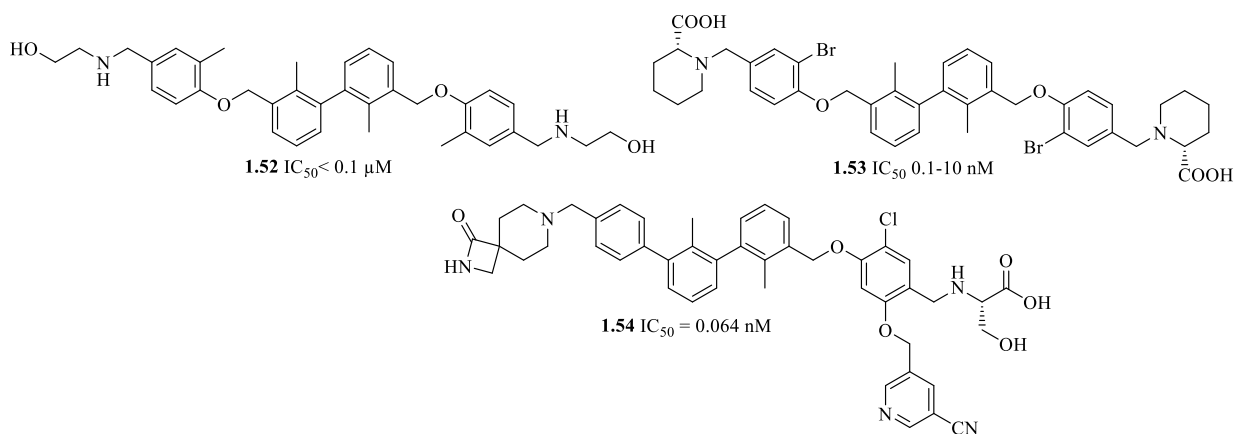


Figure 23. The compounds proposed by Arising International LLC (**1.52**), Polaris Pharmaceuticals (**1.53**) and Gilead Sciences (**1.54**) (Wang, M. *et al.*, 2019, Webber *et al.*, 2018, Aktoudianakis *et al.*, 2018).

Another company interested in the production of elongated PD-1/PD-L1 is Polaris Pharmaceutical Inc. In 2018, the company unveiled a group of (pseudo)symmetric biphenyl-based derivatives containing a system of four aromatic rings (**1.53**). Enzyme-linked immunosorbent assay (ELISA) allows to determine the IC<sub>50</sub> value of the representative compound **1.54** in the range of 0.1-10 nM. (Figure 23) (Webber *et al.*, 2018).

The next group announcing attractive PD-1/PD-L1 antagonists is Gilead Sciences Inc. Among this group of compounds, we can observe inhibitors designed as a fusion of previously reported molecules elaborated by the companies BMS (characteristic benzyl ether linkage), ChemoCentryx (rigidification), Arising International, and Incyte Corporation. The *in vitro* activities of the compounds were evaluated by the Amplified Luminescent Proximity Homogeneous Assay (ALPHA) and calculated for the low nanomolar range (**1.54**, Figure 23) (Aktoudianakis *et al.*, 2018).

Prime examples of the dimeric type of compounds are molecules presented by two research groups, Basu *et al.* and Kawashita *et al.* (Figure 24) (Basu *et al.*, 2019) (Kawashita *et al.*, 2019). The presented ICP inhibitors **1.56 - LH1306** and **1.57 - LH1307** reach IC<sub>50</sub> values in the low nanomolar range of 25 and 3 nM, respectively. Both compounds were also tested in cellular assays, restoring effector Jurkat T cells with EC<sub>50</sub> values of 4.2 and 0.76 μM, respectively. In contrast to C<sub>2</sub>-symmetric **1.56 - LH1306**, its monomeric precursor was inactive in the same cellular assay (Basu *et al.*, 2019). To compare the potency of the dimeric compounds **1.56 - LH1306** and **1.57 - LH1307** with their asymmetric analogs, a heterologous functional assay based on enzyme fragment complementation technology - the commercial PathHunter cell-based PD-1 (SHP-1) signaling assay - was performed. The results of the PathHunter cell-based PD-1 (SHP-1) assay allowed to investigate that the symmetric compounds **1.56 - LH1306** and **1.57 - LH1307** exhibit 8.2-fold (EC<sub>50</sub>, 334 nM) and 2.8-fold (EC<sub>50</sub>, 79 nM) better activity, respectively, compared to the asymmetric cognates (Basu *et al.*, 2019). Therefore, extension or in this case dimerization of the compounds is necessary for the functional design of PD-1/PD-L1 antagonists (Sasikumar *et al.*, 2022).

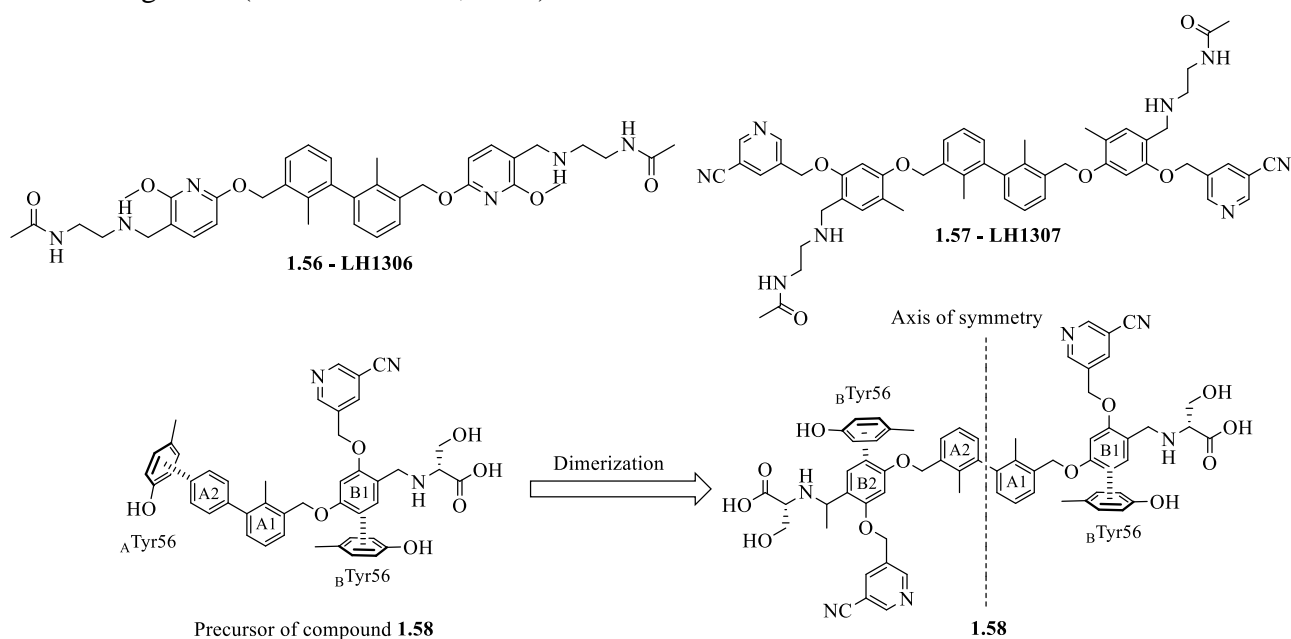


Figure 24. Examples of dimeric compounds **1.56**, **1.57** (Basu *et al.*, 2019), and **1.58** (Kawashita *et al.*, 2019).

The importance of structural elongation was also influenced by analyses such as NMR and X-ray determination of the **1.57 - LH1307** structure. These spectroscopic methods indicated the formation of a more symmetric PD-L1 dimer than previously reported for asymmetric compounds. Binding mode analysis indicated that the biphenyl core helps to anchor the hydrophobic cleft within the homodimer. The polar groups incorporated into the small molecule



structure are extended from the hydrophobic cleft and are located in the solvent-exposed region between the AG and C'C b strands of the respective PD-L1 proteins. Furthermore, solubilizing groups are responsible for assisting in bringing two PD-L1 monomers together, thanks to hydrogen bonding and electrostatic interactions with the polar residues from the AB and CC' strands of PD-L1. As proposed by Kawashita *et al.*, a symmetrical link would induce a sidechain inversion of the Tyr56 protein residue, allowing for an increase in binding affinity (Kawashita *et al.*, 2019). All described binding modes increase the potency of symmetric **1.57 - LH1307** towards PD-L1 (Basu *et al.*, 2019).

Results of recent research by Park *et al.*, 2021 present information of **1.59 - ARB 272542**, as the new release in the group of small molecules PD-1/PD-L1 antagonists. Analysis of the crystal structure of **1.59/PD-L1** showed that molecule fits in the hydrophobic cleft, composed between two PD-L1 of the homodimer. The interface of **1.59 - ARB 272542/PD-L1** interaction corresponds to the residues of PD-L1 involved in the complex with PD-1 formation. Crystallographic studies also revealed that two of the pyridine rings interact with  $\pi$ - $\pi$  stacking with Tyr56, which provides crucial interactions for compound A binding mode. Both amidic linker carboxylates form water-mediated hydrogen bond interactions with Gln66 of chain A and chain B. The two linked central benzyls are rotated by  $-106^\circ$  with respect to each other at the chain A:B interface. The central biphenyl is also involved in the binding mode, forming bonds between the Ala121 side chain of one chain and the Met115 side chain of the other chain. In addition, aryls also interact within van der Waals interactions with Asp122, Tyr123, Ile54, and Ser117. The ethanolamine moiety attached to the compound as a solubilizing group forms hydrogen bonds with the Asp122 of chain A and chain B (Park *et al.*, 2021). All described interactions are visualized in Figure 25.

The presented inhibitor was observed to exhibit a surprisingly low 17 nM EC<sub>50</sub> value, determine due to the cell-based NFAT reporter system (Jurkat-CHO-PD-1/PD-L1 bioassay). Moreover, **1.59 - ARB 272542** was found to represent different - from that presented with the use of mAbs - mechanism of PD-L1 blockade. The latter works by molecular disruption of the programmed death 1 interaction. Conversely, **1.59 - ARB 272542** reaches the PD-1/PD-L1 axis inducing cell surface PD-L1 dimerization, followed by rapid internalization into the cytosol. This process results in the effect that PD-L1 is no longer available on the cell surface to interact with its cognate receptor PD-1. In addition, **1.59 - ARB 272542** is not only a potent *in vitro* inhibitor of PD-1/PD-L1 cell signaling, but can also lead to immunostimulatory activity in human primary cells by upregulating cytomegalovirus (CMV)-specific T cell responses. **1.59 - ARB 272542** was also tested in a mouse model of the colorectal tumor where both host and

tumor expressed human PD-L1 to further determine its *in vivo* properties. The treatment provided significant tumor growth inhibition and resulted in tumor stasis with off-treatment in three out of eight animals tested and complete response in one additional animal. Notably, 7 days of **1.59 - ARB 272542** treatment provided similar tumor growth inhibition as 16 days of atezolizumab treatment in four of eight animals. In addition, **1.59 - ARB 272542** was shown to enhance hepatitis B virus-specific T and B cell responses in patient samples by inducing T cell proliferative and IFN $\gamma$  responses to HBV peptides. This could lead to the development of curative CHB immunotherapies while applying more tolerable and reversible small-molecule-based therapy (Park *et al.*, 2021).

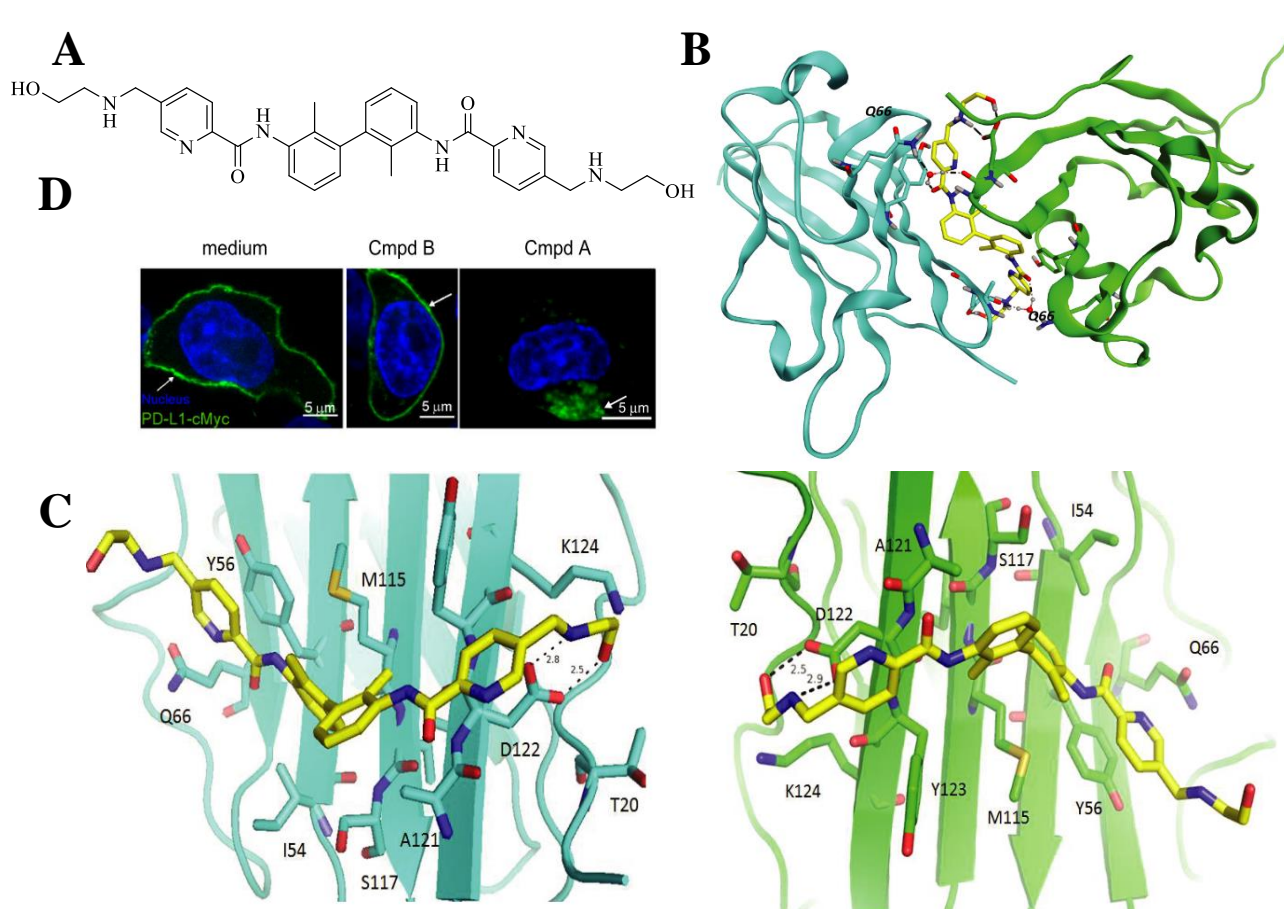


Figure 25 (A) Structure of **1.59 - ARB 272542** (B) Co-crystal X-ray structure of **1.59 - ARB 272542** and dimeric PD-L1 protein. PD-L1 presented in ribbon representation (coloured cyan and green for chains A and B) **1.59 - ARB 272542** is shown in stick representation (yellow). (C) Interaction of **1.59 - ARB 272542** with PD-L1 chain A (left panel) and with PD-L1 chain B (right panel) (D) Internalisation of PD-L1 after incubation with **1.59 - ARB 272542**. CHO-K1 cells transfected with cMyc-PD-L1 and labelled with anti-cMyc Alexa Fluor 488-conjugated antibody. The confocal fluorescence microscopy detects PD-L1-cMyc (green) and nucleus (blue) Park *et al.*, 2021).

The latest reports revealed the information about molecule **1.60 - INCB-086550** (Figure 26) disclosed by Incyte Corporations company. In 2018, the discussed compound was subjected to clinical trials, and phase 1 (NCT03762447) to study the safety, tolerability,

pharmacokinetics, and pharmacodynamics in patients with NSCLC urothelial cancer and renal cell carcinoma (Piha-Paul *et al.*, 2020). The results obtained to date, present that oral administration of **1.60 - INCB-086550** led to dose-related pharmacodynamic T-cell activation, similar to that reported for PD-L1 mAbs. Reported studies have shown that **1.60 - INCB-086550** is biologically active in disrupting the PD-1/PD-L1 pathway, leading to T-cell proliferation and activation in patients (Piha-Paul *et al.*, 2020, Sasikumar *et al.*, 2022). Research is ongoing to evaluate the intratumoral pharmacodynamic activity, safety, and efficacy of the compound.

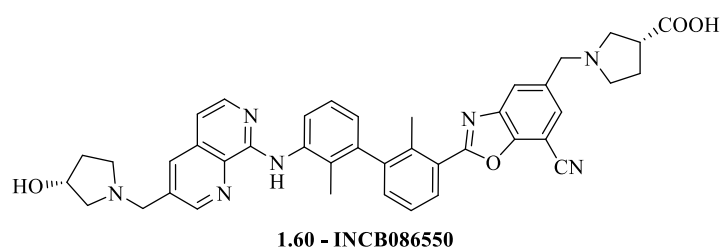


Figure 26. The structure of clinically tested molecule **1.60 - INCB-086550** (Sasikumar *et al.*, 2022).

The most recent reports revealed molecule **1.61 - IMM010** as a new drug candidate which is in phase I of clinical trials. Molecule **1.62 - YPD-29B** disclosed in the patent CN109153670 was found to possess strong potency towards PD-1/PD-L1 inhibition, and exhibit extremely low  $IC_{50}$  value of  $10^{-13}$  M in HTRF assay. Despite promising *in vitro* activity, the molecule exhibited unfavorable physicochemical properties. These problems led to the modification of **1.62 - YPD-29B** structure and the transformation of the carboxylic acid group into the corresponding ester forming **1.61 - IMM010** as **1.62 - YPD-29B** prodrug. Although having a higher  $IC_{50}$  value of  $10^{-8}$  M, **1.61 - IMM010** is expected to be converted into **1.62 - YPD-29B** during metabolic processes.

However, the latter, was essential to be studied, because the differences in metabolisms among species. Under metabolic conditions **1.61 - IMM010** transforms mainly to **1.62 - YPD-29B** and three other compounds: **1.63 - M2**, **1.64 - M3** and **1.65 - M4** and the hydrolytic process catalyzed by CES1 (Figure 27) (Wang, Y. *et al.*, 2021).

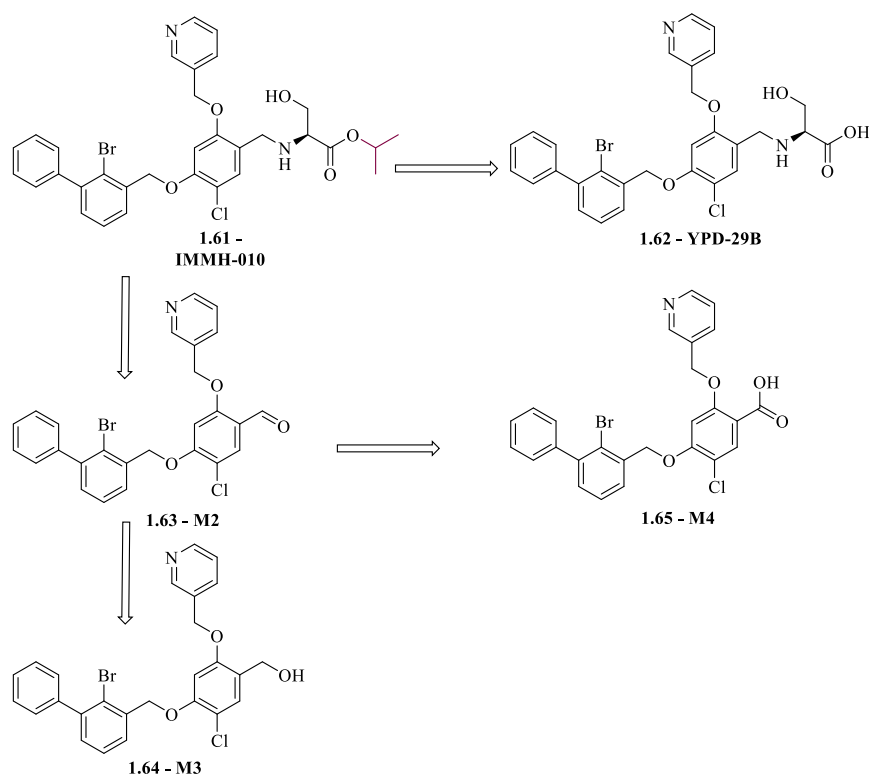


Figure 27. Metabolic profile of **1.61 - IMM-010**, where **1.62 - YPD-19B**, **1.63 - M2**, **1.64 - M3** and **1.65 - M4** were detected as metabolites due to LC-MS technique.

Metabolism studies of **1.61 - IMM-010** showed that in rat and mouse plasma it was promptly metabolized into **1.62 - YPD-29B**, in opposition to human and monkey plasma, where the compound exhibit high stability. However, the metabolism of **1.61 - IMM-010** in the liver S9 fractions exposes no differences among human, monkey, rat, and dog species. Moreover, the ratio of **1.61 - IMM-010** hydrolyses was studied in different species' intestines, showing that rat and human intestines are able to metabolite only low amounts of **1.61 - IMM-010**. The significant TGI was observed upon **1.61 - IMM-010** application in B16F10 melanoma model (for 10 mg/kg, 55% TGI,  $p < 0.001$ ,  $n = 10$ ) and MC38 (for 5 mg/kg, 75% of TGI,  $p < 0.001$ ,  $n = 10$ ) colon carcinoma xenograft mouse models. The *in vivo* studies also included the comparison of the pharmacodynamic profile of **1.61 - IMM-010** in rodent and primate animals, exhibiting lower exposure to **1.62 - YPD-29B** in primates (Wang, Y. *et al.*, 2021, Jiang *et al.*, 2021).

## 2. Performed Research

In recent years, the development of small molecule PD-1/PD-L1 inhibitors has become a widely explored scientific field. In Figure 28 and Table 1, some of the examples of already disclosed PD-L1 antagonists were correlated with clinically relevant mAbs. Two inhibitor factors such as IC<sub>50</sub> and EC<sub>50</sub> values were compared, showing that the development of small molecule inhibitors is progressing, but the search for small molecule antagonists that could replace mAbs is still highly awaited.

### THE CORELLATION OF IN VITRO ACTIVITY OF PD1/PD-L1 INHIBITORS

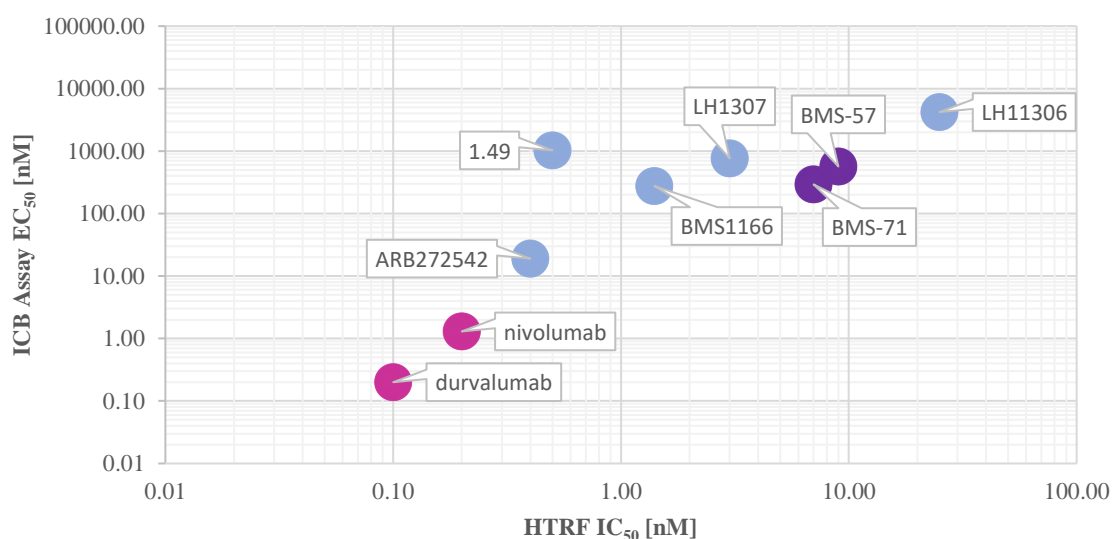


Figure 28. The comparison of the potency of known PD-1/PD-L1 inhibitors. The graph correlates IC<sub>50</sub> values from HTRF assay and EC<sub>50</sub> values from ICB assay. Various classes of compounds were visualized: blue – small molecules, violet- peptides, pink – antibodies. The numerical data on the basis of which the chart was presented have been collected in Table 1.

Table 1. The correlation of the IC<sub>50</sub>, EC<sub>50</sub> and %RLUmax values of representative various PD-L1 inhibitors. IC<sub>50</sub> values and EC<sub>50</sub> values were determined due to HTRF and ICB assay respectively. (Skalniak *et al.*, 2017; Konieczny *et al.*, 2020; Muszak *et al.*, 2021; Park *et al.*, 2021; Magiera K. *et al.*, 2017; Basu *et al.*, 2019)

Compounds	IC <sub>50</sub> (HTRF)	EC <sub>50</sub> (ICB)
<b>durvalumab</b>	0.1	0.2
<b>nivolumab</b>	0.2	1.3
<b>1.2 (BMS-57)</b>	9.0	566
<b>1.3 (BMS-71)</b>	7.0	293
<b>1.17 - BMS1166</b>	1.4	276
<b>1.49</b>	0.5	1026
<b>1.56 - LH1306</b>	25.0	4214
<b>1.57 - LH1307</b>	3.0	763
<b>1.59 - ARB 272542</b>	0.4	19

Within presented in this thesis research, ten different general structures of potential PD-1/PD-L1 inhibitors were composed. The proposed general structures are shown in Figure 29.

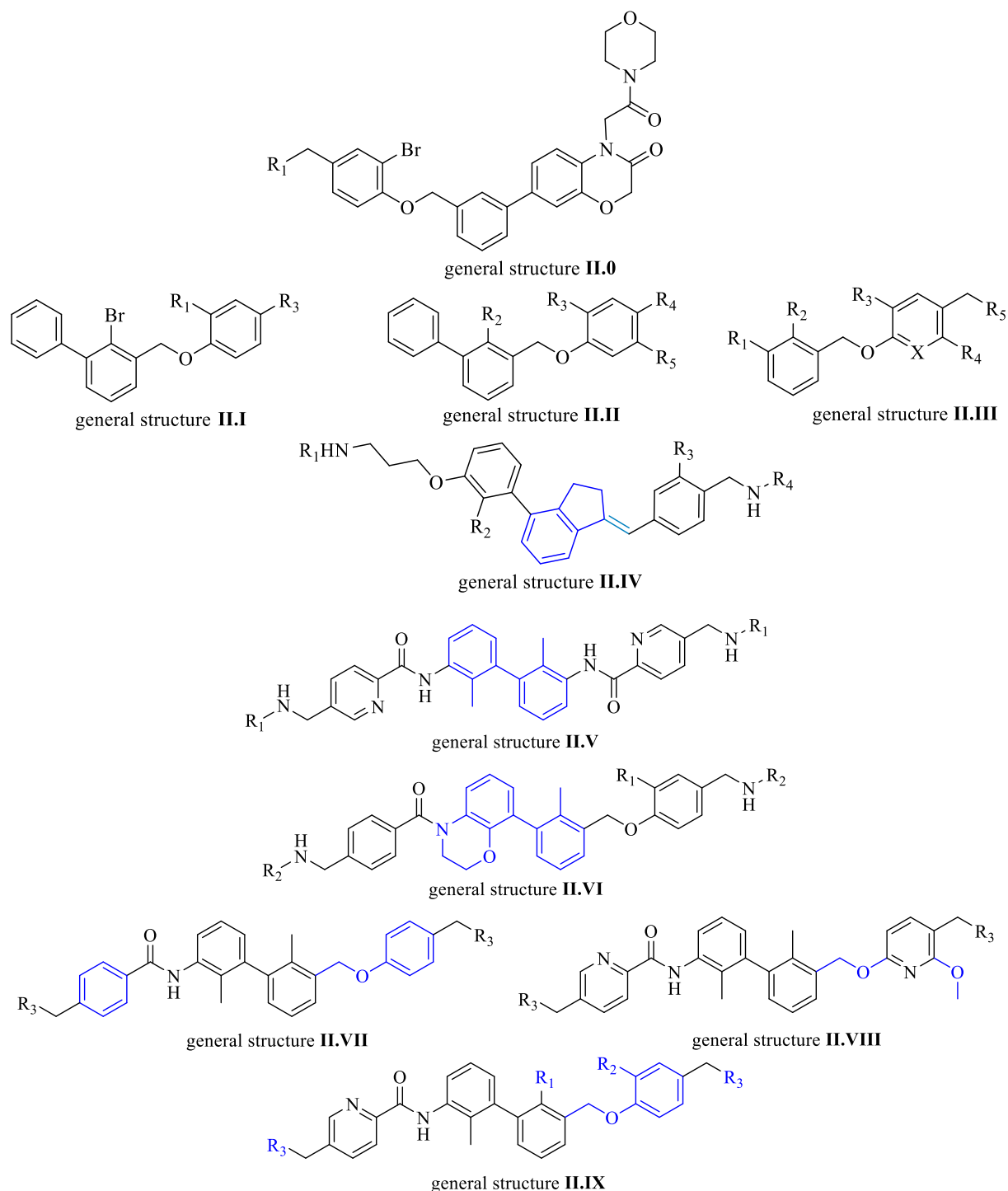


Figure 29. The plan of performed research with visualisation of the general structures of prepared groups of PD-L1 inhibitors.

Firstly, 2H-benzo[b][1,4]oxazin-3(4H)-one scaffold (general structure **II.0**) derivative was prepared. Secondly, a wide range of biphenyl-based small molecular antagonists were obtained (general structure **II.I-III**) as 2-bromo-1,1'-biphenyl, 1,1':2', 1''-terphenyl, 2-fluoro-1,1'-biphenyl, 2-chloro-1,1'-biphenyl, 2-iodo-1,1'-biphenyl derived compounds. Afterwards, to

improve the compounds' potency the attempt to synthesized elongated types of inhibitors was undertaken. Herein, the synthesis of 2,3-dihydro-1H-indene, 2,2'-dimethyl-1,1'-biphenyl, 2-fluoro-2'-methyl-1,1'-biphenyl, and 3,4-dihydro-2H-benzo[b][1,4]oxazine based molecules was described and potential PD-L1 inhibitors as derivatives of General Structures **II.IV-IX** were obtained.

## 2.1. 2H-benzo[b][1,4]oxazin-3(4H)-one's Derivatives as Potential PD-1/PD-L1 Immunomodulators

### 2.1.1. 2 Synthesis of 2H-benzo[b][1,4]oxazin-3(4H)-one's Derivative

The synthetic route shown in Figure 30 was followed to obtain the final compound based on the 2H-benzo[b][1,4]oxazin-3(4H)-one scaffold.

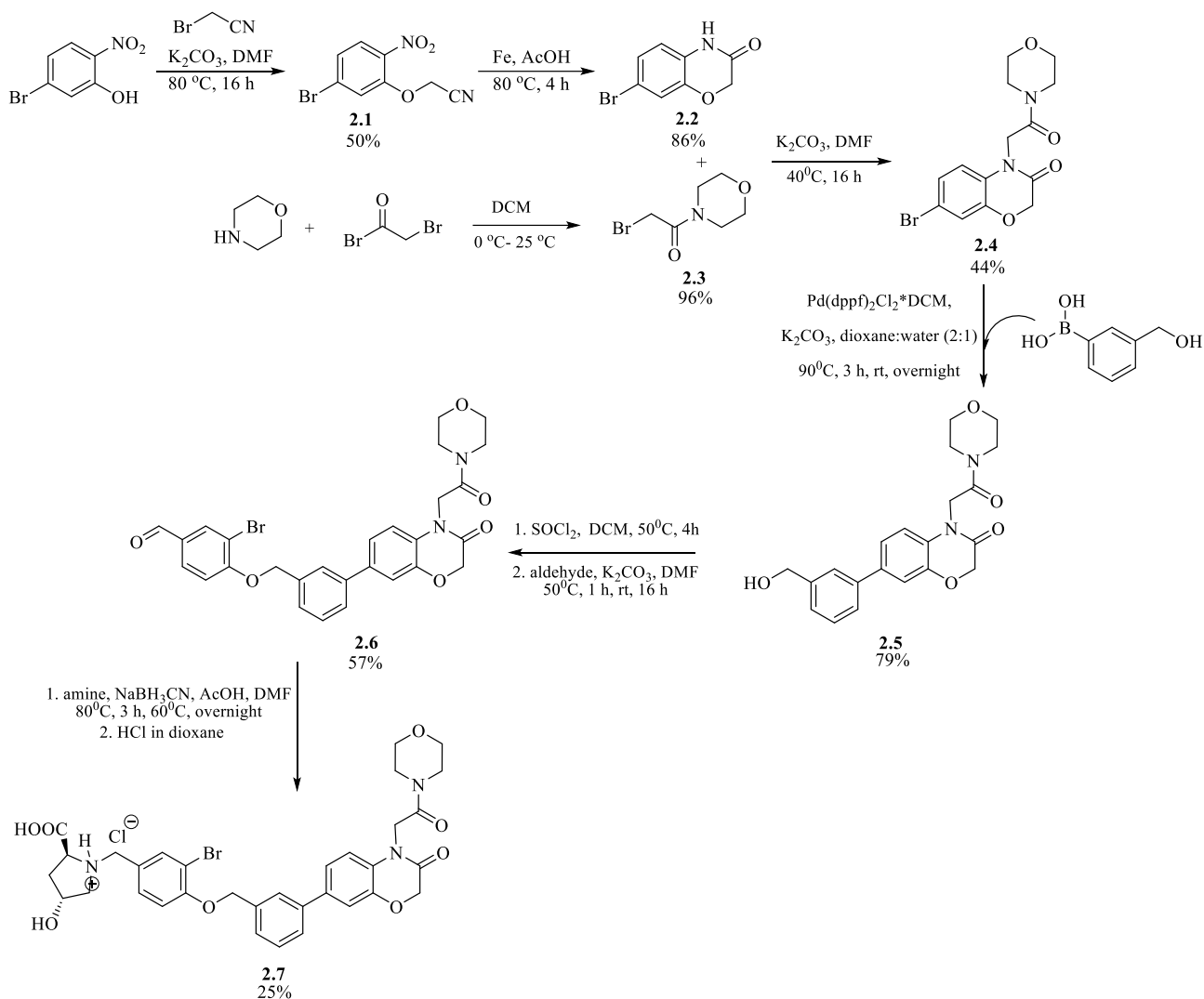


Figure 30. Synthetic route of 2H-benzo[b][1,4]oxazin-3(4H)-one's based inhibitors.

The synthetic route was started with the preparation of 7-bromo-2H-benzo[b][1,4]oxazin-3(4H)-one (**2.2**). In this case, 5-bromo-2-nitrophenol was subjected to nucleophilic substitution with bromoacetonitrile under basic conditions. Subsequently, isolated **2.1** was subjected to conditions including iron and acetic acid, which allowed reductive cyclization and ring closure of the 2H-benzo[b][1,4]oxazin-3(4H)-one (Ramesh *et al.*, 2011). In parallel, an alkylating agent (**2.3**) was prepared. Commercially available morpholine and 2-bromoacetyl bromide were



mixed to obtain 2-bromo-1-morpholinoethan-1-one as **2.3**. This product was then used as a substrate in the reaction with 7-bromo-2H-benzo[b][1,4]oxazin-3(4H)-one (**2.2**) to form the N-alkylated molecule **2.4**.

To further improve the structure of the potential inhibitor, the Suzuki cross-coupling reaction was applied. Organometallic cross-coupling reactions were found to be one of the most useful tools for C-C bond formation. Among these methods, Suzuki cross-coupling is a commonly used strategy. The reaction was first published in 1979 by Akira Suzuki, who was awarded the Noble Prize in 2010 for his discovery (Miyaura *et al.*, 1979a). In his work, he proposed the use of a palladium catalyst to promote the coupling between an aryl or vinyl boronic acid and an aryl or vinyl halide (Miyaura *et al.*, 1979a, Miyaura *et al.*, 1979b, Miyaura *et al.*, 1995). The mechanism of the discussed reaction is shown in Figure 31. The preliminary step in the Suzuki cross-coupling is the generation of Pd(0) species from Pd (I). This form of palladium is active, and in the presence of vinyl or aryl halide (A), it can participate in oxidative addition, which is the rate-determining step of the entire reaction. Oxidative addition involves the oxidation of palladium (0) to palladium (II) during the formation of organometallic intermediate (II). In the next step, a double displacement reaction between the organopalladium derivative and base takes place, yielding an intermediate (III). Subsequently, (III) participates in the transmetalation step with the formation of a more nucleophilic boronate complex (IV) from boronic compound (B) (Smith *et al.*, 1994). As a result, a transient organopalladium derivative (V) is formed. The final step of the catalytic cycle involves reductive elimination. Bulky substituents of palladium ligands enhance the elimination step and promote the formation of the desired product with the newly formed C-C bond. At the same time, the palladium catalyst is restored, allowing a new catalytic cycle to begin. The main role in the discussed reaction is played by the presence of the base. Besides taking part in a double displacement reaction (from II to III), it generates Lewis acid (IV) for the transmetalation step and promotes reductive elimination by reaction with palladium complex (Amatore *et al.*, 2011). Discussing the superiority of Suzuki coupling over the other organometallic reactions, Suzuki's substrates - boron derivatives - are less toxic and more available in comparison to organozinc or organotin compounds.

Moreover, mild conditions and a relatively wide variety of reagents that can be used in this reaction cause its wide applications in performed work and a special role in the preparation of **2.5** fragment.

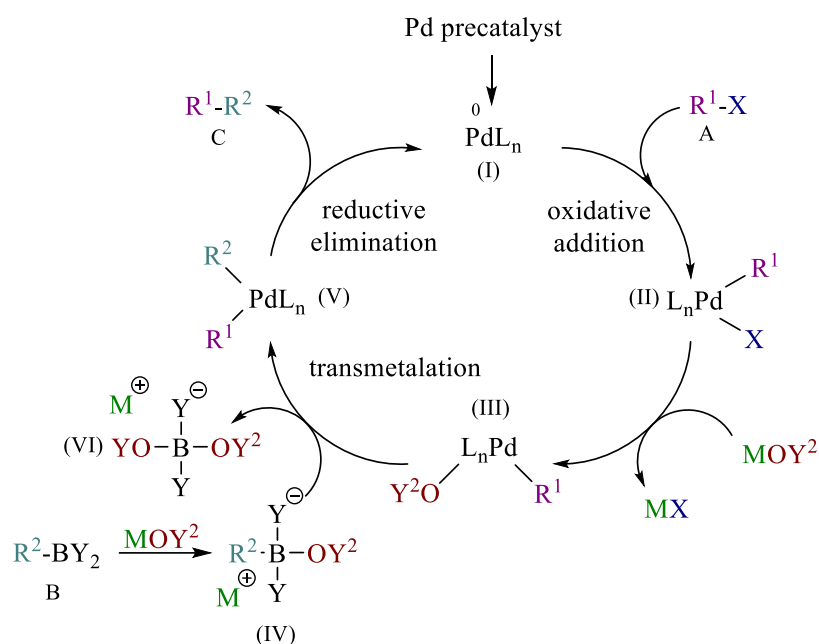


Figure 31. The mechanism of Suzuki cross-coupling, where (A)-vinyl/aryl halide, (B)-boronic compound, (C)-desired product, (I)-active palladium catalyst, (II)-organopalladium intermediate, (III)-intermediate after double displacement reaction, (IV)-boronate complex, (V)-transient organopalladium derivative.

The next step of the presented synthetic route (Figure 30) is the Williamson etherification carried out on the prepared form **2.5** benzylic chloride. This reaction is a useful way to prepare phenyl-benzyl ethers and proceeds according to the S<sub>N</sub>2 mechanism. The reaction conditions include the use of base, which is essential for the formation of alkoxyl anion. The phenoxyl anion formed in the reaction presents the increased nucleophilicity of the oxygen atom, thus providing the nucleophilic attack on the positively charged carbon atom of the benzylic halide (Williamson, 1850). Consequently, the conditions applied lead to the isolation of *O*-alkylated **2.6**.

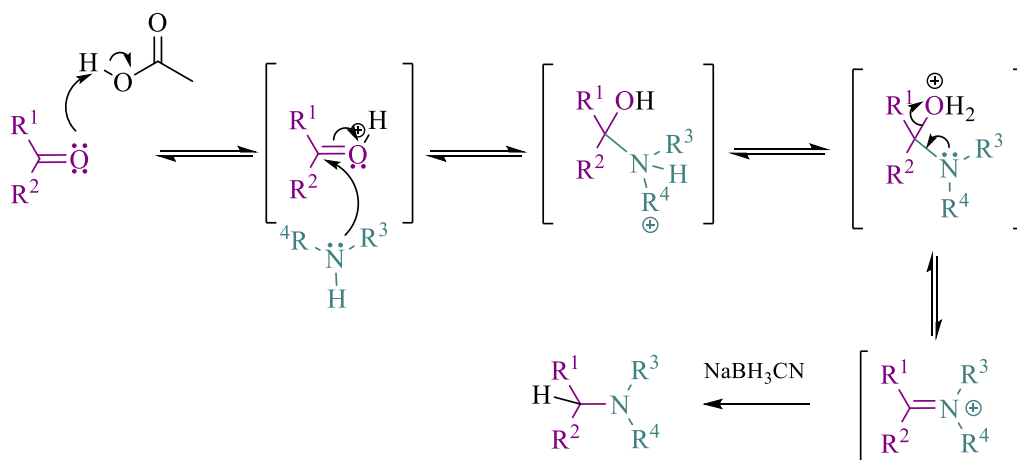


Figure 32. Reductive amination-condensation of carbonyl compound and amine via iminium ion as the intermediate – mechanism.

The final step of the synthetic route shown in Figure 30 involves the conversion of **2.6** to **2.7** via reductive amination. The latter is a versatile strategy to create a C-N bond and can be used to attach a variety of different alkyl groups to an amine. In the research conducted, this reaction was studied as a powerful tool to convert the carbonyl group to the corresponding amine (Figure 32). A more detailed look at the discussed process, reveals the crucial role of catalytic amounts of acetic acid. The latter, protonates oxygen from the carbonyl group, thus increasing the electrophilicity of carbon atom from carbonyl moiety. However, too much acidic conditions might not be preferred because of the possible protonation of amine and its conversion to non-nucleophilic ammonium salt. Therefore, in slightly acidic conditions, the more electrophilic carbonyl group is formed, each attacked by lone electron pair of nitrogen atom from an amine compound. A tetrahedral hemiaminal intermediate is formed, which undergoes proton transfer and water elimination according to alkylimino-de-oxo-bisubstitution. As a result, an imine ion (or in the case of a secondary amine, an iminium ion) is formed. The *in situ* reduction of the imine allows the isolation of the corresponding amine as a product of reductive amination. Sodium cyanoborohydride ( $\text{NaBH}_3\text{CN}$ ) and sodium triacetoxyborohydride ( $\text{NaBH}(\text{OCOCH}_3)_3$ ) are commonly used in this case because of their stability in mildly acidic conditions (Baxter *et al.*, 2004, Ahmed *et al.*, 1996). The use of such reductants also avoids side reactions and enhances the selectivity of the reaction. Generated iminium ion reacts with reductant much more readily than carbonyl compound, thus providing amine rather than alcohol as a product. The compound obtained after reductive amination was transformed into corresponding hydrochloric salt, which allowed isolation of **2.7** as the final product of carried synthetic route.

### 2.1.2. Activity Evaluation of 2H-benzo[b][1,4]oxazin-3(4H)-one Derivatives

The biochemical activity of the final compound – **2.7** - and its intermediates – **2.4**, **2.5**, **2.6** - for PD-1/PD-L1 complex dissociation was evaluated. The interaction of the obtained compounds with PD-L1 protein was preliminarily tested by  $^1\text{H}$  NMR. The  $^1\text{H}$  NMR measurements of apo-PD-L1 and apo-PD-L1 with different 2H-benzo[b][1,4]oxazin-3(4H)-one's derivatives were performed and visualized in Figure 33. Compounds **2.4**, **2.5**, **2.6**, and **2.7** were measured with the ratio 1:10 protein: compound concentration. The  $^1\text{H}$  NMR spectra of the **2.8** – **STD4** compound (Kitel *et al.*, 2022), which has already been shown to bind to short apo-PD-L1, were used as a reference for the measurements. The binding of all molecules was confirmed by broadening of NMR signals after the addition of an inhibitor to apo-PD-L1. The

observed broadening is the effect of ligand-induced interaction with the protein, although it is evident that the proposed compounds are only weak binders.

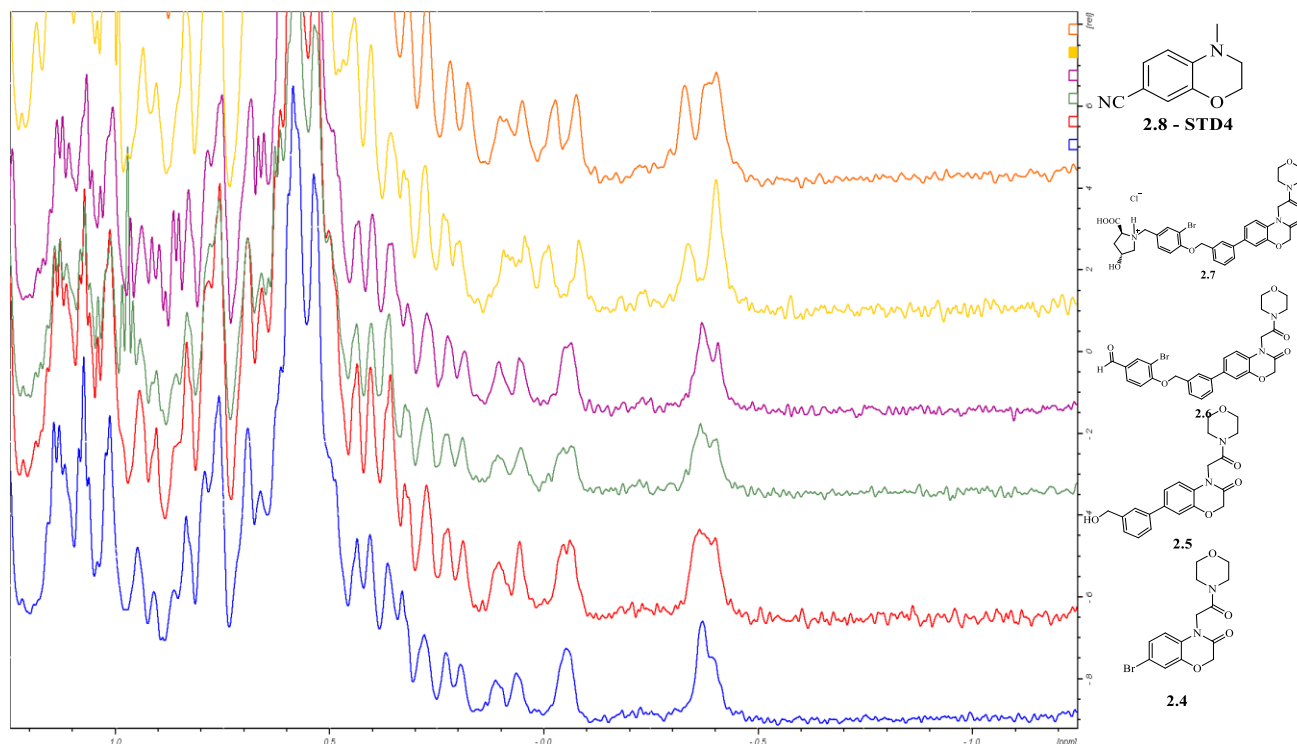


Figure 33. <sup>1</sup>H NMR spectra of apo-PD-L1 protein (blue line) and apo-PD-L1 protein with different 2H-benzo[b][1,4]oxazin-3(4H)-one's derivatives (red line – **2.4** measured at 1:10, protein: compound concentration, green line – **2.5** measured at 1:10, protein: compound concentration, violet line – **2.6** measured at 1:10, protein: compound concentration, yellow line – **2.7** measured at 1:10, protein: compound concentration, orange line – **2.8 - STD4** measured at 1:5, protein: compound concentration).

To confirm and quantify the results obtained, a homogeneous time-resolved fluorescence (HTRF) assay was performed. This technique (Degorce *et al.*, 2009) utilizes the Fluorescence Resonance Energy Transfer (FRET) phenomenon and is a relatively simple and rapid method for monitoring the PD-1/PD-L1 interaction. The detection of PD-1/PD-L1 interaction can be observed due to the presence of HTRF donor - anti-Tag1-Europium and HTRF acceptor - anti-Tag2-XL665. When PD-1 and PD-L1 bind, the HTRF donor and HTRF acceptor are close enough to trigger fluorescence energy transfer (FRET) from the excited donor to the acceptor. Consequently, this energy transfer results in specific emission of the HTRF acceptor at a wavelength of 665 nm, which is proportional to the extent of PD-1/PD-L1 interaction. Therefore, PD-L1 antagonists promote the reduction of HTRF signal by blocking PD-1/PD-L1 interaction.

Two of 2H-benzo[b][1,4]oxazin-3(4H)-one's derivatives with relatively good solubility were subjected to HTRF assay to evaluate their affinity toward PD-1/PD-L1 immune complex<sup>1</sup> (Table 2).

Table 2. Results of HTRF assay carried out for 2H-benzo[b][1,4]oxazin-3(4H)-one's derivatives

<b>Compound name</b>	<b>The presentage of undissociated PD-1/PD-L1 complex [%]</b>	<b>The concentration of the compound</b>
<b>2.5</b>	36.1	50 $\mu$ M
<b>2.7</b>	26.5	50 $\mu$ M

The results summarized in Table 2 show that after the addition of **2.5** and **2.7**, 36.1% and 26.5% of the PD-1/PD-L1 complex remained undissociated, respectively. The HTRF results confirmed that the 2H-benzo[b][1,4]oxazin-3(4H)-one derivatives belong to the group of 'weak PD-L1 binders'. Therefore, the modifications of the proposed scaffold are necessary for the evaluation of inhibitor activity.

<sup>1</sup> Presented in this thesis HTRF analysis were performed by dr Jacek Plewka and dr Ewa Surmiak from Bioorganic and Medicinal Chemistry Group, Faculty of Chemistry, Jagiellonian University, Krakow.

## 2.2. Synthesis of Biphenyl Based Small-molecule Inhibitors of the PD-1/PD-L1 Immune Checkpoint

### 2.2.1. Identification of the Short Fragments That Bind to PD-L1

To enhance the activity of the obtained PD-1/PD-L antagonists, substituent rearrangement within the biphenyl scaffold was proposed. *In silico* screening of designed short fragments was performed by AutoDock Vina integrated with PyRx software (Trott *et al.*, 2009)<sup>2</sup>. The screening involved the use of the dimeric structure of PD-L1 with BMS-1166 (PDB ID: 5NIX) to which short fragments were docked for structure-activity relationship (SAR) elucidation. *In silico* screening clearly showed a preference for hydrophobic substituents over hydrophilic ones. Therefore, the introduction of nitril group or hydroxyl group to the biphenyl scaffold negatively influences its binding affinity. Conversely, decoration of the biphenyl scaffold with halides can lead to a decrease in binding affinities down to -9.3 kcal/mol for compounds **3.1** and **3.7** (Figure 34). Although it is easy to see that the enlargement of the structure to 2,3-dihydrobenzo[b][1,4]dioxine (**3.3**, **3.6**) or 1,1':2',1''-terphenyl (**3.2**) derivatives is not preferred according to *in silico* studies (Konieczny *et al.*, 2020).

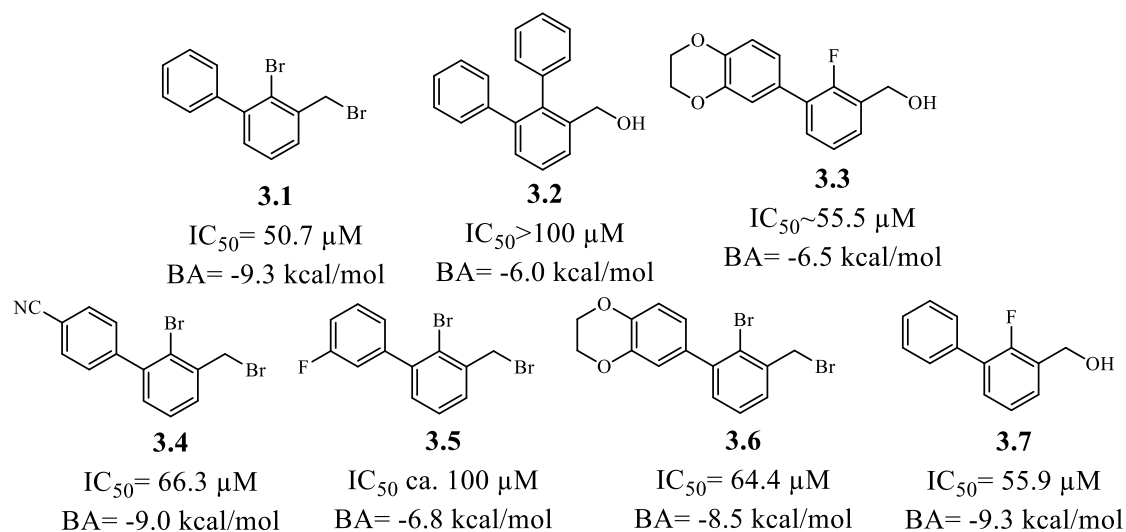


Figure 34. The synthesised short, biphenyl based fragments with their binding affinities (BA) and IC<sub>50</sub> values (Konieczny *et al.*, 2020).

Results obtained by molecular modeling encouraged to obtain synthetically the above mentioned compounds. To prepare compounds **3.1**, **3.4**, **3.5** and **3.6** 3-step synthetic pathway was carried out. The starting material - 2-bromo-3-methylaniline - was subjected to Sandmeyer reaction to exchange amine and introduce iodine into aromatic ring (**3.1.1.1**, A, Table 3). Since

<sup>2</sup> *In silico* screening was performed by dr Jacek Plewka from Bioorganic and Medicinal Chemistry Group, Faculty of Chemistry, Jagiellonian University, Krakow.

iodine is a better leaving group, its introduction allowed to selectively perform Suzuki coupling in the presence of bromide substituent (B, Table 3). Consequently, **3.1.1**, **3.4.1**, **3.5.1**, **3.6.1** were isolated. The final step in the preparation of short biphenyl fragments was radical bromination with NBS and benzoyl peroxide (C, Table 3), which led to the isolation of **3.1**, **3.4**, **3.5**, **3.6**. Reaction conditions and yields are summarized in Table 3.

Table 3. Preparation of 2-bromo-3-(bromomethyl)-1,1'-biphenyl scaffold derivatives.

Name	R <sub>1</sub>	Yield	Name	Yield
<b>3.1.1</b>		65%	<b>3.1</b>	59%
<b>3.4.1</b>		68%	<b>3.4</b>	43%
<b>3.5.1</b>		91%	<b>3.5</b>	68%
<b>3.6.1</b>		64%	<b>3.6</b>	41%

Reagents and conditions: (A) H<sub>2</sub>SO<sub>4</sub>, KI, NaNO<sub>2</sub>, water, 0 °C, 3 h, 68% for **3.1.1.1** (B) phenylboronic acid (**3.1.1**)/ (4-cyanophenyl)boronic acid (**3.4.1**)/ (3-fluorophenyl)boronic acid (**3.5.1**)/ (2,3-dihydrobenzo[b][1,4]dioxin-6-yl)boronic acid (**3.6.1**) Pd(dppf)Cl<sub>2</sub>·DCM, K<sub>2</sub>CO<sub>3</sub>, 1,4-dioxane/water, 80 °C, 4 h, rt, overnight, 65% (**3.1.1**)/ 68% (**3.4.1**)/ 91% (**3.5.1**) /64% (**3.6.1**) (C) NBS, benzoyl peroxide, CCl<sub>4</sub>, 80 °C, 5 h, 59% (**3.1**)/ 43% (**3.4**)/ 68% (**3.5**)/ 41% (**3.6**).

To prepare fragments **3.2**, **3.3** another synthetic manner was used. Respective alcohols were directly subjected to Suzuki cross-coupling. Applied conditions and reaction yields are correlated in the Table 4.

Table 4. Preparation of [1,1':2',1''-terphenyl]-3'-ylmethanol (**3.2**), (3-(2,3-dihydrobenzo[b][1,4]dioxin-6-yl)-2-fluorophenyl)methanol (**3.3**) and (2-fluoro-[1,1'-biphenyl]-3-yl)methanol (**3.7**) fragments.

Name	R <sub>0</sub>	R <sub>1</sub>	R <sub>2</sub>	Yield
<b>3.2</b>	-Br			82%
<b>3.3</b>	-F	-F		75%
<b>3.7</b>	-F	-F		97%

Reagents and conditions (A): phenylboronic acid (**3.2**, **3.7**)/ (2,3-dihydrobenzo[b][1,4]dioxin-6-yl)boronic acid (**3.3**), Pd(dppf)Cl<sub>2</sub>·DCM, K<sub>2</sub>CO<sub>3</sub>, 1,4-dioxane/water, 80 °C, 3 h, rt, overnight, 82% (**3.2**) 75% (**3.7**)/ 97% (**3.3**).

To verify the *in silico* studies were consistent with the actual biochemical activity of prepared compounds, **3.1-3.7** were subjected to HTRF assay. The half maximal inhibitory concentration (IC<sub>50</sub>) values determined for compounds **3.1-3.7** were in micromolar range. The most prominent compounds – **3.1** and **3.7**– were found to possess IC<sub>50</sub> values as 51 and 56 μM, respectively. The obtained results are relatively good, since the short fragment shows tolerable solubility in aqueous media. The biochemical validation of the *in silico* studies proved their accuracy and allowed the selection **3.1** and **3.7** as the best candidates for further development.

Although HTRF is a rapid and convenient assay widely used in *in vitro* activity evaluation, the approach is associated with some possible inconveniences such as autofluorescence of the compound and aggregation possibility. Therefore, an additional method - w-AIDA NMR assay - was used to check the affinity of the proposed short fragments towards the target. The w-AIDA NMR is a weak antagonist dissociation assay in which the specific N66A mutation of PD-1 is responsible for the decrease in binding affinity to the PD-L1 protein within the complex (Musielak *et al.*, 2020). However, the interface of PD-L1 involved in the binding remains unaltered, regardless of the introduction of PD-1 mutations. The w-AIDA NMR competition assay allows the indication of "short fragments" with promising potency as good candidates for further evaluation. Analyzing the aliphatic part of the 1D <sup>1</sup>H NMR spectra



of  $^{66}\text{N}$ -labeled PD-1 (blue line) and PD-L1 (red line), we can observe that the spectra appear more flattened (marked gray) after N66-PD-1/PD-L1 complex formation (green line). In the situation where weak binders – **3.1** (purple spectra) or **3.7** (yellow spectra) - are added to the N66-PD-1/PD-L1 complex, we can observe the restoration of the characteristic PD-1 peaks caused by the dissociation of the protein complex. The fact that **3.1** and **3.7** are able to target the PD-1/PD-L1 immune checkpoint is also well visible in 2D  $^1\text{H}$ - $^{15}\text{N}$  HSQC NMR spectra. Figure 35 presents respectively the spectrum of  $^{15}\text{N}$ -labeled N66A-PD-1 (A) and the spectrum of the N66A-PD-1/PD-L1 complex with  $^{15}\text{N}$ -labeled PD-1 (B). The red boxes (B) highlight the changes in peak pattern associated with complex formation. However, after the addition of **3.1** or **3.7** (C and D), we can observe the restoration of the characteristic for N66-PD-1 peak pattern, which proves the ability of small molecule for PD-1/PD-L1 complex dissociation (Konieczny *et al.*, 2020).

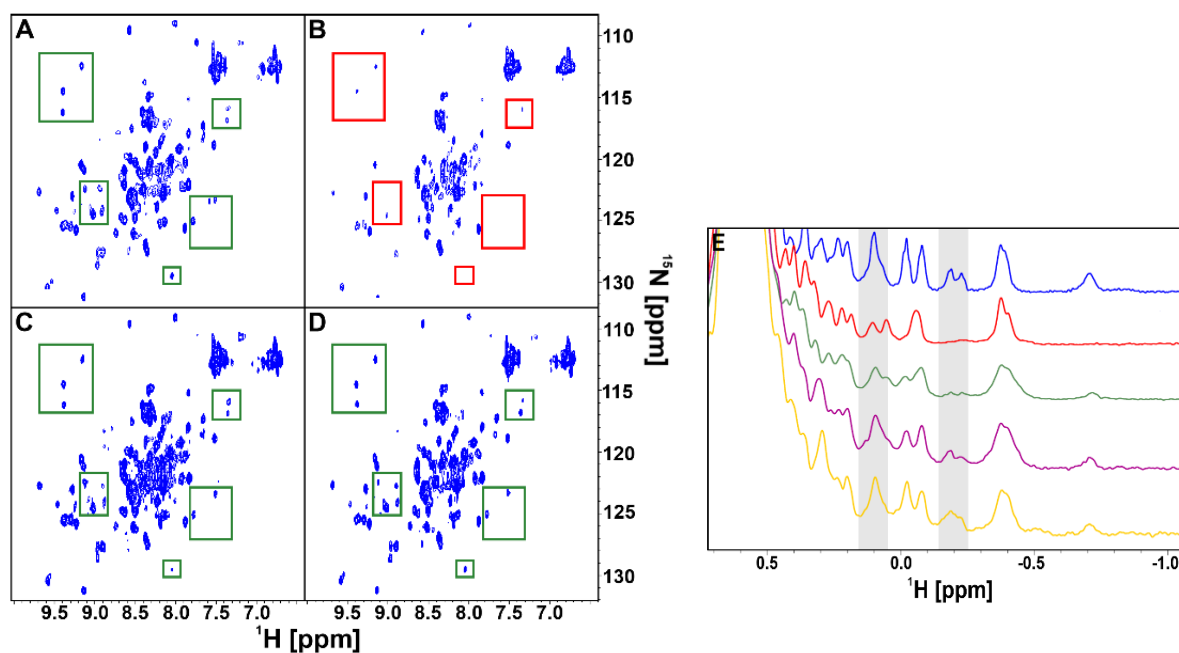


Figure 35. w-AIDA- $^1\text{H}$ - $^{15}\text{N}$  NMR HSQC (A-D) and 1D NMR spectra E. A) spectrum of N66A-PD-1 with marked characteristic peak pattern B) spectrum of N66A labelled PD-1/PD-L1 complex C) N66A-PD-1/PD-L1 complex + **3.1** – restoration of spectrum A after addition of **3.1** D) N66A-PD-1/PD-L1 complex + **3.7** – restoration of spectrum A after addition of **3.7**; E) 1D NMR spectrum of N66A-PD-1 (blue line), PD-L1 spectrum (red line), flattened spectrum of N66A-PD-1/PD-L1 complex (green line), restoration of spectrum A after addition of **3.1** to N66A-PD-1/PD-L1 complex (purple line), restoration of spectrum A after addition of **3.7** to N66A-PD-1/PD-L1 complex (yellow line) (Konieczny *et al.*, 2020).

## 2.2.2. Development of the 2-Bromo-1,1'-Biphenyl-Based Antagonists of PD-L1 – Synthesis and Activity Determination

Following the demonstration of *in vitro* activity of the 2-bromo-1,1'-biphenyl fragment, further development of inhibitors was undertaken. Another advantageous extension was the addition of a third aromatic ring *via* an ether linker. Therefore, 2-bromo-3-(bromomethyl)-1,1'-biphenyl (**3.1**) was subjected to Williamson etherification with various *p*-hydroxybenzaldehyde derivatives/methyl-4-hydroxybenzoate to form molecules **3.8-3.12**. Subsequently, the aldehydes (**3.8-3.11**) obtained were subjected to the NaBH<sub>3</sub>CN-mediated reductive amination to give the final compounds (**3.13-3.17**). In the case of ester (**3.12**), the final compound (**3.18**) was isolated after introduction of amine component in the presence of DBU. The obtained compounds were subjected to HTRF assay to evaluate their ability for PD-1 displacement from PD-1/PD-L1 complex. The structures of the synthesized compounds as general structure **II.I** derivatives with their IC<sub>50</sub> values were summarized in Table 5.

Table 5. Synthetic Pathway of Preparation of compounds consistent with general structure **II.I** as 2-bromo-1,1'-biphenyl Derivatives (Konieczny et al., 2020).

A				B			
Name	R <sub>1</sub>	R <sub>2</sub>	IC <sub>50</sub> [nM]	Name	R <sub>1</sub>	R <sub>3</sub>	IC <sub>50</sub> [nM]
<b>3.8</b>	-H		~50000	<b>3.13</b>	-Br		12.2 ±0.2
<b>3.9</b>	-Br		~50000	<b>3.14</b>	-H		522.0 ±0.5
<b>3.10</b>	-Me		~50000	<b>3.15</b>	-Me		175.1 ±13.3
<b>3.11</b>	-OMe		>100000	<b>3.16</b>	-OMe		203.9 ±6.4
<b>3.12<sup>a</sup></b>	-Br		28 600 ±500	<b>3.17</b>	-Br		15.0 ±0.2
				<b>3.18<sup>a</sup></b>	-Br		13200 ±150

Reagents and conditions: (A) substituted 4-hydroxybenzaldehyde, potassium carbonate, DMF, rt, overnight (43% yield for **3.8**, 39% yield for **3.9**, 38% yield for **3.10**, 52% yield for **3.11**) (B) NHR, sodium cyanoborohydride, acetic acid, DMF, rt, overnight (53% yield for **3.13**, 65% yield for **3.14**, 56% yield for **3.15**, 72% yield for **3.16**, 51% yield for **3.17**). <sup>a</sup>(A) methyl 3-bromo-4-hydroxybenzoate, potassium carbonate, DMF, rt, overnight (45% yield for **3.12**); (B) NHR, 1,8-Diazabicyclo[5.4.0]undec-7-en (25% yield for **3.18**).

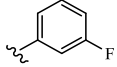
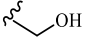
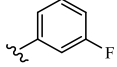
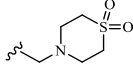
Analysing the obtained results, it is not difficult to see the correlation between solubility of a compound and its biochemical activity. If we compare the IC<sub>50</sub> values of aldehydes and their corresponding final compounds - equipped with a solubilizing group - we can observe the significant decrease of the maximal half inhibitory concentrations. The most prominent example is aldehyde **3.9** (IC<sub>50</sub> = 50000 nM), which is transformed into final compound **3.17** (IC<sub>50</sub> = 15 nM), presenting more than 3000 better activity in HTRF assay.

The satisfactory results obtained encouraged further development of PD-L1 antagonists based on **3.2-3.7** fragments. The synthesis of small molecule antagonists based on [1,1':2',1''-terphenyl]-3'-ylmethanol (**3.2**) and (3-(2,3-dihydrobenzo[b][1,4]dioxin-6-yl)-2-fluorophenyl)methanol (**3.3**) involved the conversion of the respective alcohols to the corresponding chlorides and the alkylation of deprotonated 3-bromo-4-hydroxybenzaldehyde under basic conditions. This resulted in the formation of 1,1':2',1''-terphenyl- and 6-(2-fluorophenyl)-2,3-dihydrobenzo[b][1,4]dioxine-based aldehydes (**3.21, 3.23**), which were subsequently subjected to sodium cyanoborohydride-mediated reductive amination to give **3.22** and **3.24**. Inhibitors constructed from **3.23-3.25** fragments were prepared using a similar method. Williamson etherification of deprotonated *p*-hydroxyaldehyde/*p*-hydroxyalcohol derivatives afforded the compounds (**3.19, 3.25, 3.27, 3.31**). Subsequently, the isolated aldehydes were subjected to NaBH<sub>3</sub>CN-mediated reductive amination to introduce different amine moieties, giving the final inhibitors (**3.20,3.26,3.28,3.29,3.30**). For the preparation of compound **3.32**, benzylic chloride was generated from (3-((2-bromo-[1,1'-biphenyl]-3-yl)methoxy)phenyl)methanol (**3.31**) and S<sub>N</sub>2 reaction was performed with thiomorpholine. All obtained compounds as general structure **II.II** derivatives and their IC<sub>50</sub> values are summarized in Table 6.

Analyses of the obtained compounds lead to the conclusion that besides -Br, -F is also considered as a promising candidate for the R<sub>2</sub> substituent. On the contrary, -Ph was found to be unsuitable in this position. Also, introduction of 4-cyanophenyl moiety in R<sub>1</sub> position instead of phenyl ring is not beneficial. Moreover, it was found that, enhancement of the molecule with 2,3-dihydrobenzo[b][1,4]dioxine provided different, depending on single molecule influence on enhancement of its properties (see examples **3.20, 3.22**). Interestingly, after studying the results collected in Table 5 and in Table 6, -Br was found to be the best option for R<sub>3</sub> substituent. Considering the best amine moiety (R<sub>4</sub>), the attachment of L-pipecolinic acid most positively influences the molecules affinity for PD-1/PD-L1 targeting in HTRF assay.

Table 6. Synthetic Pathway of Preparation of 2-bromo-1,1'-biphenyl compounds as 6-(2-bromo-3-(bromomethyl)phenyl)-2,3-dihydrobenzo[b][1,4]dioxine (**3.6**), 1,1':2,1''-terphenyl (**3.2**), 6-(3-(bromomethyl)-2-fluorophenyl)-2,3-dihydrobenzo[b][1,4]dioxine (**3.3**), [1,1':2,1''-terphenyl]-3'-ylmethanol, 2-bromo-3-(bromomethyl)-3'-fluoro-1,1'-biphenyl (**3.5**) and 2'-bromo-3'-(bromomethyl)-[1,1'-biphenyl]-4-carbonitrile (**3.4**) derivatives (**3.19-3.32**) (Konieczny et al., 2020).

	<b>R<sub>1</sub></b>	<b>R<sub>2</sub></b>	<b>R<sub>3</sub></b>	<b>R<sub>4</sub></b>	<b>R<sub>5</sub></b>	<b>IC<sub>50</sub> [nM]</b>
<b>3.19</b>		-Br	-Br		-H	35400±300
<b>3.20</b>		-Br	-Br		-H	401.0±2.1
<b>3.21</b>		-F	-Br		-H	>100000
<b>3.22</b>		-F	-Br		-H	22.7±1.0
<b>3.23</b>	-Ph	-Ph	-Br		-H	>100000
<b>3.24</b>	-Ph	-Ph	-Br		-H	29400±450
<b>3.25</b>		-Br	-Br		-H	>100000
<b>3.26</b>		-Br	-Br		-H	5114±58
<b>3.27</b>		-Br	-Br		-H	~55000
<b>3.28</b>		-Br	-Br		-H	65.3±0.7
<b>3.29</b>		-Br	-Br		-H	106.8±20.8
<b>3.30</b>		-Br	-Br		-H	4238±86

<b>3.31</b>		-Br	-H	-H		>100000
<b>3.32</b>		-Br	-H	-H		22300±230

Reagents and conditions: (A) for compounds **3.4-3.6** where X is -Br: derivatives of *p*-hydroxybenzaldehyde, potassium carbonate, DMF, rt, overnight (88% yield for **3.19**, 61% yield for **3.25**, 57% yield for **3.27**, 52% yield for **3.31**) for compounds **3.2**, **3.3** where X is -OH: 1. thionyl chloride, DCM, 40 °C 2. Derivatives of *p*-hydroxybenzaldehyde, potassium carbonate, DMF, rt, overnight (30% yield for **3.21**, 60% yield for **3.23**) (B) for compounds **3.19**, **3.21**, **3.23**, **3.25**, **3.27**: amine component, sodium cyanoborohydride, acetic acid, DMF, rt, overnight (43% yield for **3.20**, 61% yield for **3.22**, 37% yield for **3.24**, 26% yield for **3.26**, 44% yield for **3.28**, 67% yield for **3.29**, 33% yield for **3.30**) for compounds **3.31** 1. thionyl chloride, DCM, 40 °C 2. amine component, potassium carbonate, DMF, rt, overnight (29% yield for **3.32**).

Some of the compounds obtained were further investigated to determine their biochemical activity. Compound **3.17** was tested in competitive ELISA (Enzyme-linked Immunosorbent Assay) to determine its activity against hPD-L1 in comparison to **1.17 - BMS-1166** (strong PD-1/PD-L1 antagonist developed by Bristol-Meyer Squibb)<sup>3</sup>. The data obtained clearly showed the advantage of **3.17** over **1.17 - BMS-1166**, indicating **3.17** as stronger PD-L1 antagonist ( $1.47 \pm 0.05$  nM and  $28.04 \pm 0.36$  nM, respectively) (Konieczny, *et al*, 2020).

The compounds that showed promising activities in the HTRF assay were further evaluated in the PD-1/PD-L1 immune checkpoint blockade cell-based assay<sup>4</sup>. The co-cultured artificial antigen presenting cells (aAPCs) and Jurkat reporter T cells in the experiment provide the PD-1/PD-L1 interaction. Inhibitors capable of targeting the PD-1/PD-L1 interaction lead to TCR-mediated activation of Jurkat cells, as evidenced by an increase in luciferase activity. Thus, luciferase activity represents the level of stimulation of Jurkat T cells. According to the fitting of Hill's equation to the experimental data, durvalumab, a therapeutically applicable PD-L1 blocking antibody, unleashed TCR signalling with an EC<sub>50</sub> value of  $0.2 \pm 0.06$  nM. (Figure 36). Analysing results obtained, most of the compounds tested, as well as durvalumab, possess the ability to boost effector cell activation, but at much higher concentrations than the antibody. In the tests performed, the inhibitor **3.17** as the best of all the compounds. **3.17** was calculated to have the lowest EC<sub>50</sub> value of  $6.6 \mu\text{M} \pm 0.8$  M and the highest degree of Jurkat T cell activation (2.1-fold at 50 M compound concentration). (Figure 36). Promising results (EC<sub>50</sub> value of  $6.8 \pm 1.1 \mu\text{M}$ ) were also obtained for compound **3.13**, but due to its cytotoxicity above 10  $\mu\text{M}$  concentration, the maximal half inhibitory value was calculated from partial data. The

<sup>3</sup> ELISA test was performed by mgr Maja Myrcha from Recepton Sp. z o.o., Gdańsk Science and Technology Park

<sup>4</sup> Presented in this thesis cells based assays were performed by mgr Justyna Kocik-Król and dr hab. Łukasz Skalniak from Bioorganic and Medicinal Chemistry Group, Faculty of Chemistry, Jagiellonian University, Krakow.

other compounds tested were found to provide only low levels of TCR-inducible expression of luciferase activity, with EC<sub>50</sub> values above 40 μM.

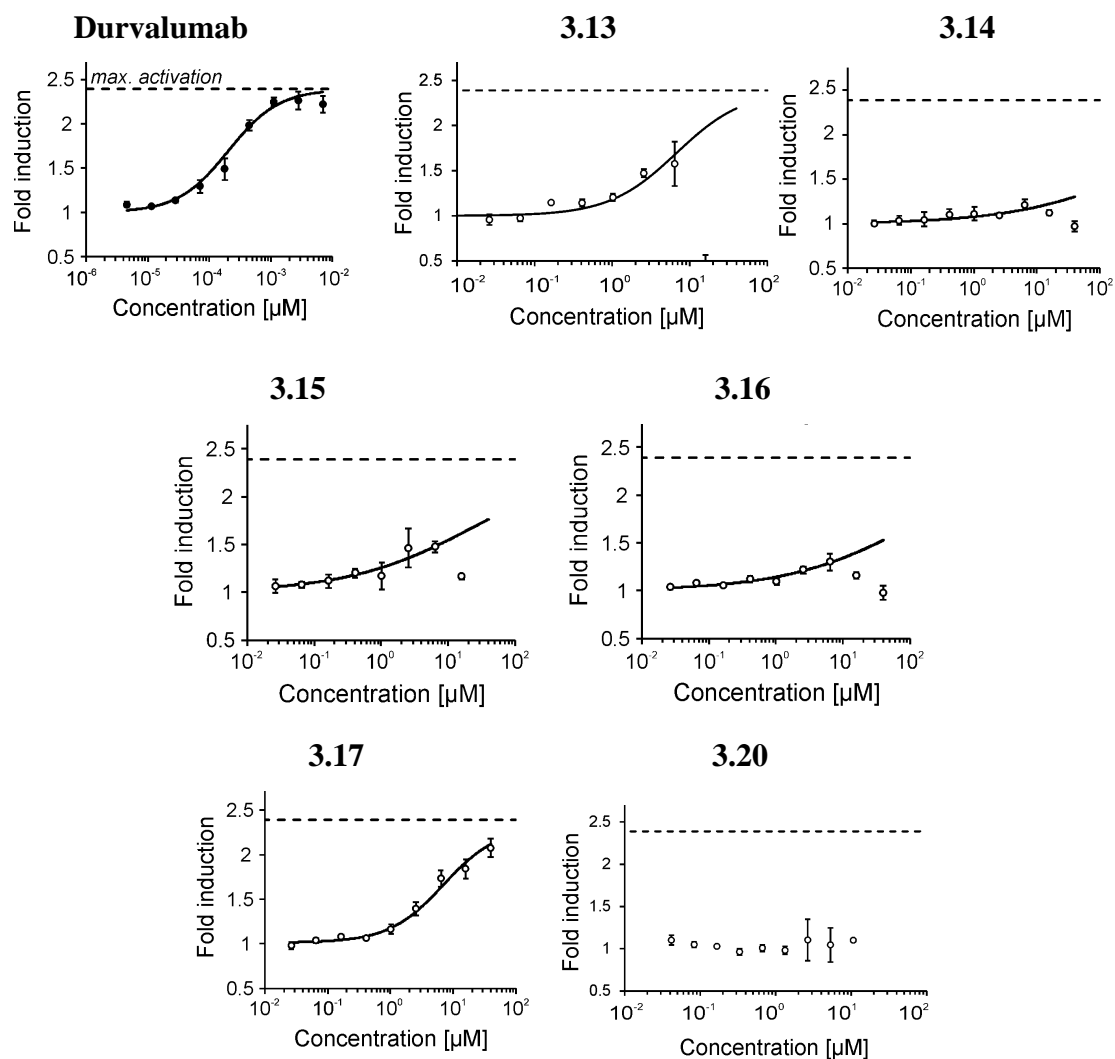


Figure 36. The profiles of PD-1/PD-L1 immune checkpoint blockade cell-based assay for compounds **3.13**, **3.14**, **3.15**, **3.16**, **3.17** and **3.20**. Activities of the compound are presented in correspondence to durvalumab-clinically relevant anti-PD-L1 antibody (Konieczny et al., 2020).

Additionally, the cytotoxic effect of the small molecules tested was determined in a cell-based assay for PD-1/PD-L1 immune checkpoint blockade. Jurkat PD-1 effector cells alone or in co-culture with CHO K-1 PD-L1 aAPCs were treated with increasing concentrations of the compounds. The most prominent compound **3.17** provided also satisfying results in the cell viability assay, being non-toxic up to a final concentration of 100 μM (Konieczny *et al.*, 2020). This is a much better outcome than for the compound **1.17 - BMS-1166** compound (Skalniak

*et al.*, 2017, Figure 2a), as **1.17 - BMS-1166** reduced cell viability by 50% at a concentration of 40  $\mu\text{M}$ , while other BMS compounds did so at even lower inhibitor concentrations.

### 2.2.3. Modeling the Interactions with Dimeric PD-L1

In addition, by docking the inhibitor to a dimeric PD-L1 using PyRx software, we were able to study the molecular interactions of the most potent compound (**3.17**) with PD-L1<sup>5</sup>. Protein-Ligand Interaction Profiler was then used to evaluate the binding profile (Figure 37) (Konieczny *et al.*, 2020).

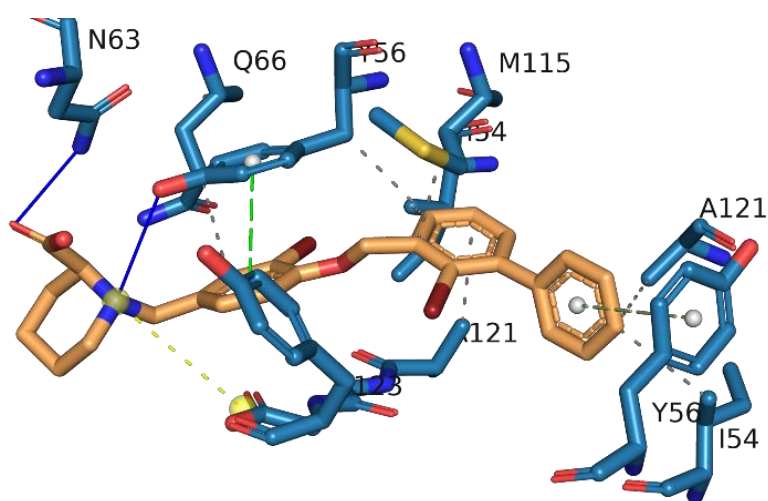


Figure 37. Visualisation of interactions between PD-L1 and compound **3.17**. Inhibitor was docked into dimeric PD-L1 (PDB ID: 5NIX). Detected interactions: hydrophobic interactions (grey dashed lines) with residues Ile54A Tyr56A and B, Gln66B, Met115B, Ala121B and Tyr123A,  $\pi$ -stacking (green dashed line) between distal phenyl ring within biphenyl scaffold and Tyr56A and between phenyl from phenoxymethyl with Tyr56B, hydrogen bonds (blue solid line) between Tyr56B hydroxyl group and tertiary amine in piperidine solubilizer and Asn63B amide nitrogen and oxygen from carboxylic group of solubilizer (Konieczny *et al.*, 2020).

The most important interactions observed are those within the biphenyl core. This fragment is responsible for anchoring the dimeric PD-L1 due to  $\pi$ - $\pi$  stacking with Tyr56A and an aromatic phenyl ring with Tyr56B. Hydrogen bonding between the OH group of Tyr56B and the N atom of the solubilizer and between the N atom of Asn63B and the O atom of the -COOH group of L-pipecolic acid also have a stabilizing effect on binding of the molecule. Analysing the docking profile, we can also distinguish the salt bridge formed between tertiary amine solubilizer and -COOH group of Asp122A. Furthermore, hydrophobic interactions of the compound with Tyr56A, Tyr56B, Gln66B, Ile54A, Met115B, Ala121A stabilize the whole complex.

<sup>5</sup> Molecular docking performer by dr Jacek Plewka from Bioorganic and Medicinal Chemistry Group, Faculty of Chemistry, Jagiellonian University, Krakow.

## 2.3. Preparation of 2-Substituted 1,1'-Biphenyl Derivatives

### 2.3.1. Optimisation of the 1,1'-Biphenyl Fragment

As a continuation of the promising results obtained for the group of 2-bromo-1,1'-biphenyl derivatives, another group of compounds derived from the biphenyl scaffold was obtained. The subject of further studies was to investigate how the replacement of the bromine from the 2-bromo-1,1'-biphenyl core with another halide of different size and electronegativity influences the activity of the compound. Moreover, the optimization of the biphenyl core also involved the preparation of 2-bromo-1,1'-biphenyl derived short fragments with introduced hydrophobic motif. All proposed fragments are shown in Figure 38.

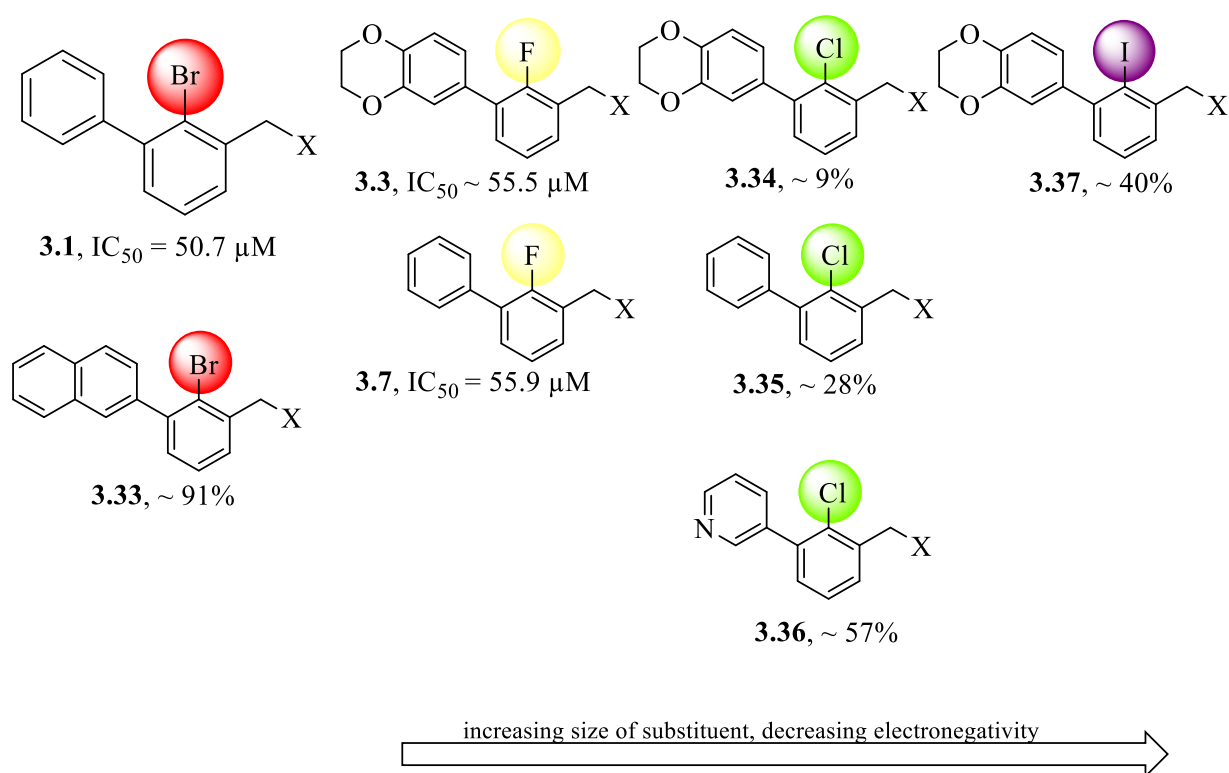


Figure 38. Modification on biphenyl core based short fragments and the affinity of the short fragments presented as  $IC_{50}$  values or as the percentage of dissociated PD-1/PD-L1 complex with  $50 \mu M$  concentration of the compound.

To identify the fragments that bind to PD-L1 with the satisfying affinity, the dissociation of PD-1/PD-L1 for **3.3**, **3.7**, **3.33-3.37** compounds was determined. The reference for obtained results was the affinity of 2-bromo-3-(bromomethyl)-1,1'-biphenyl (**3.1**), for which the  $IC_{50}$  value was calculated to be  $50.7 \mu M$ . This result corresponds to a dissociation of 53% of the present PD-1/PD-L1 complex in the presence of a  $5 \mu M$  concentration of fragment **3.1**. The data obtained for **3.3**, **3.7**, **3.34**, **3.35**, and **3.37** are shown in Figure 38. These results present



that the structural modifications on the biphenyl core based on the hit compound led to a moderate improvement of the activity, but in general, the affinity of the fragments is in the same range. The best results were obtained for 2-chloro-1,1'-biphenyl derivatives (**3.34**, **3.35**). Taking into account the data obtained for (2-chloro-3-(pyridin-3-yl)phenyl)methanol (**3.36**) (dissociation of 43% of the present PD-1/PD-L1 complex) and 2-(2-bromo-3-(bromomethyl)phenyl)naphthalene (**3.33**) (dissociation of around 9% of the present PD-1/PD-L1 complex), they do not seem advantageous. All in all, building final small molecules on short, hydrophobic biphenyl fragments is constructive and favorable for their affinity to the hydrophobic cleft of the target. Based on the promising results of the HTRF assay, we decided to use some of the prepared short fragments as starting points for further synthesis of final PD-1/PD-L1 inhibitors.

### 2.3.2. Synthesis of the PD-1/PD-L1 Inhibitors 3.46-3.60

Figure 39 comprises the synthetic route to obtain compounds **3.44-3.58** as final structures. The strategy of short biphenyl-based fragments (**3.3**, **3.7**, **3.34**, **3.35**, **3.37**) preparation is described in Sections 4.2.2 and 4.2.3. The series of final inhibitors was constructed using three different methods. In order to extend the short fragment (**3.7**) with an additional heteroaromatic ring, palladium-mediated Buchwald-Hartwig cross-coupling was performed with 2-chloro-6-methoxy-3-pyridinecarboxaldehyde, which provided the aldehyde (**3.38**). In the case of the formation of the aldehyde (**3.43**) Williamson etherification with **3.33** and 3-bromo-4-hydroxybenzaldehyde was followed. The third method involves the generation of benzylic chloride from various benzylic alcohols (**3.3**, **3.7**, **3.34-3.37**) and subsequent *O*-alkylation of phenolic aldehydes. The final synthetic step, common to all aldehydes isolated, was sodium cyanoborohydride-mediated reductive amination, which allowed the incorporation of the various amines into the structure of the compounds. The amine reagents used included ethanolamine, 2-amino-1,3-propanediol, tris(hydroxymethyl)aminomethane, *N*-(2-aminoethyl)acetamide, and amino acids: L-pipecolic acid and L-serine. The structures of the isolated compounds as general structure **II.III** derivatives were gathered in Table 7.

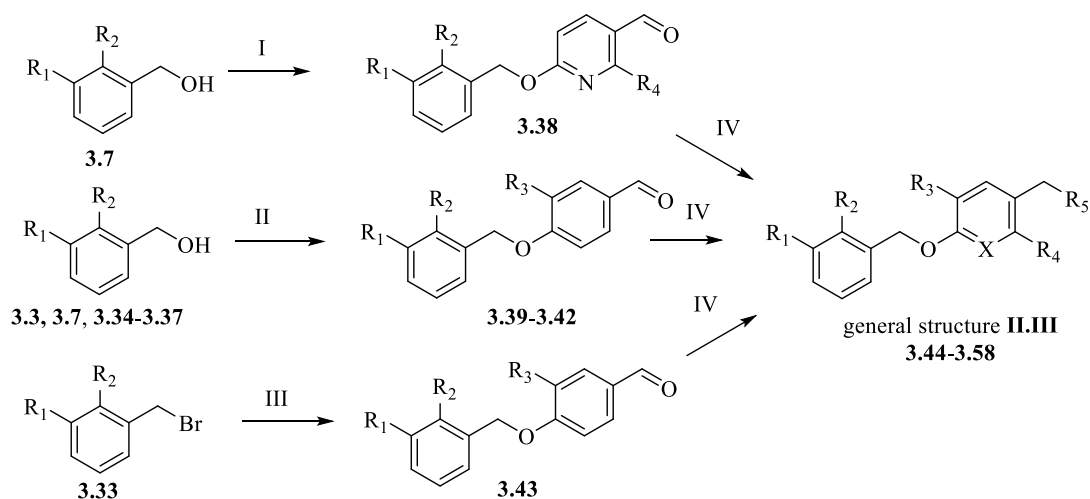
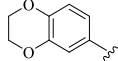
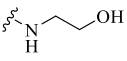
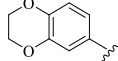
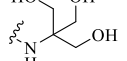
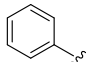
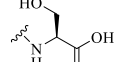
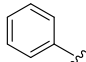
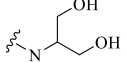
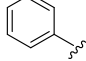
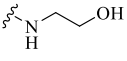
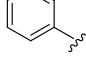
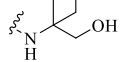


Figure 39. General Pathway for the synthesis of small molecules **3.44-3.58** as II.III derivatives. Reagents and conditions: (I) 2-chloro-6-methoxy-3-pyridinecarboxaldehyde, t-BuXPhos, Cs<sub>2</sub>CO<sub>3</sub>, Pd(OAc)<sub>2</sub>, toluene, 80 °C, 4 h (49% for **3.38**), (II) 1. SOCl<sub>2</sub>, DCM, 40 °C 2. 3-bromo-4-hydroxybenzaldehyde, K<sub>2</sub>CO<sub>3</sub>, DMF, rt, overnight (38% for **3.39**, 47% for **3.40**, 56% for **3.41**, 51% for **3.42**), (III) 3-bromo-4-hydroxybenzaldehyde, K<sub>2</sub>CO<sub>3</sub>, DMF, rt, overnight (41% for **3.43**), (IV) amine component, NaBH<sub>3</sub>CN, AcOH, DMF, rt, overnight (32% for **3.44**, 66% for **3.45**, 72% for **3.46**, 33% for **3.47**, 51% for **3.48**, 59% for **3.49**, 30% for **3.50**, 31% for **3.51**, 54% for **3.52**, 56% for **3.53**, 31% for **3.54**, 33% for **3.55**, 42% for **3.56**, 46% for **3.57**, 82% for **3.58**).

Table 7. General structure **II.III** of obtained inhibitors and substituents arrangement in particular final compounds.

 II.III						
ID	R <sub>1</sub>	R <sub>2</sub>	R <sub>3</sub>	R <sub>4</sub>	X	R <sub>5</sub>
<b>3.44</b>		-Br	-Br	-H	C	
<b>3.45</b>		-Cl	-Br	-H	C	
<b>3.46</b>		-F	-Br	-H	C	
<b>3.47</b>		-F	-Br	-H	C	
<b>3.48</b>		-F	-Br	-H	C	
<b>3.49</b>		-Cl	-Br	-H	C	
<b>3.50</b>		-I	-Br	-H	C	
<b>3.51</b>		-I	-Br	-H	C	
<b>3.52</b>		-F	-Br	-H	C	

<b>3.53</b>		-F	-Br	-H	C	
<b>3.54</b>		-F	-Br	-H	C	
<b>3.55</b>		-F	-H	-OMe	N	
<b>3.56</b>		-F	-H	-OMe	N	
<b>3.57</b>		-F	-Br	-H	C	
<b>3.58</b>		-F	-Br	-H	C	

### 2.3.3. Activity Evaluation of 1,1'-Biphenyl Fragment Based Inhibitors

Selected synthesized compounds were tested by homogeneous time-resolved fluorescence (HTRF) assay for their ability to displace PD-1 from the complex with PD-L1. The measurements were performed at 5 nM PD-L1 and 50 nM PD-1 final concentrations after 2 h incubation with the compounds. The ability of the compounds to dissociate the PD-1/PD-L1 complex was determined with 5 nM concentration of the compounds. For selected inhibitors maximal half inhibitory concentration was also calculated, by fitting the experimental dataset with a modified Hill's equation. Obtained results of the HTRF assay were reported in Table 8.

Table 8. The activity of obtained compounds determined due to HTRF assay with the comparison to the anti-PD-L1 activity of **3.17**.

<b>ID</b>	<b>Anti-PD-L1 activity*/IC<sub>50</sub></b>	<b>ID</b>	<b>Anti-PD-L1 activity*/IC<sub>50</sub></b>
<b>3.44</b>	86.9 ± 19.2%	<b>3.52</b>	IC <sub>50</sub> = 73.6 ± 3.3 nM
<b>3.45</b>	IC <sub>50</sub> = 70.2 ± 18.4 nM	<b>3.53</b>	86.5 ± 9.9%
<b>3.46</b>	45.8 ± 21.6%	<b>3.54</b>	IC <sub>50</sub> = 142.18 ± 3.60 nM
<b>3.47</b>	54.7 ± 40.6%	<b>3.55</b>	83.8 ± 0.1%
<b>3.48</b>	79.2 ± 4.3%	<b>3.56</b>	86.3 ± 6.3%
<b>3.49</b>	49.6 ± 28.9%	<b>3.57</b>	71.0 ± 9.2

<b>3.50</b>	IC <sub>50</sub> = 71.1 ± 29.1 nM	<b>3.58</b>	31.9 ± 1.5
<b>3.51</b>	IC <sub>50</sub> = 78.2 ± 6.2 nM	<b>3.17</b>	IC <sub>50</sub> = 15.0 ± 0.2 nM

\*Anti-PD-L1 activity is as the percentage of undissociated PD-1/PD-L1 complex with 5 nM concentration of inhibitor.

The structure-activity relationship analyses and preliminary *in vitro* biochemical analyses showed that the incorporation of a proper modification on the biphenyl core and the use of a favorable solubilizing group in the small molecule structure is essential for tuning the compatibility of the inhibitor against PD-L1. After optimization of the tail group, it has been investigated that inhibitors with solubilizers containing -OH group provide the best anti-PD-L1 activity. Prime examples are molecules **3.46**, **3.49**, and **3.58**, containing 2-amino-1,3-propanediol and tris(hydroxymethyl)aminomethane moieties. Discussed molecules were able to displace PD-1 from PD-1/PD-L1 complex in around 55%, 50%, and in around 70% for **3.46**, **3.49** and **3.58** respectively with 5 nM compound concentration. On the other hand, molecules **3.53** and **3.57** containing ethanolamine as the solubilizing agent does not provide such satisfying results. 5 nM concentrations of compounds provide only around 14% and around 29% of PD-1/PD-L1 complex disruption, for **3.53** and **3.57** respectively.

To further study SAR, the activities of two inhibitors **3.50** and **3.52** differing from each other with just one atom of halide introduced into the 1,1'-biphenyl scaffold were compared. The correlation of activities of 2-fluoro-1,1'-biphenyl- based inhibitor (**3.52**) and 2-iodo-1,1'-biphenyl derived inhibitor (**3.50**) lead to the conclusion that the exchange of F- into I- substituent does not affect compound's activity in HTRF assay. The maximal half inhibitory values of both **3.50** and **3.52** are around 70 nM values. As well, inhibitor **3.45** as 2-chloro-1,1'-biphenyl derivative was determined to possess the value of IC<sub>50</sub> equal to 70 nM.

Further analyses proved that extension of the distal phenyl ring to naphthalen-2-yl in **3.44** does not provide a beneficial influence on the compound's activity. A negative effect was also observed after the introduction of heteroatom into the central aromatic ring of the molecule. **3.55** and **3.56** compounds, bearing pyridine moiety were barely able to dissociate 15% of the present PD-1/PD-L1 complex.

The homogeneous time-resolved fluorescence assay also provided compelling data showing that the presence of the 2,3-dihydrobenzo[b][1,4]dioxine moiety is not essential for the activity of the compounds, what was previously proposed to be fundamental (Skalniak, *et al.*, 2017, Magiera, *et al.*, 2017). For example, in the case of our equivalent compounds **3.47**

and **3.48** 2,3-dihydrobenzo[b][1,4]dioxine's presence does not significantly affect the potency of the compounds. In this case, even a compound without 2,3-dihydrobenzo[b][1,4]dioxine fragment gave better results related to around 45% of PD-1/PD-L1 complex dissociation.

To further verify the affinity of the tested compounds for the long PD-L1 protein, proton  $^1\text{H}$  spectra was recorded (Figure 40). After the addition of **3.46** compound to the protein, we observed the broadening of the PD-L1 proton signals in the NMR spectra. The binding of **3.46** caused a flattening of the signals in 1D spectra already at a 1:1 molar ratio of protein to compound, which is characteristic for oligomerization of hPD-L1 and is observed for compounds with a biphenyl core. Further addition of the compound did not change the spectra, suggesting a  $K_d$  in the millimolar range.

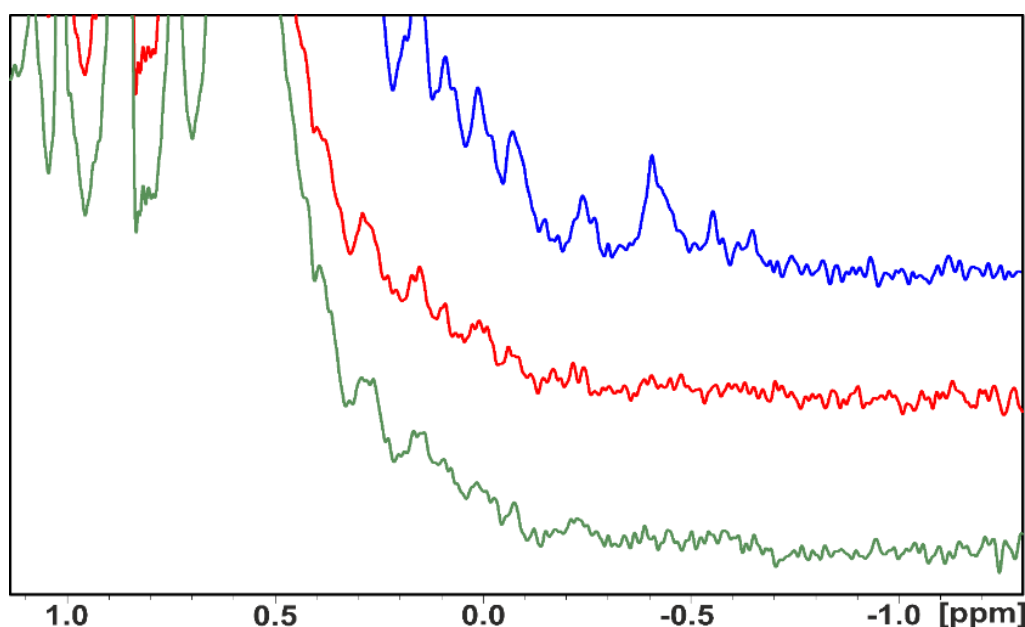


Figure 40. The aliphatic part of  $^1\text{H}$  NMR spectra of long PD-L1 (blue) with **3.46** in the molar ratio 1:1 (red), and 1:10 (green) protein to compound.

Moreover, crystallization probes to obtain the co-crystal structure of PD-L1 with **3.54** were undertaken. High-quality crystals with a final resolution of 3.2 Å of the complex of PD-L1 and **3.54** were obtained, what provided insight into the molecular interactions of **3.54** with the target.<sup>6</sup> Purified human PD-L1 was isolated, concentrated to 5 mg/ml, and then mixed in a 1:3 molar ratio with a 3-molar excess of the **3.54** compound. Diffraction-quality crystals were collected at room temperature under the conditions described in Section 4.9.

<sup>6</sup> Crystals of **3.56**/PD-L1 were obtained by mgr Ismael Rodriguez. Crystal structure of **3.56**/PD-L1 was analysed by mgr Katarzyna Magiera-Mularz.

Firstly binding mode of **3.54** with dimeric PD-L1 was analyzed with BIOVIA Discovery Studio Visualizer and then it was viewed in PyMOL Molecular Graphics System (Figure 41).

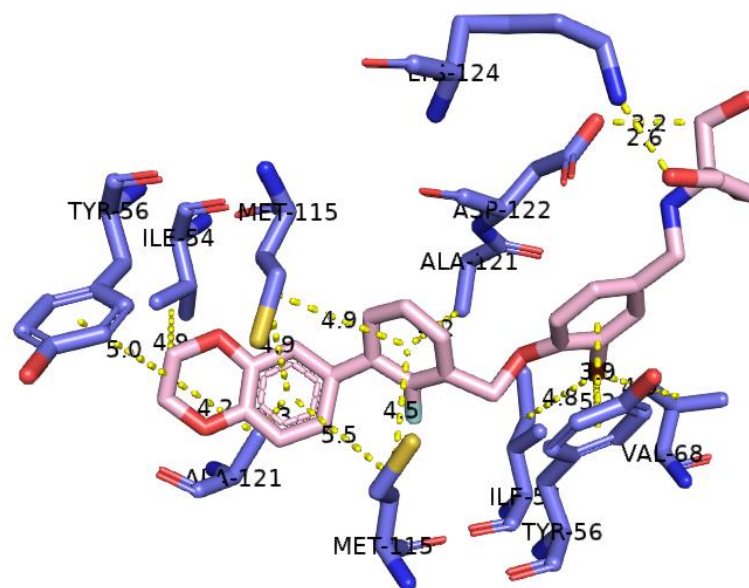


Figure 41. Visualization of interactions within co-crystallized **3.54** (pink) and dimeric hPD-L1 (violet). Detected interactions (yellow) and distance between respective residues are presented.

Analyses of the crystal structure show that molecule **3.54** is locked within a hydrophobic cleft between two PD-L1 residues. The 1,4-benzodioxane moiety being engaged in the  $\pi$ -alkyl interaction with Tyr56<sub>A</sub> and providing further hydrophobic contacts with Ile54<sub>A</sub> and Ala121<sub>B</sub> stabilizes the complex. Furthermore, both aromatic rings from the biphenyl core are involved in numerous  $\pi$ -alkyl interactions with residues from both PD-L1 chains such as Ala121<sub>B</sub>, Met115<sub>A</sub>, Met115<sub>B</sub>, and Ala121<sub>A</sub>. Moreover, central aromatic ring of the molecule provides  $\pi$ - $\pi$  stacking interaction with Tyr56<sub>B</sub> sidechain. Also -Br substituent attached to the central aromatic ring of the molecule is engaged in ligand non-bond hydrophobic contacts with Ile54<sub>B</sub> and Val68<sub>B</sub> and  $\pi$ -alkyl interaction with Tyr56<sub>B</sub>. Binding mode analyses provide also information about the significant impact of tris(hydroxymethyl)aminomethane, which allows hydrogen bonding with Lys124<sub>A</sub> and Asp122<sub>A</sub>. However, unlike to previously reported crystal structure containing the terphenyl scaffold (Muszak *et al.*, 2021) halogen form 2-fluoro-1,1'-biphenyl core of **3.54** do not interacts with PD-L1. That might partially explain the less potency of **3.54** in the biophysical experiments when compared with small molecules containing the terphenyl scaffold.

The compounds **3.46** – **3.50**, **3.54**, **3.57** presenting the best results in HTRF tests, were further subjected to cell-based immune checkpoint blockade assay. PD-1/PD-L1 interaction was provided by Jurkat T cells, expressing PD-1 co-cultured with PD-L1 equipped CHO cells.

The compounds presenting ability to block the PD-1/PD-L1 complex, led to increase of luciferase luminescence, what proved the activation of effector cells. (Figure 42). For the antagonists, exhibiting the highest fold induction, maximal half effective concentrations were determined and summarized in Table 9.

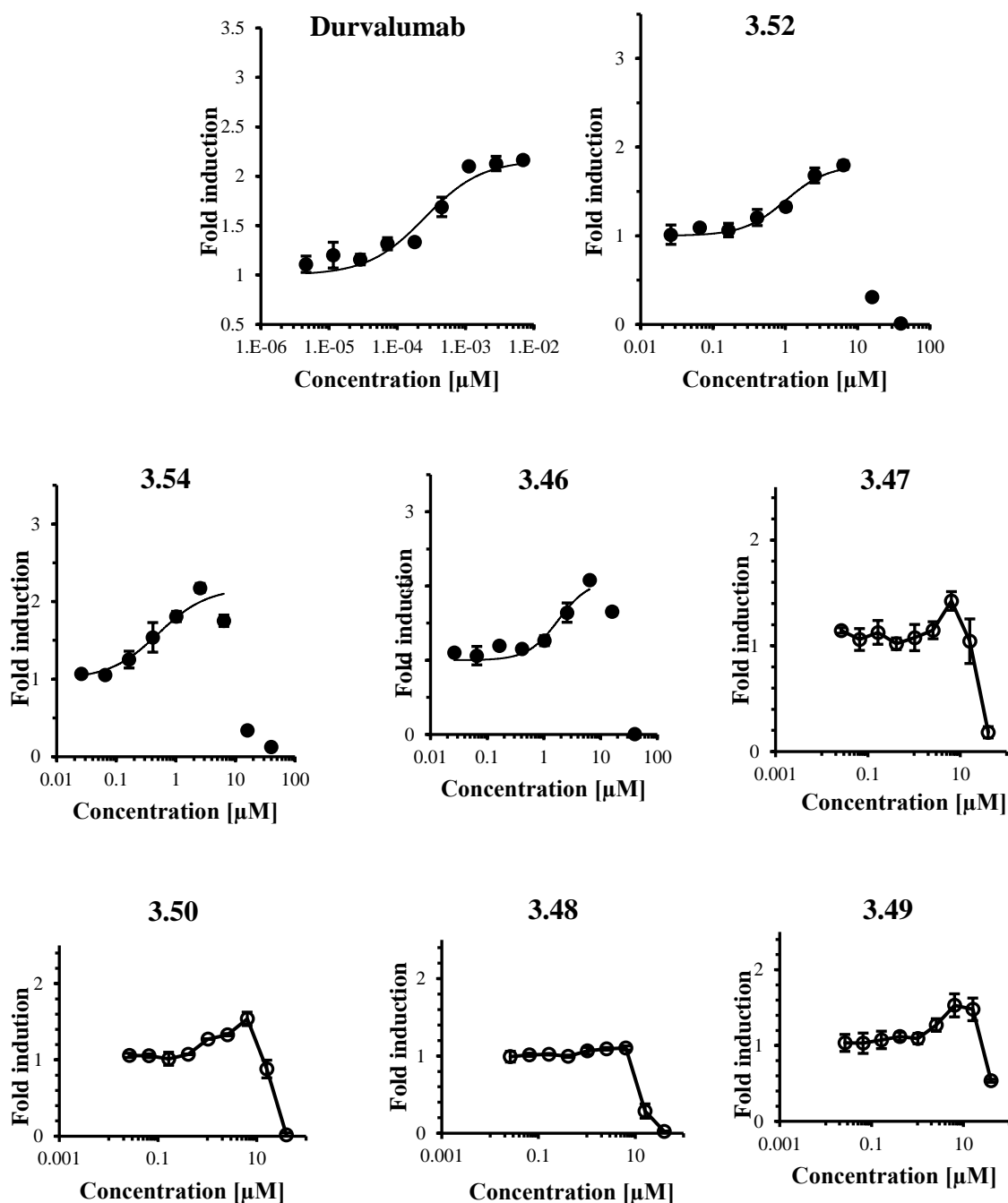


Figure 42. The activity of 2-fluoro-1,1'-biphenyl (3.46-3.48, 3.54, 3.57), 2-chloro-1,1'-biphenyl (3.48), 2-iodo-1,1'-biphenyl (3.50) derived compounds in PD-1/PD-L1 ICB cell-based assay. Data for durvalumab presented as positive control of PD-1/PD-L1 monoclonal antibody.

Table 9. EC<sub>50</sub> values calculated for **3.46**,**3.52** and **3.54** inhibitors in PD-1/PD-L1 immune checkpoint blockade cell-based assay. Values for durvalumab presented as positive control of PD-1/PD-L1 monoclonal antibody.

Name of the compound	EC <sub>50</sub> [μM]	Cytotoxic concentration [μM]
<b>3.52</b>	1.01 ± 0.15	16
<b>3.54</b>	0.51 ± 0.16	16
<b>3.46</b>	1.79 ± 0.36	40
<b>Durvalumab</b>	0.25 ± 0.06	n.o.

\* n.o. – not observed in the tested range of concentrations

Among the tested inhibitors **3.54** exhibit the lowest EC<sub>50</sub> value of 0.51 ± 0.16 μM. Two other compounds – **3.46** and **3.52** – provided maximal half inhibitory values 1.01 ± 0.15 μM and 1.79 ± 0.36 μM respectively. However, further analyses showed the relative luminescence decrease in higher concentrations of inhibitors. This observation is correlated with the cytotoxic effect of tested compounds from 16 μM concentrations of **3.52** and **3.54**. In contrast, presented previously 2-bromo-1,1'-biphenyl- based inhibitor **3.17**, characterized with EC<sub>50</sub> = 6.6 ± 0.8 μM. (Section 2.2.2) did not cause toxicity up to 100 μM concentration. The cytotoxic effect could be potentially, related to the exchange of 2-bromo-1,1'-biphenyl to the 2-fluoro-1,1'-biphenyl fragment. The performed analyses prove that a low half maximal effective value is not sufficient criterium to analyze compounds potency.



## 2.4. 2,3-dihydro-1H-indene Derivative as the Elongated Potential PD-L1 Antagonists

The next generation of compounds involves modification of the compound structure based on the idea of increasing the solubility of the inhibitors. Solubility is one of the critical factors in achieving the necessary drug concentration in the systemic circulation for the intended pharmacological response. Therefore, to increase this factor, the structure of the compound was extended and equipped with a second solubilizing group. The inspiration of the proposed new scaffold was based on the structure revealed by ChemoCentryx, in which 2,3-dihydro-1H-indene was introduced by fusing the cyclopentane ring to the biphenyl core (Figure 16). Also, based on compounds disclosed by Guangzhou Maxinovel Corporation (Figure 17, Wang, Y. *et al.*, 2018a), ether linker between biphenyl core and third aromatic ring was replaced with ethenyl moiety. Consequently, general structure **II.IV** was formed as showed on the Figure 43.

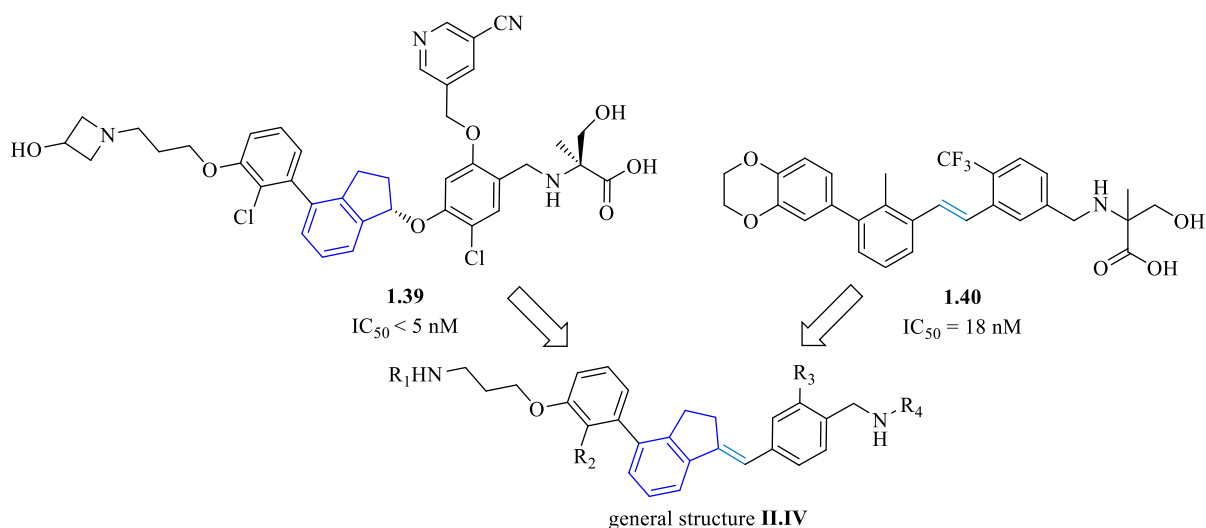


Figure 43. The formation of new, potential, 2,3-dihydro-1H-indene based PD-1/PD-L1 inhibitor consistent with general structure **II.IV**.

### 2.4.1. Synthesis of Potential 2,3-dihydro-1H-indene Based Derivative

The synthetic pathway to obtain a derivative of 2,3-dihydro-1H-indene-based inhibitor within the following set of substituents - R<sub>1</sub> = 4-piperidinol, R<sub>2</sub> = CH<sub>3</sub>, R<sub>3</sub> = OCH<sub>3</sub>, R<sub>4</sub> = serine) - was designed and involved 13 steps (Figure 44). 3 parallel synthetic routes were followed to prepare the corresponding co-substrates.

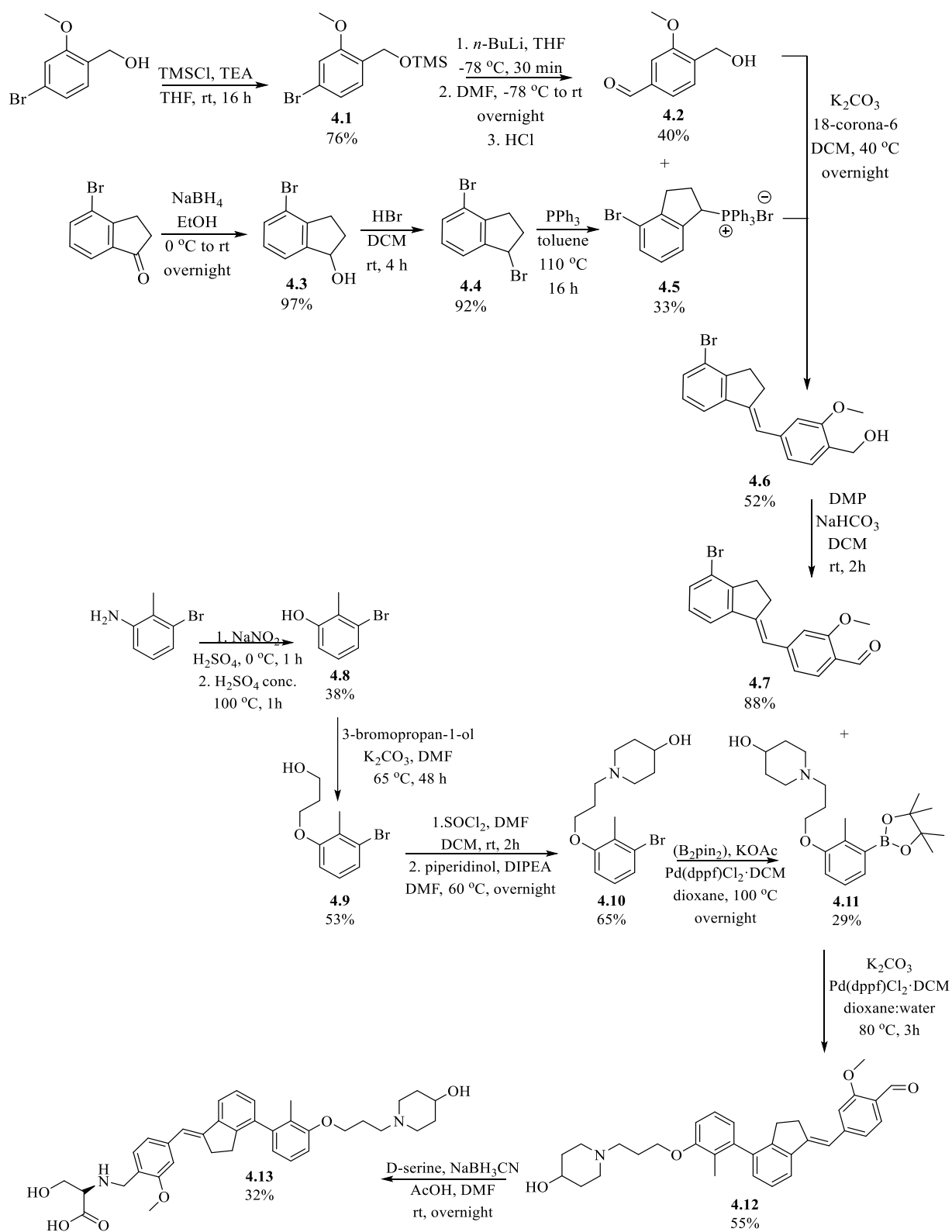


Figure 44. Synthesis of 2,3-dihydro-1H-indene derivative as elongated potential PD-1/PD-L1 antagonists.

The first synthetic route (I) was started from commercially available (4-bromo-2-methoxyphenyl)methanol. The following alcohol was protected with  $\text{TMSCl}$  to isolate the

corresponding trimethylsilyl ether **4.1**. During the next step, the formyl group was introduced into the aromatic ring. In this case, *n*-butyllithium with its highly polarized Li-C bond was used. The nucleophilicity of the carbon atom, caused by the concentration of most of electron density on this atom, allows nucleophilic attack and conversion of Ar-Br into the corresponding Ar-Li compound. Subsequently, the Ar-Li compound reacts with an excess of DMF to form a formylated compound, releasing lithium dimethylamide. Application of acidic conditions allows removal of TMS group and isolation of 4-(hydroxymethyl)-3-methoxybenzaldehyde (**4.2**) with 40% yield.

In parallel, the second co-substrate was prepared, starting from 4-bromo-2,3-dihydro-1H-inden-1-one. The cyclic ketone was subjected to reaction with the use of sodium borohydride, which plays the role of reducing agent as it is the source of hydride ion (-H-). Isolated almost equivalent amounts of alcohol (**4.3**) were converted to the corresponding bromide (**4.4**) after addition of hydrobromic acid. In the next step, **4.4** was heated in the presence of triphenylphosphine in toluene, which allowed precipitation of the corresponding triphenylphosphonium bromide (**4.5**) after cooling the reaction mixture.

Two of the prepared co-substrates - aldehyde (**4.3**) and ylide (**4.5**)- were further coupled *via* Wittig reaction, which led to the formation of **4.6** as alkene product. In this reaction, the presence of two isomers of the product was detected, which will be further discussed in **2.4.2** chapter. The *E* and *Z* diastereoisomers were separated by chromatographic methods and the *E* isomer was selected based on analyses of 2D NOESY spectroscopic results. **4.6** was further subjected to reaction with Dess-Martin periodinane reagent (DMP) for oxidation of alcohol (**4.6**) into respective aldehyde (**4.7**). During reaction DMP reagent possesses ability for effective complexation of hydroxyl group forming diacetoxyalkoxyperiodinane intermediate (Dess *et al.*, 1983). This species is further deprotonated by previously released acetates, allowing the formation of the corresponding aldehyde. The use of DMP instead of other commonly used oxidizing agents, such as pyridinium chlorochromate (PCC) and DMSO-based reagents, allows the application of less stringent reaction conditions, shorter reaction time, and has been associated with simplified workup.

Collaterally, the third synthetic route was carried out to provide the co-substrate for further modification of **4.7**. For this purpose, 3-bromo-2-methylaniline was used as the starting material. The addition of sodium nitrite under strong acid conditions, provided by the presence of sulfuric acid, led to the formation of 3-bromo-2-methylbenzenediazonium salt. The diazonium salt was then hydrolyzed by heating in an aqueous solution of sulfuric acid, yielding the corresponding phenol (**4.8**) as the product. In the next step, the phenolic compound was

further deprotonated with potassium carbonate and substituted with 3-bromopropan-1-ol to give the compound **4.9**. Obtained alcohol was then converted to the corresponding chloride and substituted with 4-piperidinol to allow the isolation of **4.10**. The application of conditions including bis(pinacolato)diboron, potassium acetate, Pd(dppf)Cl<sub>2</sub>·DCM and anhydrous dioxane led to the isolation of the boronic acid ester (**4.11**), which represents the third co-substrate necessary for the formation of the final inhibitor.

Subsequently, compound **4.11** was coupled to the previously prepared molecule **4.7**. C-C bond formation was enabled by the use of palladium-mediated Suzuki cross-coupling, which allowed the isolation of **4.12**. The last step of the whole synthetic pathway involved sodium cyanoborohydride mediated reductive amination to introduce second solubilizing group. The final compound with D-serine and 4-piperidinol was purified on silica using column chromatography to give the molecule **4.13** as the final product.

#### 2.4.2. The Study of Geometric Isomerism of the Products of the Wittig Reaction

2D NOESY spectroscopy is a powerful tool to study the configurational isomerism of organic compounds. The method is based on the nuclear Overhauser effect (NOE), which concerns cross-relaxation as the transfer of nuclear spin polarization between two populations of spin-active nuclei (Overhauser, 1953). In solutions of organic compounds, cross-relaxation is expressed by <sup>1</sup>H dipole-dipole couplings of protons in close proximity. Thus, the cross peaks of a NOESY spectrum show the protons that are close to each other.

In my work, this 2D NOESY spectroscopic approach was used to determine which of the two diastereoisomeric products of the Wittig reaction is the desired E-isomer (Figure 45). Analysing structure of the E isomer, cross relaxation peaks should be observed between protons bonded to C2 of the cyclopentane ring and C3 of the aromatic ring. Also signals related to coupling of ethylene proton and protons attached to C5 of aromatic moiety should be well visualized. Conversely, in the case of Z-isomer, the cross-relaxation effect between ethylene proton (1) and proton nuclei forming cyclopentane ring (2) should appear.

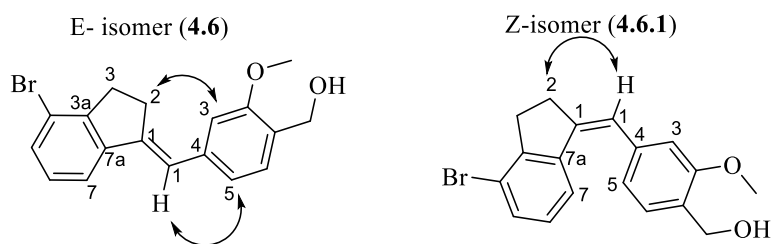


Figure 45. Two possible isomers of **4.5** and their possible cross-relaxations.

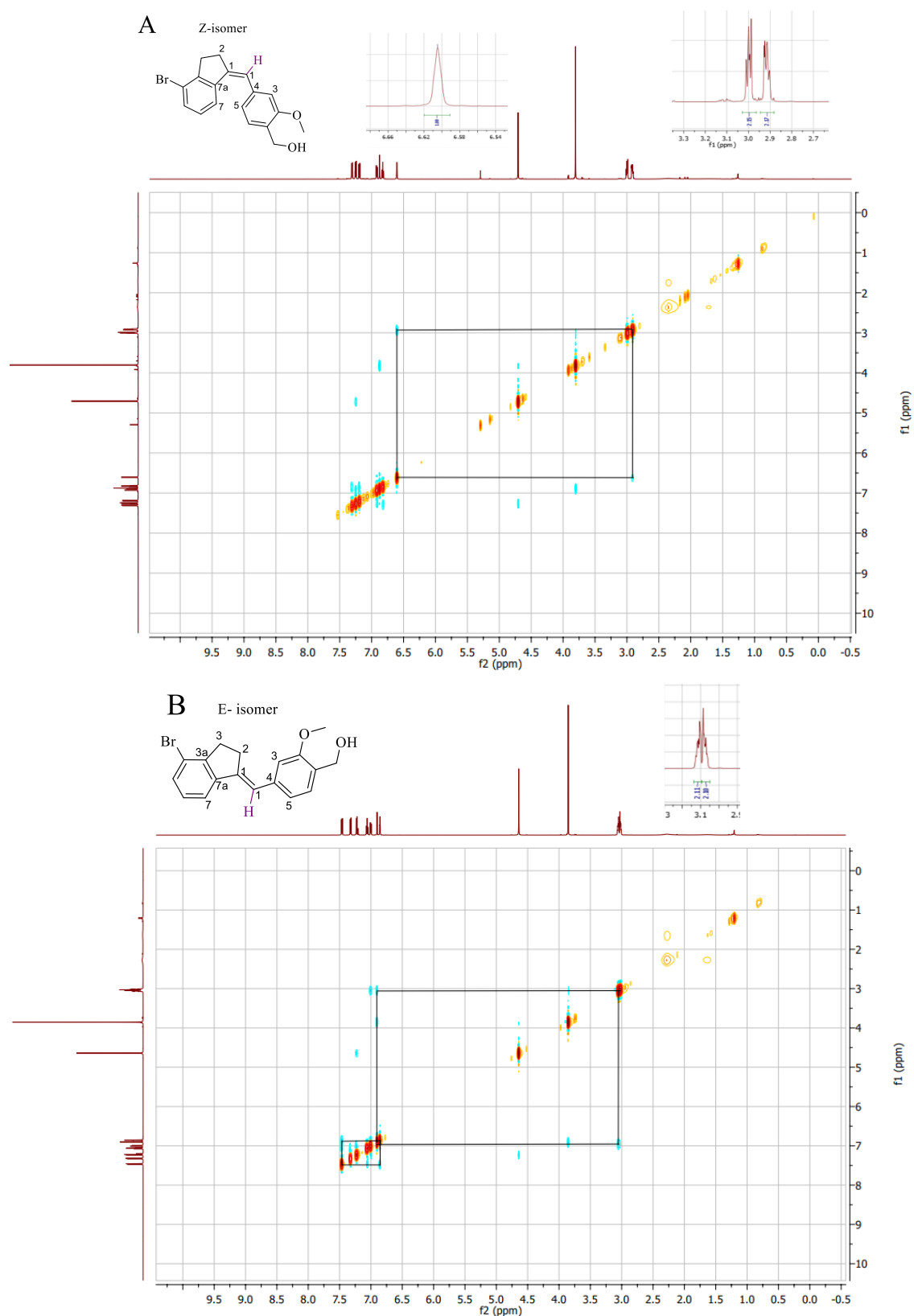


Figure 46. The NOESY spectrum of the two isomers of **4.6**. A) The NOESY spectrum of isomer Z with presented coupling between ethylene proton ( $\delta = 6.60$  ppm) and protons from aliphatic range ( $\delta = 2.91$  ppm). B) The NOESY spectrum of the isomer E. The coupling corresponding to the interaction between aliphatic protons (related to the carbon 2) ( $\delta = 3.11$  ppm) and aromatic proton (related to the carbon 3) ( $\delta = 6.96$  ppm) and the coupling between ethylene proton ( $\delta = 6.91$  ppm) and aromatic proton (related to the carbon 5) ( $\delta = 7.52$  ppm) are demonstrated.

To determine the configurational isomerism of the two isolated compounds, the 2D NOESY NMR spectra were recorded, what is visualized in Figure 46. After of the obtained results, the correct structures were assigned to both 2D NOESY spectra. Figure 46A was correlated with isomer Z as there is a coupling between ethylene proton ( $\delta = 6.60$  ppm) and protons from the aliphatic region ( $\delta = 2.91$  ppm) is present. Followingly, observed on the Figure 46B cross relaxation peaks between aliphatic protons (related to the carbon 2) ( $\delta = 3.11$  ppm) and aromatic proton (related to the carbon 3) ( $\delta = 6.96$  ppm) and the coupling between ethylene proton ( $\delta = 6.91$  ppm) and aromatic proton (related to the carbon 5) ( $\delta = 7.52$  ppm) were assigned to isomer E.

## 2.4 Assessment of *in vitro* Activity of 2,3-Dihydro-1H-Indene Derivative Towards PD-1/PD-L1

Successfully synthesized molecule (**4.13**) was tested in HTRF assay to check its ability for PD-1/PD-L1 disruption. Results indicate that after introduction of 5 nM concentration of molecule **4.13**, 68.8% of PD-1/PD-L1 complex still remained undissociated. This result is still not satisfying, therefore proposed modifications of the structure didn't provide improvement of activity.

Despite these results, compound **4.13** was further investigated in PD-1/PD-L1 immune checkpoint blockade cell-based assay to determine its ability to block PD-1/PD-L1 pathway. The results obtained showed a slightly increasing activity observed for the concentration range of 3–30  $\mu\text{M}$ . This corresponds to an  $\text{EC}_{50}$  value of about 10  $\mu\text{M}$ , which is not a spectacular result (Figure 47).

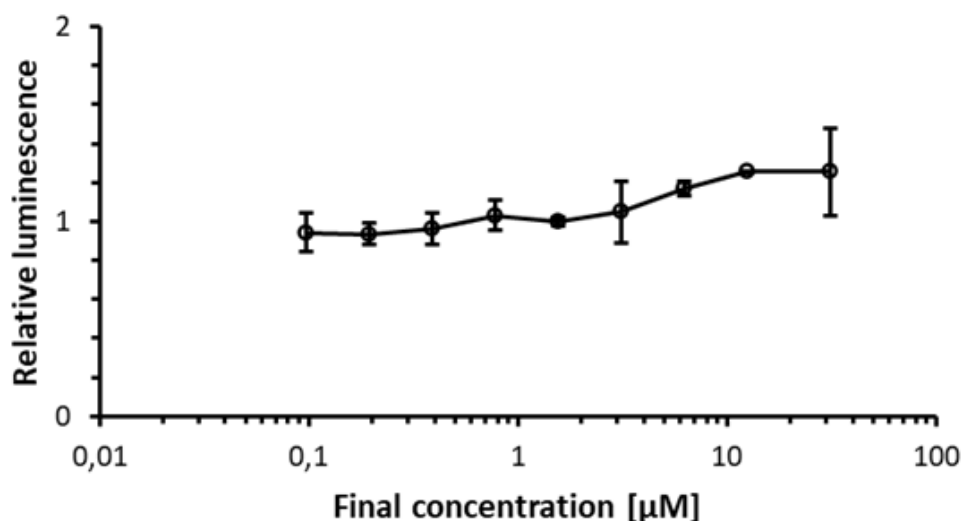


Figure 47. The profile of PD-1/PD-L1 immune checkpoint blockade cell-based assay for compound **4.13**.

Proposed modification of the scaffold did not meet the desired expectations. The introduction of 2,3-dihydro-1H-indene ring and connecting it *via* ethenyl moiety with third aromatic ring caused that compound has decreased affinity towards PD-L1 target. Therefore, some other means need to be applied to increase the compound's solubility and enhance its potency to disrupt PD-L1 from the complex.

## 2.5. Preparation of ARB272542 Derivatives as Potential PD-1/PD-L1 Inhibitors – Synthesis and Activity Determination

The subject of further experimental work was the development of a potential PD-L1 inhibitor structure. The following work describes the preparation of **1.59 - ARB 272542** derivatives (general structure **II.V**), which structure was inspiration for further research (Park *et al.*, 2021). The first modifications performed involved the exchange of solubilizing groups with retention of the core consisting of four aromatic rings of the molecule. The idea was to see how the introduction of different solubilizing agents affected the potency of the compound. Figure 48 illustrates the synthetic route followed to get **1.59 - ARB 272542** derivatives.

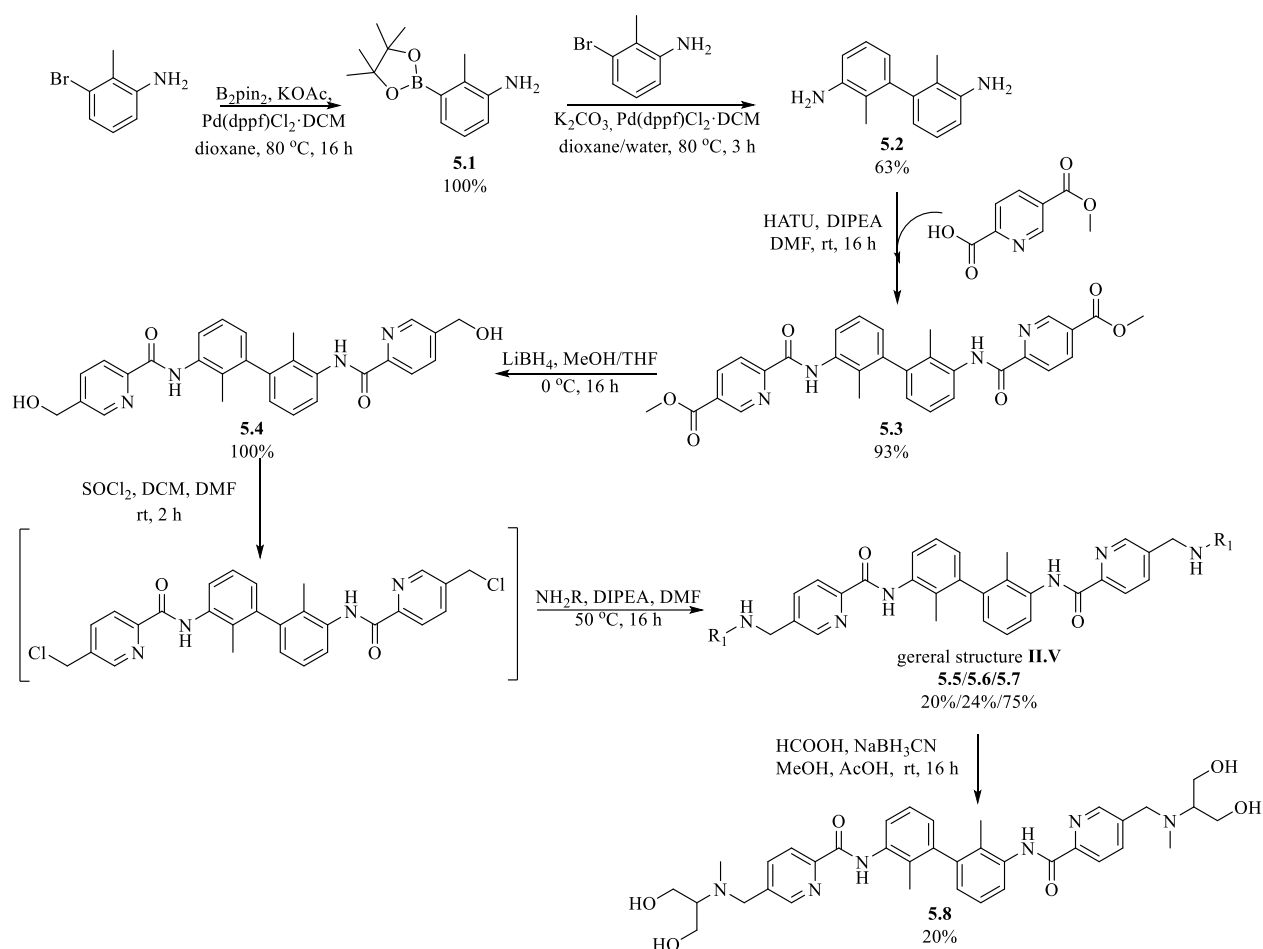


Figure 48. The synthetic pathway performed to obtain compound **1.59 - ARB272542** derivatives.

First synthetic step involved the quantitative conversion of 3-bromo-2-methylaniline to the corresponding boronic ester (**5.1**). Then, biphenyl core (**5.2**) was constructed by coupling the prepared boronic ester (**5.1**) with 3-bromo-2-methylaniline. The next synthetic step involved the elongation of the structure with two pyridine moieties *via* an amide bond. For this purpose, HATU was used as a coupling agent. The mechanism of this coupling involved two main steps.



First, deprotonated carboxylic acid attacks HATU, resulting in the formation of *O*-acyl(tetramethyl)isouronium salt. Next, the anion formed from 1-hydroxy-7-azabenzotriazole (AtO<sup>-</sup>) attacks the isouronium salt, resulting in the formation of the OAt-active ester and the release of tetramethylurea. The next step involves acylation of the amine derivative by the OAt-active ester and formation of the desired amide bond (Carpino *et al.*, 1993, Carpino *et al.*, 2000). The application of this coupling agent allowed the isolation of compound **5.3** with 93% yield. The ester groups were then selectively reduced to alcohols in the presence of amide bonds. Such a treatment was possible thanks to the application of lithium borohydride, which is a stronger reducing agent than its equivalent sodium borohydride, which is not able to reduce esters. The properties of LiBH<sub>4</sub> are attributed to the presence of the lithium cation, which allows a higher polarization of the -C=O bond by participating in the complexation of the carbonyl structure (Banfi *et al.*, 2001).

The use of this reducing agent allowed the almost quantitative isolation of **5.4**. Followingly, benzylic alcohol moieties of **5.4** were converted into respective chlorides to equipped the compound in good leaving groups. The generated chloride derivative was subjected to S<sub>N</sub>2 reaction with 3 different amine components to afford **5.5**, **5.6** and **5.7** compounds with rather low reaction yields. In addition, compound **5.8** was subjected to a second reductive amination to form a tertiary amine. For this purpose, conditions including addition of formaldehyde, acetic acid and sodium cyanoborohydride were applied. Overnight stirring of the resulting reaction mixture allowed formation of the final compound **5.8** with 20% yield.

The obtained compounds – **5.5**, **5.6**, **5.7** and **5.8**- were subjected to HTRF assay and ICB cell based assay to evaluate their ability for inhibition of PD-1/PD-L1 pathway. The collected data were correlated in Table 10.

Table 10. The comparison of **II.V** derivatives biochemical activity in HTRF and ICB assays.

Name of the compound	R <sub>1</sub>	HTRF [%]*	EC <sub>50</sub> [nM]
<b>5.5</b>		0.33 ± 0.14 (5 nM)	282
<b>5.6</b>		0.03 (5 nM)	45
<b>5.7</b>		0.06 ± 0.08 (5 nM)	19
<b>5.8</b>		0.64 ± 0.19 (5 nM) 1.06 ± 0.001 (0.5 nM)	119
<b>1.59 - ARB272542**</b>		IC <sub>50</sub> = 400 pM	17

\*results shown as the percentage of undissociated PD-1/PD-L1 complex in conditions of 5 nM or 0.5 nM compound's concentration

\*\*data from Park *et al.*, 2021.

Analysing obtained results, we can deduce that of solubilizing group of compound **1.59 - ARB272542** does not affect its potency much. The best of the obtained compound – **5.7** with R<sub>1</sub> as 2-(methylamino)ethan-1-ol was determined to possess EC<sub>50</sub> of 19 nM what is comparable to the EC<sub>50</sub> of **1.59 - ARB272542**. Moreover, we can observe the tendency of decrease of the compound's affinity towards PD-L1 with the increase of the bulkiness of the solubilizing group. Among the tested inhibitors, molecule **5.5**, with R<sub>1</sub> = tris(hydroxymethyl)aminomethane, was determined to give the less satisfactory results. Probably the molecule's solubilizing group formed to large steric hindrance and inhibit targeting PD-L1. Also, the presence of additional methyl group on nitrogen atom of amine moiety slightly influences its biochemical properties, leading to equal or lower inhibitor's potency. Besides the above observations, all solubilizing groups provided inhibitors with significant potency when comparing the obtained results with other disclosed PD-L1 inhibitors. The tested solubilizers will continue to be used to evaluate next generation inhibitor structures.

## 2.6. 3,4-dihydro-2H-benzo[b][1,4]oxazine Derivatives as Potential PD-1/PD-L1 Antagonists

### 2.6.1. 3,4-Dihydro-2H-Benzo[b][1,4]Oxazine - Fragment Identification

The next proposal of scaffold modification concerns the fusion of the morpholine ring with the biphenyl core for the construction of 3,4-dihydro-2H-benzo[b][1,4]oxazine derivatives (general structure **II.VI**). The idea originated from the satisfactory results obtained for the short fragment **2.8 - STD-4** described by Kitel *et al.*, 2022. The presented compound **2.8 - STD-4** was found to bind to PD-L1 ectodomain with  $K_D = 2.21 \pm 0.33$  mM, which was demonstrated by superimposing  $^1\text{H}$ - $^{15}\text{N}$  HSQC spectra of apo-short PD-1 and PD-L1 with **2.8 - STD-4** (Figure S1, Kitel *et al.*, 2022). That is an unexpectedly satisfying result for such a small fragment. Therefore, the decision was made to enlarge the molecular structure and improve the properties of the compound. As a result, a short biphenyl-derived fragment was composed and then a long pseudo- $\text{C}_2$  dimeric inhibitor was proposed, which is shown in Figure 49.

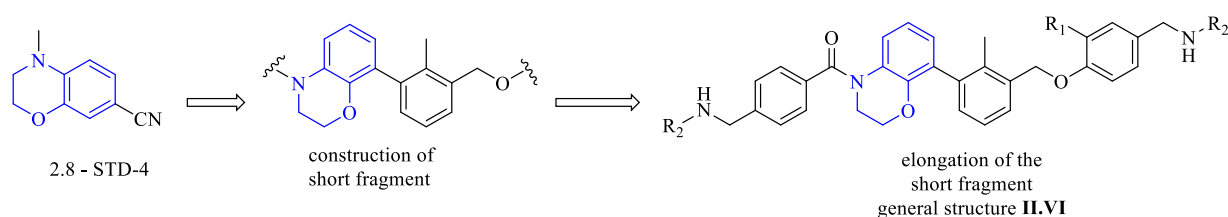


Figure 49. Conceptualisation of 3,4-dihydro-2H-benzo[b][1,4]oxazine derivatives.

### 2.6.2. Synthesis of 3,4-Dihydro-2H-Benzo[b][1,4]Oxazine Derivatives

A convergent synthesis was carried out to obtain the 3,4-dihydro-2H-benzo[b][1,4]oxazine derivatives, which are shown in Figure 50. Synthesis of the first intermediate (**6.2**) was started from 2-amino-6-bromophenol which was heated overnight in 125 °C with 1,2-dibromoethane, potassium carbonate and DMF allowing the ring closure and composition of small 3,4-dihydro-2H-benzo[b][1,4]oxazine derived fragment (**6.1**). The latter was coupled with generated from 4-formylbenzoic acid chloride to form amide bond and compose **6.2** intermediate. The second intermediate was prepared from (3-bromo-2-methylphenyl)methanol, which was converted to the corresponding boronic acid ester - **6.3**. The obtained alcohol was converted to corresponding benzylic chloride and used as alkylating agent for *O*-alkylation of meta  $\text{R}_1$  substituted 4-hydroxobenzaldehydes. Subsequently, the isolated aldehydes - were subjected to palladium-mediated cross-coupling with the previously **6.2** fragment. Thus obtained dialdehydes

– **6.7–6.9** – were converted into corresponding dialcohols – **6.10**, **6.11**, **6.12**. The applied reduction conditions included dropwise addition of 2 M solution of lithium borohydride in THF, which resulted in product formation after 2 h. Conversion of -OH groups into better leaving groups allows substitution of various amine components optimized previously in Section 2.5, which led to formation of the series of final potential PD-1/PD-L1 inhibitors **6.13–6.20**.

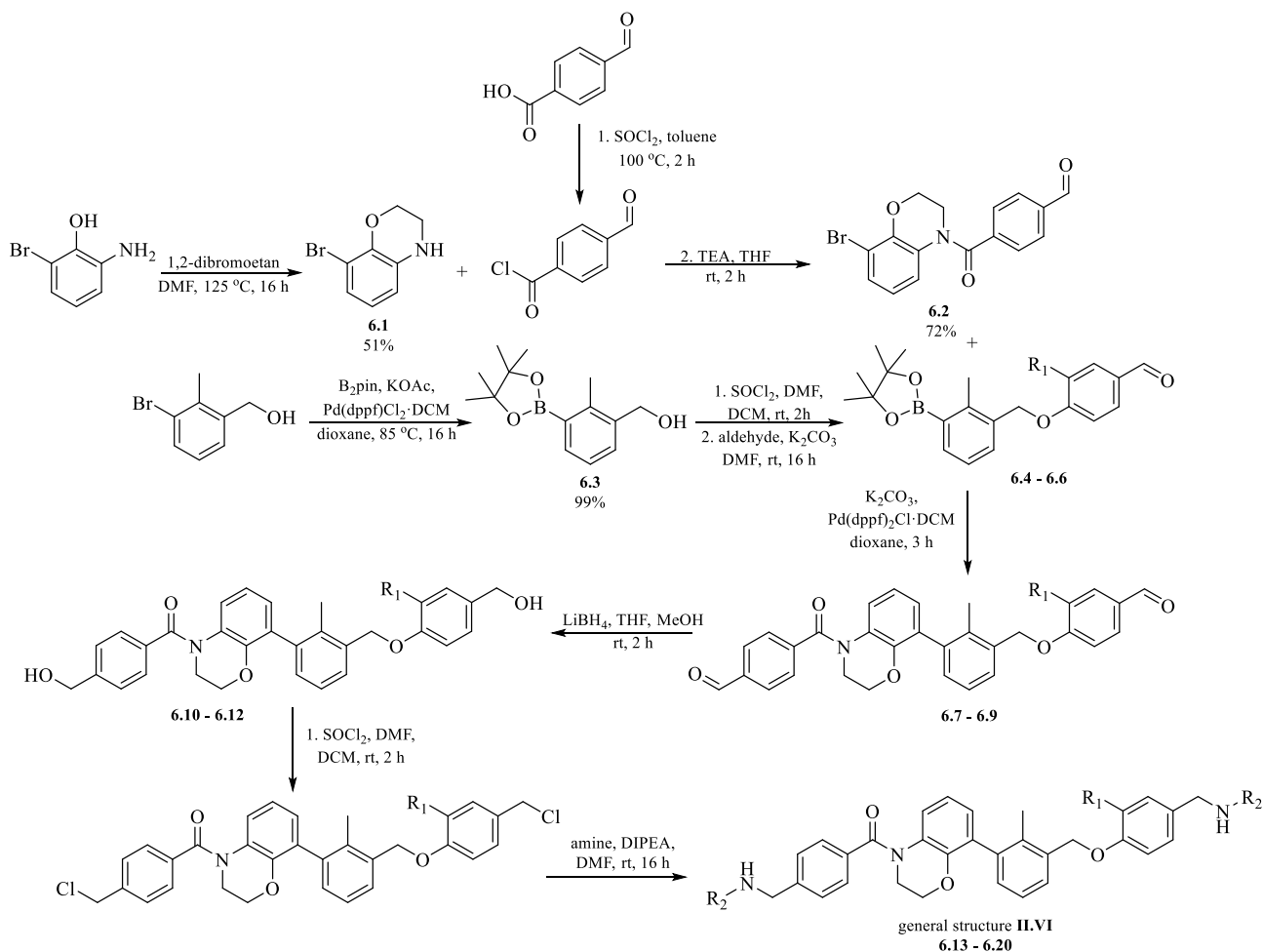


Figure 50. Synthetic pathway to obtain series of dimeric, pseudo C<sub>2</sub>-symmetric 3,4-dihydro-2H-benzo[b][1,4]oxazine derived PD-L1 inhibitors (general structure **II.VI**). Yields of obtained compounds: **6.4** (where R<sub>1</sub> is -OMe: 68%), **6.5** (where R<sub>1</sub> is -H: 57%), **6.6** (where R<sub>1</sub> is -CH<sub>3</sub>: 40%), **6.7** (where R<sub>1</sub> is -OMe: 68%), **6.8** (where R<sub>1</sub> is -H: 76%), **6.9** (where R<sub>1</sub> is -Me: 51%), **6.10** (where R<sub>1</sub> is -OMe: 85%), **6.11** (where R<sub>1</sub> is -H: 82%), **6.12** (where R<sub>1</sub> is -Me: 52%). The sets of all R<sub>1</sub>, R<sub>2</sub> R<sub>3</sub> substituents and respective reaction yields for products after last reaction step (**6.13 – 6.20**) are correlated in the Table 11.

### 2.6.3. Assessment of Biochemical Activity of 3,4-Dihydro-2H-Benzo[b][1,4]-Oxazine Derivatives towards PD-1/PD-L1

3,4-dihydro-2H-benzo[b][1,4]oxazine derived PD-L1 inhibitors were subjected to HTRF assay to estimate their affinity towards the target. Obtained results as percentage of undissociated PD-1/PD-L1 complex were collected in Table 11 of the determined values

suggests that none of the obtained compounds -**6.13-6.20**- exhibit satisfactory potency. With 5 nM and even 0.5  $\mu$ M concentration of the compound almost all PD-1/PD-L1 complex remained undissociated. The best of the obtained compound - **6.18** - give the result of 27% inhibition of PD-1/PD-L1 pathway with 0.5  $\mu$ M concentration, which is an undesirable result. To better understand the low affinity of the generated series of 3,4-dihydro-2H-benzo[b][1,4]oxazine derivatives, further structural analyses were performed. It turns out that the introduction of the 3,4-dihydro-2H-benzo[b][1,4]oxazine moiety linked to the rest of the scaffold *via* an amide bond is highly inadvisable. The generated rigidity of the scaffold causes that the compounds are not flexible enough to reach the protein binding hot spot. Therefore, the introduction of 3,4-dihydro-2H-benzo[b][1,4]oxazine in this position on the scaffold is not suitable.

Table 11. The comparison of general structure **II.VI** derivatives and their activity in HTRF assay.

Name of the compound	R <sub>1</sub>	R <sub>2</sub>	Y[%]	HTRF [%]*
<b>6.13</b>	-OCH <sub>3</sub>		56	101.3 $\pm$ 13.8 at 5 nM
<b>6.14</b>	-OCH <sub>3</sub>		55	110.2 $\pm$ 3.6 at 0.5 $\mu$ M
<b>6.15</b>	-OCH <sub>3</sub>		61	88.4 $\pm$ 5.0% at 0.5 $\mu$ M; 82.6 $\pm$ 1.3% at 5 nM
<b>6.16</b>	-H		25	119.0 $\pm$ 1.1 at 5 nM
<b>6.17</b>	-H		37	98.8 $\pm$ 0.7 at 0.5 $\mu$ M
<b>6.18</b>	-H		56	73.0 $\pm$ 3.9 at 0.5 $\mu$ M
<b>6.19</b>	-H		37	113.9 $\pm$ 3.0 at 0.5 $\mu$ M
<b>6.20</b>	-CH <sub>3</sub>		38	93.8 $\pm$ 6.4 at 0.5 $\mu$ M

\*results shown as the percentage of undissociated PD-1/PD-L1 complex

## 2.7. Elongated *Pseudo C*<sub>2</sub>- PD-1/PD-L1 Inhibitors

### 2.7.1. Elongated *Pseudo C*<sub>2</sub>-Symmetric PD-1/PD-L1 Inhibitors – Evolution

In the next stage of the research, elongated types of PD-1/PD-L1 inhibitors were developed and structure-activity relationship (SAR) analysis was performed. Modification of small molecules related to their elongation and enlargement of their structure could potentially improve the binding strength of inhibitors by increasing the interaction with the PD-L1 protein. In Figure 51 three new general structures of potential PD-1/PD-L1 inhibitors have been proposed (general structure **II.VII**, general structure **II.VIII**, general structure **II.IX**). The changes in the general structures were determined in comparison to the known dimeric compound **1.59 - ARB 272542**.

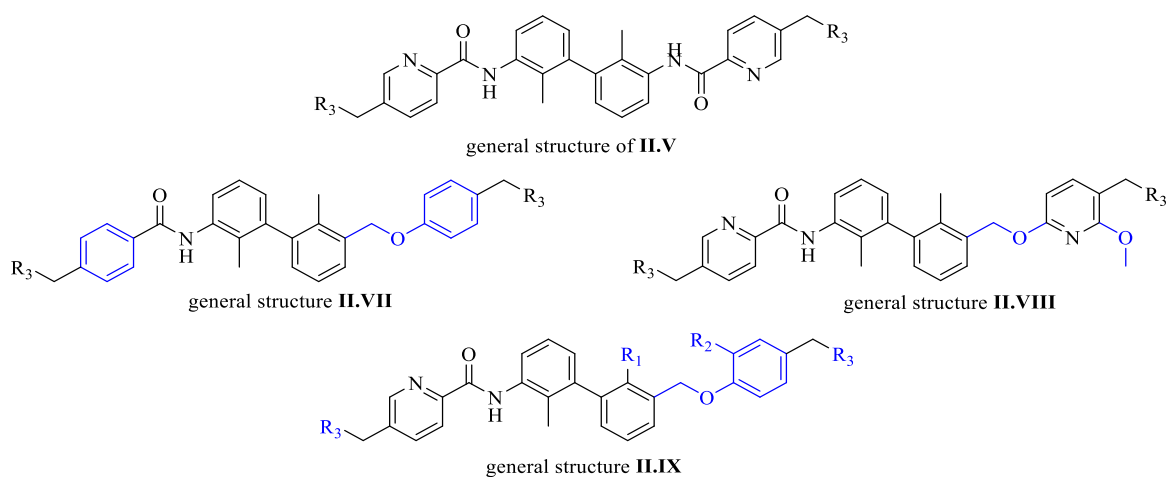


Figure 51. General structure **II.V** and three proposed modifications of dimeric pseudo *C*<sub>2</sub>-symmetric potential PD-1/PD-L1 immunomodulators (general structure **II.VII**, general structure **II.VIII** general structure **II.IX**).

In all general structures main modification concerned the desymmetrization of the scaffold by exchange of one amide bond into an etheric linker. Moreover, additional modification proposed within general structure **II.VII** involve the adjustment of the type of aromatic moieties within the scaffold. Thus, in the general structure **II.V** both of pyridine moieties were exchanged into phenyl components. According to the general structure **II.VIII** except the introduction of ether linker, -OMe substituent within pyridine moiety was added. Furthermore, the general structure **II.IX** propose the exchange of both: linker and aromatic moiety. Consequently, ether bond appears between phenyl ring of biphenyl nucleus and distal phenylic ring. Furthermore, the proposal of the third general structure **II.IX** corresponds to the adjustment of the R<sub>1</sub> substituent within the biphenyl core, the elaboration of the R<sub>2</sub> substituent on the one of the aryl component and the optimization of the solubilizing agent R<sub>3</sub>.

## 2.7.2. Synthesis and Activity Determination of Elongated *Pseudo C*<sub>2</sub>-symmetric PD-1/PD-L1 inhibitors

The synthetic pathway to obtain dimeric pseudo *C*<sub>2</sub>-symmetric compound according to the structure was presented in Figure 52.

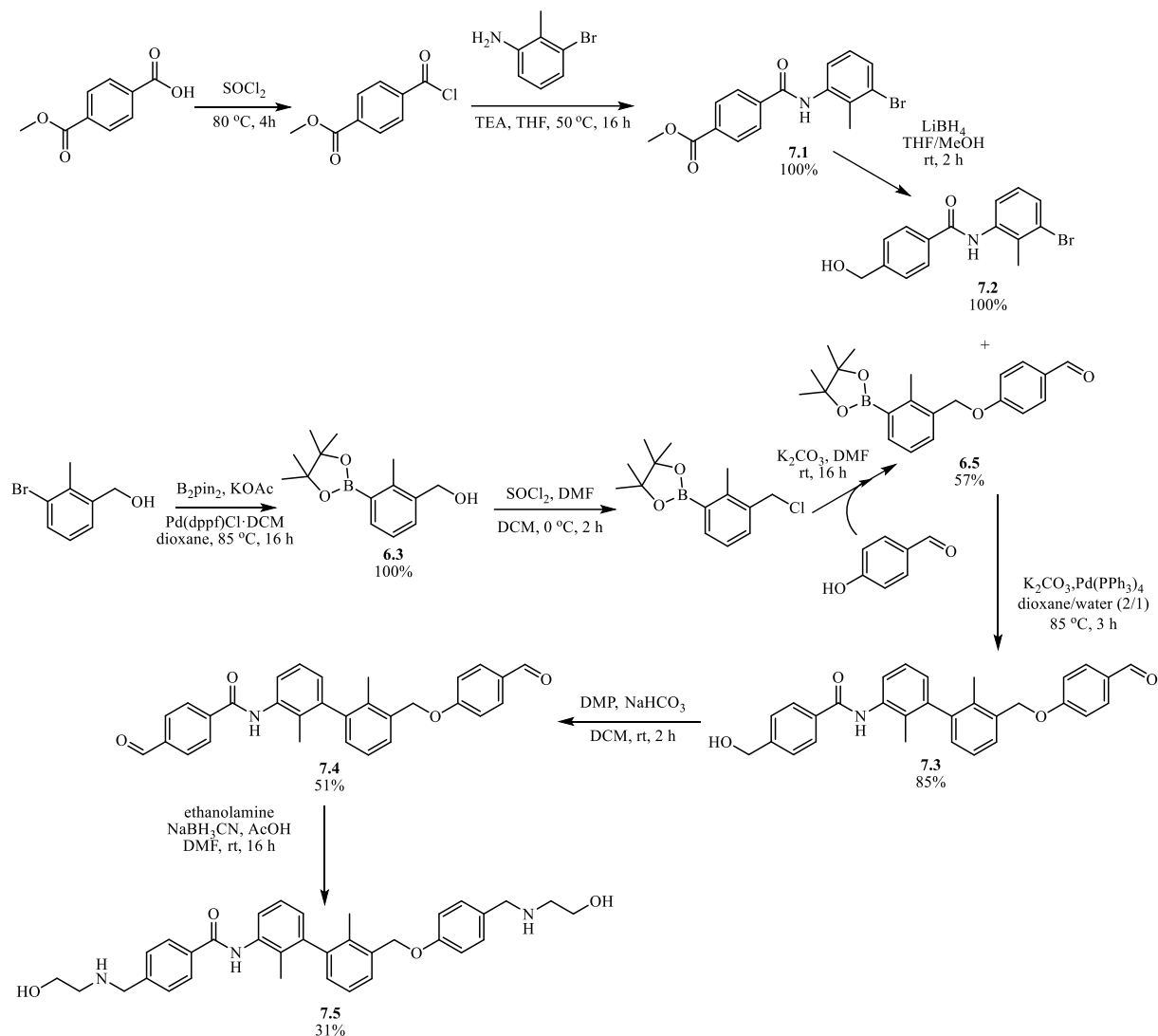


Figure 52. Synthetic pathway to obtain dimeric pseudo *C*<sub>2</sub>-symmetric elongated PD-L1 inhibitor – **7.5** (derivative of general structure **II.VII**).

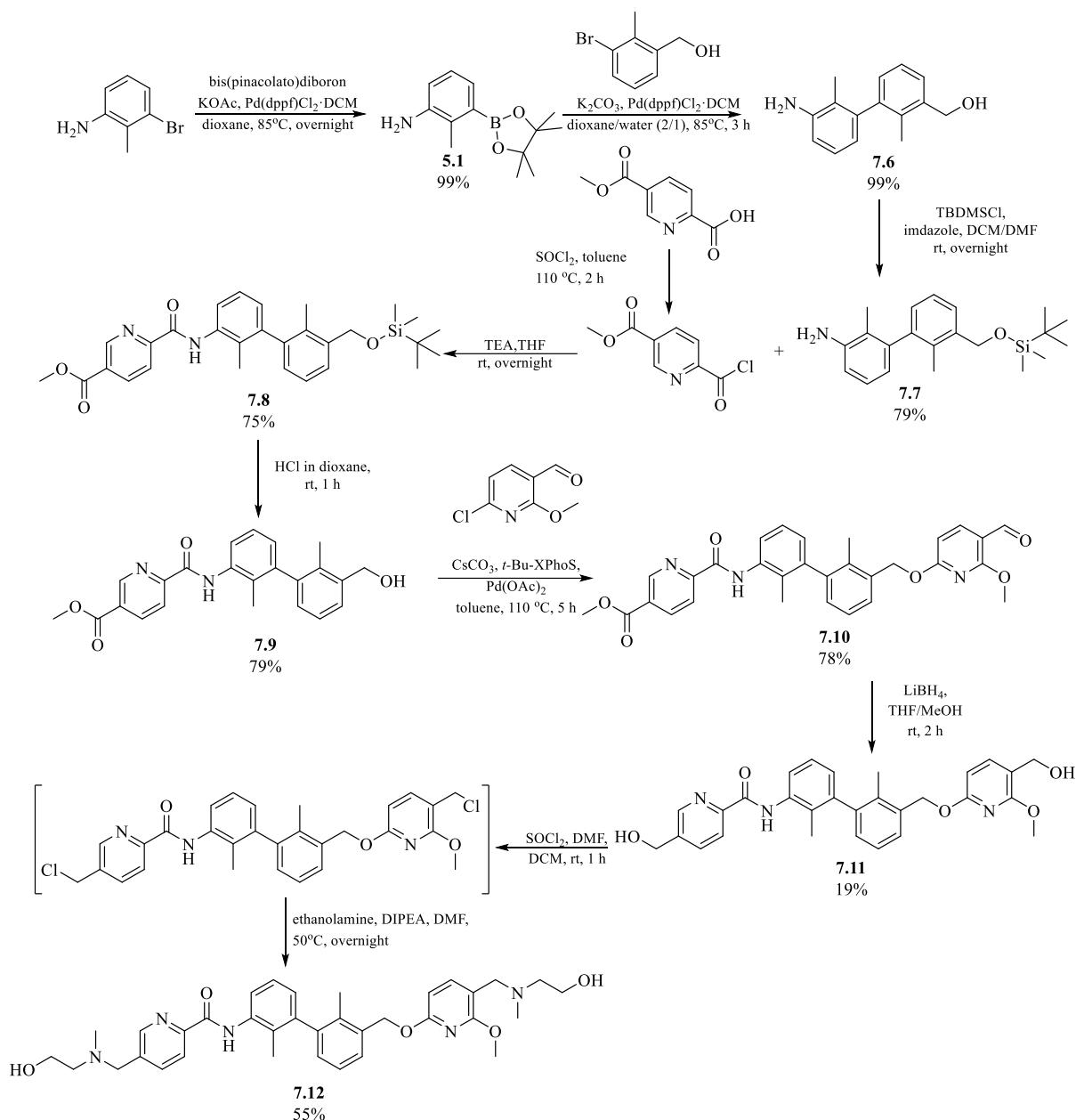
Two parallel synthetic routes were followed to prepare suitable co-substrates for further coupling. The first one started from 4-(methoxycarbonyl)benzoic acid, which was heated in thionyl chloride under anhydrous conditions, allowing its conversion to the corresponding acid chloride. After removing the excess of thionyl chloride under reduced pressure, 3-bromo-2-methylaniline and triethylamine were added dropwise, resulting in the precipitation of **7.1**. Following, ester group of **7.1** was selectively reduced by the application of  $\text{LiBH}_4$  to form the

alcohol **7.2**. In the same time, a second co-substrate was prepared. For this purpose, boronic acid ester was obtained from (3-bromo-2-methylphenyl)methanol *via* Suzuki-Miyaura reaction. The obtained boronic ester was transferred to 1-bromo-3-(chloromethyl)-2-methylbenzene and used for *O*-alkylation of deprotonated 4-hydroxybenzaldehyde. Subsequently, the isolated boronic ester – **6.5** – was coupled to the previously prepared aryl bromide – **7.2** – by palladium-mediated Suzuki cross-coupling. Formed **7.3** was further subjected to reaction with Dess-Martin periodinane to oxidize molecule's hydroxyl group and provide compound with two formyl substituents (**7.4**). Finally, reductive amination with ethanolamine performed on both formyl groups of the molecule afforded the final compound **7.5** with 31% yield.

The synthesis of the final compound related to the general structure **II.VIII** was started from 3-bromo-2-methylaniline (Figure 53). Substrate as aryl bromide was converted to the corresponding boronic acid ester *via* a palladium-assisted Suzuki-Miyaura reaction. The reaction was carried out under anhydrous conditions to avoid coupling of the formed boronic derivative with unreacted bromoaryl. Further, the formed **5.1** underwent reaction with (3-bromo-2-methylphenyl)methanol to form C-C bond between two phenyl rings and consequently to construct biphenylic derivative (**7.6**). In the next step, the hydroxyl group was protected with trimethylsilyl chloride, forming **7.7**, what provide the selectivity of the next reaction step. Subsequently, compound **7.7** was subjected to acylation of its -NH<sub>2</sub> group with previously prepared acid chloride, which led to precipitation of the reaction product after addition of triethylamine. Subsequently, the isolated compound **7.8** was deprotected and the removal of the TMS group appeared after application of strong acidic conditions.

To further elongate the structure of the molecule, Buchwald-Hartwig coupling was applied and the fourth aromatic ring was attached by C-O bond formation. Usually, Buchwald-Hartwig reaction involves the formation of C-N bond between aryl halide and amine moiety. Furthermore, the bond formation occurs after the support of palladium catalyst and ligand under basic conditions (Forero-Cortés *et al.*, 2019). However, it has been shown that alcohols, as another class of nucleophiles, can also be coupled with aryl halides to form the corresponding aryl ethers (Mann *et al.*, 1999). Subsequently, an excess of lithium borohydride was applied, what provided the simultaneous reduction of both ester and formyl groups. This allowed the formation of compound **7.11**, bearing two hydroxyl groups, which were further converted to good leaving groups in the Vilsmeier-Haack reaction. In the final step, 2-(methylamino)ethan-1-ol was introduced *via* S<sub>N</sub>2 reaction, leading to the final molecule **7.12**.





A synthetic route similar to that presented for molecule **7.12** was used to generate Figure 53. Synthetic pathway to obtain dimeric pseudo C<sub>2</sub>-symmetric elongated PD-L1 inhibitor – **7.12** (derivative of general structure **II.VIII**).

derivatives of general structure **II.IX** (Figure 54). Likewise in the previous synthetic scheme, boronic acid ester (**5.1**) was coupled with two different benzyl alcohol derivatives to form **7.6** ( $R_1 = \text{CH}_3$ ) and **7.13** ( $R_2 = \text{F}$ ). In the next steps, the corresponding alcohols were protected (**7.7**, **7.14**) and amides –**7.8**, **7.15** –were formed by acylation of aniline derivatives. Subsequently, hydroxyl groups were released by removal of the -TMS groups. The hydroxyl groups of isolated alcohols (**7.9**, **7.16**) were converted into corresponding chlorides and Williamson etherification was performed with various  $R_2$ -substituted 4-hydroxyaldehydes. The obtained compounds – **7.17-7.20** – underwent lithium borohydride assisted reduction to form analogous dialcohols –

**7.21-7.24.** The latest one converted to the corresponding chlorides, were subjected to nucleophilic substitution with various amine moieties to generate a series of final small molecule inhibitors.

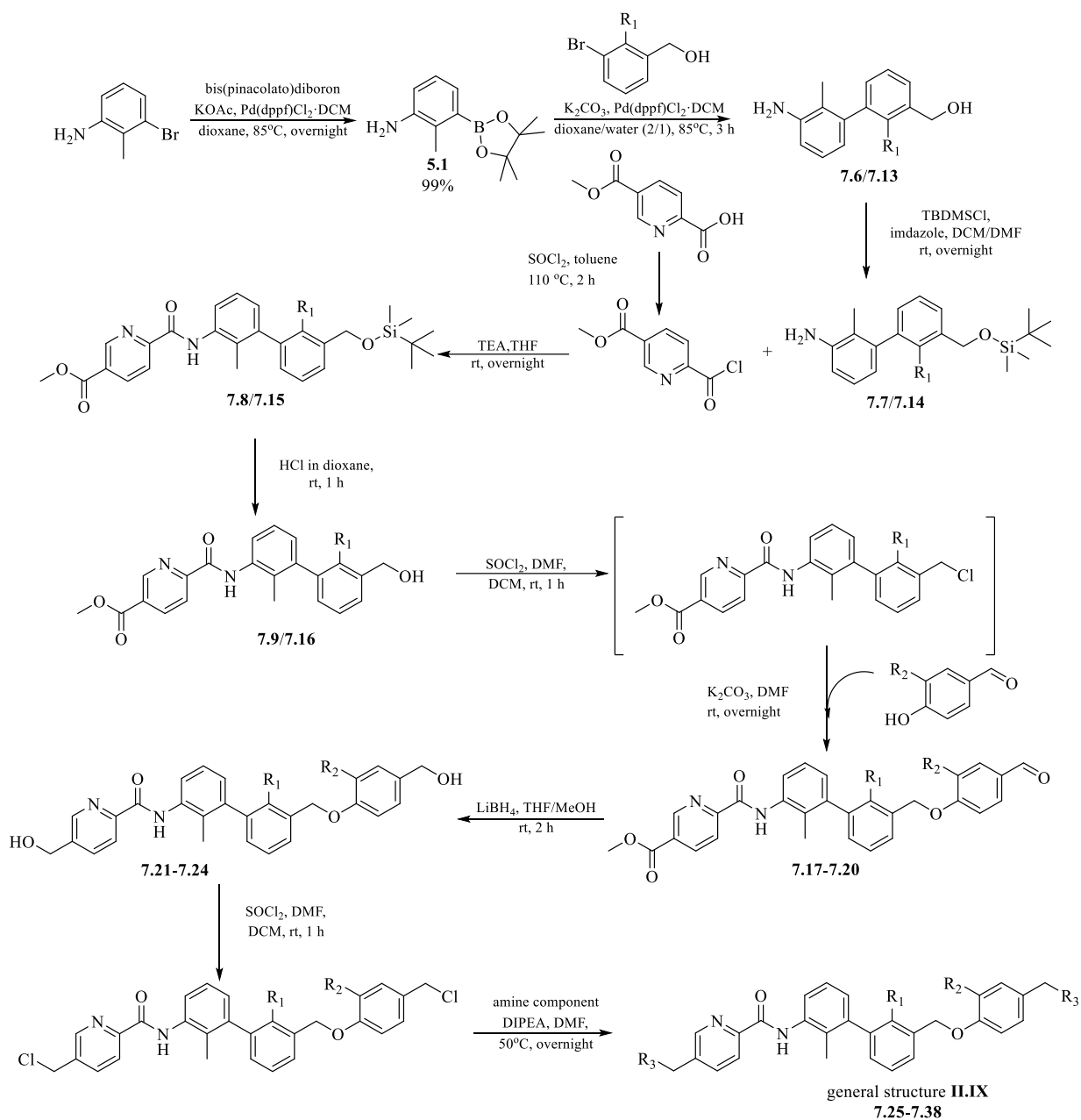
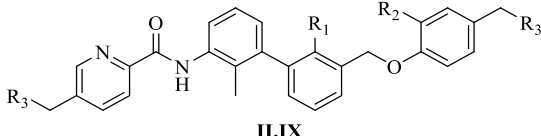
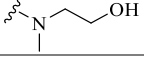
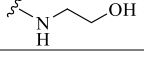
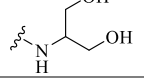
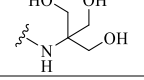
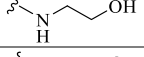
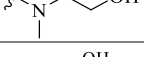
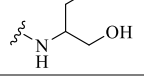
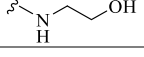
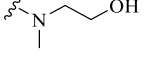
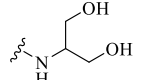
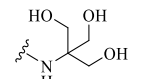
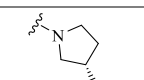
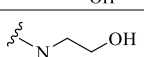
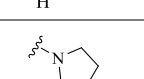


Figure 54. Synthetic pathway to obtain series of dimeric pseudo C<sub>2</sub>-symmetric elongated PD-L1 inhibitors as general structure **II.IX** derivatives. Yields of obtained compounds: **7.6** (where R<sub>1</sub> is -Me: 99%), **7.13** (where R<sub>1</sub> is -F: 74%), **7.7** (where R<sub>1</sub> is -Me: 79%), **7.14** (where R<sub>1</sub> is -F: 92%), **7.8** (where R<sub>1</sub> is -Me: 75%), **7.15** (where R<sub>1</sub> is -F: 85%), **7.9** (where R<sub>1</sub> is -Me: 100%), **7.16** (where R<sub>1</sub> is -F: 81%), **7.17** (where R<sub>1</sub> is -Me and R<sub>2</sub> is Br: 77%), **7.18** (where R<sub>1</sub> is -F and R<sub>2</sub> is Br: 76%), **7.19** (where R<sub>1</sub> is -Me and R<sub>2</sub> is Me: 71%), **7.20** (where R<sub>1</sub> is -Me and R<sub>2</sub> is -OMe: 88%), **7.21** (where R<sub>1</sub> is -Me and R<sub>2</sub> is Br: 71%), **7.22** (where R<sub>1</sub> is -F and R<sub>2</sub> is Br: 46%), **7.23** (where R<sub>1</sub> is -Me and R<sub>2</sub> is Me: 99%), **7.24** (where R<sub>1</sub> is -Me and R<sub>2</sub> is -OMe: 82%). The sets of all R<sub>1</sub>, R<sub>2</sub> R<sub>3</sub> substituents and respective reaction yields for products after last reaction step are illustrated in the Table 12.

The Table 12 comprises the characterization of all obtained final products with applied set of R<sub>1</sub>, R<sub>2</sub> and R<sub>3</sub> substituents. In addition, the reaction yields associated with the generation of each of the listed compounds have been correlated.

Table 12. The comparison of inhibitors' substituents arrangement within general structure **II.IX**.

 <b>II.IX</b>				
Name of the compound	R <sub>1</sub>	R <sub>2</sub>	R <sub>3</sub>	Y [%]
<b>7.25</b>	-CH <sub>3</sub>	-OCH <sub>3</sub>		61
<b>7.26</b>	-CH <sub>3</sub>	-OCH <sub>3</sub>		44
<b>7.27</b>	-CH <sub>3</sub>	-OCH <sub>3</sub>		26
<b>7.28</b>	-CH <sub>3</sub>	-OCH <sub>3</sub>		35
<b>7.29</b>	-CH <sub>3</sub>	-CH <sub>3</sub>		58
<b>7.30</b>	-CH <sub>3</sub>	-CH <sub>3</sub>		46
<b>7.31</b>	-CH <sub>3</sub>	-CH <sub>3</sub>		38
<b>7.32</b>	-CH <sub>3</sub>	-Br		32
<b>7.33</b>	-CH <sub>3</sub>	-Br		50
<b>7.34</b>	-CH <sub>3</sub>	-Br		32
<b>7.35</b>	-CH <sub>3</sub>	-Br		36
<b>7.36</b>	-CH <sub>3</sub>	-Br		54
<b>7.37</b>	-F	-Br		34
<b>7.38</b>	-F	-Br		47

To assess the ability of **7.5**, **7.12**, **7.25-7.38** to displace PD-1 from PD-1/PD-L1 complex HTRF assay and ICB cell-based tests were conducted and obtained results are summarized in Table 13.

Table 13. The biochemical activity of inhibitors obtained as general structures **II.VII-IX** derivatives.

Name of the compound	HTRF*	EC <sub>50</sub> [nM]
<b>7.25</b>	24% (5 nM)	n.a.
<b>7.26</b>	9% (5 nM)	10228
<b>7.27</b>	43 ± 5.0% (5 nM)	4585
<b>7.28</b>	53.2 ± 5.4% (5 nM)	1886
<b>7.29</b>	9 ± 1% (5 nM) IC <sub>50</sub> = 1.11 ± 0.00 nM	1255
<b>7.30</b>	1 ± 0% (5 nM)	1721
<b>7.31</b>	4 ± 1% (5 nM) IC <sub>50</sub> = 0.60 ± 0.02 nM	225
<b>7.32</b>	3.0 ± 3.1% (50 nM) 91.6 ± 1.2% (5 nM) IC <sub>50</sub> = 0.92 ± 0.01 nM	321
<b>7.33</b>	4 ± 0% (5 nM) IC <sub>50</sub> = 0.05 ± 0.01 nM	334
<b>7.34</b>	3.5 ± 0.5% (5 nM) IC <sub>50</sub> = 6.1 ± 0.2 nM	219
<b>7.35</b>	1.8 ± 1.4% (50 nM) 83.9 ± 2.6% (5 nM) IC <sub>50</sub> = 0.47 ± 0.03 nM	54
<b>7.36</b>	2.9 ± 0.5% (5 nM) IC <sub>50</sub> = 13.6 ± 0.50 nM	491
<b>7.37</b>	4 ± 1% (5 nM) IC <sub>50</sub> = 0.22 ± 0.01 nM	1238
<b>7.38</b>	7 ± 1% (5 nM)	n.a.
<b>7.12</b>	86 ± 2% (5 nM)	687
<b>7.5</b>	82.6 ± 1.3 (5 nM)	n.t.

\*results shown as the percentage of undissociated PD-1/PD-L1 complex in conditions of 5 nM or 0.5 nM compound's concentration

\*\* n.a. refers to not active

\*\*\* n.t. refers to not tested

Preliminary, all the compounds were tested in HTRF assay with 0.5 nM or 5 nM antagonist concentration. Selected compounds were further tested to determine their IC<sub>50</sub> values. Analyzing the obtained results, eight of obtained compounds – **7.29, 7.31- 7.37** featured IC<sub>50</sub> values below 15 nM. Among these inhibitors, six molecules – **7.29, 7.31-7.33, 7.35, and 7.37** exhibit maximal half inhibitory concentrations around 1 nM values.

Although HTRF provides a relatively rapid and convenient method for determining  $IC_{50}$ , the half-maximal inhibitory concentration values depend on several factors such as ligand and protein concentration and process environment. In addition, HTRF is a much simpler experimental model, accordingly, we need to assess compound activity together with an immune checkpoint cell-based assay. Derived from the cell-based assay, the half-maximal effective concentration ( $EC_{50}$ ) is calculated from the experimental responses of a much more complicated system where whole cells are treated with inhibitors. This is in contrast to the HTRF assay where the isolated proteins are used. Thus, in ICB, where protein systems are subject to effects such as post-translational modifications of receptors including glycosylation and molecular crowding,  $EC_{50}$  values are more reliable for characterizing the potency of compounds.

Therefore, to further study compounds' affinity toward PD-L1 target, a cell-based ICB assay was conducted. Obtained values showed that seven out of all tested compounds exhibit half maximal effective concentrations below 1  $\mu$ M values, what proves the significant ability of compounds **7.31-7.36** and **7.12** to induce effector T cells. The best of the synthesized within this group of compounds – inhibitor **7.35** - exhibits the ability to unleash TCR signaling with an  $EC_{50}$  value of 54 nM.

Moreover, to understand the obtained results structure-activity relationship was studied. SAR analyses proved that additional modifications were proposed within general structure **II.VII** (compound **7.5**) did not provide the enhancement of the compound's potency. Exchanging both pyridine moieties from **1.59 - ARB272542** into phenyl components resulted that composed compound **7.5** was able to dissociate only 17% of the present PD-1/PD-L1 complex with 5 nM concentration.

According to modifications introduced within general structure **II.VIII**, result of ICB test shows that compound **7.12** exhibit  $EC_{50}$  value of 687 nM. This quiet satisfying result was obtained after elongation of short inhibitors and desymmetrization of **1.59 - ARB272542** by the introduction of ether linker between -OMe bearing pyridine moiety and biphenyl core.

Further analyses prove that most of the compounds, which exhibit the lowest  $EC_{50}$  values are derivatives of general structure **II.IX** with a specific arrangement of substituents. Studies showed that definitely, -CH<sub>3</sub> is more favored in R<sub>1</sub> position than -F substituent. For example, compounds **7.32** and **7.37** differing only with substituent R<sub>1</sub> (**7.32**, R<sub>1</sub> = -CH<sub>3</sub> and **7.37**, R<sub>1</sub> = -F) presents completely different  $EC_{50}$  values. Half maximal inhibitory value for molecule **7.32** is  $EC_{50}$  = 321 nM, while compound **7.37** can be characterized with  $EC_{50}$  = 1238 nM.

Additionally, the best substituent in R<sub>2</sub> position was found to be -Br. Similarly in this case we can compare how the exchange of substituent R<sub>2</sub> influences the potency of the molecule towards PD-L1 inhibition. For example here, compounds **7.32**, **7.29**, and **7.26** are modified only at R<sub>2</sub> position (**7.32**, R<sub>2</sub> = -Br; **7.29**, R<sub>2</sub> = -CH<sub>3</sub> and **7.26**, R<sub>2</sub> = -OCH<sub>3</sub>), but EC<sub>50</sub> values differ substantially. We can observe the increase in half maximal effective value from EC<sub>50</sub> = 321 nM for **7.32** to EC<sub>50</sub> = 1255 nM for **7.29** and to EC<sub>50</sub> = 10228 nM for **7.26** while changing R<sub>2</sub> from -Br to -CH<sub>3</sub> and -OCH<sub>3</sub> respectively.

Definitely, the crucial role in molecule activity has the proper choice of the solubilizing agent, which not only provides the essential solubility but also generates numerous interactions with PD-L1. Generally, all tested -OH containing groups from the range of ethanolamine, 2-amino-1,3-propanediol, N-methylethanolamine, and tris(hydroxymethyl)aminomethane were suitable. However, tris(hydroxymethyl)aminomethane was found to be the best choice and second best was 2-amino-1,3-propanediol. The incorporation of tris(hydroxymethyl)aminomethane agent into the structure of inhibitor **7.35** provided the best results of 54 nM EC<sub>50</sub> value.

Additionally the cytotoxic effect of synthesized molecules was studied. Unfortunately, the best inhibitor **7.35** was found to be toxic above 1.2 μM concentration of the compound. Toxicity tests performed on the other inhibitors, which exhibit promising low EC<sub>50</sub> values (**7.31-7.34**, **7.35**, and **7.12**) confirmed the cytotoxic effect of these compounds around 1 μM concentrations of small molecules. Therefore, these features rather limit inhibitors' further application, but encourages to further work on elongated inhibitors' structure to keep both: low half maximal effective concentration and infinitesimal cytotoxicity.

### 3. Conclusions and Perspectives

Direct clinical evidence that cancer can be treated through the manipulation of immunity has emerged from the recent clinical success of inhibitors that target immunological checkpoint proteins. Among them, PD-1/PD-L1 immune-checkpoint targeting therapy is becoming the pathway utilized to modulate immune responses. As an alternative to mAbs, small-molecule drugs are arising as promising immunological drug candidates, providing novel strategies for tumor treatment. Better tumor penetration, fewer immune-related adverse effects, and improved oral availability are just some of the advantages associated with the use of small molecules. In addition, the use of small molecular inhibitors could not only improve treatment efficacy but also reduce the high cost of therapy. The simplicity of small molecules preparation and not as rigorous as mAbs' storage conditions strengthened their candidacy on the position of immunological strategies of cancer treatment.

The research presented in this thesis concerns the design, preparation, and characterization of potential PD-1/PD-L1 inhibitors. The first synthetic subject of attention was the preparation of 2H-benzo[b][1,4]oxazin-3(4H)-one's derivatives. The interaction of obtained compounds with PD-L1 protein was preliminarily tested due to  $^1\text{H}$  NMR. The observed broadening of the peaks proved the effect of ligand-induced interaction with protein, although it was evident that the proposed compounds are only weak binders. The weak activity of compounds was also affirmed by HTRF technique, which confirmed the need for further scaffold evaluation.

In the next phase of work, biphenyl-based small-molecule inhibitors of the PD-1/PD-L1 were synthesized. The structure of the inhibitor core was optimized due to techniques such as molecular docking, *weak* AIDA NMR, and HTRF. The application of such methods allows to point out the preferable substituents' arrangement within 1,1'-biphenyl scaffold. The optimized short fragments were further extended to obtain a wide range of 29 final inhibitors. All compounds were characterized by  $^1\text{H}$ NMR,  $^{13}\text{C}$ NMR, LCMS, and HRMS techniques. The preliminary biochemical activity of the prepared molecules was assessed due to HTRF assay, which allowed to estimate the percentage of undissociated PD-1/PD-L1 complex. The compounds with the most promising results were further evaluated in the PD-1/PD-L1 immune checkpoint blockade cell-based assay. Analyses of obtained activities proved, that most of the tested compounds, as well as durvalumab possess the ability to boost effector cell activation, but at much greater concentrations than the antibody. In the tests performed, inhibitor **3.17** emerged as the best of all tested compounds. **3.17** was calculated to have the lowest  $\text{EC}_{50}$  value

of  $6.6 \mu\text{M} \pm 0.8 \text{ M}$  and the highest degree of Jurkat T cell activation (2.1-fold at 50 M compound concentration). The most prominent compound **3.17** provided also satisfying results in the cell viability assay, thus being not toxic up to 100  $\mu\text{M}$  final concentration (Konieczny *et al.*, 2020). This is a much superior outcome than for the BMS-1166 compound (Skalniak *et al.*, 2017, Figure 2a), as BMS-1166 reduced cell viability by 50% at a concentration of 40  $\mu\text{M}$  while other BMS compounds did so at even lower inhibitor concentrations.

The next chapter of the presented thesis comprises the preparation of extended PD-L1 antagonists. The proposed generation of the inhibitors involves the modification of compounds' structure based on the idea to increase the solubility of the inhibitors. Therefore, to increase this factor, the structure of the compounds was elongated and equipped with the second solubilizing group. The first of the proposed structure was prepared as 2,3-dihydro-1H-indene derivative. Evaluation of *in vitro* activity of 2,3-dihydro-1H-indene based inhibitor involved HTRF and ICB cell-based assays. However, the proposed modification of the scaffold did not meet the desired expectations. The introduction of 2,3-dihydro-1H-indene ring and its connection *via* ethenyl moiety with the third aromatic ring caused that compound has decreased affinity towards PD-L1 target.

Subsequently, the described work draws attention to 3,4-dihydro-2H-benzo[b][1,4]oxazine derivatives as potential PD-1/PD-L1 inhibitors. The convergent synthesis allowed to obtain 8 final products with molecules' core based on 3,4-dihydro-2H-benzo[b][1,4]oxazine. However, also at this stage, the introduction of 3,4-dihydro-2H-benzo[b][1,4]oxazine moiety linked to the rest of the scaffold *via* an amide bond, proved to be highly inadvisable. The generated rigidity of the scaffold causes compounds are not flexible enough to reach the protein binding hot spot.

Consequently, further development of the elongated inhibitors and proposal of pseudo- $\text{C}_2$ -symmetric inhibitors emerged. Three new general structures **II.VII-IX** of potential PD-1/PD-L1 inhibitors were proposed as a consequence of the modification of compound **1.59 - ARB272542**. 16 of obtained within this project inhibitors were tested in HTRF and most of them were subjected to ICB cell-based assay, to determine their affinity towards the target. The obtained results clearly demonstrated improved properties of antagonists. Calculated  $\text{IC}_{50}$  values showed that most of the presented compounds were characterized with maximal half inhibitory value in the low nanomolar range. Five from obtained compounds – **7.31-7.33**, **7.35**, and **7.37** featured with  $\text{IC}_{50}$  values below 1 nM. In addition, analyses of  $\text{EC}_{50}$  values showed that six of the synthesized within this group molecules **7.31 - 7.36** possess maximal half



inhibitory values in the range of 0 – 500 nM. The best of the compound exhibit ability to unleash TCR signaling with an EC<sub>50</sub> value of 54 nM.

Analyses of the best results obtained within performed research are presented in the Figure 55 and in the Table 14.

## THE CORELLATION OF IN VITRO ACTIVITY OF PD1/PD-L1 INHIBITORS

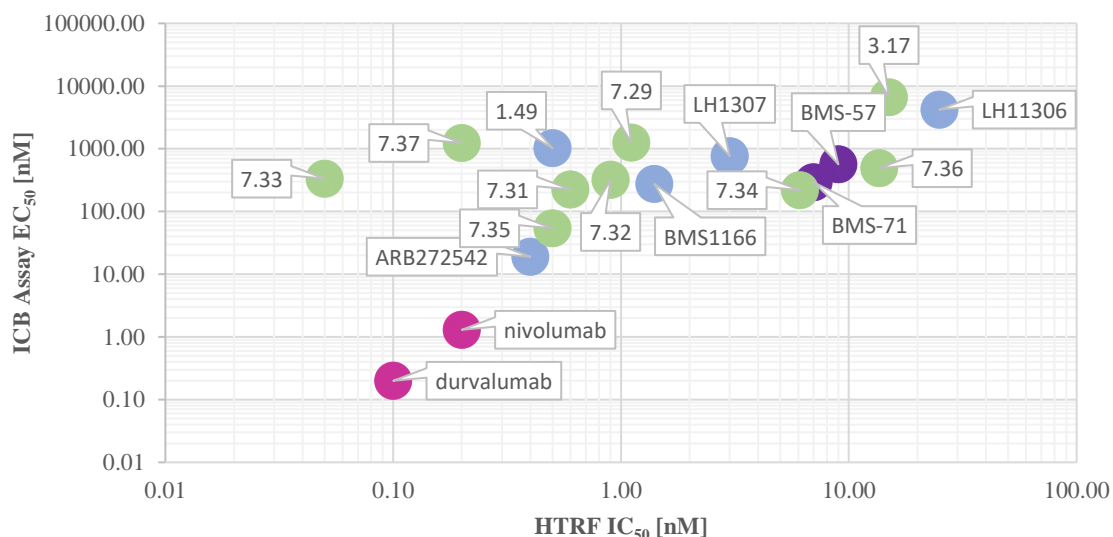


Figure 55. The comparison of the potency of PD-1/PD-L1 inhibitors known in literature and for the synthesized PD-L1 antagonists. The graph correlates IC<sub>50</sub> values from HTRF assay and EC<sub>50</sub> values from ICB assay. Various classes of compounds were visualized in different colours: blue – small molecules known from literature, violet-peptides, pink – antibodies, green – synthesised molecules. The numerical data on the basis of which the chart was presented have been collected in Table 14.

Table 14. The correlation of the IC<sub>50</sub> and EC<sub>50</sub> values of representative PD-L1 inhibitors known from the literature and for the synthesized PD-L1 antagonists. IC<sub>50</sub> values and EC<sub>50</sub> values were determined due to HTRF and ICB assay respectively. (Skalniak *et al.*, 2017; Konieczny *et al.*, 2020; Muszak *et al.*, 2021; Park *et al.*, 2021; Magiera K. *et al.*, 2017; Basu *et al.*, 2019).

Compounds	IC <sub>50</sub> (HTRF)	EC <sub>50</sub> (ICB)
<b>durvalumab</b>	0.1	0.2
<b>nivolumab</b>	0.2	1.3
<b>1.2 (BMS-57)</b>	9.0	566
<b>1.3 (BMS-71)</b>	7.0	293
<b>1.17 - BMS1166</b>	1.4	276
<b>1.49</b>	0.5	1026
<b>1.56 - LH1306</b>	25.0	4214
<b>1.57 - LH1307</b>	3.0	763
<b>1.59 - ARB 272542</b>	0.4	19
<b>3.17</b>	15.0	6632
<b>7.29</b>	1.11	1255
<b>7.31</b>	0.6	225
<b>7.32</b>	0.9	321
<b>7.33</b>	0.05	334
<b>7.34</b>	6.1	219

<b>7.35</b>	0.5	54
<b>7.36</b>	13.6	491
<b>7.37</b>	0.2	1238

The obtained PD-L1 antagonists are correlated to the previously published, outstanding examples of PD-1/PD-L1 inhibitors. Well-known and novel PD-L1 inhibitors were compared with their IC<sub>50</sub> and EC<sub>50</sub> values determine due to HTRF and ICB assays. The investigation proved that the best of synthesized novel PD-L1 inhibitors show similar activity to the previously known small molecular references of PD-L1 inhibitors. Research proved that apart from the difficulties of targeting flat and hydrophobic site of PD-1/PD-L1 interaction it is possible to disrupt PD-1/PD-L1 pathway with the use of small molecules. However, to further enhance small-molecule activity and avoid cytotoxic effects, additional evaluation of the small-molecules' structure is still needed.

## 4. Materials and Methods

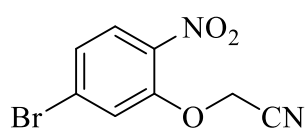
### 4.1. General Information – Organic Synthesis

All solvents, reagents, and starting materials were purchased from commercial sources and were used without prior purification, unless otherwise noted in the procedure. Anhydrous magnesium sulfate was used to dry the solutions. Argon was used as an inert gas. The progress of the reaction was monitored by Thin-layer chromatography (TLC), performed on silica plates (60 F<sub>254</sub>). Chromatograms were visualized with UV radiation (254 nm) or by heating the plates previously placed in solutions with particular TLC stains. <sup>1</sup>H and <sup>13</sup>C NMR spectra were recorded on Bruker Avance 300 or 600 MHz spectrometers with the report of chemical shifts ( $\delta$ ) in ppm and coupling constants ( $J$ ) in Hz. Chemical shifts were related to the internal standard TMS with a singlet at  $\delta$  0 ppm and were analysed in correspondence to the solvent peaks (DMSO-d<sub>6</sub>, CDCl<sub>3</sub>, MeOD-d<sub>4</sub>). Infrared spectra were determined with a Nicolet IR200 spectrometer using ATR technique. High resolution mass spectrometry (HRMS) spectra were performed on microTOF-QII spectrometer using ESI ionisation mode. The UPLC-MS measurements were performed on the UPLC Waters Acquity chromatographic system (column: Acquity UPLC BEH C<sub>18</sub> 1.7  $\mu$ m particle size, 2.1 mm  $\times$  100 mm, equipped with Acquity UPLC BEH C<sub>18</sub> VanGuard pre-column: 1.7  $\mu$ m particle size, 2.1 mm  $\times$  5 mm; method: 12 min, linear gradient 95% - 0% H<sub>2</sub>O (0.1% HCOOH) with acetonitrile (0.1% HCOOH), 0.3 mL/min, detector: Waters Acquity PDE e $\lambda$  UV/Vis). The UPLC Waters Acquity chromatographic system was coupled with Waters TQD mass analyser. The purity of final compounds determined using chromatographic LC-MS was over 95%. Purification of some compounds involved the use of Grace Reveleris X2 Flash Chromatography System with Grace Resolv Silica Cartridges. Melting points were recorded on an Ascon-M5 apparatus.

### 4.2. Synthetic Protocols

#### 4.2.1. Synthesis of 2H-benzo[b][1,4]oxazin-3(4H)-one's Derivative

##### 2-(5-bromo-2-nitrophenoxy)acetonitrile (2.1)

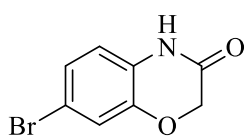


5-bromo-2-nitrophenol (4.00 g, 18.35) and potassium carbonate (6.81 g, 49.35 mmol) were placed in the round bottom flask under argon.

Then, anhydrous DMF (25 mL) was added and the mixture was stirred at room temperature for 30 minutes. Afterwards, bromoacetonitrile (1.58 mL, 2.72 g,

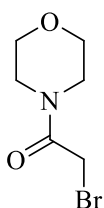
22.67 mmol) was added dropwise. The reaction mixture was stirred at 80 °C for 4 hours, then it was allowed to cool to room temperature and it was stirred overnight. Solvent was removed under reduced pressure and the crude product was purified by flash chromatography (silica gel, 0-100% ethyl acetate in hexane). A yellow solid **2.1** (2.37 g, yield: 50%) was obtained as the product. <sup>1</sup>H NMR (600 MHz, CDCl<sub>3</sub>) δ 7.84 (d, *J* = 8.4 Hz, 1H), 7.44 – 7.38 (m, 2H), 4.93 (s, 2H). <sup>13</sup>C NMR (151 MHz, CDCl<sub>3</sub>) δ 150.1, 139.7, 128.8, 127.4, 127.1, 120.1, 113.7, 55.5.

### 7-bromo-2H-benzo[b][1,4]oxazin-3(4H)-one (2.2)



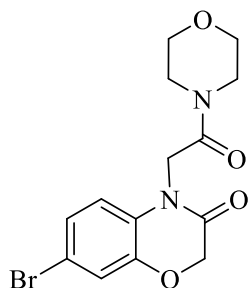
To the mixture of **2.1** (2.37 g, 9.25 mmol) and acetic acid (46 mL), iron (3.03 g, 56 mmol) was added portionwise. The resulted mixture was refluxed for 2 hours and then it was filtered through Celite to separate iron residues. The filtrate was cooled to room temperature, it was diluted with water (100 mL) and it was extracted with ethyl acetate (2x100 mL). The organic layers were combined, dried over anhydrous MgSO<sub>4</sub>, filtered, and the solvent was removed under reduced pressure. The crude product was purified by flash chromatography (silica gel, 0-100% ethyl acetate in hexane). A brown solid **2.2** (1.82 g, yield: 86%) was obtained as the product. <sup>1</sup>H NMR (600 MHz, DMSO) δ 10.79 (s, 1H), 7.14 (d, *J* = 2.1 Hz, 1H), 7.10 (dd, *J* = 8.3, *J* = 2.1 Hz, 1H), 6.81 (d, *J* = 8.3 Hz, 1H), 4.57 (s, 2H). <sup>13</sup>C NMR (151 MHz, DMSO) δ 164.9, 144.6, 127.3, 125.5, 119.4, 117.7, 114.2, 67.2.

### 2-bromo-1-morpholinoethan-1-one (2.3)



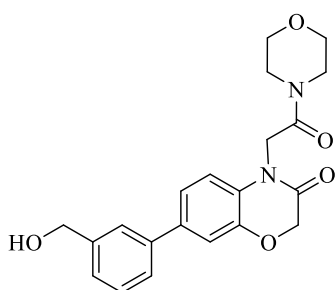
Morpholine (1.73 mL, 1.73 g, 19.82 mmol) was added dropwise to the solution of bromoacetyl bromide (0.86 mL, 2.00 g, 9.91 mmol) in DCM (66 mL) at 0 °C. After 25 minutes of stirring at 0 °C, reaction mixture was warmed up to room temperature and NH<sub>4</sub>Cl was added dropwise. Afterwards, water (100 mL) was added to the reaction mixture and it was washed with dichlorometane (2x100 mL). The organic layers were combined, dried over anhydrous Na<sub>2</sub>SO<sub>4</sub>, filtered, and the solvent was removed under reduced pressure. A colorless oil was obtained as **2.3** (2.08 g, 96% yield). <sup>1</sup>H NMR (600 MHz, CDCl<sub>3</sub>) δ 3.84 (s, 2H), 3.74 – 3.71 (m, 2H), 3.70 – 3.66 (m, 2H), 3.64 – 3.60 (m, 2H), 3.53 – 3.49 (m, 2H). <sup>13</sup>C NMR (151 MHz, CDCl<sub>3</sub>) δ 165.6, 66.7, 66.4, 47.3, 42.5, 25.5.

### 7-bromo-4-(2-morpholino-2-oxoethyl)-2H-benzo[b][1,4]oxazin-3(4H)-one (2.4)



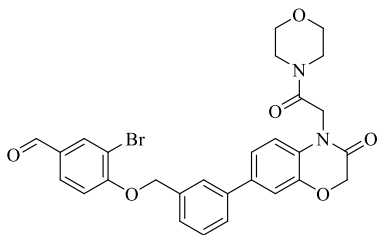
**2.2** (0.80 g, 3.51 mmol) and potassium carbonate (1.94 g, 14.06 mmol) were placed in the round bottom flask under argon and anhydrous DMF (12 mL) was added. Then, **2.3** (1.80 g, 8.75 mmol) was added dropwise and reaction mixture was heated overnight at 50 °C. After that time, solvent was removed under reduced pressure and water (100 mL) was added. Extraction with ethyl acetate (100 mL x 2) was followed to separate the phases. The organic layers were combined, dried over anhydrous MgSO<sub>4</sub>, filtered, and the solvent was removed under reduced pressure. The crude product was purified by flash chromatography (silica gel, 0-100% ethyl acetate in hexane). A colorless solid **2.4** (0.54 g, yield: 44%) was obtained as the product. <sup>1</sup>H NMR (600 MHz, CDCl<sub>3</sub>) δ 7.16 (d, *J* = 2.1 Hz, 1H), 7.11 (dd, *J* = 8.6, 2.2 Hz, 1H), 6.65 (d, *J* = 8.6 Hz, 1H), 4.67 (s, 2H), 4.66 (s, 2H), 3.80 – 3.75 (m, 2H), 3.73 – 3.66 (m, 2H), 3.66 – 3.60 (m, 2H), 3.59 – 3.51 (m, 2H). <sup>13</sup>C NMR (151 MHz, CDCl<sub>3</sub>) δ 164.8, 164.8, 145.9, 128.5, 125.9, 120.4, 116.3, 116.3, 67.6, 66.9, 66.5, 45.6, 43.0, 42.6.

### 7-(3-(hydroxymethyl)phenyl)-4-(2-morpholino-2-oxoethyl)-2H-benzo[b][1,4]oxazin-3(4H)-one (2.5)



**2.4** (450 mg, 1.27 mmol), (3-(hydroxymethyl)phenyl)boronic acid (230 mg, 1.52 mmol), and potassium carbonate (525 mg, 3.80 mmol) were dissolved in mixture of dioxane and water (8:4 mL, v:v). The mixture was deoxygenated by rinsing with argon for 15 min. Then, resulting mixture was heated up to 85 °C and Pd(dppf)Cl<sub>2</sub>·DCM complex (52 mg, 0.06 mmol) was added. The mixture was stirred at 85 °C for 3 hours. Afterwards, water (100 mL) was added to the reaction mixture and it was extracted with ethyl acetate (2x100 mL). The organic layers were combined, dried over anhydrous MgSO<sub>4</sub>, filtered, and the solvent was removed under reduced pressure. The crude product was purified by flash chromatography (silica gel, 0-100% ethyl acetate in hexane) to give a colorless solid as **2.5** (385 mg, yield: 79%). <sup>1</sup>H NMR (600 MHz, CDCl<sub>3</sub>) δ 7.54 (s, 1H), 7.46 (d, *J* = 7.7 Hz, 1H), 7.42 (t, *J* = 7.6 Hz, 1H), 7.34 (d, *J* = 7.5 Hz, 1H), 7.26 – 7.22 (m, 2H), 6.85 (d, *J* = 8.3 Hz, 1H), 4.76 (s, 2H), 4.73 (s, 2H), 4.72 (s, 2H), 3.80 – 3.76 (m, 2H), 3.75 – 3.71 (m, 2H), 3.69 – 3.64 (m, 2H), 3.62 – 3.57 (m, 2H). <sup>13</sup>C NMR (151 MHz, CDCl<sub>3</sub>) δ 165.2, 164.9, 145.5, 141.7, 140.3, 137.4, 129.3, 128.4, 126.2, 126.2, 125.5, 121.7, 115.8, 115.4, 67.8, 67.0, 66.6, 65.4, 45.6, 43.0, 42.7.

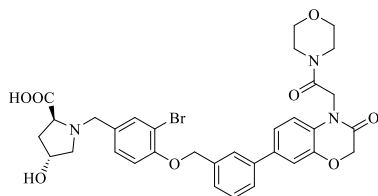
**3-bromo-4-((3-(4-(2-morpholino-2-oxoethyl)-3-oxo-3,4-dihydro-2H-benzo[b][1,4]oxazin-7-yl)benzyl)oxy)benzaldehyde (2.6)**



**2.5** (363 mg, 0.95 mmol) was dissolved in dry DCM (4 mL) and it was cooled to 0 °C. Then SOCl<sub>2</sub> (1.2 mL, 16.54 mmol) was added portionwise. Resulted mixture was refluxed for 3 hours. After that time, NaHCO<sub>3</sub> (50 mL) was added and it was washed with DCM (2 x 50 mL). Organic layers were extracted with water

(50 mL), combined, dried over anhydrous MgSO<sub>4</sub>, filtered, and concentrated under reduced pressure. After drying of the product, K<sub>2</sub>CO<sub>3</sub> (263 g, 1.90 mmol), 3-bromo-4-hydroxybenzaldehyde (197 mg, 0.98 mmol) and anhydrous DMF (5 mL) were added and resulted mixture was stirred overnight at 90 °C. Afterwards, mixture was concentrated under reduced pressure, water was added (50 mL) and it was extracted with ethyl acetate (2 x 50 mL). The organic layers were combined, dried over anhydrous MgSO<sub>4</sub>, filtered, and concentrated. The crude product was purified by flash chromatography (silica gel, 0-100% AcOEt in hexane). The product was obtained as a colorless solid (307 mg, 57%). <sup>1</sup>H NMR (600 MHz, CDCl<sub>3</sub>) δ 9.85 (s, 1H), 8.12 (d, *J* = 2.0 Hz, 1H), 7.80 (dd, *J* = 8.5, 2.0 Hz, 1H), 7.65 (s, 1H), 7.52 (d, *J* = 7.6 Hz, 1H), 7.49 – 7.41 (m, 2H), 7.24 (dd, *J* = 8.3, 2.0 Hz, 2H), 7.07 (d, *J* = 8.5 Hz, 1H), 6.87 (d, *J* = 8.3 Hz, 1H), 5.31 (s, 2H), 4.74 (s, 2H), 4.73 (s, 2H), 3.82 – 3.77 (m, 2H), 3.75 – 3.71 (m, 2H), 3.69 – 3.63 (m, 2H), 3.63 – 3.56 (m, 2H). <sup>13</sup>C NMR (151 MHz, CDCl<sub>3</sub>) δ 189.7, 165.2, 164.8, 159.8, 145.6, 140.5, 137.0, 136.3, 134.9, 131.2, 129.5, 128.6, 126.9, 126.1, 125.5, 121.7, 115.8, 115.5, 113.5, 113.2, 77.2, 71.1, 67.8, 67.0, 66.6, 45.6, 43.0, 42.7.

**(2S,4R)-1-(3-bromo-4-((3-(4-(2-morpholino-2-oxoethyl)-3-oxo-3,4-dihydro-2H-benzo[b][1,4]oxazin-7-yl)benzyl)oxy)benzyl)-4-hydroxypyrrolidine-2-carboxylic acid (2.7)**



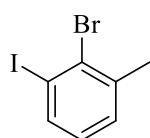
**2.6** (167 mg, 0.30 mmol) and (2S,4R)-4-hydroxypyrrolidine-2-carboxylic acid (253 mg, 1.93 mmol) were dissolved in anhydrous DMF (5 mL) and AcOH (8 droplets) was added. The resulted mixture was stirred for 3 hours at 80 °C. After that time,

NaBH<sub>3</sub>CN (79 mg, 1.25 mmol) was added and reaction mixture was stirred overnight at 60 °C. Solvent was removed under reduced pressure. The crude product was purified by column chromatography (silica gel, 4:1, AcOEt: MeOH) to give the product **2.7** as a colorless solid (50 mg, 25%). <sup>1</sup>H NMR (600 MHz, DMSO) δ 7.77 (s, 1H), 7.65 – 7.61 (m, 2H), 7.51 – 7.43 (m, 2H), 7.36 – 7.31 (m, 3H), 7.20 (d, *J* = 8.5 Hz, 1H), 7.07 (d, *J* = 8.3 Hz, 1H), 5.26 (s, 2H), 4.86

(s, 2H), 4.74 (s, 2H), 4.20 (s, 1H), 3.94 (d,  $J = 12.8$  Hz, 1H), 3.72 – 3.63 (m, 2H), 3.59 (m, 2H), 3.46 – 3.41 (m, 2H), 2.95 – 2.85 (m, 1H), 2.69 – 2.57 (m, 1H), 2.44 – 2.34 (m, 1H), 1.84 – 1.75 (m, 1H). UPLC–MS (DAD/ESI):  $t_R = 4.60$  min, for  $C_{33}H_{34}BrN_3O_8$   $[M + H]^+$  found: 680.38  $m/z$ ; calc. mass: 680.16. HRMS ESI-MS-q-TOF for  $C_{33}H_{34}BrN_3O_8$   $[M + Na]^+$  found: 702.1421  $m/z$ ; calc. mass: 702.1427.

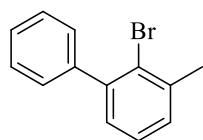
## 4.2.2. Synthesis of Biphenyl Based Small-molecule Inhibitors of the PD-1/PD-L1 Immune Checkpoint

### 2-bromo-1-iodo-3-methylbenzene (3.1.1.1)



Mixture of 95% sulfuric acid (3.3 mL) and water (12.2 mL) was placed in the round bottom, three-neck flask and it was cooled to 0 °C in the ice bath. Afterwards, 2-bromo-3-methylaniline (3.00 g, 16.12 mmol) was added in one portion. To the resulted mixture, aqueous solution of sodium nitrate (19%, 4.4 mL) was added dropwise over 30 minutes and then solution was allowed to stir at 0 °C for 1 h. Subsequently, an aqueous solution of potassium iodine (39%, 4.4 mL) was added carefully to the reaction mixture. The reaction was stopped after 1 h of stirring at room temperature. Saturated aqueous solution of sodium thiosulfate (50 mL) was added and the mixture was extracted with ethyl acetate (100 mL x 3). Organic layers were collected together, dried over  $MgSO_4$  and concentrated under reduced pressure. The crude product was purified by flash chromatography (silica gel, 0-20% AcOEt in hexane) to give orange oil (3.27 g, yield: 68%).  $^1H$  NMR (600 MHz,  $CDCl_3$ )  $\delta$  7.70 (d,  $J = 7.9$  Hz, 1H), 7.18 (d,  $J = 7.5$  Hz, 1H), 6.90 (t,  $J = 7.7$  Hz, 1H), 2.50 (s, 3H).  $^{13}C$  NMR (151 MHz,  $CDCl_3$ )  $\delta$  140.3, 138.1, 131.8, 130.3, 128.6, 102.6, 26.20. (Konieczny *et al.*, 2020).

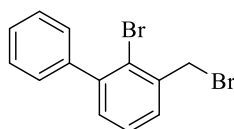
### 2-bromo-3-methyl-1,1'-biphenyl (3.1.1)



**3.1.1.1** (5.63 g, 18.98 mmol), phenylboronic acid (2.32 g, 19.06 mmol), potassium carbonate (9.84 g, 71.27 mmol), and  $Pd(dppf)Cl_2 \cdot DCM$  (0.17 g, 0.08 mmol) were placed in a round-bottom flask under argon. Resulted mixture was solubilized in a mixture of degassed dioxane/water (0.5 M, 2:1, v:v). Reaction was conducted under argon atmosphere by stirring at 85 °C during first 4 h. Then stirring was continued overnight at room temperature. Afterwards, crude mixture was diluted with AcOEt and filtered through Celite. Filtrate was concentrated under reduced pressure. Purification

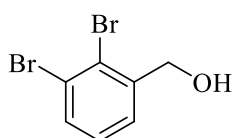
involved flash chromatography (silica gel, 0-20% AcOEt in hexane) and yielded **3.1.1** (3.06 g, 65%) as colorless oil.  $^1\text{H}$  NMR (600 MHz,  $\text{CDCl}_3$ )  $\delta$  7.48 – 7.39 (m, 6H), 7.27 (d,  $J = 1.9$  Hz, 1H), 7.18 – 7.15 (m, 1H), 2.53 (s, 3H).  $^{13}\text{C}$  NMR (151 MHz,  $\text{CDCl}_3$ )  $\delta$  143.5, 142.2, 139.0, 129.8, 129.5, 128.8, 128.0, 127.5, 126.9, 125.5, 24.4. (Konieczny *et al.*, 2020).

### 2-bromo-3-(bromomethyl)-1,1'-biphenyl (**3.1**)



**3.1.1** (970 mg, 3.92 mmol) and NBS (776 mg, 4.36 mmol) were placed in the round bottom flask and were dissolved in tetrachloromethane (86 mL). Resulted mixture was heated to 80 °C. Afterwards, benzoyl peroxide (17 mg, 0.07 mmol) was added. After 2 h of refluxing, second portion of benzoyl peroxide (17 mg, 0.07 mmol) was added to the reaction. Mixture was refluxed for 2 more hours, it was cooled to room temperature and it was concentrated under reduced pressure. The crude product was purified by flash chromatography (silica gel, 0-15% AcOEt in hexane) to give colorless oil (758 mg, yield: 59%).  $^1\text{H}$  NMR (600 MHz,  $\text{CDCl}_3$ )  $\delta$ : 7.47 (dd,  $J = 7.6, 1.7$  Hz, 1H), 7.45 – 7.36 (m, 5H), 7.34 (t,  $J = 7.6$  Hz, 1H), 7.26 (dd,  $J = 7.6, 1.7$  Hz, 1H), 4.72 (s, 2H).  $^{13}\text{C}$  NMR (151 MHz,  $\text{CDCl}_3$ )  $\delta$ : 144.5, 141.5, 138.0, 131.5, 130.5, 129.5, 128.1, 127.9, 125.1. (Konieczny *et al.*, 2020).

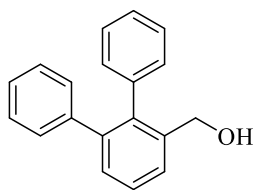
### (2,3-dibromophenyl)methanol (**3.2.1**)



2,3-dibromobenzoic acid (4.00 g, 14.29 mmol) was dissolved in anhydrous THF (15 mL) and it was cooled to °C. To the ice-cooled resulted solution  $\text{BH}_3 \cdot \text{THF}$  complex (1 M, 21.5 mL) was added dropwise over a period of 3 hours. Solution was allowed to warm to room temperature and was stirred for additional 20 h. Subsequently, the mixture was poured into cooled solution of hydrochloric acid (1M, 100 mL) and then it was extracted with  $\text{Et}_2\text{O}$  (2 x 150 mL). The organic layers were collected together, dried over anhydrous  $\text{MgSO}_4$  filtered and concentrated. The crude product was purified by flash chromatography (silica gel, 0-100% AcOEt in hexane) to give colorless solid (3.36 g, yield: 91%).  $^1\text{H}$  NMR (600 MHz,  $\text{CDCl}_3$ )  $\delta$  7.58 (dd,  $J = 7.9, 1.5$  Hz, 1H), 7.47 – 7.43 (m, 1H), 7.22 (t,  $J = 7.8$  Hz, 1H), 4.77 (d,  $J = 6.3$  Hz, 2H), 2.07 (t,  $J = 6.3$  Hz, 1H).  $^{13}\text{C}$  NMR (151 MHz,  $\text{CDCl}_3$ )  $\delta$  142.7, 132.8, 128.7, 127.2, 125.9, 124.5, 66.2. (Konieczny *et al.*, 2020).

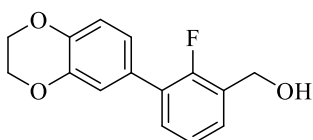


### [1,1':2',1''-terphenyl]-3'-ylmethanol (**3.2**)



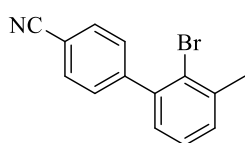
**3.2.1** (3.00 g, 11.32 mmol), potassium carbonate (7.85 g; 56.60 mmol), phenylboronic acid (4.13 g, 33.96 mmol) and Pd(dppf)Cl<sub>2</sub>·DCM (0.10 g, 0.05 mmol) were placed in a round-bottom flask under argon. Resulted mixture was solubilized in a mixture of degassed dioxane/water (0.5 M, 2:1, v:v). Reaction was conducted under argon atmosphere by stirring at 85 °C during first 3 h. Then stirring was continued overnight at room temperature. Afterwards, crude mixture was diluted with AcOEt and filtered through Celite. Filtrate was concentrated under reduced pressure. The crude product was chromatographed on silica gel eluting with 0-40% AcOEt in hexane to give 2.41 g of an colorless solid with yield: 82%. <sup>1</sup>H NMR (600 MHz, CDCl<sub>3</sub>) δ: 7.58 (dd, *J* = 7.6, 0.6 Hz, 1H), 7.47 (t, *J* = 7.6 Hz, 1H), 7.38 (dd, *J* = 7.6, 1.1 Hz, 1H), 7.25 – 7.19 (m, 3H), 7.17 – 7.11 (m, 3H), 7.11 – 7.04 (m, 4H), 4.52 (d, *J* = 5.7 Hz, 2H), 1.59 – 1.54 (m, 1H). <sup>13</sup>C NMR (151 MHz, CDCl<sub>3</sub>) δ: 142.0, 141.6, 139.6, 139.2, 138.9, 130.4, 129.9, 129.7, 128.0, 127.9, 127.6, 127.1, 126.9, 126.4, 63.8. HRMS ESI-MS-q-TOF for C<sub>19</sub>H<sub>16</sub>O [M + Na]<sup>+</sup> found: 283.1092 *m/z*; calc. mass: 283.1099. (Konieczny *et al.*, 2020).

### (3-(2,3-dihydrobenzo[b][1,4]dioxin-6-yl)-2-fluorophenyl)methanol (**3.3**)



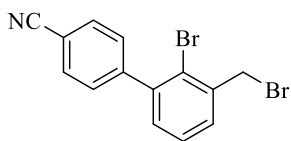
Reaction was conducted in the similar manner as described in case of **3.1.1** (yielded **3.3**: 2.46 g, 97%). <sup>1</sup>H NMR (600 MHz, CDCl<sub>3</sub>) δ: 7.37 (td, *J* = 7.5, 1.7 Hz, 1H), 7.34 (td, *J* = 7.6, 1.8 Hz, 1H), 7.18 (t, *J* = 7.6 Hz, 1H), 7.07 (t, *J* = 1.8 Hz, 1H), 7.04 – 7.01 (m, 1H), 6.93 (d, *J* = 8.4 Hz, 1H), 4.81 (d, *J* = 5.8 Hz, 2H), 4.30 (s, 4H), 1.92 (t, *J* = 6.1 Hz, 1H). <sup>13</sup>C NMR (151 MHz, CDCl<sub>3</sub>) δ: 157.6 (d, 1 *J*<sub>CF</sub> = 247.7 Hz), 143.5, 130.2 (d, *J*<sub>C-F</sub> = 3.3 Hz), 129.0, 128.6 (d, *J*<sub>C-F</sub> = 3.7 Hz), 128.6 (d, *J*<sub>C-F</sub> = 6.3 Hz), 128.0 (d, *J*<sub>C-F</sub> = 4.4 Hz), 124.4 (d, *J*<sub>C-F</sub> = 4.0 Hz), 122.4 (d, *J*<sub>C-F</sub> = 2.4 Hz), 118.1 (d, *J*<sub>C-F</sub> = 2.3 Hz), 117.4, 64.6 (2C), 59.8 (d, <sup>3</sup>*J*<sub>C-F</sub> = 5.6 Hz). HRMS ESI-MS-q-TOF for C<sub>15</sub>H<sub>13</sub>FO<sub>3</sub> [M + Na]<sup>+</sup> found: 283.0740 *m/z*; calc. mass: 283.0746. (Konieczny *et al.*, 2020).

### 2-bromo-4'-isocyano-3-methyl-1,1'-biphenyl (**3.4.1**)



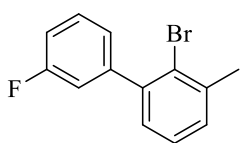
Reaction was conducted in the similar manner as described in case of **3.1.1** (yielded **3.4.1**: 1.86 g, 68%). <sup>1</sup>H NMR (600 MHz, CDCl<sub>3</sub>) δ: 7.69 (d, *J* = 8.5 Hz, 2H), 7.47 (d, *J* = 8.5 Hz, 2H), 7.27 (m, 2H), 7.07 (dd, *J* = 6.8, 2.4 Hz, 1H), 2.48 (s, 3H). <sup>13</sup>C NMR (151 MHz, CDCl<sub>3</sub>) δ: 146.7, 141.5, 139.4, 131.9, 130.8, 130.4, 128.4, 127.2, 124.7, 118.9, 111.4, 24.2. (Konieczny *et al.*, 2020).

### 2-bromo-3-(bromomethyl)-4'-isocyano-1,1'-biphenyl (3.4)



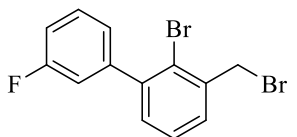
The compound was obtained in the similar way as depicted in case of **3.1** (yielded **3.4**: 0.99 g, 43%). <sup>1</sup>H NMR (600 MHz, CDCl<sub>3</sub>) δ: 7.75 – 7.71 (m, 2H), 7.52 (dd, *J* = 7.7, 1.7 Hz, 1H), 7.51 – 7.48 (m, 2H), 7.38 (t, *J* = 7.6 Hz, 1H), 7.22 (dd, *J* = 7.6, 1.7 Hz, 1H), 4.70 (s, 2H). <sup>13</sup>C NMR (151 MHz, CDCl<sub>3</sub>) δ: 145.9, 142.6, 138.5, 132.0, 131.3, 131.0, 130.4, 127.9, 124.4, 118.9, 111.9, 34.3. HRMS ESI-MS-q-TOF for C<sub>14</sub>H<sub>9</sub>Br<sub>2</sub>N [M + Na]<sup>+</sup> found: 371.8996 *m/z*; calc. mass: 371.8999. (Konieczny *et al.*, 2020).

### 2-bromo-3'-fluoro-3-methyl-1,1'-biphenyl (3.5.1)



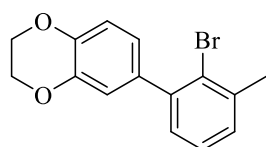
Reaction was conducted in the similar way as depicted in case of **3.1.1** (yielded **3.5.1**: 3.25 g, 91%). <sup>1</sup>H NMR (600 MHz, CDCl<sub>3</sub>) δ: 7.41 (td, *J* = 7.9, 6.0 Hz, 1H), 7.28 (dd, *J* = 6.6, 3.7 Hz, 2H), 7.19 – 7.16 (m, 1H), 7.16 – 7.08 (m, 3H), 2.52 (s, 3H). <sup>13</sup>C NMR (151 MHz, CDCl<sub>3</sub>) δ: 162.3 (d, <sup>1</sup>*J*<sub>C-F</sub> = 245.7 Hz), 144.1 (d, <sup>3</sup>*J*<sub>C-F</sub> = 7.9 Hz), 142.1, 139.0, 130.1, 129.4 (d, <sup>3</sup>*J*<sub>C-F</sub> = 8.3 Hz), 128.5, 126.8, 125.2 (d, <sup>4</sup>*J*<sub>C-F</sub> = 2.5 Hz), 125.0, 116.6 (d, <sup>2</sup>*J*<sub>C-F</sub> = 21.9 Hz), 114.3 (d, <sup>2</sup>*J*<sub>C-F</sub> = 21.0 Hz), 24.2. (Konieczny *et al.*, 2020).

### 2-bromo-3-(bromomethyl)-3'-fluoro-1,1'-biphenyl (3.5)



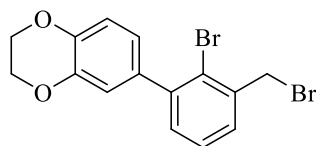
Reaction was conducted in the similar way as described for **3.1** (yielded **3.5**: 2.65 g, 68%). <sup>1</sup>H NMR (600 MHz, CDCl<sub>3</sub>) δ: 7.48 (dd, *J* = 7.6, 1.7 Hz, 1H), 7.42 – 7.37 (m, 1H), 7.35 (t, *J* = 7.6 Hz, 1H), 7.24 (dd, *J* = 7.6, 1.7 Hz, 1H), 7.16 – 7.13 (dt, *J* = 7.7, 1.3 Hz, 1H), 7.12 – 7.08 (m, 2H), 4.71 (s, 2H). <sup>13</sup>C NMR (151 MHz, CDCl<sub>3</sub>) δ: 162.4 (d, <sup>1</sup>*J*<sub>C-F</sub> = 246.3 Hz), 143.4 (d, <sup>3</sup>*J*<sub>C-F</sub> = 8.0 Hz), 143.2, 138.2, 131.3, 130.7, 129.7 (d, <sup>3</sup>*J*<sub>C-F</sub> = 8.3 Hz), 127.7, 125.3 (d, <sup>4</sup>*J*<sub>C-F</sub> = 2.5 Hz), 124.8, 116.7 (d, <sup>2</sup>*J*<sub>C-F</sub> = 22.1 Hz), 114.8 (d, <sup>2</sup>*J*<sub>C-F</sub> = 20.9 Hz), 34.6. (Konieczny *et al.*, 2020)

### 6-(2-bromo-3-methylphenyl)-2,3-dihydrobenzo[b][1,4]dioxine (3.6.1)



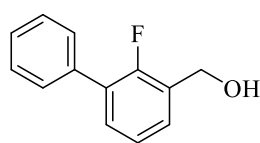
The compound was obtained identically to the compound **3.1.1** (yielded: **3.6.1**: 1.82 g, 64%). <sup>1</sup>H NMR (600 MHz, CDCl<sub>3</sub>) δ: 7.25 – 7.22 (m, 2H), 7.16 – 7.13 (m, 1H), 6.96 – 6.93 (m, 2H), 6.89 (dd, *J* = 8.3, 2.0 Hz, 1H), 4.33 (s, 4H), 2.51 (s, 3H). <sup>13</sup>C NMR (151 MHz, CDCl<sub>3</sub>) δ: 143.1, 143.0, 142.8, 138.9, 135.6, 129.6, 128.9, 126.8, 125.6, 122.8, 118.5, 116.8, 64.6, 64.5, 24.4. (Konieczny *et al.*, 2020).

### 6-(2-bromo-3-(bromomethyl)phenyl)-2,3-dihydrobenzo[b][1,4]dioxine (3.6)



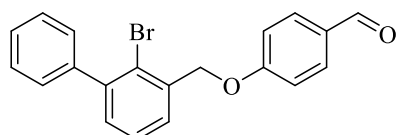
The compound was obtained identically to the compound **3.1** (yielded: **3.6**: 0.90 g, 41%). <sup>1</sup>H NMR (600 MHz, CDCl<sub>3</sub>) δ: 7.43 (dd, *J* = 7.6, 1.7 Hz, 1H), 7.30 (t, *J* = 7.6 Hz, 1H), 7.23 (dd, *J* = 7.6, 1.7 Hz, 1H), 6.93 – 6.90 (m, 2H), 6.85 (dd, *J* = 8.2, 2.2 Hz, 1H), 4.71 (s, 2H), 4.31 (s, *J* = 4.6 Hz, 4H). <sup>13</sup>C NMR (151 MHz, CDCl<sub>3</sub>) δ: 143.9, 143.4, 143.1, 137.9, 134.8, 131.6, 130.2, 127.5, 125.3, 122.8, 118.5, 116.9, 64.6, 35.0. (Konieczny *et al.*, 2020).

### (2-fluoro-[1,1'-biphenyl]-3-yl)methanol (3.7)



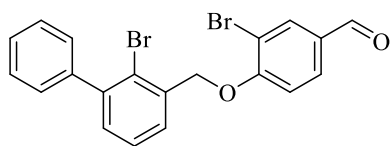
Suzuki coupling was carried out in the similar manner as described in case of **3.1.1** (yielded **3.7**: 1.53 g, 75%). <sup>1</sup>H NMR (600 MHz, CDCl<sub>3</sub>) δ: 7.57 – 7.52 (m, 2H), 7.48 – 7.36 (m, 5H), 7.22 (t, *J* = 7.6 Hz, 1H), 4.83 (d, *J* = 5.7 Hz, 2H), 1.89 (t, *J* = 6.0 Hz, 1H). <sup>13</sup>C NMR (151 MHz, CDCl<sub>3</sub>) δ: 157.6 (d, <sup>1</sup>*J*<sub>C-F</sub> = 248.0 Hz), 135.7, 130.4 (d, *J*<sub>C-F</sub> = 3.4 Hz), 129.2 (m, 2C), 128.7, 128.6 (m, 3C), 128.4 (d, *J* = 4.5 Hz), 127.9, 124.4 (d, *J*<sub>C-F</sub> = 4.1 Hz), 59.8 (d, <sup>3</sup>*J*<sub>C-F</sub> = 5.6 Hz). HRMS ESI-MS-q-TOF for C<sub>13</sub>H<sub>11</sub>FO [M + Na]<sup>+</sup> found: 225.0685 *m/z*; calc. mass: 225.0692. (Konieczny *et al.*, 2020).

### 4-((2-bromo-[1,1'-biphenyl]-3-yl)methoxy)benzaldehyde (3.8)



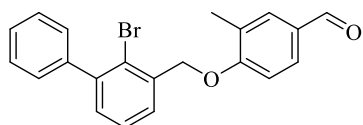
**3.1** (200 mg, 0.62 mmol), 4-hydroxybenzaldehyde (75 mg, 0.62 mmol), and potassium carbonate (170 mg, 1.23 mmol) were stirred in anhydrous DMF (3 mL) at room temperature overnight. The solvent was removed under reduced pressure. Water was added (30 mL), and the mixture was extracted with AcOEt (2 × 30 mL). Organic layers were combined and concentrated. Crude product was purified by column chromatography (silica gel, 0–100% AcOEt in hexane) and crystallized from cyclohexane to yield **3.8** (97 mg, 43%) as a colorless solid. <sup>1</sup>H NMR (600 MHz, CDCl<sub>3</sub>) δ: 9.91 (s, 1H), 7.90–7.86 (m, 2H), 7.54–7.51 (m, 1H), 7.47–7.37 (m, 6H), 7.31 (dd, *J* = 7.5, 1.7 Hz, 1H), 7.15–7.12 (m, 2H), 5.30 (s, 2H). <sup>13</sup>C NMR (151 MHz, CDCl<sub>3</sub>) δ: 190.8, 163.4, 143.7, 141.1, 136.1, 132.1, 130.9, 130.4, 129.4, 128.1, 127.8, 127.5, 127.4, 122.6, 115.2, 70.4. IR (ATR): 2916, 2849, 2835, 1684, 1598, 1591 1508, 1422, 1260, 1164, 1046 cm<sup>-1</sup>. HRMS ESI-MSq-TOF for C<sub>20</sub>H<sub>15</sub>BrO<sub>2</sub> [M + Na]<sup>+</sup> found: 389.0148 *m/z*; calc. mass: 389.0153. Mp: 87.7 °C. UPLC-MS (DAD/ESI): t<sub>R</sub> = 8.78 min, for C<sub>20</sub>H<sub>15</sub>BrO<sub>2</sub> [M + H]<sup>+</sup> found: 367.18 *m/z*; calc. mass: 367.03.

### 3-bromo-4-((2-bromo-[1,1'-biphenyl]-3-yl)methoxy)benzaldehyde (**3.9**)



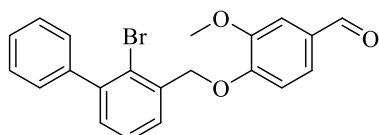
Compound **3.9** was prepared following the procedure for **3.8**. Preparation involved the use of **3.1** (220 mg, 0.68 mmol), 3-bromo-4-hydroxybenzaldehyde (136 mg, 0.68 mmol), and potassium carbonate (187 mg, 1.36 mmol), which were stirred in anhydrous DMF (3 mL) at room temperature overnight. The crude product was purified by column chromatography (silica gel, 0–100% AcOEt in hexane) and yielded **3.9** (119 mg, 39%) as a colorless solid. <sup>1</sup>H NMR (600 MHz, CDCl<sub>3</sub>) δ: 9.87 (s, 1H), 8.15 (d, *J* = 2.0 Hz, 1H), 7.83 (dd, *J* = 8.4, 2.0 Hz, 1H), 7.69 (d, *J* = 7.7 Hz, 1H), 7.49–7.37 (m, 6H), 7.32 (dd, *J* = 7.5, 1.5 Hz, 1H), 7.11 (d, *J* = 8.5 Hz, 1H), 5.36 (s, 2H). <sup>13</sup>C NMR (151 MHz, CDCl<sub>3</sub>) δ: 189.7, 159.5, 143.6, 141.1, 135.7, 134.8, 131.3, 131.3, 130.9, 129.6, 128.2, 127.9, 127.7, 127.2, 121.9, 113.4, 113.1, 71.1. IR (ATR): 3082, 2923, 2852, 1683, 1593, 1492, 1276, 1256, 1185, 1050 cm<sup>-1</sup>. HRMS ESI–MS–q–TOF for C<sub>20</sub>H<sub>14</sub>Br<sub>2</sub>O<sub>2</sub> [M + Na]<sup>+</sup> found: 466.9249 *m/z*; calc. mass, 466.9258. Mp: 151.2 °C. UPLC–MS (DAD/ESI): t<sub>R</sub> = 9.37 min, for C<sub>20</sub>H<sub>14</sub>Br<sub>2</sub>O<sub>2</sub> [M + H]<sup>+</sup> found: 447.07 *m/z*; calc. mass: 446.94.

### 4-((2-bromo-[1,1'-biphenyl]-3-yl)methoxy)-3-methylbenzaldehyde (**3.10**)



Compound **3.10** was obtained according to the procedure of **3.8**, using **3.1** (200 mg, 0.62 mmol), 4-hydroxy-3-methylbenzaldehyde (84 mg, 0.62 mmol), potassium carbonate (170 mg, 1.23 mmol), and anhydrous DMF (3 mL). The crude product was purified by column chromatography (silica gel, 0–100% AcOEt in hexane) and was crystallized from cyclohexane to yield **3.10** (90 mg, 38%) as a colorless solid. <sup>1</sup>H NMR (600 MHz, CDCl<sub>3</sub>) δ: 9.88 (s, 1H), 7.76 (d, *J* = 1.1 Hz, 1H), 7.73 (dd, *J* = 8.3, 2.0 Hz, 1H), 7.57–7.53 (m, 1H), 7.47–7.38 (m, 6H), 7.32 (dd, *J* = 7.5, 1.7 Hz, 1H), 7.03 (d, *J* = 8.4 Hz, 1H), 5.30 (s, 2H), 2.41 (s, 3H). <sup>13</sup>C NMR (151 MHz, CDCl<sub>3</sub>) δ: 191.3, 161.7, 143.7, 141.3, 136.6, 131.8, 130.8, 130.1, 129.6, 128.2, 128.1, 127.9, 127.5, 127.3, 122.5, 111.2, 70.4, 16.7. IR (ATR): 2821, 1679, 1599, 1260, 1240, 1125, cm<sup>-1</sup>. HRMS ESI–MS–q–TOF for C<sub>21</sub>H<sub>17</sub>BrO<sub>2</sub> [M + Na]<sup>+</sup> found: 403.0304 *m/z*; calc. mass: 403.0309. Mp: 144.5 °C. UPLC–MS (DAD/ESI): t<sub>R</sub> = 9.31 min, for C<sub>21</sub>H<sub>17</sub>BrO<sub>2</sub> [M + H]<sup>+</sup> found: 381.20 *m/z*; calc. mass: 381.05.

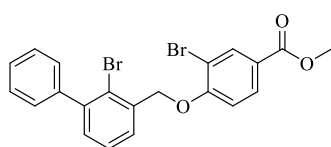
### 4-((2-bromo-[1,1'-biphenyl]-3-yl)methoxy)-3-methoxybenzaldehyde (**3.11**)



Compound **3.11** was prepared following the procedure for **3.8**. Preparation involved the use of **3.1** (300 mg, 0.93 mmol), 4-hydroxy-3-methoxybenzaldehyde (141 mg, 0.93 mmol), and

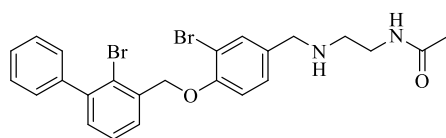
potassium carbonate (255 mg, 1.85 mmol), which were stirred in anhydrous DMF (3 mL) at room temperature overnight. The crude product was purified by column chromatography (silica gel, 0–100% AcOEt in hexane) and yielded **3.11** (192 mg, 52%) as a colorless solid. <sup>1</sup>H NMR (600 MHz, CDCl<sub>3</sub>) δ: 9.87 (s, 1H), 7.53 (ddd, *J* = 10.8, 5.8, 5.0 Hz, 1H), 7.49–7.35 (m, 8H), 7.29 (dd, *J* = 7.5, 1.6 Hz, 1H), 7.01 (d, *J* = 8.2 Hz, 1H), 5.37 (s, 2H), 4.00 (s, 3H). <sup>13</sup>C NMR (151 MHz, CDCl<sub>3</sub>) δ: 191.1, 153.4, 150.2, 143.6, 141.3, 136.2, 130.8, 130.7, 129.6, 128.2, 127.8, 127.6, 127.3, 126.8, 122.2, 112.6, 109.6, 71.0, 56.3. IR (ATR): 2916, 2850, 2834, 1683, 1588, 1507, 1421, 1265, 1235, 1134, 1031 cm<sup>-1</sup>. HRMS ESI-MS-q-TOF for C<sub>21</sub>H<sub>17</sub>BrO<sub>3</sub> [M + Na]<sup>+</sup> found: 419.0253 *m/z*; calc. mass: 419.0259. Mp: 109.0 °C. UPLC-MS (DAD/ESI): t<sub>R</sub> = 8.50 min, for C<sub>21</sub>H<sub>17</sub>BrO<sub>3</sub> [M + H]<sup>+</sup> found: 397.22 *m/z*; calc. mass: 397.04.

### methyl 3-bromo-4-((2-bromo-[1,1'-biphenyl]-3-yl)methoxy)benzoate (**3.12**)



Compound **3.12** was prepared according to the protocol for **3.8**. Preparation involved the use of **3.1** (200 mg, 0.61 mmol), methyl 3-bromo-4-hydroxybenzoate (142 mg, 0.61 mmol), and potassium carbonate (169 mg, 1.22 mmol), which were stirred in anhydrous DMF (5 mL) at room temperature overnight. The crude product was purified by precipitation from AcOEt to give **3.12** (131 mg, 45%) as a colorless solid. <sup>1</sup>H NMR (600 MHz, CDCl<sub>3</sub>) δ: 8.30 (d, *J* = 2.1 Hz, 1H), 7.99 (dd, *J* = 8.6, 2.1 Hz, 1H), 7.71–7.68 (m, 1H), 7.47–7.38 (m, 6H), 7.30 (dd, *J* = 7.5, 1.7 Hz, 1H), 7.01 (d, *J* = 8.6 Hz, 1H), 5.32 (s, 2H), 3.90 (s, 3H). <sup>13</sup>C NMR (151 MHz, CDCl<sub>3</sub>) δ: 165.7, 158.3, 143.4, 141.1, 135.9, 135.0, 130.6, 129.5, 128.0, 127.7, 127.5, 127.1, 124.3, 121.8, 112.5, 112.1, 70.8, 52.2. IR (ATR): 2948, 2163, 1981, 1781, 1599, 1498, 1431, 1363, 1311, 1269, 1240, 1108, 1054 cm<sup>-1</sup>. HRMS ESI-MS-q-TOF for C<sub>21</sub>H<sub>16</sub>Br<sub>2</sub>O<sub>3</sub> [M + Na]<sup>+</sup> found: 496.9447 *m/z*; calc. mass: 496.9364. Mp: 160.3 °C. UPLC-MS (DAD/ESI): t<sub>R</sub> = 9.99 min, for C<sub>21</sub>H<sub>16</sub>Br<sub>2</sub>O<sub>3</sub> [M + H]<sup>+</sup> found: 475.12 *m/z*; calc. mass: 474.95.

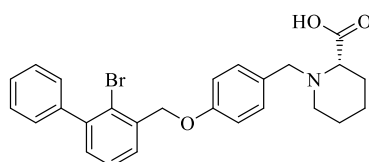
### N-(2-((3-bromo-4-((2-bromo-[1,1'-biphenyl]-3-yl)methoxy)benzyl)amino)ethyl)acetamide (**3.13**)



A solution of **3.9** (200 mg, 0.45 mmol), N-(2-aminoethyl)acetamide (209 mg, 2.05 mmol) with addition of AcOH (3 droplets) was stirred in anhydrous DMF (4 mL) at 25 °C for 2 h. Then, NaBH<sub>3</sub>CN (132 mg, 2.24 mmol) was added, and the resulted mixture was stirred additionally for 20 h. The residue was concentrated under reduced pressure. Water was added (30 mL), and the mixture was extracted with AcOEt (2 × 30 mL). Organic layers

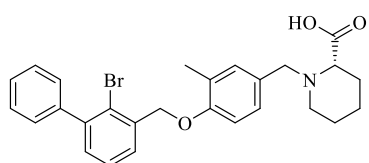
were combined, dried over MgSO<sub>4</sub>, filtered, and concentrated. The crude product was purified by column chromatography (silica gel, 0–30% MeOH in CHCl<sub>3</sub>) to give an off-white solid (126 mg, yield: 53%) as a product. <sup>1</sup>H NMR (600 MHz, DMSO) δ: 7.84 (s, 1H), 7.66 (dd, *J* = 7.6, 1.6 Hz, 1H), 7.62 (d, *J* = 1.9 Hz, 1H), 7.52 (t, *J* = 7.6 Hz, 1H), 7.49–7.45 (m, 2H), 7.44–7.30 (m, 5H), 7.17 (d, *J* = 8.5 Hz, 1H), 5.26 (s, 2H), 3.68 (s, 2H), 3.14 (q, *J* = 6.3 Hz, 2H), 2.55 (t, *J* = 6.5 Hz, 2H), 1.79 (s, 3H). <sup>13</sup>C NMR (151 MHz, DMSO) δ: 169.7, 153.6, 143.4, 141.2, 137.0, 133.2, 131.3, 129.7, 129.3, 128.8, 128.6, 128.2, 122.9, 114.2, 111.4, 71.0, 51.5, 48.2, 38.7, 23.1. IR (ATR): 3280, 3051, 2937, 2829, 2659, 1654, 1556, 1499, 1445, 1369, 1282, 1259, 1056 cm<sup>-1</sup>. HRMS ESI–MS–q–TOF for C<sub>24</sub>H<sub>24</sub>Br<sub>2</sub>N<sub>2</sub>O<sub>2</sub> [M + H]<sup>+</sup> found: 531.0274 *m/z*; calc. mass: 531.0283. Mp: 142.9 °C. UPLC–MS (DAD/ESI): t<sub>R</sub> = 6.13 min, for C<sub>24</sub>H<sub>24</sub>Br<sub>2</sub>N<sub>2</sub>O<sub>2</sub> [M + H]<sup>+</sup> found: 531.22 *m/z*; calc. mass: 531.03.

**(S)-1-(4-((2-bromo-[1,1'-biphenyl]-3-yl)methoxy)benzyl)piperidine-2-carboxylic acid (3.14)**



Compound **3.14** was prepared following the protocol of **3.13**, using **3.8** (90 mg, 0.25 mmol), L-pipecolinic acid (145 mg, 1.22 mmol), NaBH<sub>3</sub>CN (72 mg, 1.23 mmol), AcOH (3 droplets), and DMF (4 mL). The crude product was purified by flash chromatography (silica gel, 0–50% MeOH in CHCl<sub>3</sub>) to give a colorless solid (77 mg, yield: 65%) as the product. <sup>1</sup>H NMR (600 MHz, DMSO) δ: 7.59 (d, *J* = 7.1 Hz, 1H), 7.54–7.25 (m, 9H), 7.04 (d, *J* = 7.9 Hz, 2H), 5.19 (s, 2H), 4.01 (d, *J* = 11.9 Hz, 1H), 3.11 (s, 1H), 2.98 (s, 1H), 2.40 (s, 1H), 1.87 (s, 1H), 1.69 (s, 1H), 1.61–1.43 (m, 3H), 1.35 (s, 1H). <sup>13</sup>C NMR (151 MHz, DMSO) δ: 158.4, 143.5, 141.3, 137.2, 131.8, 131.4, 129.7, 129.5, 128.6, 128.2, 123.4, 115.0, 79.6, 70.3, 58.3, 49.6, 28.5, 23.9, 22.2. IR (ATR): 3055, 2940, 2862, 2352, 2251, 1610, 1513, 1447, 1413, 1386, 1242, 1180, 1028 cm<sup>-1</sup>. HRMS ESI–MS–qTOF for C<sub>26</sub>H<sub>26</sub>BrNO<sub>3</sub> [M + H]<sup>+</sup> found: 480.1169 *m/z*; calc. mass: 480.1174. Mp: 182.5 °C. UPLC–MS (DAD/ESI): t<sub>R</sub> = 6.18 min, for C<sub>26</sub>H<sub>26</sub>BrNO<sub>3</sub> [M + H]<sup>+</sup> found: 480.24 *m/z*; calc. mass: 480.12.

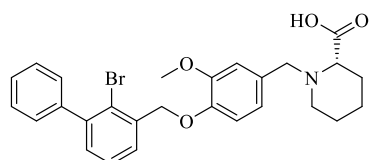
**(S)-1-(4-((2-bromo-[1,1'-biphenyl]-3-yl)methoxy)-3-methylbenzyl)piperidine-2-carboxylic acid (3.15)**



Compound **3.15** was obtained according to the procedure of **3.13**, using **3.10** (90 mg, 0.24 mmol), L-pipecolinic acid (140 mg, 1.08 mmol), NaBH<sub>3</sub>CN (69 mg, 1.18 mmol), AcOH (3 droplets), and DMF (4 mL). The crude product was purified by flash chromatography (silica

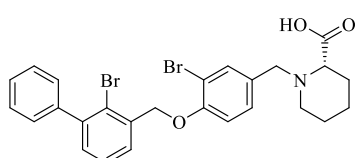
gel, 0–50% MeOH in CHCl<sub>3</sub>) to give a yellow solid (65 mg, yield: 56%) as a product. <sup>1</sup>H NMR (600 MHz, CDCl<sub>3</sub>) δ: 7.50 (d, *J* = 7.5 Hz, 1H), 7.44–7.21 (m, 9H), 6.83 (d, *J* = 7.0 Hz, 1H), 5.06 (s, 2H), 4.39 (d, *J* = 55.8 Hz, 2H), 3.42 (d, *J* = 55.1 Hz, 2H), 2.62 (s, 1H), 2.28 (s, 3H), 1.96 (d, *J* = 9.0 Hz, 2H), 1.85–1.69 (m, 2H), 1.37–1.20 (m, 2H). <sup>13</sup>C NMR (151 MHz, CDCl<sub>3</sub>) δ: 157.8, 143.5, 141.3, 137.0, 134.3, 130.9, 130.6, 129.6, 128.1, 127.9, 127.8, 127.3, 127.2, 122.4, 111.6, 70.1, 58.5, 50.9, 29.8, 28.2, 22.8, 22.1, 16.7. IR (ATR): 2943, 2862, 2390, 2250, 1613, 1505, 1447, 1410, 1288, 1258, 1137, 1003 cm<sup>-1</sup>. HRMS ESI–MS–q–TOF for C<sub>27</sub>H<sub>28</sub>BrNO<sub>3</sub> [M + H]<sup>+</sup> found: 494.1325 *m/z*; calc. mass: 494.1330. Mp: 106.3 °C. UPLC–MS (DAD/ESI): t<sub>R</sub> = 6.54 min, for C<sub>27</sub>H<sub>28</sub>BrNO<sub>3</sub> [M + H]<sup>+</sup> found: 494.26 *m/z*; calc. mass: 494.1330.

**(S)-1-(4-((2-bromo-[1,1'-biphenyl]-3-yl)methoxy)-3-methoxybenzyl)piperidine-2-carboxylic acid (3.16)**



Compound **3.16** was obtained as described for **3.13**. Preparation involved the use of **3.11** (100 mg, 0.25 mmol), L-pipecolic acid (149 mg, 1.15 mmol), NaBH<sub>3</sub>CN (74 mg, 1.26 mmol), AcOH (3 droplets), and DMF (4 mL). The crude product was purified by flash chromatography (silica gel, 0–50% MeOH in CHCl<sub>3</sub>) to give a colorless solid (93 mg, yield: 72%) as a product. <sup>1</sup>H NMR (600 MHz, DMSO) δ: 7.60 (dd, *J* = 7.6, 1.5 Hz, 1H), 7.52–7.33 (m, 7H), 7.09 (s, 1H), 7.05 (d, *J* = 8.2 Hz, 1H), 6.94 (d, *J* = 7.9 Hz, 1H), 5.17 (s, 2H), 4.08 (d, *J* = 12.8 Hz, 1H), 3.80 (s, 3H), 3.15 (s, 1H), 3.04 (s, 1H), 1.96–1.87 (m, 1H), 1.72 (d, *J* = 9.7 Hz, 1H), 1.61–1.53 (m, 3H), 1.41–1.33 (m, 1H). <sup>13</sup>C NMR (151 MHz, DMSO) δ: 149.4, 147.9, 143.4, 141.3, 137.4, 131.4, 129.7, 129.3, 128.6, 128.2, 123.3, 123.1, 114.5, 113.7, 79.6, 71.0, 58.5, 56.1, 49.7, 28.3, 23.6, 22.1. IR (ATR): 3345, 3055, 2939, 2867, 2394, 2251, 1633, 1606, 1517, 1448, 1416, 1268, 1238, 1102, 1029 cm<sup>-1</sup>. HRMS ESI–MS–q–TOF for C<sub>27</sub>H<sub>28</sub>BrNO<sub>4</sub> [M + H]<sup>+</sup> found: 510.1274 *m/z*; calc. mass: 510.1280. Mp: 154.6 °C. UPLC–MS (DAD/ESI): t<sub>R</sub> = 6.10 min, for C<sub>27</sub>H<sub>28</sub>BrNO<sub>4</sub> [M + H]<sup>+</sup> found: 510.28 *m/z*; calc. mass: 510.13.

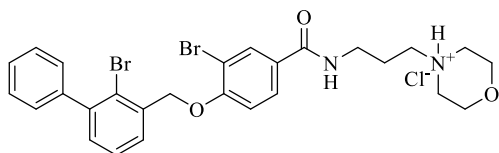
**(S)-1-(3-bromo-4-((2-bromo-[1,1'-biphenyl]-3-yl)methoxy)benzyl)piperidine-2-carboxylic acid (3.17)**



Compound **3.17** was prepared following the protocol of **3.13**, using **3.9** (119 mg, 0.27 mmol), L-pipecolic acid (158 mg, 1.22 mmol), NaBH<sub>3</sub>CN (79 mg, 1.33 mmol), and AcOH (3 droplets), which were stirred in DMF (4 mL). The crude product was purified by flash chromatography (silica gel, 0–50% MeOH in CHCl<sub>3</sub>) to give a colorless solid (77 mg, yield: 51%) as the product.

$^1\text{H}$  NMR (600 MHz, DMSO)  $\delta$ : 7.67 (d,  $J = 6.5$  Hz, 1H), 7.62 (s, 1H), 7.52 (t,  $J = 7.6$  Hz, 1H), 7.50–7.35 (m, 6H), 7.32 (d,  $J = 7.9$  Hz, 1H), 7.18 (d,  $J = 8.4$  Hz, 1H), 5.26 (s, 2H), 3.84 (d,  $J = 13.3$  Hz, 1H), 3.49–3.39 (m, 1H), 3.05 (s, 1H), 2.90–2.83 (m, 1H), 2.24–2.16 (m, 1H), 1.86–1.76 (m, 1H), 1.74–1.62 (m, 1H), 1.58–1.40 (m, 3H), 1.39–1.29 (m, 1H).  $^{13}\text{C}$  NMR (151 MHz, DMSO)  $\delta$ : 153.4, 142.9, 140.7, 136.5, 133.7, 130.9, 129.8, 129.2, 128.3, 128.2, 127.7, 122.4, 113.6, 110.9, 70.6, 64.4, 57.8, 49.2, 28.7, 24.4, 22.0. IR (ATR): 3649, 3075, 2941, 2859, 2392, 2251, 1621, 1496, 1411, 1288, 1260, 1102, 1055  $\text{cm}^{-1}$ . HRMS ESI–MS–q–TOF for  $\text{C}_{26}\text{H}_{25}\text{Br}_2\text{NO}_3$   $[\text{M} + \text{Na}]^+$  found: 580.0097  $m/z$ ; calc. mass: 580.0099. Mp: 129.1  $^\circ\text{C}$ . UPLC–MS (DAD/ESI):  $t_{\text{R}} = 6.51$  min, for  $\text{C}_{26}\text{H}_{25}\text{Br}_2\text{NO}_3$   $[\text{M} + \text{H}]^+$  found: 558.20  $m/z$ ; calc. mass: 558.02.

#### 4-(3-(3-bromo-4-((2-bromo-[1,1'-biphenyl]-3-yl)methoxy)benzamido)propyl)morpholin-4-ium chloride (3.18)

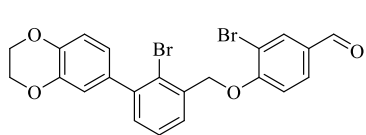


**3.18** (100 mg, 0.21 mmol) and DBU (350  $\mu\text{l}$ ) were stirred in 3-morpholinopropan-1-amine (1.5 mL) at room temperature for 2 days. Afterward, the reaction mixture was solubilized with AcOEt (30 mL).

Following that, water was added ( $30 \times 2$  mL) to wash out the excess of amine from organic layers. Organic layers were dried, combined, and concentrated. Purification involved column chromatography (silica gel, 0–10%  $\text{CHCl}_3$  in MeOH). After purification, compound was converted into the corresponding hydrochloride salt, and product was precipitated from AcOEt to give **3.18** (30 mg, 25%) as a colorless solid.  $^1\text{H}$  NMR (600 MHz,  $\text{CDCl}_3$ )  $\delta$ : 8.14 (t,  $J = 4.0$  Hz, 1H), 8.06 (d,  $J = 2.2$  Hz, 1H), 7.82 (dd,  $J = 8.6, 2.2$  Hz, 1H), 7.73–7.69 (m, 1H), 7.48–7.37 (m, 5H), 7.30 (dd,  $J = 7.5, 1.7$  Hz, 1H), 7.03 (d,  $J = 8.6$  Hz, 1H), 5.31 (s, 2H), 3.78 (t,  $J = 4.6$  Hz, 4H), 3.57 (dd,  $J = 10.9, 5.8$  Hz, 2H), 2.58 (t,  $J = 5.7$  Hz, 2H), 2.53 (s, 4H), 1.84–1.74 (m, 2H).  $^{13}\text{C}$  NMR (151 MHz,  $\text{CDCl}_3$ )  $\delta$ : 165.6, 157.1, 143.5, 141.2, 136.2, 132.1, 130.7, 129.6, 129.0, 128.2, 128.2, 127.8, 127.6, 127.2, 121.9, 113.0, 112.3, 70.9, 67.1, 59.2, 54.1, 41.1, 23.9. IR (ATR): 3460, 3299, 2951, 2856, 2822, 1626, 1604, 1553, 1497, 1285, 1267, 1118, 1056  $\text{cm}^{-1}$ . HRMS ESI–MS–q–TOF for  $[\text{C}_{27}\text{H}_{29}\text{Br}_2\text{N}_2\text{O}_3]^+$   $[\text{M}]$  found: 587.0556  $m/z$ ; calc. mass: 587.0545. Mp: 128.9  $^\circ\text{C}$ . UPLC–MS (DAD/ESI):  $t_{\text{R}} = 6.75$  min, for  $[\text{C}_{27}\text{H}_{29}\text{Br}_2\text{N}_2\text{O}_3]^+$   $[\text{M}]$  found: 587.12  $m/z$ ; calc. mass: 587.05.



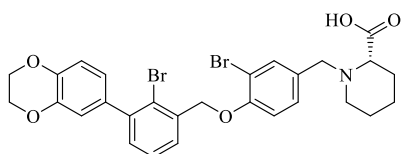
### 3-bromo-4-((2-bromo-3-(2,3-dihydrobenzo[b][1,4]dioxin-6-yl)benzyl)oxy)benzaldehyde



(3.19)

Compound 4a was prepared as described in the protocol of **3.8**, using **3.6** (250 mg, 0.65 mmol), 3-bromo-4-hydroxybenzaldehyde (130 mg, 0.65 mmol), potassium carbonate (180 mg, 1.31 mmol), and anhydrous DMF (4 mL). The crude product was purified by column chromatography (silica gel, 0–100% AcOEt in hexane) and yielded **3.19** (291 mg, 88%) as a colorless solid. <sup>1</sup>H NMR (600 MHz, DMSO)  $\delta$ : 9.88 (s, 1H), 8.15 (d,  $J = 2.0$  Hz, 1H), 7.97 (dd,  $J = 8.5, 2.0$  Hz, 1H), 7.64 (dd,  $J = 7.6, 1.6$  Hz, 1H), 7.52–7.44 (m, 2H), 7.35 (dd,  $J = 7.6, 1.7$  Hz, 1H), 6.94 (d,  $J = 8.3$  Hz, 1H), 6.87 (d,  $J = 2.1$  Hz, 1H), 6.84 (dd,  $J = 8.2, 2.1$  Hz, 1H), 5.40 (s, 2H), 4.29 (s,  $J = 4.6$  Hz, 4H). <sup>13</sup>C NMR (151 MHz, DMSO)  $\delta$ : 190.7, 159.0, 143.2, 142.9, 142.5, 135.8, 134.1, 133.8, 131.3, 131.2, 131.0, 128.5, 127.8, 122.9, 122.3, 118.0, 116.8, 114.1, 111.9, 71.2, 64.2. IR (ATR): 2983, 2952, 1685, 1598, 1494, 1314, 1275, 1258, 1243, 1190, 1062  $\text{cm}^{-1}$ . HRMS ESI-MS-q-TOF for  $\text{C}_{22}\text{H}_{16}\text{Br}_2\text{O}_4$   $[\text{M} + \text{Na}]^+$  found: 524.9348  $m/z$ ; calc. mass: 524.9313. Mp: 196.2 °C. UPLC-MS (DAD/ESI):  $t_{\text{R}} = 8.98$  min, for  $\text{C}_{22}\text{H}_{16}\text{Br}_2\text{O}_4$   $[\text{M} + \text{H}]^+$  found: 503.04  $m/z$ ; calc. mass: 502.95.

### (S)-1-(3-bromo-4-((2-bromo-3-(2,3-dihydrobenzo[b][1,4]dioxin-6-yl)benzyl)oxy)benzyl)piperidine-2-carboxylic acid (3.20)

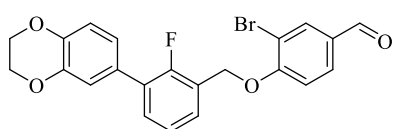


Compound **3.20** was prepared according to the procedure of **3.13**, using **3.19** (310 mg, 0.61 mmol), L-pipecolic acid (364 mg, 2.82 mmol),  $\text{NaBH}_3\text{CN}$  (181 mg, 3.07 mmol), addition of AcOH (3 droplets), and anhydrous DMF (4 mL) as a solvent. The crude product was purified by flash chromatography (silica gel, 0–50% MeOH in  $\text{CHCl}_3$ ) to give a white solid (164 mg, yield: 43%) as the product.

<sup>1</sup>H NMR (600 MHz, DMSO)  $\delta$ : 7.66–7.59 (m, 2H), 7.48 (t,  $J = 7.6$  Hz, 1H), 7.35–7.29 (m, 2H), 7.18 (d,  $J = 8.5$  Hz, 1H), 6.93 (d,  $J = 8.2$  Hz, 1H), 6.86 (d,  $J = 2.1$  Hz, 1H), 6.83 (dd,  $J = 8.3, 2.1$  Hz, 1H), 5.24 (s, 2H), 4.28 (s, 4H), 3.85 (d,  $J = 13.4$  Hz, 1H), 3.06 (dd,  $J = 8.2, 3.8$  Hz, 1H), 2.93–2.81 (m, 1H), 2.30–2.17 (m,  $J = 16.9, 8.1$  Hz, 1H), 1.86–1.77 (m, 1H), 1.74–1.61 (m,  $J = 12.6, 6.6$  Hz, 1H), 1.57–1.41 (m, 3H), 1.38–1.28 (m, 1H), 1.23 (s, 1H). <sup>13</sup>C NMR (151 MHz, DMSO)  $\delta$ : 153.6, 143.1, 142.8, 142.4, 136.5, 133.8, 133.7, 131.0, 129.9, 128.2, 127.7, 122.7, 122.3, 118.0, 116.8, 113.7, 111.0, 70.7, 64.2, 57.9, 49.2, 28.6, 28.5, 24.1, 22.0. IR (ATR): 2932, 2864, 2356, 2323, 2286, 1728, 1634, 1589, 1500, 1454, 1368, 1315, 1278, 1260, 1246, 1197, 1065  $\text{cm}^{-1}$ . HRMS ESI-MS-q-TOF for  $\text{C}_{28}\text{H}_{27}\text{Br}_2\text{NO}_5$   $[\text{M} + \text{H}]^+$

found: 616.0327 *m/z*; calc. mass: 616.0334. Mp: decomposition at 191.9 °C. UPLC-MS (DAD/ESI): *t<sub>R</sub>* = 6.25 min, for C<sub>28</sub>H<sub>27</sub>Br<sub>2</sub>NO<sub>5</sub> [M + H]<sup>+</sup> found: 616.23 *m/z*; calc. mass: 616.03.

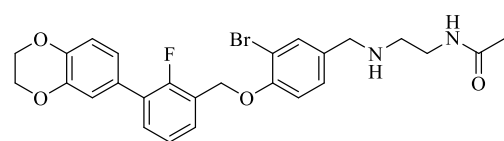
**3-bromo-4-((3-(2,3-dihydrobenzo[*b*][1,4]dioxin-6-yl)-2-fluorobenzyl)oxy)benzaldehyde (3.21)**



**3.3** (700 mg, 2.69 mmol) was dissolved in anhydrous DCM (10 mL) under Ar. SOCl<sub>2</sub> (3.2 mL) was added carefully, and the resulted mixture was stirred at 45 °C. After 3 h the reaction

was stopped, and the mixture was concentrated under reduced pressure. Generated in situ chloride, 3-bromo-4-hydroxybenzaldehyde (1.6 g, 8.08 mmol), and K<sub>2</sub>CO<sub>3</sub> (1.8 g, 13.46 mmol) were stirred in anhydrous DMF (10 mL) at room temperature overnight. The solvent was removed under reduced pressure. Water was added (100 mL), and the mixture was extracted with AcOEt (2 × 100 mL). Organic layers were combined and concentrated. The crude product was chromatographed on silica gel eluting with 0–60% AcOEt in hexane to give 180 mg of a colorless solid with a yield of 30%. <sup>1</sup>H NMR (600 MHz, CDCl<sub>3</sub>) δ: 9.85 (s, 1H), 8.12 (d, *J* = 2.0 Hz, 1H), 7.81 (dd, *J* = 8.5, 2.0 Hz, 1H), 7.55 (t, *J* = 7.1 Hz, 1H), 7.39 (td, *J* = 7.6, 1.6 Hz, 1H), 7.23 (t, *J* = 7.7 Hz, 1H), 7.12 (d, *J* = 8.5 Hz, 1H), 7.09 (t, *J* = 1.7 Hz, 1H), 7.04 (dt, *J* = 8.3, 1.8 Hz, 1H), 6.95 (d, *J* = 8.4 Hz, 1H), 5.36 (s, 2H), 4.31 (s, 4H). <sup>13</sup>C NMR (151 MHz, CDCl<sub>3</sub>) δ: 189.7, 159.7, 157.0 (d, <sup>1</sup>*J*<sub>C-F</sub> = 248.2 Hz), 143.6 (d, <sup>2</sup>*J*<sub>C-F</sub> = 14.0 Hz), 134.8, 131.3, 131.2, 130.7 (d, <sup>3</sup>*J*<sub>C-F</sub> = 3.1 Hz), 128.8, 128.7, 128.7, 127.8 (d, <sup>3</sup>*J*<sub>C-F</sub> = 3.1 Hz), 124.7 (d, <sup>3</sup>*J*<sub>C-F</sub> = 3.8 Hz), 123.6 (d, <sup>2</sup>*J*<sub>C-F</sub> = 15.1 Hz), 122.4, 118.1, 117.5, 113.4, 113.0, 65.2 (d, <sup>3</sup>*J*<sub>C-F</sub> = 6.3 Hz), 64.6, 64.5. IR (ATR): 2927, 2823, 2738, 1691, 1592, 1493, 1450, 1323, 1278, 1191, 1064, 1047 cm<sup>-1</sup>. HRMS ESI-MS-q-TOF for C<sub>22</sub>H<sub>16</sub>BrFO<sub>4</sub> [M + Na]<sup>+</sup> found: 465.0109 *m/z*; calc. mass: 465.0114. Mp: 118.0 °C. UPLC-MS (DAD/ESI): *t<sub>R</sub>* = 8.56 min, for C<sub>22</sub>H<sub>16</sub>BrFO<sub>4</sub> [M + H]<sup>+</sup> found: 443.15 *m/z*; calc. mass: 443.03.

**N-(2-((3-bromo-4-((3-(2,3-dihydrobenzo[*b*][1,4]dioxin-6-yl)-2-fluorobenzyl)oxy)benzyl)amino)ethyl)acetamide (3.22)**

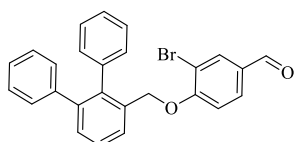


Compound **3.22** was prepared following the procedure of **3.13**, using **3.21** (120 mg, 0.27 mmol), N-(2-aminoethyl)acetamide (126 mg, 1.24 mmol),

NaBH<sub>3</sub>CN (79 mg, 1.35 mmol), addition of AcOH (3 droplets), and anhydrous DMF (4 mL) as a solvent. The crude product was purified by column chromatography (silica gel, 0–30% MeOH in CHCl<sub>3</sub>) to give a colorless solid (88 mg, yield: 61%) as the product. <sup>1</sup>H NMR (600 MHz,

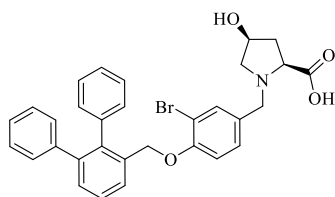
CDCl<sub>3</sub>)  $\delta$ : 7.60 (d,  $J$  = 2.0 Hz, 1H), 7.55 (t,  $J$  = 6.4 Hz, 1H), 7.36 (td,  $J$  = 7.6, 1.6 Hz, 1H), 7.25 (d,  $J$  = 2.0 Hz, 1H), 7.21 (t,  $J$  = 7.6 Hz, 1H), 7.08 (t,  $J$  = 1.5 Hz, 1H), 7.04 (dt,  $J$  = 8.4, 1.8 Hz, 1H), 6.97 (d,  $J$  = 8.4 Hz, 1H), 6.94 (d,  $J$  = 8.4 Hz, 1H), 6.30 (s, 1H), 5.25 (s, 2H), 4.30 (s, 4H), 3.79 (s, 2H), 3.39 (dd,  $J$  = 11.1, 5.5 Hz, 2H), 2.84 (t,  $J$  = 5.6 Hz, 2H), 2.00 (s, 3H). <sup>13</sup>C NMR (151 MHz, CDCl<sub>3</sub>)  $\delta$ : 171.0, 157.0 (d, <sup>1</sup> $J_{C-F}$  = 248.1 Hz), 154.6, 143.6 (d, <sup>3</sup> $J_{C-F}$  = 6.9 Hz), 133.8, 131.5, 130.4 (d, <sup>4</sup> $J_{C-F}$  = 2.6 Hz), 129.1, 128.8, 128.6 (d, <sup>2</sup> $J_{C-F}$  = 13.3 Hz), 127.9 (d, <sup>3</sup> $J_{C-F}$  = 3.2 Hz), 124.5 (d, <sup>3</sup> $J_{C-F}$  = 3.7 Hz), 124.4 (d, <sup>2</sup> $J_{C-F}$  = 15.2 Hz), 122.4, 118.1, 117.4, 113.9, 112.8, 65.0 (d, <sup>3</sup> $J_{C-F}$  = 6.0 Hz), 64.6, 64.5, 52.1, 47.9, 38.7, 23.4. IR (ATR): 3283, 2925, 2803, 2163, 1692, 1655, 1578, 1502, 1454, 1417, 1373, 1319, 1283, 1261, 1244, 1192, 1128, 1066, 1048 cm<sup>-1</sup>. HRMS ESI-MS-q-TOF for C<sub>26</sub>H<sub>26</sub>BrFN<sub>2</sub>O<sub>4</sub> [M + H]<sup>+</sup> found: 529.1135  $m/z$ ; calc. mass: 529.1138. Mp: 121.6 °C. UPLC-MS (DAD/ESI):  $t_R$  = 5.66 min, C<sub>26</sub>H<sub>26</sub>BrFN<sub>2</sub>O<sub>4</sub> [M + H]<sup>+</sup> found: 529.22  $m/z$ ; calc. mass: 529.11.

#### 4-([1,1':2',1''-terphenyl]-3'-ylmethoxy)-3-bromobenzaldehyde (3.23)



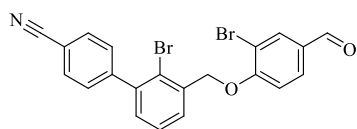
Compound **3.23** was prepared following the procedure of **3.21**. Preparation of chloride involved the use of **1b** (300 mg, 1.15 mmol), which was dissolved in anhydrous DCM (4.5 mL) with the addition of SOCl<sub>2</sub> (1.4 mL) under Ar. In the second step, generated in situ chloride was stirred with 3-bromo-4-hydroxybenzaldehyde (231 mg, 1.15 mmol) and potassium carbonate (319 mg, 2.31 mmol) in anhydrous DMF (3.3 mL) at room temperature overnight. The crude product was chromatographed on silica gel, eluting with 0–60% AcOEt in hexane to give 308 mg of an off-white solid with yield: 60%. <sup>1</sup>H NMR (600 MHz, CDCl<sub>3</sub>)  $\delta$ : 9.8 (s, 1H), 8.1 (d,  $J$  = 2.0 Hz, 1H), 7.7 (m, 1H), 7.7 (dd,  $J$  = 8.5, 2.0 Hz, 1H), 7.5 (t,  $J$  = 7.7 Hz, 1H), 7.4 (dd,  $J$  = 7.7, 1.2 Hz, 1H), 7.2 – 7.0 (m, 10H), 6.7 (d,  $J$  = 8.5 Hz, 1H), 5.0 (s, 2H). <sup>13</sup>C NMR (151 MHz, CDCl<sub>3</sub>)  $\delta$ : 189.7, 159.8, 142.0, 141.3, 139.8, 138.4, 134.7, 133.9, 131.1, 130.9, 130.4, 130.3, 129.9, 128.1, 128.0, 127.7, 127.3, 127.2, 126.5, 113.2, 112.9, 69.7. IR (ATR): 3029, 2733, 1685, 1592, 1285, 1263, 1194, 1005 cm<sup>-1</sup>. HRMS ESI-MS-q-TOF for C<sub>26</sub>H<sub>19</sub>BrO<sub>2</sub> [M + Na]<sup>+</sup> found: 465.0465  $m/z$ ; calc. mass: 465.0466. Mp: 142.3 °C. UPLC-MS (DAD/ESI):  $t_R$  = 9.51 min, for C<sub>26</sub>H<sub>19</sub>BrO<sub>2</sub> [M + H]<sup>+</sup> found: 445.34  $m/z$ ; calc. mass: 445.06.

**(2S,4S)-1-(4-([1,1':2',1''-terphenyl]-3'-ylmethoxy)-3-bromobenzyl)-4-hydroxypyrrolidine-2-carboxylic acid (3.24)**



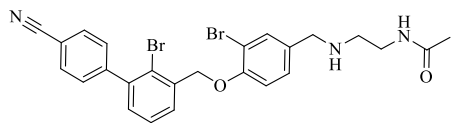
The synthesis of compound **3.24** was performed following the procedure of **3.13**. Preparation included the use of **3.23** (200 mg, 0.45 mmol), (2R,4R)-4-hydroxypyrrolidine-2-carboxylic acid (272 mg, 2.07 mmol), NaBH<sub>3</sub>CN (142 mg, 2.26 mmol), AcOH (3 droplets), and anhydrous DMF (6.0 mL). The crude product was purified by flash chromatography (silica gel, 0–50% MeOH in AcOEt) to give a colorless solid (93 mg, yield: 37%) as the product. <sup>1</sup>H NMR (600 MHz, CDCl<sub>3</sub>) δ: 7.7 (d, *J* = 7.2 Hz, 1H), 7.6 – 7.5 (m, 2H), 7.4 (dd, *J* = 7.7, 1.1 Hz, 1H), 7.2 – 7.1 (m, 9H), 7.1 – 7.0 (m, 2H), 6.7 (d, *J* = 8.4 Hz, 1H), 4.8 (s, 2H), 4.1 (s, 1H), 3.9 (d, *J* = 13.1 Hz, 1H), 3.5 (d, *J* = 13.0 Hz, 1H), 3.1 (s, *J* = 19.4 Hz, 1H), 2.8 (d, *J* = 9.4 Hz, 1H), 2.4 (s, 1H), 2.2 (s, 1H), 1.7 (d, *J* = 8.8 Hz, 1H), 1.2 (s, 1H). <sup>13</sup>C NMR (151 MHz, CDCl<sub>3</sub>) δ: 153.4, 141.3, 141.0, 139.8, 138.0, 134.6, 133.6, 130.1, 129.9, 129.7, 129.5, 129.0, 127.8, 127.7, 127.7, 127.7, 126.9, 126.4, 113.2, 110.7, 68.8, 68.6, 65.4, 60.7, 55.8, 48.6. IR (ATR): 3297, 3057, 2659, 1600, 1494, 1410, 1253, 1050 cm<sup>-1</sup>. HRMS ESI-MS-q-TOF for C<sub>31</sub>H<sub>28</sub>BrNO<sub>4</sub> [M + Na]<sup>+</sup> found: 580.1078 *m/z*; calc. mass: 580.1099. Mp: 152.3 °C. UPLC-MS (DAD/ESI): t<sub>R</sub> = 6.55 min, for C<sub>31</sub>H<sub>28</sub>BrNO<sub>4</sub> [M + H]<sup>+</sup> found: 558.27 *m/z*; calc. mass: 558.13.

**2'-bromo-3'-((2-bromo-4-formylphenoxy)methyl)-[1,1'-biphenyl]-4-carbonitrile (3.25)**



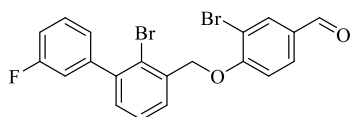
The synthesis of compound **3.25** was performed according to the procedure of **3.8**, using **3.4** (559 mg, 1.59 mmol), 3-bromo-4-hydroxybenzaldehyde (320 mg, 1.59 mmol), potassium carbonate (440 mg, 3.18 mmol), and anhydrous DMF (8 mL). The product was precipitated from AcOEt and yielded **3.25** (461 mg, 61%) as a colorless solid. <sup>1</sup>H NMR (600 MHz, CDCl<sub>3</sub>) δ: 9.88 (s, 1H), 8.15 (d, *J* = 2.0 Hz, 1H), 7.84 (dd, *J* = 8.4, 2.0 Hz, 1H), 7.79 – 7.73 (m, 3H), 7.53 – 7.50 (m, 2H), 7.48 (t, *J* = 7.7 Hz, 1H), 7.28 (dd, *J* = 7.6, 1.6 Hz, 1H), 7.11 (d, *J* = 8.5 Hz, 1H), 5.34 (s, 2H). <sup>13</sup>C NMR (151 MHz, CDCl<sub>3</sub>) δ: 189.6, 159.4, 145.6, 141.7, 136.3, 134.9, 132.1, 131.4, 131.3, 130.5, 128.3, 128.0, 121.3, 118.8, 113.4, 113.1, 111.9, 70.9. IR (ATR): 2844, 2227, 1688, 1590, 1566, 1489, 1276, 1256, 1184, 1050 cm<sup>-1</sup>. HRMS ESI-MS-q-TOF for C<sub>21</sub>H<sub>13</sub>Br<sub>2</sub>NO<sub>2</sub> [M + Na]<sup>+</sup> found: 491.9203 *m/z*; calc. mass: 491.9211. Mp: over 200 °C. UPLC-MS (DAD/ESI): t<sub>R</sub> = 8.71 min, for C<sub>21</sub>H<sub>13</sub>Br<sub>2</sub>NO<sub>2</sub> [M + H]<sup>+</sup> found: 469.93 *m/z*; calc. mass: 469.94.

**N-(2-((3-bromo-4-((2-bromo-4'-cyano-[1,1'-biphenyl]-3-yl)methoxy)benzyl)amino)ethyl)acetamide (3.26)**



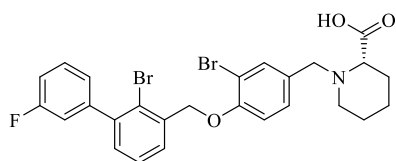
Compound **3.26** was prepared following the procedure of **3.13**, using **3.25** (100 mg, 0.21 mmol), N-(2-aminoethyl)acetamide (99 mg, 0.97 mmol), NaBH<sub>3</sub>CN (63 mg, 1.06 mmol), addition of AcOH (3 droplets), and anhydrous DMF (5 mL) as a solvent. The crude product was purified by column chromatography (silica gel, 0 – 30% MeOH in CHCl<sub>3</sub>) to give an off-white solid (30 mg, yield: 26%) as a product. <sup>1</sup>H NMR (600 MHz, CDCl<sub>3</sub>) δ: 7.79 (d, *J* = 7.7 Hz, 1H), 7.74 (d, *J* = 8.3 Hz, 2H), 7.58 (d, *J* = 1.9 Hz, 1H), 7.51 (d, *J* = 8.3 Hz, 2H), 7.46 (t, *J* = 7.7 Hz, 1H), 7.25 (dd, *J* = 7.6, 1.5 Hz, 1H), 7.21 (dd, *J* = 8.3, 1.9 Hz, 1H), 6.94 (d, *J* = 8.4 Hz, 1H), 6.00 (s, 1H), 5.23 (s, 2H), 3.73 (s, 2H), 3.35 (dd, *J* = 11.3, 5.6 Hz, 2H), 2.76 (t, *J* = 5.8 Hz, 2H), 1.99 (s, 3H). <sup>13</sup>C NMR (151 MHz, CDCl<sub>3</sub>) δ: 170.5, 153.9, 145.8, 141.5, 137.3, 134.5, 133.3, 132.1, 130.5, 130.1, 128.4, 128.4, 127.9, 121.2, 118.9, 113.7, 112.5, 111.8, 70.8, 52.5, 48.1, 39.2, 23.5. IR (ATR): 3282, 2925, 2228, 1688, 1654, 1591, 1554, 1490, 1447, 1362, 1279, 1256, 1185, 1052, 1025 cm<sup>-1</sup>. HRMS ESI-MS-q-TOF for C<sub>25</sub>H<sub>23</sub>Br<sub>2</sub>N<sub>3</sub>O<sub>2</sub> [M + H]<sup>+</sup> found: 556.0230 *m/z*; calc. mass: 556.0235. Mp: 152.8 °C. UPLC-MS (DAD/ESI): t<sub>R</sub> = 5.67 min, for C<sub>25</sub>H<sub>23</sub>Br<sub>2</sub>N<sub>3</sub>O<sub>2</sub> [M + H]<sup>+</sup> found: 556.21 *m/z*; calc. mass: 556.02.

**3-bromo-4-((2-bromo-3'-fluoro-[1,1'-biphenyl]-3-yl)methoxy)benzaldehyde (3.27)**



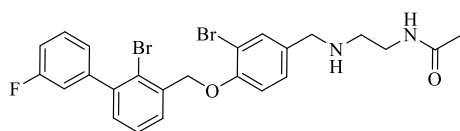
Compound **3.27** was obtained according to the procedure of **3.8**, using **3.5** (700 mg, 2.03 mmol), 4-hydroxy-3-methylbenzaldehyde (409 mg, 2.03 mmol), potassium carbonate (562 mg, 4.07 mmol), and anhydrous DMF (10 mL). Product was purified by precipitation from AcOEt and yielded **3.27** (534 mg, 57%) as a colorless solid. <sup>1</sup>H NMR (600 MHz, CDCl<sub>3</sub>) δ: 9.87 (s, 1H), 8.15 (d, *J* = 2.0 Hz, 1H), 7.83 (dd, *J* = 8.4, 2.0 Hz, 1H), 7.75 – 7.69 (m, 1H), 7.44 (t, *J* = 7.6 Hz, 1H), 7.42 – 7.38 (m, 1H), 7.30 (dd, *J* = 7.5, 1.7 Hz, 1H), 7.19 – 7.14 (m, 1H), 7.14 – 7.05 (m, 3H), 5.35 (s, 2H). <sup>13</sup>C NMR (151 MHz, CDCl<sub>3</sub>) δ: 189.6, 162.5 (d, <sup>1</sup>J<sub>C-F</sub> = 246.4 Hz), 159.5, 143.1 (d, <sup>3</sup>J<sub>C-F</sub> = 7.9 Hz), 142.3, 135.9, 134.8, 131.3, 130.7, 129.8 (d, <sup>3</sup>J<sub>C-F</sub> = 8.3 Hz), 127.8, 127.6, 125.4 (d, <sup>4</sup>J<sub>C-F</sub> = 2.2 Hz), 121.7, 116.8 (d, <sup>2</sup>J<sub>C-F</sub> = 22.0 Hz), 114.8 (d, <sup>2</sup>J<sub>C-F</sub> = 21.0 Hz), 113.4, 113.1, 71.0. IR (ATR): 3060, 2922, 2853, 1683, 1594, 1490, 1461, 1418, 1368, 1313, 1278, 1255, 1190, 1049 cm<sup>-1</sup>. HRMS ESI-MS-q-TOF for C<sub>20</sub>H<sub>13</sub>Br<sub>2</sub>FO<sub>2</sub> [M + Na]<sup>+</sup> found: 484.9150 *m/z*; calc. mass: 484.9164. Mp: 168.1 °C. UPLC-MS (DAD/ESI): t<sub>R</sub> = 9.32 min, for C<sub>20</sub>H<sub>13</sub>Br<sub>2</sub>FO<sub>2</sub> [M + H]<sup>+</sup> found: 463.02 *m/z*; calc. mass: 462.93.

**(S)-1-(3-bromo-4-((2-bromo-3'-fluoro-[1,1'-biphenyl]-3-yl)methoxy)benzyl)piperidine-2-carboxylic acid (3.28)**



Compound **3.28** was prepared following the procedure of **3.13**, using **3.27** (135 mg, 0.29 mmol), L-pipecolinic acid (172 mg, 1.33 mmol), NaBH<sub>3</sub>CN (86 mg, 1.45 mmol), addition of AcOH (3 droplets), and anhydrous DMF (5 mL) as a solvent. The crude product was purified by column chromatography (silica gel, 0–40% MeOH in CHCl<sub>3</sub>) to give a colorless solid (73 mg, yield: 44%) as the product. <sup>1</sup>H NMR (600 MHz, DMF) δ: 7.82 (dd, *J* = 7.7, 1.5 Hz, 1H), 7.73 (s, 1H), 7.63 – 7.56 (m, 2H), 7.46 – 7.41 (m, 2H), 7.33 – 7.27 (m, 4H), 5.36 (s, 2H), 3.97 (d, *J* = 13.3 Hz, 1H), 3.56 (d, *J* = 12.8 Hz, 1H), 3.29 – 3.23 (m, 1H), 3.03 – 2.97 (m, 1H), 2.39 – 2.30 (m, 1H), 1.95 – 1.89 (m, 1H), 1.85 – 1.77 (m, 1H), 1.62 – 1.48 (m, 3H), 1.48 – 1.39 (m, 1H). <sup>13</sup>C NMR (151 MHz, DMF) δ: 175.0, 167.2 (d, <sup>1</sup>*J*<sub>C-F</sub> = 63.5 Hz), 155.0, 144.4 (d, <sup>3</sup>*J*<sub>C-F</sub> = 7.9 Hz), 143.1, 138.1, 134.9, 131.9, 131.2 (d, <sup>3</sup>*J*<sub>C-F</sub> = 8.4 Hz), 130.9, 129.8, 128.9, 126.7, 123.2, 117.4 (d, <sup>2</sup>*J*<sub>C-F</sub> = 22.2 Hz), 115.6 (d, <sup>2</sup>*J*<sub>C-F</sub> = 21.0 Hz), 114.7, 112.3, 71.9, 65.4, 59.4, 50.5, 25.7, 24.0, 23.2. IR (ATR): 2923, 2853, 1614, 1495, 1461, 1363, 1288, 1259, 1196, 1157, 1055, 1023 cm<sup>-1</sup>. HRMS ESI-MS-q-TOF for C<sub>26</sub>H<sub>24</sub>Br<sub>2</sub>FNO<sub>3</sub> [M + H]<sup>+</sup> found: 576.0180 *m/z*; calc. mass: 576.0185. Mp: 175.6 °C. UPLC-MS (DAD/ESI): t<sub>R</sub> = 6.65 min, for C<sub>26</sub>H<sub>24</sub>Br<sub>2</sub>FNO<sub>3</sub> [M + H]<sup>+</sup> found: 576.15 *m/z*; calc. mass: 576.02.

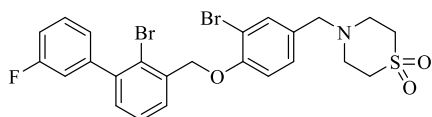
**N-(2-((3-bromo-4-((2-bromo-3'-fluoro-[1,1'-biphenyl]-3-yl)methoxy)benzyl)amino)ethyl)acetamide (3.29)**



Compound **3.29** was prepared according to the procedure of **3.13**, using **3.27** (200 mg, 0.43 mmol), N-(2-aminoethyl)acetamide (201 mg, 1.97 mmol), NaBH<sub>3</sub>CN (127 mg, 2.16 mmol), addition of AcOH (3 droplets), and anhydrous DMF (4 mL) as a solvent. The crude product was purified by column chromatography (silica gel, 0–40% MeOH in CHCl<sub>3</sub>) to give a colorless solid (159 mg, yield: 67%) as the product. <sup>1</sup>H NMR (600 MHz, DMSO) δ: 7.98 (t, *J* = 5.2 Hz, 1H), 7.70 (d, *J* = 1.9 Hz, 1H), 7.68 (dd, *J* = 7.7, 1.6 Hz, 1H), 7.56 – 7.49 (m, 2H), 7.41 – 7.37 (m, 2H), 7.30 – 7.19 (m, 4H), 5.27 (s, 2H), 3.81 (s, 2H), 3.21 (dd, *J* = 12.2, 6.2 Hz, 2H), 2.67 (t, *J* = 6.4 Hz, 2H), 1.80 (s, 3H). <sup>13</sup>C NMR (151 MHz, DMSO) δ: 169.6, 161.7 (d, <sup>1</sup>*J*<sub>C-F</sub> = 244.0 Hz), 153.6, 142.9 (d, <sup>3</sup>*J*<sub>C-F</sub> = 8.0 Hz), 141.7, 136.6, 133.4, 130.9, 130.3 (d, <sup>3</sup>*J*<sub>C-F</sub> = 8.5 Hz), 129.6, 128.8, 127.9, 125.6, 122.3, 116.3 (d, <sup>2</sup>*J*<sub>C-F</sub> = 22.0 Hz), 114.7 (d, <sup>2</sup>*J*<sub>C-F</sub> = 20.8 Hz), 113.8, 111.0, 70.6, 50.4, 47.2, 37.3, 22.7. IR (ATR): 3282, 2934, 2774, 2427, 1656, 1557, 1500, 1446, 1363, 1291, 1261, 1195, 1070, 1056 cm<sup>-1</sup>. HRMS ESI-

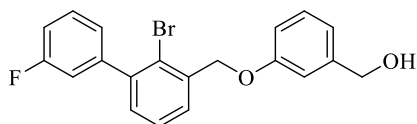
MS-q-TOF for  $C_{24}H_{23}Br_2FN_2O_2$   $[M + H]^+$  found: 549.0176  $m/z$ ; calc. mass: 549.0189. Mp: 151.2 °C. UPLC-MS (DAD/ESI):  $t_R = 6.21$  min, for  $C_{24}H_{23}Br_2FN_2O_2$   $[M + H]^+$  found: 549.16  $m/z$ ; calc. mass: 549.02.

#### 4-(3-bromo-4-((2-bromo-3'-fluoro-[1,1'-biphenyl]-3-yl)methoxy)benzyl)thiomorpholine 1,1-dioxide (3.30)



The synthesis of compound **3.30** was performed following the procedure of **3.13**. Preparation included the use of **3.27** (100 mg, 0.22 mmol), thiomorpholine 1,1-dioxide (133 mg, 0.99 mmol),  $NaBH_3CN$  (64 mg, 1.08 mmol), AcOH (3 droplets), and anhydrous DMF (4.0 mL). The crude product was purified by column chromatography (silica gel, 0–10% MeOH in  $CHCl_3$ ) to give an off-white solid (41 mg, yield: 33%) as a product.  $^1H$  NMR (600 MHz,  $CDCl_3$ )  $\delta$ : 7.75 (dd,  $J = 7.7, 0.7$  Hz, 1H), 7.57 (d,  $J = 2.0$  Hz, 1H), 7.41 (m, 2H), 7.28 (dd,  $J = 7.5, 1.5$  Hz, 1H), 7.20 (dd,  $J = 8.4, 2.0$  Hz, 1H), 7.16 (d,  $J = 7.6$  Hz, 1H), 7.13 – 7.08 (m, 2H), 6.95 (d,  $J = 8.4$  Hz, 1H), 5.25 (s, 2H), 3.58 (s, 2H), 3.08 – 3.05 (m, 4H), 2.99 – 2.96 (m, 4H).  $^{13}C$  NMR (151 MHz,  $CDCl_3$ )  $\delta$ : 162.4 (d,  $^1J_{C-F} = 246.1$  Hz), 154.4, 143.2 (d,  $^3J_{C-F} = 7.9$  Hz), 142.2, 136.8, 133.8, 131.7, 130.4, 129.7 (d,  $^3J_{C-F} = 8.3$  Hz), 129.0, 127.7, 127.7, 125.4, 121.6, 116.8 (d,  $^2J_{C-F} = 22.0$  Hz), 114.8 (d,  $^2J_{C-F} = 21.0$  Hz), 113.6, 112.7, 70.9, 60.5, 51.6, 50.7. IR (ATR): 3079, 2818, 1608, 1584, 1494, 1463, 1363, 1328, 1301, 1253, 1199, 1124, 1110  $cm^{-1}$ . HRMS ESI-MS-q-TOF for  $C_{24}H_{22}Br_2FNO_3S$   $[M + Na]^+$  found: 603.9573  $m/z$ ; calc. mass: 603.9569. Mp: 183.0 °C. UPLC-MS (DAD/ESI):  $t_R = 8.81$  min, for  $C_{24}H_{22}Br_2FNO_3S$   $[M + H]^+$  found: 582.13  $m/z$ ; calc. mass: 581.97.

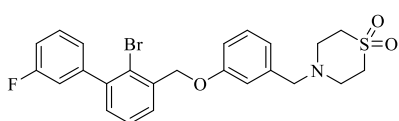
#### (3-((2-bromo-3'-fluoro-[1,1'-biphenyl]-3-yl)methoxy)phenyl)methanol (3.31)



Compound **3.31** was obtained following the protocol of **3.8**, using **3.5** (700 mg, 2.03 mmol), 3-(hydroxymethyl)phenol (252 mg, 2.03 mmol), potassium carbonate (562 mg, 4.07 mmol), and anhydrous DMF (10 mL). The crude product was purified by column chromatography (silica gel, 0–100% AcOEt in hexane) and yielded **3.31** (408 mg, 52%) as a colorless solid.  $^1H$  NMR (600 MHz,  $CDCl_3$ )  $\delta$ : 7.61 – 7.57 (m, 1H), 7.44 – 7.37 (m, 2H), 7.31 (t,  $J = 7.9$  Hz, 1H), 7.27 (d,  $J = 1.7$  Hz, 1H), 7.19 – 7.16 (m, 1H), 7.14 – 7.08 (m, 2H), 7.07 (s, 1H), 7.00 (dd,  $J = 7.5, 0.6$  Hz, 1H), 6.95 (dd,  $J = 8.2, 2.4$  Hz, 1H), 5.21 (s, 2H), 4.70 (d,  $J = 5.8$  Hz, 2H), 1.73 (t,  $J = 6.0$  Hz, 1H).  $^{13}C$  NMR (151 MHz,  $CDCl_3$ )  $\delta$ : 162.4 (d,  $^1J_{C-F} = 246.2$  Hz), 158.9, 143.4 (d,  $^3J_{C-F} = 7.9$  Hz), 142.8, 142.3, 137.4, 130.5, 129.9, 129.7 (d,  $^3J_{C-F}$

$J_{\text{C-F}} = 8.3$  Hz), 128.1, 127.5, 125.4 (d,  $^4J_{\text{C-F}} = 2.3$  Hz), 122.4, 119.9, 116.8 (d,  $^2J_{\text{C-F}} = 22.0$  Hz), 114.7 (d,  $^2J_{\text{C-F}} = 21.0$  Hz), 114.2, 113.5, 70.2, 65.4. IR (ATR): 3233, 2854, 1601, 1584, 1493, 1448, 1417, 1365, 1258, 1196, 1173, 1155, 1068, 1055  $\text{cm}^{-1}$ . HRMS ESI-MS-q-TOF for  $\text{C}_{20}\text{H}_{16}\text{BrFO}_2$   $[\text{M} + \text{Na}]^+$  found: 409.0207  $m/z$ ; calc. mass: 409.0215. Mp: 59.0 °C. UPLC-MS (DAD/ESI):  $t_{\text{R}} = 8.05$  min, for  $\text{C}_{20}\text{H}_{16}\text{BrFO}_2$   $[(\text{M}-\text{H}_2\text{O}) + \text{H}]^+$  found: 369.17  $m/z$ ; calc. mass: 369.02.

#### 4-(3-((2-bromo-3'-fluoro-[1,1'-biphenyl]-3-yl)methoxy)benzyl)thiomorpholine 1,1-dioxide (3.32)

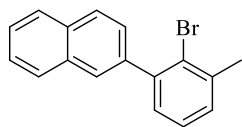


Compound **3.31** (100 mg, 0.26 mmol) was dissolved in anhydrous DCM (3 mL) under Ar.  $\text{SOCl}_2$  (1.0 mL) was added carefully, and the resulted mixture was stirred at 45 °C for 3 h. Afterward, the reaction was stopped, and the mixture was concentrated under reduced pressure. Generated *in situ* chloride, thiomorpholine 1,1-dioxide (105 mg, 0.78 mmol), and potassium carbonate (178 mg, 1.29 mmol) were stirred in anhydrous DMF (5 mL) at room temperature overnight. The solvent was removed under reduced pressure. Water was added (30 mL), and the mixture was extracted with AcOEt ( $2 \times 30$  mL). Organic layers were combined and concentrated. The crude product was chromatographed (silica gel, 0– 60% AcOEt in hexane) to give 38 mg of an off-white solid with a yield of 29%.  $^1\text{H}$  NMR (600 MHz,  $\text{CDCl}_3$ )  $\delta$ : 7.58 (dd,  $J = 7.6, 1.0$  Hz, 1H), 7.44 – 7.37 (m, 2H), 7.31 – 7.27 (m, 2H), 7.17 (d,  $J = 7.6$  Hz, 1H), 7.13 – 7.08 (m, 2H), 6.99 (s, 1H), 6.94 (m, 2H), 5.20 (s, 2H), 3.65 (s, 2H), 3.08 – 3.03 (m, 4H), 2.99 (m, 4H).  $^{13}\text{C}$  NMR (151 MHz,  $\text{CDCl}_3$ )  $\delta$ : 162.4 (d,  $^1J_{\text{C-F}} = 246.2$  Hz), 158.9, 143.3 (d,  $^3J_{\text{C-F}} = 8.0$  Hz), 142.4, 139.3, 137.3, 130.5, 129.9, 129.7 (d,  $^3J_{\text{C-F}} = 8.3$  Hz), 128.1, 127.5, 125.4, 122.4, 121.7, 116.8 (d,  $^2J_{\text{C-F}} = 22.0$  Hz), 115.5, 114.8 (d,  $^2J_{\text{C-F}} = 20.9$  Hz), 114.0, 70.2, 61.5, 51.7, 50.8. IR (ATR): 2918, 2849, 1583, 1487, 1462, 1364, 1290, 1269, 1195, 1153, 1123, 1049  $\text{cm}^{-1}$ . HRMS ESI-MS-q-TOF for  $\text{C}_{24}\text{H}_{23}\text{BrFNO}_3\text{S}$   $[\text{M} + \text{Na}]^+$  found: 526.0454  $m/z$ ; calc. mass: 526.0464. Mp: 94.2 °C. UPLC-MS (DAD/ESI):  $t_{\text{R}} = 8.28$  min, for  $\text{C}_{24}\text{H}_{23}\text{BrFNO}_3\text{S}$   $[\text{M} + \text{H}]^+$  found: 504.17  $m/z$ ; calc. mass: 504.06.



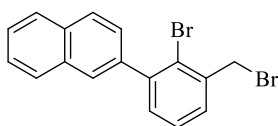
### 4.2.3. Preparation of 2-substituted 1,1'-biphenyl Derivatives

#### 2-(2-bromo-3-methylphenyl)naphthalene (3.33.1)



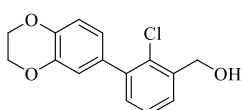
**3.33.1.1** (4.50 g, 15.16 mmol), naphthalen-2-ylboronic acid (2.61 g, 15.16 mmol) and potassium carbonate (6.27 g, 45.47 mmol) were dissolved in mixture of dioxane and water (44:22 mL, v:v). The mixture was deoxygenated by rinsing with argon for 15 min. Then, resulting mixture was heated up to 85 °C and Pd(dppf)Cl<sub>2</sub>·DCM complex (621 mg, 0.76 mmol) was added. The mixture was stirred at 85 °C for 3 hours. Afterwards, water (100 mL) was added to the reaction mixture and it was extracted with ethyl acetate (2 x 100 mL). The organic layers were combined, dried over anhydrous MgSO<sub>4</sub>, filtered, and the solvent was removed under reduced pressure. The crude product was purified by flash chromatography (silica gel, 0-20% ethyl acetate in hexane) to give a beige solid (1.78 g, yield: 40%). <sup>1</sup>H NMR (600 MHz, CDCl<sub>3</sub>) δ 7.92 – 7.86 (m, 3H), 7.85 – 7.81 (m, 1H), 7.55 (dd, *J* = 8.4, 1.7 Hz, 1H), 7.53 – 7.49 (m, 2H), 7.30 – 7.27 (m, 2H), 7.25 – 7.22 (m, 1H), 2.53 (s, 3H). <sup>13</sup>C NMR (151 MHz, CDCl<sub>3</sub>) δ 143.4, 139.8, 139.1, 133.2, 132.7, 129.9, 129.1, 128.3, 128.2, 128.0, 127.9, 127.3, 127.0, 126.3, 126.3, 125.6, 24.4.

#### 2-(2-bromo-3-(bromomethyl)phenyl)naphthalene (3.33)



**3.33.1** (1480.0 mg, 4.98 mmol) was dissolved in chloroform (83 mL) and then NBS (1327 mg, 7.45 mmol) was added. Resulted mixture was heated to 80 °C, what was followed by addition of benzoyl peroxide (22.0 mg, 0.09 mmol). After 2 h of refluxing, second portion of benzoyl peroxide (22.0 mg, 0.09 mmol) was added. Mixture was refluxed for 2 more hours, it was cooled to room temperature and it was concentrated under reduced pressure. The crude product was purified by flash chromatography on silica gel using 0-15% AcOEt in hexane to give colorless oil (757.7 mg, yield: 59%). <sup>1</sup>H NMR (600 MHz, CDCl<sub>3</sub>) δ 7.89 (m, 3H), 7.83 (d, *J* = 1.0 Hz, 1H), 7.52 (m, 4H), 7.36 (m, 2H), 4.75 (s, 2H). <sup>13</sup>C NMR (151 MHz, CDCl<sub>3</sub>) δ 144.4, 139.0, 138.1, 133.2, 132.8, 131.8, 130.5, 128.4, 128.3, 127.9, 127.7, 127.7, 127.6, 126.5, 125.3, 34.82.

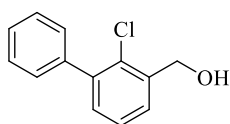
#### (2-chloro-3-(2,3-dihydrobenzo[b][1,4]dioxin-6-yl)phenyl)methanol (3.34)



(3-bromo-2-chlorophenyl)methanol (1.00 g, 3.72 mmol), (2,3-dihydrobenzo[b][1,4]dioxin-6-yl)boronic acid (2.01 g, 11.17 mmol), potassium carbonate (2.57 g; 18.62 mmol), and catalytic amount of Pd(dppf)Cl<sub>2</sub>·DCM were placed in a round-bottom flask under argon. Resulted mixture was

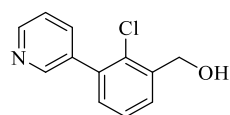
solubilized in a mixture of degassed dioxane/water (0.5 M, 2/1). Reaction was conducted under argon atmosphere by stirring at 90 °C during first 3 h. Then stirring was continued overnight at room temperature. Afterwards, crude mixture was diluted with AcOEt and filtered through Celite. Filtrate was concentrated under reduced pressure. Purification involved flash chromatography (0-60% AcOEt in hexane) and yielded **3.34** (737 mg, 72%) as colorless crystals. <sup>1</sup>H NMR (600 MHz, CDCl<sub>3</sub>) δ 7.47 (dd, *J* = 7.5, 1.7 Hz, 1H), 7.31 (t, *J* = 7.6 Hz, 1H), 7.26 (dd, *J* = 7.6, 1.8 Hz, 1H), 6.95 (d, *J* = 2.0 Hz, 1H), 6.92 (d, *J* = 8.3 Hz, 1H), 6.89 (dd, *J* = 8.3, 2.0 Hz, 1H), 4.84 (d, *J* = 5.8 Hz, 2H), 4.30 (s, 4H), 2.16 (t, *J* = 6.0 Hz, 1H). <sup>13</sup>C NMR (151 MHz, CDCl<sub>3</sub>) δ 143.3, 143.1, 140.7, 139.1, 132.9, 131.2, 130.7, 127.5, 126.8, 122.9, 118.6, 117.0, 64.6, 64.5, 63.6. UPLC-MS (DAD/ESI): *t*<sub>R</sub> = 6.10 min, for C<sub>15</sub>H<sub>13</sub>ClO<sub>3</sub> [M-OH]<sup>+</sup> found: 259.12 *m/z*; calc. mass: 259.05.

### (2-chloro-[1,1'-biphenyl]-3-yl)methanol (**3.35**)



(3-bromo-2-chlorophenyl)methanol (780 mg, 2.90 mmol), phenylboronic acid (280 mg, 2.19 mmol), potassium carbonate (70 mg; 0.55 mmol), and catalytic amount of Pd(dppf)Cl<sub>2</sub>·DCM were placed in a round-bottom flask under argon. Resulted mixture was solubilized in a mixture of degassed dioxane/water (0.5 M, 2/1). Reaction was conducted under argon atmosphere by stirring at 90 °C during first 3 h. Then stirring was continued overnight at room temperature. Afterwards, crude mixture was diluted with AcOEt and filtered through Celite. Filtrate was concentrated under reduced pressure. Purification involved flash chromatography (0-60% AcOEt in hexane) and yielded **3.35** (254 mg, 40%) as colorless crystals. <sup>1</sup>H NMR (600 MHz, CDCl<sub>3</sub>) δ 7.51 (m, 1H), 7.42 (m, 5H), 7.35 (t, *J* = 7.6 Hz, 1H), 7.29 (dd, *J* = 7.6, 1.8 Hz, 1H), 4.86 (d, *J* = 5.9 Hz, 2H), 2.12 (t, *J* = 6.2 Hz, 1H). <sup>13</sup>C NMR (151 MHz, CDCl<sub>3</sub>) δ 141.3, 139.6, 139.1, 131.2, 130.7, 129.6, 128.2, 127.8, 126.9, 63.7. UPLC-MS (DAD/ESI): *t*<sub>R</sub> = 6.49 min, C<sub>13</sub>H<sub>11</sub>ClO [M - OH]<sup>+</sup> found: 201.23 *m/z*; calc. mass: 201.04.

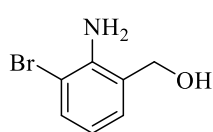
### (2-chloro-3-(pyridin-3-yl)phenyl)methanol (**3.36**)



(3-bromo-2-chlorophenyl)methanol (1.00 g, 3.73 mmol), 3-pyridinylboronic acid (0.60 g, 4.84 mmol), potassium carbonate (1.54 g; 11.18 mmol) and catalytic amount of Pd(dppf)Cl<sub>2</sub>·DCM were placed in a round-bottom flask under argon. Resulted mixture was solubilized in a mixture of degassed dioxane/water (0.5 M, 2/1). Reaction was conducted under argon atmosphere by stirring at 90 °C during first 3 h. Then stirring was continued overnight at room temperature. Afterwards,

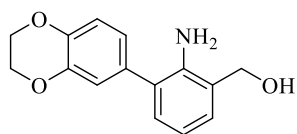
crude mixture was diluted with AcOEt and filtered through Celite. Filtrate was concentrated under reduced pressure. Purification involved flash chromatography (0-60% AcOEt in hexane) and yielded **3.36** (631 mg, 77%) as brown crystals.  $^1\text{H}$  NMR (600 MHz, DMSO)  $\delta$  8.61 (d,  $J$  = 5.2 Hz, 1H), 7.85 (m, 1H), 7.64 (m, 1H), 7.49 (m, 2H), 7.34 (dd,  $J$  = 7.5, 1.4 Hz, 1H), 5.50 (t,  $J$  = 5.6 Hz, 1H), 4.63 (d,  $J$  = 5.6 Hz, 2H).  $^{13}\text{C}$  NMR (151 MHz, DMSO)  $\delta$  149.5, 148.7, 140.7, 136.9, 136.7, 134.8, 129.7, 129.3, 127.6, 127.1, 123.3, 60.7. UPLC-MS (DAD/ESI):  $t_{\text{R}}$  = 2.46 min, for  $\text{C}_{12}\text{H}_{10}\text{ClNO}$   $[\text{M} + \text{H}]^+$  found: 220.05  $m/z$ ; calc. mass: 220.24.

### (2-amino-3-bromophenyl)methanol (**3.37.1.1**)



2-amino-3-bromobenzoic acid (4.00 g, 18.52 mmol) was dissolved in anhydrous THF (20 mL) and it was cooled to  $^{\circ}\text{C}$ . To the ice-cooled resulted solution  $\text{BH}_3\cdot\text{THF}$  complex (1 M, 28 mL) was added dropwise over a period of 3 hours. Solution was allowed to warm to room temperature and was stirred for additional 20 h. Subsequently, the mixture was poured into cooled solution of hydrochloric acid (1M, 100 mL) and then it was extracted with  $\text{Et}_2\text{O}$  (2 x 150 mL). The organic layers were collected together, dried over anhydrous  $\text{MgSO}_4$  filtered and concentrated. The crude product was purified by flash chromatography (silica gel, 0-100% AcOEt in hexane) to give colorless solid (2.43 g, yield: 65%).  $^1\text{H}$  NMR (600 MHz,  $\text{CDCl}_3$ )  $\delta$  7.39 (dd,  $J$  = 8.0, 1.4 Hz, 1H), 7.00 (dd,  $J$  = 7.4, 1.4 Hz, 1H), 6.58 (t,  $J$  = 7.6 Hz, 1H), 4.67 (s, 2H).  $^{13}\text{C}$  NMR (151 MHz,  $\text{CDCl}_3$ )  $\delta$  143.9, 132.7, 128.3, 125.8, 118.6, 110.5, 64.75.

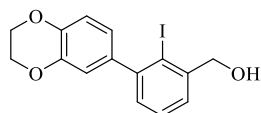
### (2-amino-3-(2,3-dihydrobenzo[b][1,4]dioxin-6-yl)phenyl)methanol (**3.37.1**)



**3.37.1.1** (800 mg, 3.96 mmol), (2,3-dihydrobenzo[b][1,4]dioxin-6-yl)boronic acid (852 mg, 4.75 mmol) and potassium carbonate (1.37 g, 9.93 mmol) were dissolved in mixture of dioxane and water (24:12 mL, v:v). The mixture was deoxygenated by rinsing with argon for 15 min. Then, resulting mixture was heated up to  $85^{\circ}\text{C}$  and  $\text{Pd}(\text{dppf})\text{Cl}_2\cdot\text{DCM}$  complex (162 mg, 0.20 mmol) was added. The mixture was stirred at  $85^{\circ}\text{C}$  for 3 hours. Afterwards, water (100 mL) was added to the reaction mixture and it was extracted with ethyl acetate (2x100 mL). The organic layers were combined, dried over anhydrous  $\text{MgSO}_4$ , filtered, and the solvent was removed under reduced pressure. The crude product was purified by flash chromatography (silica gel, 0-100% ethyl acetate in hexane) to give a colorless solid (823 mg, yield: 81%).  $^1\text{H}$  NMR (600 MHz,  $\text{CDCl}_3$ )  $\delta$  7.09 (dd,  $J$  = 7.5, 1.6 Hz, 1H), 7.07 (dd,  $J$  = 7.4, 1.5 Hz, 1H), 6.96 – 6.93 (m, 2H), 6.90 (dd,  $J$  = 8.2, 2.0 Hz, 1H), 6.76 (t,  $J$  = 7.5 Hz, 1H), 4.73 (s, 2H), 4.30 (s, 4H).  $^{13}\text{C}$  NMR

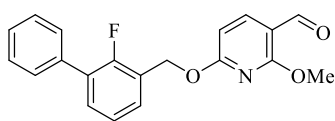
(151 MHz, CDCl<sub>3</sub>)  $\delta$  143.9, 143.1, 132.5, 130.7, 128.6, 128.3, 125.1, 122.4, 118.2, 118.0, 117.8, 64.9, 64.6.

### (3-(2,3-dihydrobenzo[b][1,4]dioxin-6-yl)-2-iodophenyl)methanol (3.37)



**3.37.1** (790 mg, 3.07 mmol) in H<sub>2</sub>SO<sub>4</sub> (6.0 mL of 22% H<sub>2</sub>SO<sub>4</sub>) was placed in the three-neck round-bottom flask and it was cooled to 0 °C. To the resulted mixture, aqueous solution of sodium nitrate (2.0 mL, 16%) was added dropwise over 30 minutes and then solution was allowed to stir at 0 °C for 1 h. Then an aqueous solution of potassium iodine (2.0 mL, 26%) was added carefully to the reaction mixture. The reaction was stopped after 1 h of stirring at room temperature. Saturated aqueous solution of sodium thiosulfate (50 mL) was added and the mixture was extracted with ethyl acetate (50 mL x 3). Organic layers were collected together and they were dried over MgSO<sub>4</sub> and concentrated under reduced pressure. The crude product was purified by column chromatography on silica gel using 0-20% AcOEt in hexane to give orange oil (402 mg, yield: 36%). <sup>1</sup>H NMR (600 MHz, CDCl<sub>3</sub>)  $\delta$  7.41 (dd, *J* = 7.6, 1.7 Hz, 1H), 7.35 (t, *J* = 7.5 Hz, 1H), 7.20 (dd, *J* = 7.4, 1.8 Hz, 1H), 6.91 (d, *J* = 8.2 Hz, 1H), 6.81 (d, *J* = 2.1 Hz, 1H), 6.76 (dd, *J* = 8.2, 2.1 Hz, 1H), 4.76 (s, 2H), 4.31 (s, *J* = 4.7 Hz, 4H). <sup>13</sup>C NMR (151 MHz, CDCl<sub>3</sub>)  $\delta$  147.15, 143.39, 143.09, 142.78, 138.24, 129.24, 127.99, 126.98, 122.58, 118.30, 116.65, 102.74, 70.56, 64.36, 64.33. UPLC-MS (DAD/ESI): *t*<sub>R</sub> = 6.39 min, C<sub>15</sub>H<sub>13</sub>IO<sub>3</sub> [M – OH]<sup>+</sup> found: 350.87 *m/z*; calc. mass: 350.99.

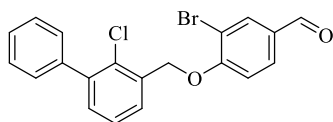
### 6-((2-fluoro-[1,1'-biphenyl]-3-yl)methoxy)-2-methoxynicotinaldehyde (3.38)



**3.7** (500 mg, 2.47 mmol), 2-chloro-6-methoxy-3-pyridinecarboxaldehyde (251 mg, 1.90 mmol), Cs<sub>2</sub>CO<sub>3</sub> (0.96 g, 3.81 mmol), *t*-BuXPhos (126 mg, 0.38 mmol) and palladium(II) acetate (33 mg, 0.19 mmol) were combined and purged with argon. Then, anhydrous toluene (13 mL) was added and the reaction mixture was heated at 80 °C for 4 h. Then, water was added (100 mL) and mixture was extracted with AcOEt (2x100 mL). Organic layers were combined and dried over MgSO<sub>4</sub>. Filtrate was concentrated under reduced pressure. The product was purified by flash chromatography on silica gel using 0–60% EtOAc in hexane to give pure product (423 mg, 49%). <sup>1</sup>H NMR (600 MHz, CDCl<sub>3</sub>)  $\delta$  10.13 (s, 1H), 7.99 (d, *J* = 8.3 Hz, 1H), 7.47 (m, 2H), 7.34 (m, 5H), 7.15 (t, *J* = 7.6 Hz, 1H), 6.39 (dd, *J* = 8.3, 0.7 Hz, 1H), 5.51 (s, 2H), 3.96 (s, 3H). <sup>13</sup>C NMR (151 MHz, CDCl<sub>3</sub>)  $\delta$  187.8, 166.2, 165.1, 157.8 (d, *J* = 249.7 Hz), 140.6, 135.6, 131.0 (d, *J* = 3.3 Hz), 129.4 (d, *J* = 13.8 Hz), 129.2 (m, 2C), 128.6, 128.0, 124.5

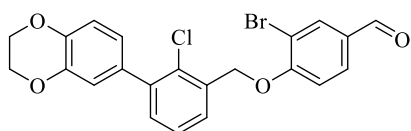
(d,  $J = 15.6$  Hz), 124.4 (d,  $J = 4.1$  Hz), 112.6, 103.9, 62.6 (d,  $J = 5.7$  Hz), 54.1. UPLC-MS (DAD/ESI):  $t_R = 8.87$  min,  $C_{20}H_{16}FNO_3$   $[M + H]^+$  found: 338.05  $m/z$ ; calc. mass: 338.12.

### 3-bromo-4-((2-chloro-[1,1'-biphenyl]-3-yl)methoxy)benzaldehyde (3.39)



**3.35** (200 mg, 0.94 mmol) was dissolved in anhydrous DCM (4 mL) under Ar.  $SOCl_2$  (1.14 mL) was added carefully and resulted mixture was stirred at 45 °C. After 3 h reaction was stopped and mixture was concentrated under reduced pressure. Generated *in situ* chloride, 3-bromo-4-hydroxybenzaldehyde (180 mg, 0.90 mmol) and  $K_2CO_3$  (230 mg, 1.67 mmol) were stirred in anhydrous DMF (4 mL) at room temperature overnight. The solvent was removed under reduced pressure. Water was added (100 mL) and mixture was extracted with AcOEt (2x100 mL). Organic layers were combined and concentrated. The crude product was chromatographed on silica gel eluting with 0-60% AcOEt in hexane to give 143 mg of a white solid colorless yield: 38%.  $^1H$  NMR (600 MHz,  $CDCl_3$ )  $\delta$  9.87 (s, 1H), 8.15 (d,  $J = 2.0$  Hz, 1H), 7.83 (dd,  $J = 8.4, 2.0$  Hz, 1H), 7.71 (m, 1H), 7.43 (m, 6H), 7.35 (dd,  $J = 7.6, 1.7$  Hz, 1H), 7.12 (d,  $J = 8.5$  Hz, 1H), 5.40 (s, 2H).  $^{13}C$  NMR (151 MHz,  $CDCl_3$ )  $\delta$  189.7, 159.6, 141.4, 139.3, 134.9, 134.2, 131.3, 131.3, 131.1, 130.3, 129.6, 128.3, 127.9, 127.1, 113.4, 113.1, 68.7. UPLC-MS (DAD/ESI):  $t_R = 8.93$  min, for  $C_{20}H_{14}BrClO_2$   $[M + H]^+$  found: 401.19  $m/z$ ; calc. mass: 400.99.

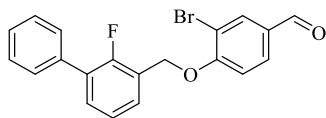
### 3-bromo-4-((2-chloro-3-(2,3-dihydrobenzo[b][1,4]dioxin-6-yl)benzyl)oxy)benzaldehyde (3.40)



**3.34** (700 mg, 2.53 mmol) was dissolved in anhydrous DCM (9 mL) under Ar.  $SOCl_2$  (3 mL) was added carefully and resulted mixture was stirred at 45 °C. After 3 h reaction was stopped and mixture was concentrated under reduced pressure. Generated *in situ* chloride, 3-bromo-4-hydroxybenzaldehyde (1.5 g, 7.58 mmol) and  $K_2CO_3$  (1.75 g, 12.64 mmol) were stirred in anhydrous DMF (10 mL) at room temperature overnight. The solvent was removed under reduced pressure. Water was added (100 mL) and mixture was extracted with AcOEt (2x100 mL). Organic layers were combined and concentrated. The crude product was chromatographed on silica gel eluting with 0-60% AcOEt in hexane to give 540 mg of a colorless solid with yield: 47%.  $^1H$  NMR (600 MHz,  $CDCl_3$ )  $\delta$  9.87 (s, 1H), 8.14 (d,  $J = 2.0$  Hz, 1H), 7.82 (dd,  $J = 8.5, 2.0$  Hz, 1H), 7.67 (dd,  $J = 7.6, 0.8$  Hz, 1H), 7.36 (t,  $J = 7.6$  Hz, 1H), 7.32 (dd,  $J = 7.6, 1.6$  Hz, 1H), 7.11 (d,  $J = 8.5$  Hz, 1H), 6.97 (d,  $J = 2.0$  Hz, 1H), 6.93 (m, 2H), 5.38 (s, 2H), 4.32 (s, 4H).  $^{13}C$  NMR (151 MHz,  $CDCl_3$ )  $\delta$  189.7, 159.6, 143.5, 143.2, 140.8, 134.8,

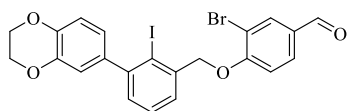
134.2, 132.5, 131.3, 131.2, 131.1, 130.4, 127.1, 126.9, 122.9, 118.6, 117.1, 113.4, 113.1, 68.7, 64.6, 64.5. UPLC-MS (DAD/ESI):  $t_R = 8.93$  min, for  $C_{22}H_{16}BrClO_4$   $[M + H]^+$  found: 459.17  $m/z$ ; calc. mass: 458.99.

### 3-bromo-4-((2-fluoro-[1,1'-biphenyl]-3-yl)methoxy)benzaldehyde (3.41)



**3.7** (700 mg, 3.47 mmol) was dissolved in anhydrous DCM (11 mL) under Ar.  $SOCl_2$  (4 mL) was added carefully and resulted mixture was stirred at 45 °C. After 3 h reaction was stopped and mixture was concentrated under reduced pressure. Generated *in situ* chloride, 3-bromo-4-hydroxybenzaldehyde (1.4 g, 6.93 mmol) and  $K_2CO_3$  (1.43 g, 10.39 mmol) were stirred in anhydrous DMF (10 mL) at room temperature overnight. The solvent was removed under reduced pressure. Water was added (100 mL) and mixture was extracted with AcOEt (2x100 mL). Organic layers were combined and concentrated. The crude product was chromatographed on silica gel eluting with 0-60% AcOEt in hexane to give 748 mg of a colorless solid with yield: 56%.  $^1H$  NMR (600 MHz,  $CDCl_3$ )  $\delta$  9.9 (s, 1H), 8.1 (d,  $J = 2.0$  Hz, 1H), 7.8 (dd,  $J = 8.5, 2.0$  Hz, 1H), 7.6 (td,  $J = 7.6, 1.7$  Hz, 1H), 7.6 (m, 2H), 7.5 (m, 3H), 7.4 (tt,  $J = 7.4, 1.2$  Hz, 1H), 7.3 (t,  $J = 7.7$  Hz, 1H), 7.1 (d,  $J = 8.5$  Hz, 1H), 5.4 (s, 2H).  $^{13}C$  NMR (151 MHz,  $CDCl_3$ )  $\delta$  189.69, 159.65, 157.08 (d,  $J = 248.6$  Hz), 135.43, 134.84, 131.27, 131.23, 131.02 (d,  $J = 3.2$  Hz), 129.33 (d,  $J = 13.6$  Hz), 129.22 (d,  $J = 1.9$  Hz), 128.67, 128.19 (d,  $J = 3.3$  Hz), 128.06, 124.75 (d,  $J = 3.9$  Hz), 123.59 (d,  $J = 15.0$  Hz), 113.43, 113.03, 65.17 (d,  $J = 6.2$  Hz). UPLC-MS (DAD/ESI):  $t_R = 8.92$  min,  $C_{20}H_{14}BrFO_2$   $[M + H]^+$  found: 384.96  $m/z$ ; calc. mass: 385.02.

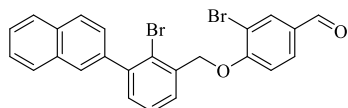
### 3-bromo-4-((3-(2,3-dihydrobenzo[b][1,4]dioxin-6-yl)-2-iodobenzyl)oxy)benzaldehyde (3.42)



**3.37** (668 mg, 1.81 mmol) was dissolved in anhydrous DCM (4 mL) and resulted mixture was cooled to 0°C.  $SOCl_2$  (0.7 mL) and 200  $\mu$ L of DMF was added carefully at 0°C and resulted mixture was stirred at ambient temperature for 1 h. Mixture was concentrated under reduced pressure. Generated *in situ* chloride, 3-bromo-4-hydroxybenzaldehyde (547 mg, 2.72 mmol) and  $K_2CO_3$  (500 mg, 3.63 mmol) were stirred in anhydrous DMF (6 mL) at room temperature overnight. The solvent was removed under reduced pressure. Water was added (100 mL) and mixture was extracted with AcOEt (2x100 mL). Organic layers were combined and concentrated. The crude product was chromatographed on silica gel eluting with 0-60% AcOEt in hexane to give 507 mg of a white solid with yield: 51%.  $^1H$  NMR (600 MHz,  $CDCl_3$ )  $\delta$  9.87 (s, 1H), 8.15 (d,  $J =$

2.0 Hz, 1H), 7.83 (dd,  $J = 8.4, 2.0$  Hz, 1H), 7.58 (m, 1H), 7.41 (t,  $J = 7.6$  Hz, 1H), 7.26 (dd,  $J = 7.5, 1.6$  Hz, 1H), 7.08 (d,  $J = 8.5$  Hz, 1H), 6.93 (d,  $J = 8.2$  Hz, 1H), 6.84 (d,  $J = 2.1$  Hz, 1H), 6.79 (dd,  $J = 8.2, 2.1$  Hz, 1H), 5.27 (s, 2H), 4.32 (s,  $J = 12.2$  Hz, 4H).  $^{13}\text{C}$  NMR (151 MHz,  $\text{CDCl}_3$ )  $\delta$  189.7, 159.5, 147.4, 143.4, 143.0, 138.5, 138.1, 134.8, 131.4, 131.2, 129.8, 128.4, 126.7, 122.8, 118.5, 116.9, 113.3, 113.2, 101.6, 76.3, 64.6, 64.5.

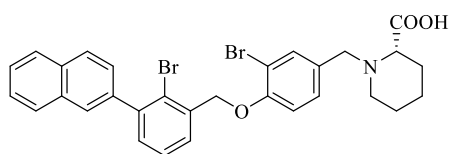
### 3-bromo-4-((2-bromo-3-(naphthalen-2-yl)benzyl)oxy)benzaldehyde (3.43)



**3.33** (200 mg, 0.53 mmol), 3-bromo-4-hydroxybenzaldehyde (107 mg, 0.53 mmol), potassium carbonate (146 mg, 1.06 mmol) were stirred in anhydrous DMF (3 mL) at room temperature overnight.

Then, solvent was removed under reduced pressure. The residue was dissolved in AcOEt (50 mL) and it was washed with water (2 x 30 mL). Organic layers were collected and concentrated. The crude product was chromatographed on silica gel eluting with 0-60% AcOEt in hexane to give 107 mg of a colorless solid with yield: 41%.  $^1\text{H}$  NMR (600 MHz,  $\text{CDCl}_3$ )  $\delta$ : 9.88 (s, 1H), 8.16 (d,  $J = 2.0$  Hz, 1H), 7.90 (m, 3H), 7.85 (m, 1H), 7.83 (d,  $J = 2.0$  Hz, 1H), 7.73 (dd,  $J = 7.7, 0.9$  Hz, 1H), 7.54 (m, 3H), 7.48 (t,  $J = 7.6$  Hz, 1H), 7.41 (dd,  $J = 7.5, 1.5$  Hz, 1H), 7.12 (d,  $J = 8.5$  Hz, 1H), 5.39 (s, 2H).  $^{13}\text{C}$  NMR (151 MHz,  $\text{CDCl}_3$ )  $\delta$ : 189.5, 159.4, 143.5, 138.5, 135.7, 134.7, 133.1, 132.7, 131.2, 131.2, 131.0, 128.3, 128.2, 127.8, 127.6, 127.6, 127.5, 127.2, 126.4, 122.0, 113.3, 113.0, 71.0. UPLC-MS (DAD/ESI):  $t_{\text{R}} = 10.02$  min, for  $\text{C}_{24}\text{H}_{16}\text{Br}_2\text{O}_2$   $[\text{M} + \text{H}]^+$  found: 494.93  $m/z$ ; calc. mass: 494.95.

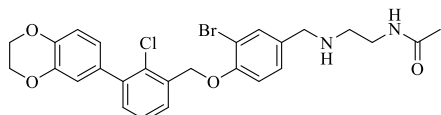
### (S)-1-(3-bromo-4-((2-bromo-3-(naphthalen-2-yl)benzyl)oxy)benzyl)piperidine-2-carboxylic acid (3.44)



Compound **3.44** was prepared following to the procedure of **3.13**, using **3.43** (90 mg, 0.18 mmol), L-pipecolic acid (107 mg, 0.83 mmol),  $\text{NaBH}_3\text{CN}$  (53 mg, 0.89 mmol), addition of AcOH (3 droplets) and anhydrous DMF (4 mL) as a solvent. The crude product was purified by column chromatography (silica gel, 0-30% MeOH in  $\text{CHCl}_3$ ) to give white solid (35 mg, yield: 32%) as a product.  $^1\text{H}$  NMR (600 MHz, DMSO)  $\delta$ : 7.99 (m, 3H), 7.93 (d,  $J = 1.1$  Hz, 1H), 7.72 (dd,  $J = 7.7, 1.6$  Hz, 1H), 7.63 (d,  $J = 1.9$  Hz, 1H), 7.57 (m, 4H), 7.48 (dd,  $J = 7.5, 1.7$  Hz, 1H), 7.33 (dd,  $J = 8.4, 1.9$  Hz, 1H), 7.21 (d,  $J = 8.5$  Hz, 1H), 5.30 (s, 2H), 3.85 (d,  $J = 13.4$  Hz, 1H), 3.47 (d,  $J = 13.4$  Hz, 1H), 3.08 (dd,  $J = 8.2, 3.9$  Hz, 1H), 2.88 (m, 1H), 2.23 (t,  $J = 8.3$  Hz, 1H), 1.82 (m, 1H), 1.69 (m, 1H), 1.49 (m, 3H), 1.35 (m, 1H).  $^{13}\text{C}$  NMR (151 MHz, DMSO)  $\delta$ : 153.9, 143.4, 138.8, 137.0, 134.1, 133.2, 132.7, 131.6, 130.3, 129.0, 128.6,

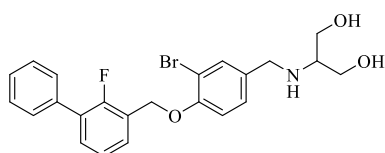
128.5, 128.3, 128.0, 127.9, 127.9, 126.9, 126.9, 123.1, 114.1, 111.4, 71.0, 64.5, 58.2, 49.6, 29.1, 24.7, 22.5. HRMS ESI-MS-q-TOF for C<sub>30</sub>H<sub>27</sub>Br<sub>2</sub>NO<sub>3</sub> [M + H]<sup>+</sup> found: 608.0432 *m/z*; calc. mass: 608.0436. UPLC-MS (DAD/ESI): t<sub>R</sub> = 7.37 min, for C<sub>30</sub>H<sub>27</sub>Br<sub>2</sub>NO<sub>3</sub> [M+H]<sup>+</sup> found: 608.19 *m/z*; calc. mass: 608.04.

**N-(2-((3-bromo-4-((2-chloro-3-(2,3-dihydrobenzo[b][1,4]dioxin-6-yl)benzyl)oxy)benzyl)amino)ethyl)acetamide (3.45)**



Compound **3.45** was prepared following to the procedure of **3.13**, using **3.40** (120 mg, 0.26 mmol), N-(2-aminoethyl)acetamide (122 mg, 1.20 mmol), NaBH<sub>3</sub>CN (76 mg, 1.31 mmol), addition of AcOH (3 droplets) and anhydrous DMF (4 mL) as a solvent. The crude product was purified by column chromatography (silica gel, 0-30% MeOH in CHCl<sub>3</sub>) to give white solid (94 mg, yield: 66%) as a product. <sup>1</sup>H NMR (600 MHz, DMSO) δ 7.87 (t, *J* = 5.4 Hz, 1H), 7.63 (dd, *J* = 7.6, 1.6 Hz, 1H), 7.62 (d, *J* = 2.0 Hz, 1H), 7.44 (t, *J* = 7.6 Hz, 1H), 7.36 (dd, *J* = 7.6, 1.6 Hz, 1H), 7.32 (dd, *J* = 8.4, 2.0 Hz, 1H), 7.19 (d, *J* = 8.5 Hz, 1H), 6.95 (d, *J* = 8.3 Hz, 1H), 6.91 (d, *J* = 2.1 Hz, 1H), 6.88 (dd, *J* = 8.3, 2.1 Hz, 1H), 5.27 (s, 2H), 4.28 (s, 4H), 3.69 (s, 2H), 3.15 (q, *J* = 6.3 Hz, 2H), 2.57 (t, *J* = 6.5 Hz, 2H), 1.80 (s, *J* = 7.2 Hz, 3H). <sup>13</sup>C NMR (151 MHz, DMSO) δ 169.67, 153.31, 143.30, 143.04, 140.17, 135.03, 132.91, 131.90, 131.17, 130.58, 129.05, 128.21, 127.30, 122.49, 118.08, 117.01, 113.92, 111.08, 68.36, 64.29, 64.24, 51.09, 47.74, 38.29, 22.74. HRMS ESI-MS-q-TOF for C<sub>26</sub>H<sub>26</sub>BrClN<sub>2</sub>O<sub>4</sub> [M + H]<sup>+</sup> found: 545.0836 *m/z*; calc. mass: 545.0842. UPLC-MS (DAD/ESI): t<sub>R</sub> = 5.85 min, C<sub>26</sub>H<sub>26</sub>BrClN<sub>2</sub>O<sub>4</sub> [M + H]<sup>+</sup> found: 545.24 *m/z*; calc. mass: 545.08.

**2-((3-bromo-4-((2-fluoro-[1,1'-biphenyl]-3-yl)methoxy)benzyl)amino)propane-1,3-diol (3.46)**

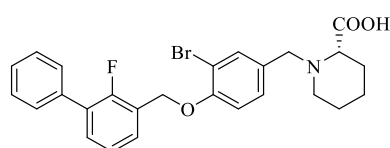


Compound **3.46** was prepared following to the procedure of **3.13**, using **3.41** (120 mg, 0.31 mmol), 2-amino-1,3-propanediol (129 mg, 1.42 mmol), NaBH<sub>3</sub>CN (90 mg, 1.56 mmol), addition of AcOH (3 droplets) and anhydrous DMF (4 mL) as a solvent. The crude product was purified by column chromatography (silica gel, 0-30% MeOH in CHCl<sub>3</sub>) to give colorless solid (104 mg, yield: 72%) as a product. <sup>1</sup>H NMR (600 MHz, CDCl<sub>3</sub>) δ 7.61 (t, *J* = 6.4 Hz, 1H), 7.56 (m, 3H), 7.46 (t, *J* = 7.6 Hz, 2H), 7.40 (m, 2H), 7.25 (m, 2H), 6.96 (d, *J* = 8.4 Hz, 1H), 5.27 (s, 2H), 3.76 (s, 2H), 3.73 (dd, *J* = 10.9, 4.5 Hz, 2H), 3.61 (dd, *J* = 10.9, 5.1 Hz,



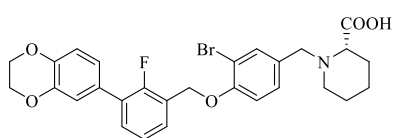
2H), 2.79 (p,  $J = 4.8$  Hz, 1H).  $^{13}\text{C}$  NMR (151 MHz,  $\text{CDCl}_3$ )  $\delta$  157.1 (d,  $^1J_{\text{C-F}} = 248.4$  Hz), 154.1, 135.6, 134.5, 133.3, 130.6 (d,  $J_{\text{C-F}} = 3.0$  Hz), 129.2 (d,  $^4J_{\text{C-F}} = 1.7$  Hz), 129.1 (d,  $^2J_{\text{C-F}} = 13.6$  Hz), 128.6, 128.3, 127.9, 124.6 (m, 2C), 113.9, 112.7, 65.0 (d,  $^3J_{\text{C-F}} = 6.1$  Hz), 62.4, 59.0, 50.2. HRMS ESI-MS-q-TOF for  $\text{C}_{23}\text{H}_{23}\text{BrFNO}_3$   $[\text{M} + \text{H}]^+$  found: 460.0919  $m/z$ ; calc. mass: 460.0923. UPLC-MS (DAD/ESI):  $t_{\text{R}} = 5.67$  min,  $\text{C}_{23}\text{H}_{23}\text{BrFNO}_3$   $[\text{M} + \text{H}]^+$  found: 460.04  $m/z$ ; calc. mass: 460.09.

**(S)-1-(3-bromo-4-((2-fluoro-[1,1'-biphenyl]-3-yl)methoxy)benzyl)piperidine-2-carboxylic acid (3.47)**



Compound **3.47** was prepared following to the procedure of **3.13**, using **3.41** (120 mg, 0.31 mmol), L-pipecolic acid (183 mg, 1.42 mmol),  $\text{NaBH}_3\text{CN}$  (90 mg, 1.56 mmol), addition of AcOH (3 droplets) and anhydrous DMF (4 mL) as a solvent. The crude product was purified by column chromatography (silica gel, 0-30% MeOH in  $\text{CHCl}_3$ ) to give colorless solid (51 mg, yield: 33%) as a product.  $^1\text{H}$  NMR (600 MHz,  $\text{CDCl}_3$ )  $\delta$  7.68 (m, 1H), 7.55 (m, 3H), 7.40 (m, 5H), 7.23 (t,  $J = 7.6$  Hz, 1H), 6.99 (d,  $J = 8.2$  Hz, 1H), 5.22 (s, 2H), 4.26 (m, 2H), 3.41 (d,  $J = 39.9$  Hz, 2H), 2.62 (m, 1H), 2.24 (m, 1H), 1.95 (m, 2H), 1.79 (m, 2H), 1.36 (m, 1H).  $^{13}\text{C}$  NMR (151 MHz,  $\text{CDCl}_3$ )  $\delta$  157.1 (d,  $^1J_{\text{C-F}} = 248.7$  Hz), 156.0, 136.3 (d,  $J_{\text{C-F}} = 3.8$  Hz), 135.5, 132.2, 130.8, 129.2 (3C), 128.6 (3C), 128.3 (d,  $^4J_{\text{C-F}} = 2.1$  Hz), 128.0, 124.6 (d,  $J_{\text{C-F}} = 3.3$  Hz), 124.1 (d,  $^2J_{\text{C-F}} = 15.2$  Hz), 113.7, 112.9, 65.0 (d,  $^3J_{\text{C-F}} = 5.5$  Hz), 57.6, 50.8, 29.8, 27.9, 22.8, 22.0. HRMS ESI-MS-q-TOF for  $\text{C}_{26}\text{H}_{25}\text{BrFNO}_3$   $[\text{M} + \text{Na}]^+$  found: 520.0892  $m/z$ ; calc. mass: 520.0899. UPLC-MS (DAD/ESI):  $t_{\text{R}} = 6.22$  min,  $\text{C}_{26}\text{H}_{25}\text{BrFNO}_3$   $[\text{M} + \text{H}]^+$  found: 498.26  $m/z$ ; calc. mass: 498.10.

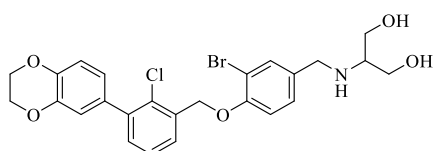
**(S)-1-(3-bromo-4-((3-(2,3-dihydrobenzo[b][1,4]dioxin-6-yl)-2-fluorobenzyl)oxy)benzyl)piperidine-2-carboxylic acid (3.48)**



Compound **3.48** was prepared following to the procedure of **3.13**, using **3.21** (110 mg, 0.25 mmol), L-pipecolic acid (145 mg, 1.13 mmol),  $\text{NaBH}_3\text{CN}$  (78 mg, 1.24 mmol), addition of AcOH (3 droplets) and anhydrous DMF (4 mL) as a solvent. The crude product was purified by column chromatography (silica gel, 0-30% MeOH in  $\text{CHCl}_3$ ) to give white solid (71 mg, yield: 51%) as a product.  $^1\text{H}$  NMR (600 MHz, DMSO)  $\delta$  7.58 (d,  $J = 1.5$  Hz, 1H), 7.51 (dt,  $J = 42.8, 7.1$  Hz, 2H), 7.30 (m, 2H), 7.23 (d,  $J = 8.5$  Hz, 1H), 7.03 (m, 2H), 6.96 (d,  $J = 8.3$  Hz,

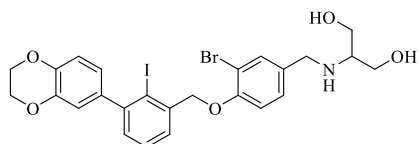
1H), 5.27 (s, 2H), 4.28 (s, 4H), 3.83 (d,  $J = 13.4$  Hz, 1H), 3.45 (d,  $J = 13.3$  Hz, 1H), 3.06 (dd,  $J = 8.1, 3.7$  Hz, 1H), 2.86 (m, 1H), 2.21 (t,  $J = 8.1$  Hz, 1H), 1.80 (m, 1H), 1.70 (m, 1H), 1.50 (m, 3H), 1.30 (m, 1H).  $^{13}\text{C}$  NMR (151 MHz, DMSO)  $\delta$  157.4 (d,  $^1J_{\text{C-F}} = 248.3$  Hz), 154.0, 143.8 (d,  $J_{\text{C-F}} = 10.2$  Hz), 134.0, 131.0, 130.2, 129.3, 128.3, 125.1, 122.3, 117.9, 117.7, 114.3, 111.5, 65.2 (d,  $^3J_{\text{C-F}} = 3.7$  Hz), 64.6, 64.5, 58.3, 49.6, 29.1, 24.8, 22.5. HRMS ESI-MS-q-TOF for  $\text{C}_{28}\text{H}_{27}\text{BrFNO}_5$   $[\text{M} + \text{H}]^+$  found: 556.1128  $m/z$ ; calc. mass: 556.1135. UPLC-MS (DAD/ESI):  $t_{\text{R}} = 6.03$  min,  $\text{C}_{28}\text{H}_{27}\text{BrFNO}_5$   $[\text{M} + \text{H}]^+$  found: 556.16  $m/z$ ; calc. mass: 556.11.

**2-((3-bromo-4-((2-chloro-3-(2,3-dihydrobenzo[b][1,4]dioxin-6-yl)benzyl)oxy)benzyl)amino)propane-1,3-diol (3.49)**



Compound **3.49** was prepared following to the procedure of **3.13**, using **3.40** (104 mg, 0.23 mmol), 2-amino-1,3-propanediol (94 mg, 1.03 mmol),  $\text{NaBH}_3\text{CN}$  (66 mg, 1.05 mmol), addition of AcOH (3 droplets) and anhydrous DMF (4 mL) as a solvent. The crude product was purified by column chromatography (silica gel, 0-30% MeOH in  $\text{CHCl}_3$ ) to give white solid (71 mg, yield: 59%) as a product.  $^1\text{H}$  NMR (600 MHz, DMSO)  $\delta$  7.64 (dd,  $J = 7.6, 1.5$  Hz, 1H), 7.62 (d,  $J = 1.9$  Hz, 1H), 7.45 (t,  $J = 7.6$  Hz, 1H), 7.34 (ddd,  $J = 10.3, 8.0, 1.8$  Hz, 2H), 7.17 (d,  $J = 8.5$  Hz, 1H), 6.95 (d,  $J = 8.3$  Hz, 1H), 6.92 (d,  $J = 2.1$  Hz, 1H), 6.88 (dd,  $J = 8.3, 2.1$  Hz, 1H), 5.27 (s, 2H), 4.29 (s,  $J = 4.4$  Hz, 4H), 3.73 (s, 2H), 3.38 (m, 5H), 2.5 (m, 1H).  $^{13}\text{C}$  NMR (151 MHz, DMSO)  $\delta$  152.9, 143.2, 142.9, 140.0, 135.0, 132.5, 131.8, 131.0, 130.4, 128.5, 128.0, 127.1, 122.3, 118.0, 116.9, 113.7, 110.9, 68.2, 64.2, 64.1, 60.9, 60.1, 49.4. HRMS ESI-MS-q-TOF for  $\text{C}_{25}\text{H}_{25}\text{BrClNO}_5$   $[\text{M} + \text{H}]^+$  found: 534.0676  $m/z$ ; calc. mass: 534.0683. UPLC-MS (DAD/ESI):  $t_{\text{R}} = 5.68$  min,  $\text{C}_{25}\text{H}_{25}\text{BrClNO}_5$   $[\text{M} + \text{H}]^+$  found: 534.08  $m/z$ ; calc. mass: 534.07.

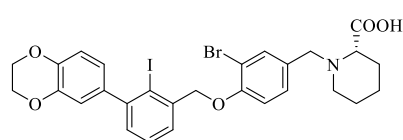
**2-((3-bromo-4-((3-(2,3-dihydrobenzo[b][1,4]dioxin-6-yl)-2-iodobenzyl)oxy)benzyl)amino)propane-1,3-diol (3.50)**



Compound **3.50** was prepared following to the procedure of **3.13**, using **3.44** (130 mg, 0.24 mmol), 2-amino-1,3-propanediol (98 mg, 1.08 mmol),  $\text{NaBH}_3\text{CN}$  (68 mg, 1.18 mmol), addition of AcOH (3 droplets) and anhydrous DMF (4 mL) as a solvent. The crude product was purified by column chromatography (silica gel, 0-30% MeOH in  $\text{CHCl}_3$ ) to give colorless solid (44 mg, yield: 30%) as a product.  $^1\text{H}$  NMR (600 MHz, DMSO)  $\delta$  7.62 (d,  $J =$

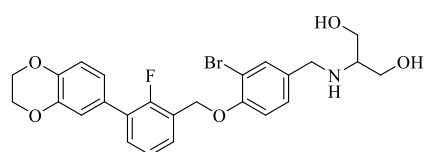
1.8 Hz, 1H), 7.54 (dd,  $J = 7.6, 1.4$  Hz, 1H), 7.46 (t,  $J = 7.6$  Hz, 1H), 7.33 (dd,  $J = 8.4, 1.8$  Hz, 1H), 7.25 (dd,  $J = 7.5, 1.5$  Hz, 1H), 7.13 (d,  $J = 8.5$  Hz, 1H), 6.92 (d,  $J = 8.2$  Hz, 1H), 6.78 (d,  $J = 2.1$  Hz, 1H), 6.74 (dd,  $J = 8.2, 2.1$  Hz, 1H), 5.16 (s, 2H), 4.29 (s, 4H), 3.72 (s, 2H), 3.38 (ddd,  $J = 34.9, 10.7, 5.5$  Hz, 4H), 2.53 (m, 1H).  $^{13}\text{C}$  NMR (151 MHz, DMSO)  $\delta$  153.0, 146.9, 143.0, 142.7, 139.5, 137.7, 132.6, 129.6, 128.6, 128.2, 127.7, 122.3, 117.9, 116.7, 113.7, 110.9, 103.5, 75.5, 64.2, 60.9, 60.1, 49.4. HRMS ESI-MS-q-TOF for  $\text{C}_{25}\text{H}_{25}\text{BrINO}_5$   $[\text{M} + \text{H}]^+$  found: 626.0034  $m/z$ ; calc. mass: 626.0039. UPLC-MS (DAD/ESI):  $t_{\text{R}} = 5.78$  min  $\text{C}_{25}\text{H}_{25}\text{BrINO}_5$   $[\text{M} + \text{H}]^+$  found: 626.06  $m/z$ ; calc. mass: 626.00.

**(S)-1-(3-bromo-4-((3-(2,3-dihydrobenzo[b][1,4]dioxin-6-yl)-2-iodobenzyl)oxy)benzyl)piperidine-2-carboxylic acid (3.53)**



Compound **3.53** was prepared following to the procedure of **3.13**, using **3.42** (130 mg, 0.24 mmol), L-pipecolic acid (140 mg, 1.08 mmol),  $\text{NaBH}_3\text{CN}$  (68 mg, 1.08 mmol), addition of AcOH (3 droplets) and anhydrous DMF (4 mL) as a solvent. The crude product was purified by column chromatography (silica gel, 0-30% MeOH in  $\text{CHCl}_3$ ) to give colorless solid (49 mg, yield: 31%) as a product.  $^1\text{H}$  NMR (600 MHz, DMSO)  $\delta$  7.60 (d,  $J = 1.8$  Hz, 1H), 7.55 (dd,  $J = 7.6, 1.5$  Hz, 1H), 7.46 (t,  $J = 7.6$  Hz, 1H), 7.32 (dd,  $J = 8.4, 1.8$  Hz, 1H), 7.26 (dd,  $J = 7.5, 1.6$  Hz, 1H), 7.16 (d,  $J = 8.5$  Hz, 1H), 6.92 (d,  $J = 8.2$  Hz, 1H), 6.78 (d,  $J = 2.1$  Hz, 1H), 6.75 (dd,  $J = 8.2, 2.1$  Hz, 1H), 5.18 (s, 2H), 4.29 (s, 4H), 3.81 (d,  $J = 13.4$  Hz, 1H), 3.44 (d,  $J = 13.3$  Hz, 1H), 3.06 (m, 1H), 2.85 (m, 1H), 2.20 (m, 1H), 1.81 (m, 1H), 1.68 (m, 1H), 1.47 (m, 3H), 1.35 (m, 1H).  $^{13}\text{C}$  NMR (151 MHz, DMSO)  $\delta$  153.4, 146.9, 143.0, 142.7, 139.4, 137.6, 133.5, 129.7, 129.6, 128.2, 127.7, 122.3, 117.9, 116.6, 113.6, 110.9, 103.4, 75.5, 64.1, 57.8, 49.1, 28.7, 24.4, 22.0. HRMS ESI-MS-q-TOF for  $\text{C}_{28}\text{H}_{27}\text{BrINO}_5$   $[\text{M} + \text{Na}]^+$  found: 686.0008  $m/z$ ; calc. mass: 686.0015. UPLC-MS (DAD/ESI):  $t_{\text{R}} = 6.63$  min  $\text{C}_{28}\text{H}_{27}\text{BrINO}_5$   $[\text{M} + \text{H}]^+$  found: 664.08  $m/z$ ; calc. mass: 664.02.

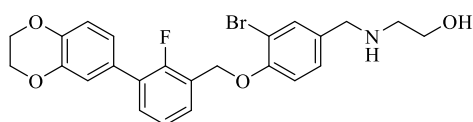
**2-(((3-bromo-4-((3-(2,3-dihydrobenzo[b][1,4]dioxin-6-yl)-2-fluorobenzyl)oxy)benzyl)amino)propane-1,3-diol (3.52)**



Compound **3.52** was prepared following to the procedure of **3.13**, using **3.21** (120 mg, 0.27 mmol), 2-amino-1,3-propanediol (112 mg, 1.23 mmol),  $\text{NaBH}_3\text{CN}$  (84 mg, 1.35 mmol), addition of AcOH (3 droplets) and anhydrous DMF (4 mL) as a solvent. The crude

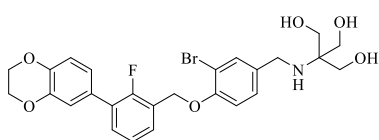
product was purified by column chromatography (silica gel, 0-30% MeOH in CHCl<sub>3</sub>) to give colorless solid (75 mg, yield: 54%) as a product. <sup>1</sup>H NMR (600 MHz, MeOD) δ 7.68 (d, *J* = 2.1 Hz, 1H), 7.49 (t, *J* = 6.4 Hz, 1H), 7.37 (m, 2H), 7.19 (t, *J* = 7.7 Hz, 1H), 7.14 (d, *J* = 8.5 Hz, 1H), 6.98 (m, 2H), 6.86 (d, *J* = 8.3 Hz, 1H), 5.25 (s, 2H), 4.24 (s, *J* = 4.1 Hz, 4H), 4.01 (s, 2H), 3.68 (ddd, *J* = 17.4, 11.6, 5.4 Hz, 4H), 3.00 (d, *J* = 5.3 Hz, 1H). <sup>13</sup>C NMR (151 MHz, MeOD) δ 158.6, 156.4, 144.9 (d, *J*<sub>C-F</sub> = 16.0 Hz), 135.4, 131.6 (d, *J*<sub>C-F</sub> = 2.9 Hz), 131.0, 129.9, 129.8 (d, *J*<sub>C-F</sub> = 4.0 Hz), 129.5 (d, *J*<sub>C-F</sub> = 3.3 Hz), 125.7, 125.5 (d, *J*<sub>C-F</sub> = 3.6 Hz), 123.1, 118.9, 118.3, 115.1, 113.4, 66.1 (d, <sup>3</sup>*J*<sub>C-F</sub> = 5.1 Hz), 65.7, 65.6, 61.2, 60.5, 49.8. HRMS ESI-MS-q-TOF for C<sub>25</sub>H<sub>25</sub>BrFNO<sub>5</sub> [M + H]<sup>+</sup> found: 518.0972 *m/z*; calc. mass: 518.0978. UPLC-MS (DAD/ESI): t<sub>R</sub> = 5.38 min C<sub>25</sub>H<sub>25</sub>BrFNO<sub>5</sub> [M + H]<sup>+</sup> found: 518.06 *m/z*; calc. mass: 518.10.

**2-((3-bromo-4-((3-(2,3-dihydrobenzo[*b*][1,4]dioxin-6-yl)-2-fluorobenzyl)oxy)benzyl)amino)ethan-1-ol (3.53)**



Compound **3.53** was prepared following to the procedure of **3.13**, using **3.21** (130 mg, 0.29 mmol), ethanolamine (82 mg, 1.34 mmol), NaBH<sub>3</sub>CN (85 mg, 1.47 mmol), addition of AcOH (3 droplets) and anhydrous DMF (4 mL) as a solvent. The crude product was purified by column chromatography (silica gel, 0-30% MeOH in CHCl<sub>3</sub>) to give colorless solid (81 mg, yield: 56%) as a product. <sup>1</sup>H NMR (600 MHz, DMSO) δ 7.57 (d, *J* = 1.9 Hz, 1H), 7.50 (dt, *J* = 15.3, 7.0 Hz, 2H), 7.29 (m, 2H), 7.20 (d, *J* = 8.4 Hz, 1H), 7.05 (s, 1H), 7.03 (d, *J* = 8.4 Hz, 1H), 6.96 (d, *J* = 8.3 Hz, 1H), 5.26 (s, 2H), 4.48 (s, 1H), 4.28 (s, 4H), 3.65 (s, 2H), 3.45 (t, *J* = 5.7 Hz, 2H), 3.33 (s, 1H), 2.53 (t, *J* = 5.8 Hz, 2H). <sup>13</sup>C NMR (151 MHz, DMSO) δ 157.4 (d, <sup>1</sup>*J*<sub>C-F</sub> = 248.1 Hz), 153.4, 143.8 (d, *J*<sub>C-F</sub> = 9.9 Hz), 135.8, 132.9, 130.93, 129.2, 128.9, 128.3, 125.1 (d, *J*<sub>C-F</sub> = 3.4 Hz), 124.9 (d, *J*<sub>C-F</sub> = 15.9 Hz), 122.30, 117.89, 117.71, 114.41, 111.48, 65.2 (d, <sup>3</sup>*J*<sub>C-F</sub> = 4.3 Hz), 64.65, 64.57, 60.78, 51.98, 51.30. HRMS ESI-MS-q-TOF for C<sub>24</sub>H<sub>23</sub>BrFNO<sub>4</sub> [M + H]<sup>+</sup> found: 488.0866 *m/z*; calc. mass: 488.0872. UPLC-MS (DAD/ESI): t<sub>R</sub> = 5.63 min C<sub>24</sub>H<sub>23</sub>BrFNO<sub>4</sub> [M + H]<sup>+</sup> found: 488.16 *m/z*; calc. mass: 488.09.

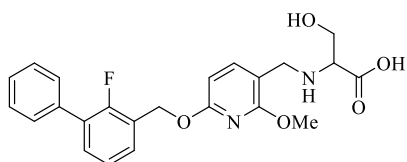
**2-((3-bromo-4-((3-(2,3-dihydrobenzo[*b*][1,4]dioxin-6-yl)-2-fluorobenzyl)oxy)benzyl)amino)-2-(hydroxymethyl)propane-1,3-diol (3.54)**



Compound **3.54** was prepared following to the procedure of **3.13**, using **3.21** (130 mg, 0.29 mmol), tris(hydroxymethyl)aminomethane (162 mg, 1.34 mmol),

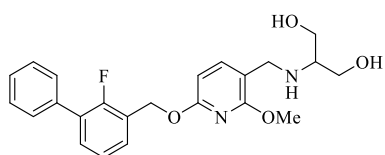
NaBH<sub>3</sub>CN (85 mg, 1.47 mmol), addition of AcOH (3 droplets) and anhydrous DMF (4 mL) as a solvent. The crude product was purified by column chromatography (silica gel, 0-30% MeOH in CHCl<sub>3</sub>) to give colorless solid (50 mg, yield: 31%) as a product. <sup>1</sup>H NMR (600 MHz, DMSO) δ 7.62 (d, *J* = 1.7 Hz, 1H), 7.50 (dt, *J* = 39.1, 7.0 Hz, 2H), 7.31 (m, 2H), 7.20 (d, *J* = 8.5 Hz, 1H), 7.05 (s, 1H), 7.03 (d, *J* = 8.5 Hz, 1H), 6.97 (d, *J* = 8.3 Hz, 1H), 5.27 (s, 2H), 4.29 (s, 4H), 3.71 (s, 2H), 3.40 (s, 6H). <sup>13</sup>C NMR (151 MHz, DMSO) δ 156.9 (d, *J*<sub>C-F</sub> = 248.1 Hz), 153.00, 143.4 (d, *J*<sub>C-F</sub> = 9.9 Hz), 132.71, 130.48, 128.7, 128.7 (d, *J*<sub>C-F</sub> = 7.1 Hz), 127.8, 127.8 (d, *J*<sub>C-F</sub> = 12.5 Hz), 124.6 (d, *J*<sub>C-F</sub> = 2.9 Hz), 124.4 (d, *J*<sub>C-F</sub> = 15.6 Hz), 121.8, 117.4, 117.2, 113.9, 110.9, 64.7 (d, *J*<sub>C-F</sub> = 4.2 Hz), 64.19, 64.10, 60.94, 60.52, 44.27. HRMS ESI-MS-q-TOF for C<sub>26</sub>H<sub>27</sub>BrFNO<sub>6</sub> [M + H]<sup>+</sup> found: 548.1078 *m/z*; calc. mass: 548.1084. UPLC-MS (DAD/ESI): *t*<sub>R</sub> = 5.50 min, C<sub>26</sub>H<sub>27</sub>BrFNO<sub>6</sub> [M + H]<sup>+</sup> found: 548.17 *m/z*; calc. mass: 548.11.

**((6-((2-fluoro-[1,1'-biphenyl]-3-yl)methoxy)-2-methoxypyridin-3-yl)methyl)serine (3.55)**



Compound **3.55** was prepared following to the procedure of **3.13**, using **3.38** (150 mg, 0.45 mmol), *L*-serine (213 mg, 2.03 mmol), NaBH<sub>3</sub>CN (140 mg, 2.23 mmol), addition of AcOH (3 droplets) and anhydrous DMF (5 mL) as a solvent. The crude product was purified by column chromatography (silica gel, 0-30% MeOH in CHCl<sub>3</sub>) to give colorless solid (63 mg, yield: 33%) as a product. <sup>1</sup>H NMR (600 MHz, DMSO) δ 7.71 (d, *J* = 8.0 Hz, 1H), 7.55 (m, 3H), 7.49 (m, 3H), 7.41 (m, 1H), 7.30 (t, *J* = 7.6 Hz, 1H), 6.47 (d, *J* = 8.0 Hz, 1H), 5.48 (s, 2H), 3.89 (m, 5H), 3.71 (dd, *J* = 11.2, 4.5 Hz, 1H), 3.62 (dd, *J* = 11.2, 6.4 Hz, 1H), 3.16 (m, 1H). <sup>13</sup>C NMR (151 MHz, DMSO) δ 169.6, 161.4, 160.1, 157.2 (d, *J* = 248.3 Hz), 142.8, 134.9, 130.7, 129.9 (d, *J* = 3.0 Hz), 128.9, 128.6, 128.4 (d, *J* = 13.5 Hz), 127.9, 124.9 (d, *J* = 15.6 Hz), 124.6 (d, *J* = 3.2 Hz), 108.7, 101.3, 77.4, 62.6, 61.5 (d, <sup>3</sup>*J*<sub>C-F</sub> = 4.0 Hz), 60.7, 53.5, 44.3. HRMS ESI-MS-q-TOF for [M + Na]<sup>+</sup> found: 449.1480 *m/z*; calc. mass: 449.1489. UPLC-MS (DAD/ESI): *t*<sub>R</sub> = 6.67 min, C<sub>23</sub>H<sub>23</sub>FN<sub>2</sub>O<sub>5</sub> [M + H]<sup>+</sup> found: 427.17 *m/z*; calc. mass: 427.17.

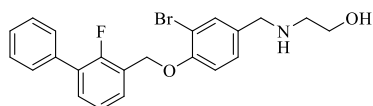
**2-(((6-((2-fluoro-[1,1'-biphenyl]-3-yl)methoxy)-2-methoxypyridin-3-yl)methyl)amino)propane-1,3-diol (3.56)**



Compound **3.56** was prepared following to the procedure of **3.13**, using **3.38** (130 mg, 0.39 mmol), 2-amino-1,3-propanediol (160 mg, 1.76 mmol), NaBH<sub>3</sub>CN (121 mg, 1.93 mmol), addition of AcOH (3 droplets) and anhydrous DMF (5 mL) as a solvent. The crude

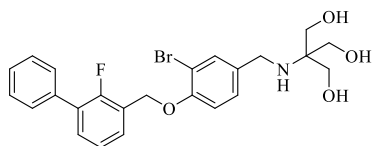
product was purified by column chromatography (silica gel, 0-30% MeOH in CHCl<sub>3</sub>) to give colorless solid (67 mg, yield: 42%) as a product. <sup>1</sup>H NMR (600 MHz, CDCl<sub>3</sub>) δ 7.54 (d, *J* = 8.2 Hz, 2H), 7.51 (d, *J* = 7.9 Hz, 1H), 7.45 (m, 3H), 7.38 (m, 2H), 7.20 (t, *J* = 7.6 Hz, 1H), 6.38 (d, *J* = 7.9 Hz, 1H), 5.49 (s, 2H), 3.96 (s, 3H), 3.85 (s, 2H), 3.77 (dd, *J* = 11.4, 4.2 Hz, 2H), 3.64 (dd, *J* = 11.4, 5.3 Hz, 2H), 2.87 (m, 1H). <sup>13</sup>C NMR (151 MHz, CDCl<sub>3</sub>) δ 162.1, 160.7, 157.7 (d, *J* = 249.4 Hz), 141.9, 135.8, 130.6 (d, *J* = 2.8 Hz), 129.3, 129.2, 128.6, 127.9, 125.4 (d, *J* = 15.7 Hz), 124.3 (d, *J* = 3.9 Hz), 110.8, 101.8, 61.9 (d, *J* = 5.6 Hz), 61.3, 59.0, 53.8, 45.3. HRMS ESI-MS-q-TOF for C<sub>23</sub>H<sub>25</sub>FN<sub>2</sub>O<sub>4</sub> [M + H]<sup>+</sup> found: 413.1870 *m/z*; calc. mass: 413.1877. UPLC-MS (DAD/ESI): t<sub>R</sub> = 6.51 min, C<sub>23</sub>H<sub>25</sub>FN<sub>2</sub>O<sub>4</sub> [M + H]<sup>+</sup> found: 413.21 *m/z*; calc. mass: 413.19.

### 2-((3-bromo-4-((2-fluoro-[1,1'-biphenyl]-3-yl)methoxy)benzyl)amino)ethan-1-ol (3.57)



Compound **3.57** was prepared following to the procedure of **3.13**, using **3.41** (150 mg, 0.39 mmol), ethanolamine (108 mg, 1.77 mmol), NaBH<sub>3</sub>CN (112 mg, 1.94 mmol), addition of AcOH (3 droplets) and anhydrous DMF (5 mL) as a solvent. The crude product was purified by column chromatography (silica gel, 0-30% MeOH in CHCl<sub>3</sub>) to give colorless solid (76 mg, yield: 46%) as a product. <sup>1</sup>H NMR (600 MHz, MeOD) δ 7.75 (d, *J* = 2.2 Hz, 1H), 7.58 (td, *J* = 7.6, 1.6 Hz, 1H), 7.56 – 7.52 (m, 2H), 7.49 – 7.43 (m, 4H), 7.40 – 7.36 (m, 1H), 7.28 (t, *J* = 7.6 Hz, 1H), 7.24 (d, *J* = 8.5 Hz, 1H), 5.33 (s, 2H), 4.12 (s, 2H), 3.81 – 3.75 (m, 2H), 3.08 – 3.05 (m, 2H). <sup>13</sup>C NMR (151 MHz, MeOD) δ 158.7 (d, <sup>1</sup>*J*<sub>C-F</sub> = 248.3 Hz), 157.0, 136.8, 135.9, 132.0 (d, *J*<sub>C-F</sub> = 3.1 Hz), 131.6, 130.5 (d, <sup>2</sup>*J*<sub>C-F</sub> = 13.7 Hz), 130.1, 130.0 (d, *J* = 3.6 Hz), 129.5, 128.9, 127.7, 125.6 (m, 2C), 115.2, 113.6, 66.2 (d, <sup>3</sup>*J*<sub>C-F</sub> = 5.6 Hz), 58.3, 51.2, 50.2. HRMS ESI-MS-q-TOF for C<sub>22</sub>H<sub>21</sub>BrFNO<sub>2</sub> [M + Na]<sup>+</sup> found: 452.0634 *m/z*; calc. mass 452.0637. UPLC-MS (DAD/ESI): t<sub>R</sub> = 5.81 min, C<sub>22</sub>H<sub>21</sub>BrFNO<sub>2</sub> [M + H]<sup>+</sup> found: 430.20 *m/z*; calc. mass: 430.08.

### 2-((3-bromo-4-((2-fluoro-[1,1'-biphenyl]-3-yl)methoxy)benzyl)amino)-2-(hydroxymethyl)propane-1,3-diol (3.58)

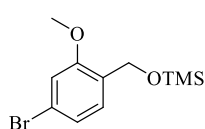


Compound **3.58** was prepared following to the procedure of **3.13**, using **3.41** (170 mg, 0.44 mmol), 2-amino-2-(hydroxymethyl)propane-1,3-diol (243 mg, 2.00 mmol), NaBH<sub>3</sub>CN (127 mg, 2.20 mmol), addition of AcOH (6 droplets) and anhydrous DMF (6 mL) as a solvent. The crude product was purified by column chromatography (silica gel, 0-30% MeOH in CHCl<sub>3</sub>) to give colorless solid (176 mg, yield: 82%) as a product. <sup>1</sup>H NMR (600 MHz, DMSO) δ 7.62 (d, *J* = 1.9 Hz, 1H), 7.61 – 7.57 (m, 1H), 7.56 (d, *J* = 8.1 Hz, 2H), 7.54 – 7.48

(m, 3H), 7.44 – 7.41 (m, 1H), 7.34 (t,  $J = 7.6$  Hz, 1H), 7.31 (dd,  $J = 8.4, 2.0$  Hz, 1H), 7.20 (d,  $J = 8.5$  Hz, 1H), 5.29 (s, 2H), 3.70 (s, 2H), 3.40 (s, 6H).  $^{13}\text{C}$  NMR (151 MHz, DMSO)  $\delta$  157.0 (d,  $^1J_{\text{C-F}} = 248.5$  Hz), 153.0, 134.9, 132.7, 130.8, 129.3 (d,  $J = 3.1$  Hz), 128.9 (2C), 128.7 (2C), 128.4 (d,  $^2J_{\text{C-F}} = 13.2$  Hz), 128.0, 124.7 (d,  $J = 3.3$  Hz), 124.4 (d,  $^2J_{\text{C-F}} = 15.4$  Hz), 113.9, 110.9, 64.7 (d,  $^3J_{\text{C-F}} = 4.4$  Hz), 61.0, 60.4, 44.3. HRMS ESI-MS-q-TOF for  $\text{C}_{24}\text{H}_{25}\text{BrFNO}_4$   $[\text{M} + \text{H}]^+$  found: 490.1023  $m/z$ ; calc. mass: 490.1029. UPLC-MS (DAD/ESI):  $t_{\text{R}} = 5.59$  min,  $\text{C}_{24}\text{H}_{25}\text{BrFNO}_4$   $[\text{M} + \text{H}]^+$  found: 490.22  $m/z$ ; calc. mass: 490.10.

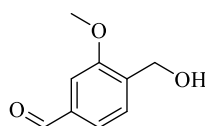
#### 4.2.4. 2,3-dihydro-1H-indene Derivative as Elongated Potential PD-L1 Antagonists

##### ((4-bromo-2-methoxybenzyl)oxy)trimethylsilane (4.1)



(4-bromo-2-methoxyphenyl)methanol (5.00 g, 23.04 mmol) and TMSCl (3.25 mL, 2.78 g, 25.59 mmol) were placed in the round bottom flask under argon. Then, anhydrous THF (93 mL) and TEA (4.80 mL, 3.49 g, 34.56 mmol) were added and resulted mixture was stirred overnight at room temperature. After that time, solvent was removed under reduced pressure and water (100 mL) was added. Ethyl acetate (100 mL x 2) was used to extract water phase. The organic layers were combined, dried over anhydrous  $\text{MgSO}_4$ , filtered, and the solvent was removed under reduced pressure. The crude product was purified by flash chromatography (silica gel, 0-50% ethyl acetate in hexane) to give the product a colorless oil (5.05 g, yield: 76%).  $^1\text{H}$  NMR (300 MHz,  $\text{CDCl}_3$ )  $\delta$  7.29 (d,  $J = 8.1$  Hz, 1H), 7.09 (dd,  $J = 8.0, 1.5$  Hz, 1H), 6.95 (d,  $J = 1.5$  Hz, 1H), 4.64 (s, 2H), 3.81 (s, 3H), 0.18 (s, 9H).

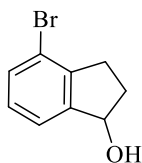
##### 4-(hydroxymethyl)-3-methoxybenzaldehyde (4.2)



**4.1** (4.28 g, 14.81 mmol) was placed under argon in the previously dried reaction tube. Then, anhydrous THF (59 mL) was added and reaction mixture was cooled to  $-78$  °C in the acetone/dry ice bath. Afterwards, 2.5 M solution of *n*-BuLi in hexane (8.9 mL, 22.22 mmol) was added dropwise for 30 minutes. Resulted solution was stirred at  $-78$  °C for next 30 minutes. Next anhydrous DMF (1.88 mL) was added dropwise for additional 30 minutes and the mixture was stirred overnight allowing the temperature to come to ambient conditions. After that time, 1 M solution of HCl (12 mL) was added dropwise. Solvent was removed under reduced pressure and water (100 mL) and DCM (100 mL x 2) were added to separate the phases. The organic layers were combined, dried over anhydrous  $\text{MgSO}_4$ , filtered, and the solvent was removed under reduced pressure. The

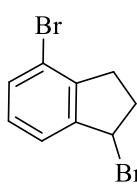
crude product was purified by flash chromatography (silica gel, 0-50% ethyl acetate in hexane) to give the product a colorless solid (0.98 g, yield: 40%).  $^1\text{H}$  NMR (600 MHz,  $\text{CDCl}_3$ )  $\delta$  9.95 (s, 1H), 7.51 (d,  $J = 7.5$  Hz, 1H), 7.45 (dd,  $J = 7.5, 1.3$  Hz, 1H), 7.37 (d,  $J = 1.1$  Hz, 1H), 4.74 (s, 2H), 3.91 (s, 3H).  $^{13}\text{C}$  NMR (151 MHz,  $\text{CDCl}_3$ )  $\delta$  192.1, 157.7, 137.1, 136.5, 128.4, 124.9, 108.3, 61.4, 55.7.

#### 4-bromo-2,3-dihydro-1H-inden-1-ol (4.3)



4-bromo-2,3-dihydro-1H-inden-1-one (4.00 g, 18.69 mmol) was placed in the round bottom flask under argon. Then, anhydrous ethanol (150 mL) was added and solution was cooled to 0 °C. Sodium borohydride (565 mg, 14.95 mmol) was added portionwise and resulted mixture was stirred overnight at room temperature. After that time, solvent was removed under reduced pressure and mixture of DCM: 10% HCl (400 mL, 1:1, v:v) was added to separate the phases. Water phase was washed with DCM (200 mL), organic layers were collected, dried with anhydrous  $\text{MgSO}_4$ , filtrated and concentrated under reduced pressure. Compound **4.3** was obtained as colorless solid (3.91 g, 97%) and was used further without additional purification.  $^1\text{H}$  NMR (600 MHz,  $\text{CDCl}_3$ )  $\delta$  7.39 (s, 1H), 7.36 (d,  $J = 8.1$  Hz, 1H), 7.26 (d,  $J = 8.0$  Hz, 1H), 5.18 (t,  $J = 6.1$  Hz, 1H), 3.03 (ddd,  $J = 16.1, 8.5, 4.7$  Hz, 1H), 2.87 – 2.74 (m, 1H), 2.54 – 2.43 (m, 1H), 2.02 – 1.89 (m, 1H).  $^{13}\text{C}$  NMR (151 MHz,  $\text{CDCl}_3$ )  $\delta$  145.8, 144.1, 130.0, 128.2, 125.9, 122.4, 75.9, 36.2, 29.8.

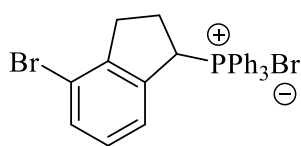
#### 1,4-dibromo-2,3-dihydro-1H-indene (4.4)



**4.3** (3.23 g, 15.17 mmol) was placed in round bottom flask and was dissolved in DCM (32 mL). Then, HBr (16.2 mL, 40%) was added dropwise and resulted mixture was stirred at room temperature for 4 hours. After that time, solution was neutralised with sodium bicarbonate and it was transferred to separatory funnel. DCM: water (200 mL, 1:1, v:v) was added to separate the phases. Water phase was additionally washed with DCM (100 mL), organic layers were collected together, dried over anhydrous  $\text{MgSO}_4$ , filtrated and concentrated under reduced pressure. Compound **4.4** was obtained as colorless solid (4.13 g, 99%) and was used further without additional purification.  $^1\text{H}$  NMR (600 MHz,  $\text{CDCl}_3$ )  $\delta$  7.42 (d,  $J = 7.9$  Hz, 1H), 7.36 (d,  $J = 7.5$  Hz, 1H), 7.12 (t,  $J = 7.7$  Hz, 1H), 5.60 (dd,  $J = 6.6, 2.3$  Hz, 1H), 3.21 – 3.12 (m, 1H), 2.96 (ddd,  $J = 16.6, 8.0, 2.7$  Hz, 1H), 2.66 – 2.59 (m, 1H), 2.53 (ddt,  $J = 14.5, 7.6, 2.5$  Hz, 1H).  $^{13}\text{C}$  NMR (151 MHz,  $\text{CDCl}_3$ )  $\delta$  145.7, 144.1, 132.0, 129.1, 124.2, 120.1, 54.3 36.7, 32.2.

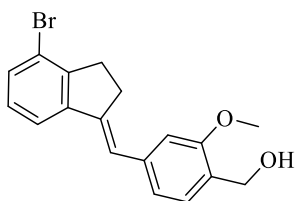


**(4-bromo-2,3-dihydro-1H-inden-1-yl)triphenylphosphonium bromide (4.5)**



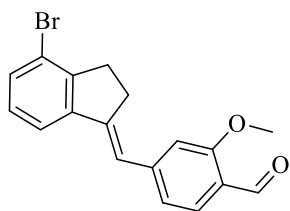
**4.4** (4.13 g, 15.02 mmol) and triphenylphosphine (4.40 g, 24.27 mmol) was solubilised in toluene (20 mL). Resulted solution was heated overnight at 110 °C. After that time, it was cooled to room temperature. The crystallised salt was filtered and it was washed with cold toluene. Obtained colorless precipitate (2.73 g, 5.08 mmol) was dried and used further without additional purification. <sup>1</sup>H NMR (600 MHz, CDCl<sub>3</sub>) δ 7.86 – 7.78 (m, 6H), 7.74 (td, *J* = 7.1, 1.1 Hz, 3H), 7.61 (td, *J* = 7.9, 3.5 Hz, 6H), 7.42 (t, *J* = 10.0 Hz, 1H), 7.32 (dd, *J* = 7.8, 2.2 Hz, 1H), 6.84 (t, *J* = 7.8 Hz, 1H), 6.77 (dd, *J* = 7.6, 2.3 Hz, 1H), 3.30 – 3.12 (m, 1H), 2.73 – 2.63 (m, 1H), 2.38 – 2.22 (m, 1H), 1.54 – 1.40 (m, 1H). <sup>13</sup>C NMR (151 MHz, CDCl<sub>3</sub>) δ 146.6 (d, *J*<sub>C-P</sub> = 6.3 Hz), 136.1 (d, *J*<sub>C-P</sub> = 5.9 Hz), 135.0 (d, <sup>4</sup>*J*<sub>C-P</sub> = 2.1 Hz, PPh<sub>3</sub>), 134.2 (d, <sup>3</sup>*J*<sub>C-P</sub> = 9.4 Hz, PPh<sub>3</sub>), 132.1 (d, *J*<sub>C-P</sub> = 3.3 Hz), 130.4 (d, <sup>2</sup>*J*<sub>C-P</sub> = 12.2 Hz, PPh<sub>3</sub>), 128.8 (d, *J*<sub>C-P</sub> = 2.9 Hz), 125.6 (d, *J*<sub>C-P</sub> = 3.7 Hz), 120.4 (d, *J*<sub>C-P</sub> = 3.2 Hz), 117.8 (d, <sup>1</sup>*J*<sub>C-P</sub> = 83.2 Hz, *ipso*-PPh<sub>3</sub>), 40.6 (d, <sup>1</sup>*J*<sub>C-P</sub> = 43.6 Hz), 32.8, 26.1.

**(E)-4-(((4-bromo-2,3-dihydro-1H-inden-1-ylidene)methyl)-2-methoxyphenyl)methanol (4.6)**



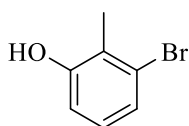
**4.5** (2.67 g, 4.84 mmol), **4.2** (712 mg, 4.17 mmol), potassium carbonate (5.91 g, 41.74 mmol) and 18-crown-6 (12 mg, 0.04 mmol) were placed in the round bottom flask. Then, DCM (28 mL) was added and reaction mixture was refluxed overnight. After cooling to room temperature, water (50 mL) was added. The mixture was washed with dichloromethane (2 x 50 mL). The organic layers were combined, dried over anhydrous MgSO<sub>4</sub>, filtered, and then the solvent was removed under reduced pressure. The crude product was purified by flash chromatography (silica gel, 0-50% AcOEt in hexane) to give the colorless solid (748 mg, yield: 52%). <sup>1</sup>H NMR (600 MHz, CDCl<sub>3</sub>) δ 7.53 (d, *J* = 7.7 Hz, 1H), 7.38 (d, *J* = 7.8 Hz, 1H), 7.29 (d, *J* = 7.7 Hz, 1H), 7.12 (t, *J* = 7.7 Hz, 1H), 7.06 (dd, *J* = 7.7, 1.1 Hz, 1H), 6.97 (s, 1H), 6.92 (t, *J* = 2.4 Hz, 1H), 4.70 (s, 2H), 3.91 (s, *J* = 7.6 Hz, 3H), 3.15 – 3.10 (m, 2H), 3.10 – 3.04 (m, 2H). <sup>13</sup>C NMR (151 MHz, CDCl<sub>3</sub>) δ 157.6, 146.0, 144.6, 144.2, 138.8, 131.1, 128.9, 128.6, 127.8, 121.1, 121.0, 120.7, 119.1, 110.7, 62.0, 55.4, 32.6, 30.2.

#### (E)-4-((4-bromo-2,3-dihydro-1H-inden-1-ylidene)methyl)-2-methoxybenzaldehyde (4.7)



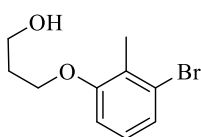
To the mixture of **4.6** (200 mg, 0.58 mmol) solubilised in DCM (6 mL), Dess-Martin Periodinane (15% solution in DCM, 2 mL) was added dropwise. Then, NaHCO<sub>3</sub> (122 mg, 1.45 mmol) was added and resulted mixture was stirred at room temperature for 2 hours. After that time, water (50 mL) was added and it was washed with dichloromethane (2 x 50 mL). The organic layers were combined, dried over anhydrous MgSO<sub>4</sub>, filtered, and then the solvent was removed under reduced pressure. The crude product was purified by flash chromatography (silica gel, 0-50% AcOEt in hexane) to give the colorless solid (176 mg, yield: 88 %). NMR (400 MHz, DMSO)  $\delta$  10.14 (s, 1H), 7.87 (d,  $J = 7.5$  Hz, 1H), 7.38 (dd,  $J = 8.0, 1.1$  Hz, 1H), 7.24 (d,  $J = 8.1$  Hz, 1H), 7.13 (t,  $J = 7.8$  Hz, 1H), 6.75 (d,  $J = 7.9$  Hz, 1H), 6.67 (s, 1H), 4.75 (s, 1H), 3.65 (s,  $J = 1.0$  Hz, 3H), 2.85 – 2.60 (m, 3H), 2.09 – 1.93 (m, 1H).

#### 3-bromo-2-methylphenol (4.8)



Mixture of 95% sulfuric acid (1.83 mL) and water (31 mL) was placed in the flask and it was cooled to 0 °C. 3-bromo-2-methylaniline (3.31 mL, 5.00 g, 26.67 mmol) was added in one portion, resulting with appearance of brown solid. To the resulted mixture, sodium nitrate (2.25 g, 32.50 mmol) was added portionwise over 30 minutes and then resulted solution was allowed to stir at 0 °C for 1 h. Next, 95% solution of H<sub>2</sub>SO<sub>4</sub> (11.7 mL) was added carefully to the reaction solution. The reaction was heated at 100 °C for 1 hour. After cooling to the room temperature, Et<sub>2</sub>O (50 mL x 3) was added to extract our product from water phase. Organic layers were collected together, dried over MgSO<sub>4</sub> and concentrated under reduced pressure. The crude product was purified by column chromatography on silica gel using 0-20% AcOEt in hexane to give colorless crystals (1.79 g, yield: 36%). <sup>1</sup>H NMR (600 MHz, CDCl<sub>3</sub>)  $\delta$  7.14 (dd,  $J = 8.0, 0.5$  Hz, 1H), 6.92 (t,  $J = 8.0$  Hz, 1H), 6.71 (d,  $J = 8.0$  Hz, 1H), 2.34 (s, 3H). <sup>13</sup>C NMR (151 MHz, CDCl<sub>3</sub>)  $\delta$  154.4, 127.6, 126.2, 125.1, 124.6, 114.2, 15.65.

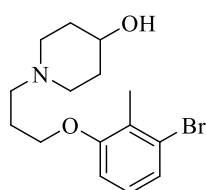
#### 3-(3-bromo-2-methylphenoxy)propan-1-ol (4.9)



**4.8** (1278 mg, 6.87 mmol), 3-bromopropan-1-ol (1.28 mL, 1.91 g, 13.74 mmol) and potassium carbonate (2.37 g, 17.18 mmol) were placed in the round bottom flask under argon. Anhydrous DMF (25 mL) was added and resulted mixture was stirred at 65 °C for 48 hours. Solvent was removed under reduced pressure and water/DCM extraction was carried out. Organic layers were collected together, dried over

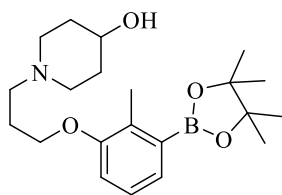
MgSO<sub>4</sub> and concentrated under reduced pressure. The crude product was purified by column chromatography on silica gel using 0-100% AcOEt in hexane to give brown oil (885 mg, yield: 53%). <sup>1</sup>H NMR (600 MHz, CDCl<sub>3</sub>) δ 7.16 (d, *J* = 8.0 Hz, 1H), 7.00 (t, *J* = 8.1 Hz, 1H), 6.79 (d, *J* = 8.2 Hz, 1H), 4.11 (t, *J* = 5.9 Hz, 2H), 3.88 (t, *J* = 6.0 Hz, 2H), 2.31 (s, 3H), 2.07 (p, *J* = 5.9 Hz, 2H). <sup>13</sup>C NMR (151 MHz, CDCl<sub>3</sub>) δ 157.7, 127.4, 127.1, 126.0, 124.9, 110.2, 66.2, 60.4, 32.2, 15.9.

#### 1-(3-(3-bromo-2-methylphenoxy)propyl)piperidin-4-ol (**4.10**)



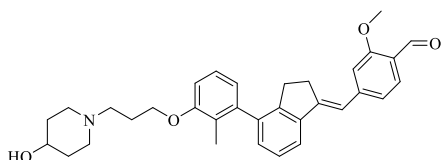
**4.9** (850 mg, 3.47 mmol) was dissolved in anhydrous DCM (33 mL). Then, catalytic amount of DMF (0.35 mL) was added and was followed by dropwise addition of SOCl<sub>2</sub> (2.06 g, 1.26 mL, 17.35 mmol). Resulted mixture was stirred at room temperature for 2 hours. Afterwards, the resulted solution was poured to the separation funnel with the 100 mL of sodium carbonate solution. Phases were separated and water phase was washed with dichloromethane (2 x 50 mL). The organic layers were combined, dried over anhydrous MgSO<sub>4</sub>, filtered, and the solvent was removed under reduced pressure. As a result yellow oil was obtained. In the second step of reaction, to the flask with resulted chloride, piperidinol (1.05 g, 10.41 mmol), anhydrous DMF (33 mL) and DIPEA (1.78 mL, 10.41 mmol) were added respectively. Resulted mixture was heated overnight at 60 °C. Afterwards, solvent was removed under reduced pressure and the mixture of water and ethyl acetate (200 mL, 1:1, v:v) was added to separate the phases. The aqueous phase was further extracted with ethyl acetate (100 mL). The organic layers were combined, dried over anhydrous MgSO<sub>4</sub>, filtered, and then concentrated under reduced pressure. The crude product was purified by column chromatography (silica gel, chloroform: methanol, 4:1). A colorless oil **4.10** (742 mg, yield: 65%) was obtained as the product. <sup>1</sup>H NMR (600 MHz, CDCl<sub>3</sub>) δ 7.14 (d, *J* = 8.0 Hz, 1H), 6.98 (t, *J* = 8.2 Hz, 1H), 6.77 (d, *J* = 8.2 Hz, 1H), 4.00 (t, *J* = 6.2 Hz, 2H), 3.73 (s, 1H), 2.85 – 2.76 (m, 2H), 2.55 (t, *J* = 7.4 Hz, 2H), 2.30 (s, 3H), 2.27 – 2.13 (m, 2H), 2.06 – 1.96 (m, 2H), 1.96 – 1.88 (m, 2H), 1.64 – 1.59 (m, 2H). <sup>13</sup>C NMR (151 MHz, CDCl<sub>3</sub>) δ 157.8, 127.3, 127.2, 125.9, 124.6, 110.2, 66.9, 55.3, 51.2, 34.5, 29.8, 27.2, 15.9.

**(1-(3-(2-methyl-3-(4,4,5,5-tetramethyl-1,3,2-dioxaborolan-2-yl)phenoxy)propyl)piperidin-4-ol (4.11)**



**4.10** (700 mg, 2.13 mmol), bis(pinacolato)diboron (650 mg, 2.56 mmol) and potassium acetate (627 mg, 6.40 mmol) were placed in the round bottom flask under argon and were dissolved in anhydrous dioxane (12 mL). The resulting solution was heated to 85 °C, then Pd(dppf)Cl<sub>2</sub>·DCM (79 mg, 0.11 mmol) was added and resulting mixture was heated overnight at 100 °C. Afterwards, the mixture was concentrated under reduced pressure, water (100 mL) was added and then, it was washed with dichloromethane (2x100 mL). The organic layers were combined, dried over anhydrous MgSO<sub>4</sub>, filtered, and the solvent was removed under reduced pressure. The crude product was purified by flash chromatography (silica gel, 0-20% chloroform: methanol) to give the product as a colorless solid (232 mg, yield: 29%). <sup>1</sup>H NMR (600 MHz, CDCl<sub>3</sub>) δ 7.31 (d, *J* = 7.4 Hz, 1H), 7.11 (t, *J* = 7.8 Hz, 1H), 6.88 (d, *J* = 8.0 Hz, 1H), 3.97 (t, *J* = 6.1 Hz, 2H), 3.68 (s, 1H), 3.22 (brs, 1H), 2.89 – 2.76 (m, 2H), 2.58 (d, *J* = 7.4 Hz, 2H), 2.40 (s, 3H), 2.22 (s, 2H), 2.05 – 1.95 (m, 2H), 1.95 – 1.85 (m, 2H), 1.67 – 1.55 (m, 2H), 1.33 (s, 12H). <sup>13</sup>C NMR (151 MHz, CDCl<sub>3</sub>) δ 156.8, 133.5, 127.6, 125.8, 113.8, 83.6, 67.3, 66.4, 55.4, 51.1, 34.1, 26.9, 24.9, 14.8.

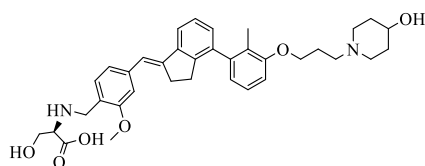
**(E)-4-((4-(3-(3-(4-hydroxypiperidin-1-yl)propoxy)-2-methylphenyl)-2,3-dihydro-1H-inden-1-ylidene)methyl)-2-methoxybenzaldehyde (4.12)**



**4.7** (176 mg, 0.51 mmol), **4.11** (230 mg, 0.61 mmol), and potassium carbonate (212 mg, 1.53 mmol) were dissolved in mixture of dioxane and water (4:2 mL, v:v). The mixture was deoxygenated by rinsing with argon for 15 min. Then, resulting mixture was heated up to 85 °C and Pd(dppf)Cl<sub>2</sub>·DCM complex (21 mg, 0.03 mmol) was added. The mixture was stirred at 85 °C for 3 hours. After cooling to room temperature, water (50 mL) was added to the reaction mixture and it was extracted with ethyl acetate (2 x 50 mL). The organic layers were combined, dried over anhydrous MgSO<sub>4</sub>, filtered, and the solvent was removed under reduced pressure. The crude product was purified by flash chromatography (silica gel, 0-25% methanol in chloroform) to give a colorless solid (143 mg, yield: 55%). <sup>1</sup>H NMR (300 MHz, CDCl<sub>3</sub>) δ 10.41 (s, 1H), 7.82 (d, *J* = 8.1 Hz, 1H), 7.63 (d, *J* = 7.2 Hz, 1H), 7.32 (t, *J* = 7.3 Hz, 1H), 7.21 – 7.07 (m, 3H), 7.01 (dd, *J* = 5.9, 3.4 Hz, 2H), 6.85 (d, *J* = 7.7 Hz, 1H), 6.77 (d, *J* = 6.9 Hz, 1H), 4.13 – 3.99 (m, 2H), 3.95 (s, 3H), 3.78 – 3.70 (m, 1H), 3.16 – 3.04 (m, 2H), 2.92 – 2.73 (m, 4H),

2.64 – 2.50 (m, 2H), 2.33 – 2.18 (m, 2H), 2.12 – 2.02 (m, 2H), 1.98 (s, 3H), 1.95 – 1.85 (m, 2H), 1.70 – 1.53 (m, 2H).

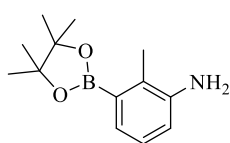
**(E)-4-(((4-(3-(3-(4-hydroxypiperidin-1-yl)propoxy)-2-methylphenyl)-2,3-dihydro-1H-inden-1-ylidene)methyl)-2-methoxybenzyl)-D-serine (4.13)**



**4.12** (120 mg, 0.23 mmol) and D-serine (112 mg, 1.07 mmol) were dissolved in anhydrous DMF (6 mL) and AcOH (3 droplets) was added. The resulted mixture was stirred for 3 hours at room temperature. After that time, NaBH<sub>3</sub>CN (74 mg, 1.17 mmol) was added and reaction mixture was stirred overnight at room temperature. Solvent was removed under reduced pressure. The crude product was purified by column chromatography (silica gel, 4:1, CHCl<sub>3</sub>: MeOH + 2% NH<sub>3</sub> in MeOH) to give the product **4.13** as a colorless solid (45 mg, 32%). <sup>1</sup>H NMR (600 MHz, DMSO) δ 7.71 (d, *J* = 7.7 Hz, 1H), 7.36 (d, *J* = 7.6 Hz, 1H), 7.33 (t, *J* = 7.5 Hz, 1H), 7.19 (t, *J* = 7.8 Hz, 1H), 7.14 – 7.08 (m, 3H), 7.03 (d, *J* = 7.3 Hz, 1H), 6.95 (t, *J* = 11.2 Hz, 1H), 6.73 (d, *J* = 7.5 Hz, 1H), 4.07 – 3.93 (m, 4H), 3.86 (s, 3H), 3.70 – 3.65 (m, 1H), 3.65 – 3.58 (m, 1H), 3.49 – 3.40 (m, 2H), 3.10 (brs, 1H), 3.04 (brs, 2H), 2.82 – 2.75 (m, 1H), 2.75 – 2.69 (m, 2H), 2.69 – 2.58 (m, 1H), 2.44 (t, *J* = 7.0 Hz, 2H), 2.07 – 1.97 (m, 2H), 1.94 – 1.82 (m, 6H), 1.70 (d, *J* = 10.0 Hz, 2H), 1.40 – 1.34 (m, 2H). <sup>13</sup>C NMR (151 MHz, DMSO) δ 157.4, 150.4, 144.0, 142.3, 141.0, 139.7, 138.9, 130.3, 127.0, 126.2, 123.5, 121.1, 120.3, 119.2, 116.2, 110.9, 110.2, 103.2, 66.4, 66.0, 62.6, 61.0, 55.5, 54.6, 51.1, 45.7, 39.5, 34.4, 34.2, 30.0, 29.7, 29.0, 26.7, 12.9. UPLC–MS (DAD/ESI): t<sub>R</sub> = 4.39 min, for C<sub>36</sub>H<sub>44</sub>N<sub>2</sub>O<sub>6</sub> [M - H]<sup>+</sup> found: 599.22 *m/z*; calc. mass: 599.31. HRMS ESI-MS-q-TOF for C<sub>36</sub>H<sub>44</sub>N<sub>2</sub>O<sub>6</sub> [M + H]<sup>+</sup> found: 601.3270 *m/z*; calc. mass: 601.3278.

**4.2.5. Preparation of ARB272542 Derivatives as Potential PD-1/PD-L1 Derivatives – Synthesis and Activity Determination**

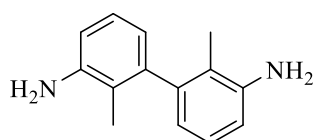
**2-methyl-3-(4,4,5,5-tetramethyl-1,3,2-dioxaborolan-2-yl)aniline (5.1)**



3-bromo-2-methylaniline (3.75 g, 20.16 mmol), bis(pinacolato)diborane (7.68 g, 30.24 mmol) and anhydrous potassium acetate (5.86 g, 60.48 mmol) were dissolved in anhydrous dioxane (150 mL) in two-neck round-bottom flask under argon atmosphere. Reaction mixture was heated up to 85 °C, Pd(dppf)Cl<sub>2</sub> dichloromethane complex (824 mg, 1.01 mmol) was added and heating was continued

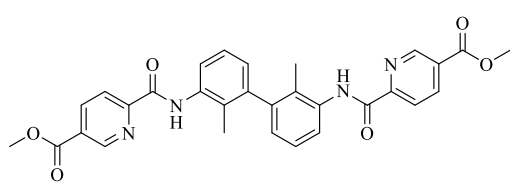
overnight. Afterwards, reaction mixture was concentrated under reduced pressure, water (200 mL) was added and extraction with ethyl acetate (2 x 200 mL) followed. Organic phases were combined, dried over anhydrous MgSO<sub>4</sub> and concentrated under reduced pressure. Crude product was purified by flash chromatography (SiO<sub>2</sub>, hexane/ethyl acetate 4:1) giving compound **5.1** (4.70 g, 100%) as colorless solid. <sup>1</sup>H NMR (600 MHz, CDCl<sub>3</sub>) δ 7.23 (dd, *J* = 7.4, 1.0 Hz, 1H), 7.04 (t, *J* = 7.6 Hz, 1H), 6.77 (dd, *J* = 7.8, 1.1 Hz, 1H), 3.60 (s, 2H), 2.38 (s, 3H), 1.35 (s, 12H). <sup>13</sup>C NMR (151 MHz, CDCl<sub>3</sub>) δ 144.6, 128.6, 126.5, 126.0, 117.8, 83.5, 77.2, 25.1, 25.0, 15.8.

### 2,2'-dimethyl-[1,1'-biphenyl]-3,3'-diamine (**5.2**)



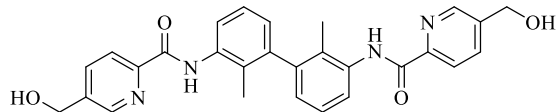
The compound **5.1** was prepared according to the procedure used for **6.7**. 3-bromo-2-methylaniline (3.13 g, 16.80 mmol), **5.1** (4.70 g, 20.16 mmol), (374 mg, 9.89 mmol), potassium carbonate (6.96 g, 50.40 mmol), Pd(dppf)Cl<sub>2</sub>·DCM (685 mg, 0.84 mmol) and mixture of deoxygenated dioxane/water (64:32 mL, v:v) were used to obtain compound **5.2** as a brown solid (2.24 g, yield: 63%). <sup>1</sup>H NMR (600 MHz, CDCl<sub>3</sub>) δ 7.06 (t, *J* = 7.7 Hz, 2H), 6.70 (dd, *J* = 7.9, 0.9 Hz, 2H), 6.61 (dd, *J* = 7.5, 1.0 Hz, 2H), 3.67 (s, 4H), 1.89 (s, 6H). <sup>13</sup>C NMR (151 MHz, CDCl<sub>3</sub>) δ 144.6, 143.0, 126.0, 120.7, 120.3, 113.8, 13.9.

### Dimethyl 6,6'-(((2,2'-dimethyl-[1,1'-biphenyl]-3,3'-diyl)bis(azanediyl))bis(carbonyl))dinicotinate (**5.3**)



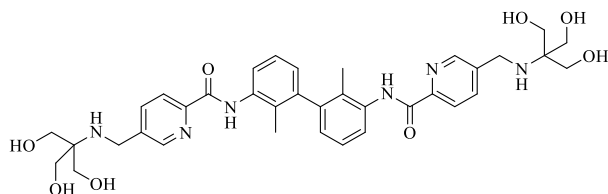
5-(methoxycarbonyl)picolinic acid (4.62 g, 25.47 mmol) and HATU (9.68 g, 25.47 mmol) were placed in the round bottom flask under argon. Then anhydrous DMF (43 mL) and DIPEA (5.6 mL, 31.84 mmol) were added and resulted mixture was stirred for 30 minutes. Afterwards, **5.2** (1.50 g, 7.08 mmol) dissolved in anhydrous DMF (40 mL) was added dropwise and resulted mixture was stirred overnight at room temperature. After that time, mixture was poured over the solution of NaHCO<sub>3</sub>. The resulting precipitate was filtered off. Solid was purified by maceration in ethyl acetate/methanol mixture, giving final product (**5.3**) as white solid (3.54 g) with 93% yield. <sup>1</sup>H NMR (600 MHz, CDCl<sub>3</sub>) δ 10.15 (s, 2H), 9.23 (s, 2H), 8.52 (dd, *J* = 8.1, 1.8 Hz, 2H), 8.41 (d, *J* = 8.1 Hz, 2H), 8.29 (d, *J* = 8.1 Hz, 2H), 7.34 (t, *J* = 7.8 Hz, 2H), 7.02 (d, *J* = 7.4 Hz, 2H), 4.00 (s, 6H), 2.14 (s, 6H). <sup>13</sup>C NMR (151 MHz, DMSO) δ 164.7, 160.9, 152.8, 149.3, 142.1, 138.8, 135.8, 128.2, 127.1, 126.2, 126.0, 121.9, 121.0, 14.3.

**N,N'-(2,2'-dimethyl-[1,1'-biphenyl]-3,3'-diyl)bis(5-(hydroxymethyl)picolinamide) (5.4)**



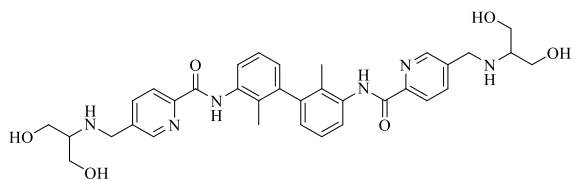
**5.3** (1.83 g, 3.41 mmol) was placed in a round bottom flask under argon and it was dissolved in a mixture of anhydrous THF and anhydrous MeOH (100:50 mL, v:v). The mixture was cooled to 0 °C and followingly sodium borohydride (685 mg, 31.45 mmol) was added portionwise. The reaction was monitored by TLC and it was completed after 5 hours. The excess of reductor was quenched by addition of ethyl acetate (5 mL), water (5 mL), and hydrochloric acid (2 mL). Then, water (25 mL) was added and the mixture was extracted with ethyl acetate (2 x 25 mL). The organic layers were combined, dried over anhydrous MgSO<sub>4</sub>, filtered, and the solvent was removed under reduced pressure. A colorless precipitate (**5.4**) was obtained (1.52 g, 100% yield). <sup>1</sup>H NMR (600 MHz, DMSO) δ 10.34 (s, 2H), 8.67 (d, *J* = 1.2 Hz, 2H), 8.15 (d, *J* = 8.0 Hz, 2H), 8.00 (dd, *J* = 8.0, 1.9 Hz, 2H), 7.88 (d, *J* = 8.0 Hz, 2H), 7.32 (t, *J* = 7.8 Hz, 2H), 6.99 (d, *J* = 7.5 Hz, 2H), 5.63 (t, *J* = 5.6 Hz, 2H), 4.65 (d, *J* = 5.6 Hz, 4H), 2.02 (s, 6H). <sup>13</sup>C NMR (151 MHz, DMSO) δ 162.2, 148.3, 146.9, 141.8, 141.5, 136.3, 136.0, 128.7, 126.1, 125.8, 122.6, 121.9, 60.3, 14.5.

**N,N'-(2,2'-dimethyl-[1,1'-biphenyl]-3,3'-diyl)bis(5-(((1,3-dihydroxy-2-(hydroxymethyl)propan-2-yl)amino)methyl)picolinamide) (5.5)**



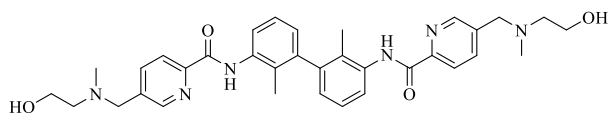
The compound **5.5** was prepared according to the procedure used for **6.13**. In the first step, **5.4** (300 mg, 0.62 mmol), anhydrous DCM (13 mL) with addition of anhydrous DMF (0.2 mL), and thionyl chloride (0.45 mL, 6.22 mmol) were used. The product from the first step was treated with 2-amino-2-hydroxymethyl-propane-1,3-diol (752 mg, 6.22 mmol), DIPEA (0.90 mL, 4.97 mmol) and anhydrous DMF (9 mL). A colorless precipitate **5.5** (87 mg, yield: 20%) was obtained as the product. <sup>1</sup>H NMR (600 MHz, DMSO) δ 10.34 (s, 2H), 8.72 (s, 2H), 8.13 (d, *J* = 8.0 Hz, 2H), 8.08 (d, *J* = 7.9 Hz, 2H), 7.90 (d, *J* = 8.0 Hz, 2H), 7.33 (t, *J* = 7.8 Hz, 2H), 6.99 (d, *J* = 7.4 Hz, 2H), 4.52 (s, *J* = 142.2 Hz, 6H), 3.98 (s, *J* = 66.3 Hz, 4H), 3.45 (s, *J* = 44.2 Hz, 12H), 2.02 (s, 6H). <sup>13</sup>C NMR (151 MHz, DMSO) δ 162.1, 148.6, 148.2, 141.8, 137.8, 136.3, 128.5, 126.0, 125.8, 122.4, 121.7, 60.8, 42.8, 39.5, 14.5. UPLC–MS (DAD/ESI): *t*<sub>R</sub> = 3.30 min, for C<sub>36</sub>H<sub>44</sub>N<sub>6</sub>O<sub>8</sub> [M + H]<sup>+</sup> found: 689.27 *m/z*; calc. mass: 689.33. HRMS ESI-MS-q-TOF for C<sub>36</sub>H<sub>44</sub>N<sub>6</sub>O<sub>8</sub> [M + H]<sup>+</sup> found: 689.3294 *m/z*; calc. mass: 689.3299.

**N,N'-(2,2'-dimethyl-[1,1'-biphenyl]-3,3'-diyl)bis(5-(((1,3-dihydroxypropan-2-yl)amino)methyl)picolinamide) (5.6)**



The compound **5.6** was prepared according to the procedure used for **6.13**. In the first step, **5.4** (250 mg, 0.52 mmol), anhydrous DCM (11 mL) with addition of anhydrous DMF (0.1 mL), and thionyl chloride (0.38 mL, 5.18 mmol) were used. The product from the first step was treated with 2-amino-1,3-propanediol (472 mg, 5.19 mmol), DIPEA (0.75 mL, 4.06 mmol) and anhydrous DMF (7 mL). A colorless precipitate **5.6** (38 mg, yield: 24%) was obtained as the product.  $^1\text{H}$  NMR (600 MHz, DMSO)  $\delta$  10.34 (s, 2H), 8.71 (d,  $J = 1.0$  Hz, 2H), 8.14 (d,  $J = 8.0$  Hz, 2H), 8.05 (dd,  $J = 8.0, 1.7$  Hz, 2H), 7.90 (d,  $J = 7.9$  Hz, 2H), 7.33 (t,  $J = 7.8$  Hz, 2H), 6.99 (d,  $J = 7.4$  Hz, 2H), 4.52 (s, 4H), 3.95 (s, 4H), 3.42 (ddd,  $J = 36.6, 10.8, 5.6$  Hz, 8H), 2.63 – 2.53 (m, 2H), 2.03 (s, 6H).  $^{13}\text{C}$  NMR (151 MHz, DMSO)  $\delta$  162.1, 148.4, 148.2, 141.8, 140.2, 137.5, 136.3, 128.6, 126.1, 125.8, 122.5, 121.8, 60.9, 60.3, 60.2, 47.7, 39.5, 14.5. UPLC–MS (DAD/ESI):  $t_{\text{R}} = 3.57$  min, for  $\text{C}_{34}\text{H}_{40}\text{N}_6\text{O}_6$   $[\text{M} - \text{H}]^+$  found: 627.06  $m/z$ ; calc. mass: 627.29. HRMS ESI-MS-q-TOF for  $\text{C}_{34}\text{H}_{40}\text{N}_6\text{O}_6$   $[\text{M} + \text{H}]^+$  found: 629.3083  $m/z$ ; calc. mass: 629.3087.

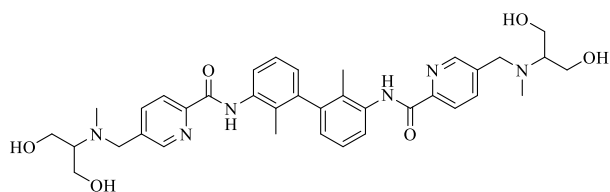
**N,N'-(2,2'-dimethyl-[1,1'-biphenyl]-3,3'-diyl)bis(5-(((2-hydroxyethyl)(methyl)amino)methyl)picolinamide) (5.7)**



The compound **5.7** was prepared according to the procedure used for **6.13**. In the first step, **5.4** (800 mg, 1.66 mmol), anhydrous DCM (14 mL) with addition of anhydrous DMF (0.2 mL), and thionyl chloride (1.20 mL, 16.54 mmol) were used. The product from the first step was treated with N-methylethanolamine (1.23 mL, 15.26 mmol), DIPEA (0.95 mL, 11.95 mmol) and anhydrous DMF (20 mL). A yellow oil **5.7** (738 mg, yield: 75%) was obtained as the product.  $^1\text{H}$  NMR (400 MHz, )  $\delta$  10.12 (s, 2H), 8.55 (dd,  $J = 1.9, 0.5$  Hz, 2H), 8.29 (d,  $J = 8.0$  Hz, 4H), 7.86 (dd,  $J = 8.0, 2.1$  Hz, 2H), 7.32 (t,  $J = 7.9$  Hz, 2H), 6.99 (dd,  $J = 7.6, 1.2$  Hz, 2H), 3.69 – 3.63 (m, 8H), 2.65 (t,  $J = 5.4$  Hz, 4H), 2.25 (s, 6H), 2.12 (s, 6H).  $^{13}\text{C}$  NMR (101 MHz,  $\text{CDCl}_3$ )  $\delta$  162.1, 149.4, 148.8, 142.3, 138.2, 137.5, 136.1, 126.6, 126.3, 126.1, 122.3, 120.8, 59.5, 58.8, 58.7, 41.7, 14.5. UPLC–MS (DAD/ESI):  $t_{\text{R}} = 4.59$  min, for  $\text{C}_{34}\text{H}_{40}\text{N}_6\text{O}_4$   $[\text{M} + \text{H}]^+$  found: 597.26  $m/z$ ; calc. mass: 596.31.



**N,N'-(2,2'-dimethyl-[1,1'-biphenyl]-3,3'-diyl)bis(5-(((1,3-dihydroxypropan-2-yl)(methyl)amino)methyl)picolinamide) (5.8)**

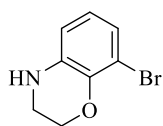


**5.6** (135 mg, 0.21 mmol) was dissolved in 6 mL of anhydrous methanol with addition of 0.3 mL of acetic acid. The reaction mixture was cooled to 0 °C and was treated

with NaBH<sub>3</sub>CN (40 mg, 0.63 mmol) and then formaldehyde (30 μL, 0.42 mmol, 37% water solution) was added. The resulted solution was mixed overnight at room temperature and then was concentrated under reduced pressure. Water (50 mL) was added and it was washed with DCM (50 mL x 2) with small addition of MeOH. Organic phases were combined, dried over anhydrous MgSO<sub>4</sub> and concentrated under reduced pressure. The crude product was purified by column chromatography (SiO<sub>2</sub>, chloroform: methanol, 4:1 + 1% solution of ammonia in methanol) giving compound **5.8** (34 mg, 24%) as colorless solid. <sup>1</sup>H NMR (600 MHz, DMSO) δ 10.33 (s, 2H), 8.68 (s, 2H), 8.13 (d, *J* = 8.0 Hz, 2H), 8.03 (d, *J* = 7.7 Hz, 2H), 7.91 (d, *J* = 7.9 Hz, 2H), 7.32 (t, *J* = 7.8 Hz, 2H), 6.99 (d, *J* = 7.2 Hz, 2H), 4.40 (brs, 4H), 3.89 (s, 4H), 3.63 – 3.56 (m, 4H), 3.56 – 3.46 (m, 4H), 2.70 (s, 2H), 2.24 (s, 6H), 2.03 (s, 6H). <sup>13</sup>C NMR (151 MHz, DMSO) δ 162.1, 148.7, 148.3, 141.8, 139.8, 137.9, 136.2, 128.4, 126.0, 125.8, 122.4, 121.8, 65.6, 59.2, 55.7, 37.6, 14.5. UPLC–MS (DAD/ESI): t<sub>R</sub> = 4.54 min, for C<sub>36</sub>H<sub>44</sub>N<sub>6</sub>O<sub>6</sub> [M - H]<sup>+</sup> found: 655.31 *m/z*; calc. mass: 655.32. HRMS ESI-MS-q-TOF for C<sub>36</sub>H<sub>44</sub>N<sub>6</sub>O<sub>6</sub> [M + H]<sup>+</sup> found: 657.3395 *m/z*; calc. mass: 657.3400.

**4.2.6. 3,4-dihydro-2H-benzo[b][1,4]oxazine Derivatives as Potential PD-1/PD-L1 Antagonists**

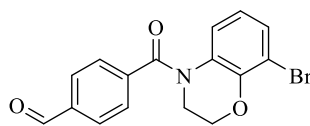
**8-bromo-3,4-dihydro-2H-benzo[b][1,4]oxazine (6.1)**



2-amino-6-bromophenol (8.00 g, 42.54 mmol), dibromoethane (4.4 mL, 51.06 mmol) and potassium carbonate (17.64 g, 127.64 mmol) were placed in the flask under argon and were dissolved in 80 mL of anhydrous DMF. The mixture was heated at 125 °C overnight. Then, the reaction mixture was concentrated under reduced pressure. After cooling to room temperature, saturated sodium chloride solution (200 mL) was added. The mixture was extracted with ethyl acetate (2 x 200 mL). The organic layers were washed with water (100 mL), combined, dried over anhydrous MgSO<sub>4</sub>, filtered, and then the solvent was removed under reduced pressure. The crude product was purified by flash chromatography (silica gel, 0-50% petroleum ether in DCM) to give the product as a brown oil

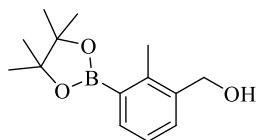
(4.64 g, yield: 51%). <sup>1</sup>H NMR (600 MHz, CDCl<sub>3</sub>) δ: 6.88 (dd, *J* = 7.9, 1.4 Hz, 1H), 6.62 (t, *J* = 7.9 Hz, 1H), 6.52 (dd, *J* = 7.9, 1.4 Hz, 1H), 4.36 – 4.30 (m, 2H), 3.83 (s, 1H), 3.49 – 3.39 (m, 2H). <sup>13</sup>C NMR (151 MHz, CDCl<sub>3</sub>) δ 140.8, 135.0, 122.3, 121.9, 114.6, 110.8, 77.2, 65.9, 40.8.

#### 4-(8-bromo-3,4-dihydro-2H-benzo[b][1,4]oxazine-4-carbonyl)benzaldehyde (6.2)



4-carboxybenzaldehyde (1.90 g, 12.66 mmol) was placed in the round bottom flask under argon. Then, anhydrous toluene (20 mL) and thionyl chloride (2.5 mL, 34.45 mmol) were added. The resulting mixture was heated at 110 °C under a cooling condenser fitted with a tube with calcium chloride. Heating was continued for 1 hour until a clear solution was obtained. The solvent was removed under reduced pressure to get the corresponding acid chloride. In the second step, the obtained acid chloride was added portionwise to a previously cooled solution of **6.1** (2.20 g, 10.28 mmol) in THF (25 mL). Afterwards, the content of the flask was stirred for 10 minutes at 0 °C and then for 30 minutes at room temperature. Saturated sodium bicarbonate solution (80 mL) was added portionwise and mixture was extracted with ethyl acetate (2 x 100 mL). The organic layers were washed with water (100 mL), combined, dried over anhydrous MgSO<sub>4</sub>, filtered, and concentrated under reduced pressure. The crude product was purified by flash chromatography (silica gel, 0-50% ethyl acetate in hexane) to give the product **6.2** as a colorless solid (2.25 g, yield: 72%). <sup>1</sup>H NMR (600 MHz, CDCl<sub>3</sub>) δ 10.04 (s, 1H), 7.89 (d, *J* = 8.1 Hz, 2H), 7.64 (d, *J* = 8.1 Hz, 2H), 7.27 (dd, *J* = 8.0, 1.0 Hz, 1H), 6.77 (s, 1H), 6.52 (m, 1H), 4.52 (s, 2H), 4.04 (s, 2H). <sup>13</sup>C NMR (151 MHz, CDCl<sub>3</sub>) δ 191.5, 167.6, 143.5, 140.4, 137.7, 129.9, 129.2, 126.9, 123.8, 120.5, 111.3, 67.5.

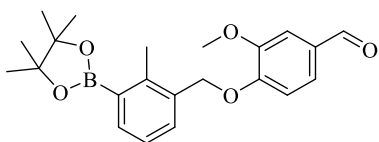
#### (2-methyl-3-(4,4,5,5-tetramethyl-1,3,2-dioxaborolan-2-yl)phenyl)methanol (6.3)



3-brom-2-methylbenzyl alcohol (2.00 g, 9.95 mmol), bis(pinacolato)diboron (3.03 g, 11.94 mmol) and potassium acetate (2.93 g, 29.84 mmol) were placed in the round bottom flask under argon and were dissolved in anhydrous dioxane (60 mL). The resulting solution was heated to 85 °C, then Pd(dppf)Cl<sub>2</sub>·DCM (406 mg, 0.50 mmol) was added and resulting mixture was heated overnight at 85 °C. The mixture was concentrated under reduced pressure, water (100 mL) was added and then, the it was washed with dichloromethane (2x100 mL).The organic layers were combined, dried over anhydrous MgSO<sub>4</sub>, filtered, and the solvent was removed under reduced pressure. The crude product was purified by flash chromatography (silica gel, 0-50% ethyl acetate in hexane) to give the product a colorless solid **6.3** (2.45 g, yield: 99%). <sup>1</sup>H NMR (600 MHz,

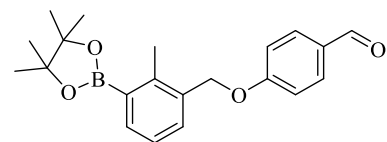
CDCl<sub>3</sub>)  $\delta$  7.71 (dd,  $J = 7.4, 1.2$  Hz, 1H), 7.43 (d,  $J = 6.8$  Hz, 1H), 7.19 (t,  $J = 7.5$  Hz, 1H), 4.70 (s, 2H), 2.54 (s, 3H), 1.35 (s, 12H). <sup>13</sup>C NMR (151 MHz, CDCl<sub>3</sub>)  $\delta$  142.7, 138.8, 135.5, 130.3, 125.3, 83.7, 63.9, 25.0, 17.5.

**3-methoxy-4-((2-methyl-3-(4,4,5,5-tetramethyl-1,3,2-dioxaborolan-2-yl)benzyl)oxy)benzaldehyde (6.4)**



**6.3** (1.55 g, 6.25 mmol) was dissolved in dry DCM (26 mL) with catalytic amount of anhydrous DMF (0.06 mL) and it was cooled to 0 °C. Then SOCl<sub>2</sub> (2.0 mL, 27.56 mmol) was added portionwise. After 2 hours, NaHCO<sub>3</sub> (80 mL) was added and it was washed with DCM (2 x 80 mL). Organic layers were extracted with water (100 mL), combined, dried over anhydrous MgSO<sub>4</sub>, filtered, and concentrated under reduced pressure. After drying of the product, K<sub>2</sub>CO<sub>3</sub> (1.73 g, 12.95 mmol), 4-hydroxy-3-methoxybenzaldehyde (1.02 g, 6.70 mmol) and anhydrous DMF (23 mL) were added and resulted mixture was stirred overnight at room temperature. Afterwards, mixture was concentrated under reduced pressure, water was added (100 mL) and it was extracted with ethyl acetate (2 x 100 mL). The organic layers were combined, dried over anhydrous MgSO<sub>4</sub>, filtered, and concentrated. The crude product was purified by flash chromatography (silica gel, 0-100% AcOEt in hexane). The product was obtained as a colorless solid (1.49 g, 68%). <sup>1</sup>H NMR (600 MHz, CDCl<sub>3</sub>)  $\delta$  9.84 (s, 1H), 7.75 (dd,  $J = 7.4, 1.1$  Hz, 1H), 7.46 (d,  $J = 7.5$  Hz, 1H), 7.43 (d,  $J = 1.9$  Hz, 1H), 7.40 (dd,  $J = 8.2, 1.9$  Hz, 1H), 7.19 (t,  $J = 7.5$  Hz, 1H), 6.98 (d,  $J = 8.2$  Hz, 1H), 5.22 (s, 2H), 3.93 (s, 3H), 2.58 (s, 3H), 1.36 (s, 12H). <sup>13</sup>C NMR (151 MHz, CDCl<sub>3</sub>)  $\delta$  191.1, 153.9, 150.3, 142.8, 136.1, 133.9, 130.7, 130.4, 126.8, 125.3, 112.4, 109.5, 83.8, 69.8, 56.2, 25.0, 17.7.

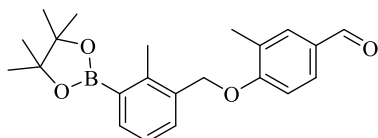
**4-((2-methyl-3-(4,4,5,5-tetramethyl-1,3,2-dioxaborolan-2-yl)benzyl)oxy)benzaldehyde (6.5)**



The compound **6.5** was prepared according to the procedure used for **6.4**. For the generation of alkylating agent were used **6.3** (2.40 g, 9.67 mmol), thionyl chloride (3.8 mL, 52.36 mmol), anhydrous DMF (0.14 mL), and anhydrous DCM (45 mL). The Williamson reaction involved the use of 4-hydroxybenzaldehyde (1.42 g, 11.64 mmol), potassium carbonate (2.68 g, 19.39 mmol) and anhydrous DMF (40 mL). A colorless solid (1.88 g, 57%) was obtained. <sup>1</sup>H NMR (600 MHz, CDCl<sub>3</sub>)  $\delta$  9.89 (s, 1H), 7.88 – 7.83 (m, 2H), 7.78 (dd,  $J = 7.5, 1.2$  Hz, 1H), 7.46 (d,  $J = 7.5$  Hz, 1H), 7.22 (t,  $J = 7.5$  Hz, 1H), 7.11 – 7.06 (m, 2H), 5.14 (s, 2H), 2.57 (s, 3H), 1.36

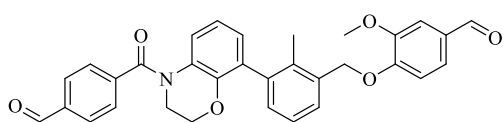
(s, 12H).  $^{13}\text{C}$  NMR (151 MHz,  $\text{CDCl}_3$ )  $\delta$  191.2, 191.1, 164.3, 143.5, 136.6, 134.1, 132.4, 131.5, 130.4, 125.6, 115.4, 84.0, 69.5, 25.2, 18.0.

**3-methyl-4-((2-methyl-3-(4,4,5,5-tetramethyl-1,3,2-dioxaborolan-2-yl)benzyl)oxy)benzaldehyde (6.6)**



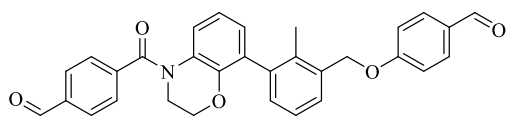
The compound **6.6** was prepared according to the procedure used for **6.4**. For the generation of alkylating agent were used **6.3** (2.00 g, 8.06 mmol), thionyl chloride (2.6 mL, 40.32 mmol), anhydrous DMF (0.8 mL), and anhydrous DCM (34 mL). The Williamson reaction involved the use of 4-hydroxy-3-methylbenzaldehyde (1.32 g, 9.68 mmol), potassium carbonate (2.23 g, 16.13 mmol) and anhydrous DMF (30 mL). A colorless solid (1.19 g, 40%) was obtained.  $^1\text{H}$  NMR (600 MHz,  $\text{CDCl}_3$ )  $\delta$  9.86 (s, 1H), 7.78 (dd,  $J = 7.5, 1.2$  Hz, 1H), 7.73 – 7.67 (m, 2H), 7.49 (d,  $J = 7.5$  Hz, 1H), 7.23 (t,  $J = 7.5$  Hz, 1H), 7.02 (d,  $J = 9.0$  Hz, 1H), 5.15 (s, 2H), 2.57 (s, 3H), 2.31 (s, 3H), 1.37 (s, 12H).  $^{13}\text{C}$  NMR (151 MHz,  $\text{CDCl}_3$ )  $\delta$  191.3, 162.2, 143.1, 136.1, 134.2, 131.7, 130.9, 130.7, 129.7, 128.2, 125.3, 111.0, 83.8, 69.2, 25.0, 17.8, 16.6.

**4-((3-(4-(4-formylbenzoyl)-3,4-dihydro-2H-benzo[b][1,4]oxazin-8-yl)-2-methylbenzyl)oxy)-3-methoxybenzaldehyde (6.7)**



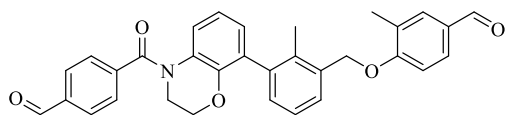
**6.2** (600 mg, 1.73 mmol), **6.4** (860 mg, 2.25 mmol), and potassium carbonate (718 mg, 5.20 mmol) were dissolved in mixture of dioxane and water (20:10 mL, v:v). The mixture was deoxygenated by rinsing with argon for 15 min. Then, resulting mixture was heated up to 85 °C and  $\text{Pd}(\text{dppf})\text{Cl}_2 \cdot \text{DCM}$  complex (70 mg, 0.09 mmol) was added. The mixture was stirred at 85 °C for 3 hours. Afterwards, water (100 mL) was added to the reaction mixture and it was extracted with ethyl acetate (2x100 mL). The organic layers were combined, dried over anhydrous  $\text{MgSO}_4$ , filtered, and the solvent was removed under reduced pressure. The crude product was purified by flash chromatography (silica gel, 0-30% ethyl acetate in hexane) to give a beige solid (584 mg, yield: 66%).  $^1\text{H}$  NMR (600 MHz,  $\text{CDCl}_3$ )  $\delta$  10.16 (s, 1H), 10.07 (s, 1H), 7.93 (d,  $J = 8.1$  Hz, 2H), 7.69 (d,  $J = 8.1$  Hz, 2H), 7.39 (dd,  $J = 7.7, 1.6$  Hz, 1H), 7.30 (dd,  $J = 7.1, 1.8$  Hz, 1H), 7.25 – 7.18 (m, 3H), 7.18 – 7.13 (m, 1H), 6.92 (d,  $J = 7.5$  Hz, 1H), 6.73 (brs, 1H), 5.27 (q,  $J = 11.5$  Hz, 2H), 4.37 (s, 2H), 4.10 – 3.99 (m, 2H), 3.97 (s, 3H), 2.24 (s, 3H).  $^{13}\text{C}$  NMR (151 MHz,  $\text{CDCl}_3$ )  $\delta$  191.6, 190.4, 153.3, 151.3, 143.8, 141.0, 138.8, 137.6, 136.1, 134.7, 131.1, 130.7, 129.9, 129.5, 129.2, 127.8, 125.7, 124.4, 123.9, 119.8, 119.1, 118.1, 75.0, 66.7, 56.3, 16.1.

**4-((3-(4-(4-formylbenzoyl)-3,4-dihydro-2H-benzo[b][1,4]oxazin-8-yl)-2-methylbenzyl)oxy)benzaldehyde (6.8)**



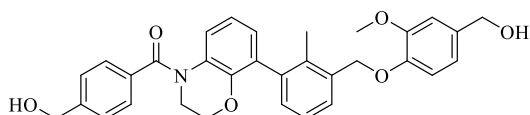
The compound **6.8** was prepared according to the procedure used for **6.7. 6.2** (700 mg, 2.02 mmol), **6.5** (925 mg, 2.63 mmol), potassium carbonate (838 mg, 6.07 mmol), Pd(dppf)Cl<sub>2</sub>·DCM complex (83 mg, 0.10 mmol), and mixture of dioxane and water (44:22 mL, v:v) were used to obtain product **6.8** as a yellow solid (753 mg, 76% yield). <sup>1</sup>H NMR (600 MHz, CDCl<sub>3</sub>) δ 10.07 (s, 1H), 9.91 (s, 1H), 7.93 (d, *J* = 8.1 Hz, 2H), 7.89 – 7.85 (m, 2H), 7.69 (d, *J* = 8.1 Hz, 2H), 7.45 (d, *J* = 6.7 Hz, 1H), 7.31 (t, *J* = 7.6 Hz, 1H), 7.26 – 7.23 (m, 1H), 7.16 – 7.10 (m, 2H), 6.94 (d, *J* = 8.4 Hz, 1H), 6.75 (brs, 1H), 5.19 (q, *J* = 11.3 Hz, 2H), 4.35 (s, 2H), 4.10 – 3.92 (m, 2H), 2.18 (s, 3H). <sup>13</sup>C NMR (151 MHz, CDCl<sub>3</sub>) δ 191.5, 190.9, 164.0, 143.7, 140.9, 138.7, 137.6, 135.6, 134.1, 132.2, 130.8, 130.6, 130.3, 129.9, 129.2, 128.4, 128.0, 125.8, 123.9, 119.8, 115.2, 69.4, 66.7, 16.0.

**4-((3-(4-(4-formylbenzoyl)-3,4-dihydro-2H-benzo[b][1,4]oxazin-8-yl)-2-methylbenzyl)oxy)-3-methylbenzaldehyde (6.9)**



The compound **6.9** was prepared according to the procedure used for **6.7. 6.2** (700 mg, 2.02 mmol), **6.6** (963 mg, 2.63 mmol), potassium carbonate (838 mg, 6.07 mmol), Pd(dppf)Cl<sub>2</sub>·DCM complex (83 mg, 0.10 mmol), and mixture of dioxane and water (44:22 mL, v:v) were used to obtain product **6.9** as a colorless solid (519 mg, 51% yield). <sup>1</sup>H NMR (600 MHz, CDCl<sub>3</sub>) δ 10.08 (s, 1H), 9.89 (s, 1H), 7.95 (d, *J* = 8.0 Hz, 2H), 7.78 – 7.69 (m, 4H), 7.51 (d, *J* = 7.4 Hz, 1H), 7.33 (t, *J* = 7.6 Hz, 1H), 7.30 – 7.24 (m, 1H), 7.10 (d, *J* = 8.2 Hz, 1H), 6.97 (d, *J* = 7.5 Hz, 1H), 6.78 (brs, 1H), 5.31 – 5.14 (m, 2H), 4.37 (brs, 2H), 4.12 – 3.97 (m, 2H), 2.35 (s, 3H), 2.22 (s, 3H). <sup>13</sup>C NMR (151 MHz, CDCl<sub>3</sub>) δ 191.5, 191.2, 162.1, 143.7, 140.9, 138.5, 137.5, 135.2, 134.4, 131.7, 130.8, 130.7, 130.3, 129.8, 129.7, 129.1, 128.0, 127.9, 127.7, 125.7, 123.9, 119.7, 111.0, 69.2, 66.7, 16.5, 15.9.

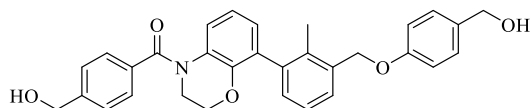
**(8-(3-((4-(hydroxymethyl)-2-methoxyphenoxy)methyl)-2-methylphenyl)-2,3-dihydro-4H-benzo[b][1,4]oxazin-4-yl)(4-(hydroxymethyl)phenyl)methanone (6.10)**



**6.7** (585 mg, 1.11 mmol) placed in a round bottom flask under argon and it was dissolved in a mixture of anhydrous THF and anhydrous MeOH (16:8 mL

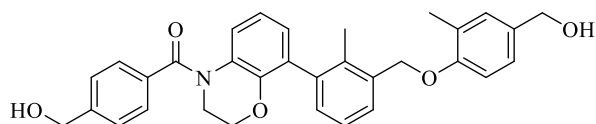
v:v). The mixture was cooled to 0 °C and followingly sodium borohydride (254 mg, 6.71 mmol) was added portionwise. The reaction was monitored by TLC and it was completed after 15 minutes. The excess of reductor was quenched by addition of ethyl acetate (5 mL), water (5 mL), and hydrochloric acid (2 mL). Then, water (25 mL) was added and the mixture was extracted with ethyl acetate (2 x 25 mL). The organic layers were combined, dried over anhydrous MgSO<sub>4</sub>, filtered, and the solvent was removed under reduced pressure. A colorless precipitate was obtained (501 mg, 85% yield). <sup>1</sup>H NMR (600 MHz, CDCl<sub>3</sub>) δ 7.52 (d, *J* = 8.2 Hz, 2H), 7.45 (d, *J* = 6.9 Hz, 1H), 7.38 (d, *J* = 8.1 Hz, 2H), 7.24 (t, *J* = 7.6 Hz, 1H), 7.18 (dd, *J* = 7.6, 1.1 Hz, 1H), 6.96 (d, *J* = 1.9 Hz, 1H), 6.93 (d, *J* = 8.1 Hz, 1H), 6.90 (dd, *J* = 7.4, 1.5 Hz, 1H), 6.86 (dd, *J* = 8.1, 1.9 Hz, 1H), 6.78 – 6.71 (m, 1H), 5.15 (q, *J* = 12.0 Hz, 2H), 4.72 (s, 2H), 4.62 (s, 2H), 4.29 (t, *J* = 4.2 Hz, 2H), 4.03 – 3.90 (m, 2H), 3.88 (s, 3H), 2.18 (s, 3H). <sup>13</sup>C NMR (151 MHz, CDCl<sub>3</sub>) δ 169.1, 150.2, 148.0, 144.0, 143.6, 138.5, 135.2, 135.1, 135.0, 134.4, 130.9, 130.0, 128.9, 128.0, 127.6, 126.8, 125.6, 123.9, 119.6, 119.5, 114.4, 111.3, 77.16, 70.39, 66.65, 65.38, 64.69, 56.11, 15.90.

**(8-(3-((4-(hydroxymethyl)phenoxy)methyl)-2-methylphenyl)-2,3-dihydro-4H-benzo[b][1,4]oxazin-4-yl)(4-(hydroxymethyl)phenyl)methanone (6.11)**



The compound **6.11** was prepared according to the procedure used for **6.10**. **6.8** (810 mg, 1.65 mmol) sodium borohydride (374 mg, 9.89 mmol) and mixture of anhydrous THF/MeOH (22:11 mL, v:v) were used to obtain compound **6.11** as a colorless foam (667 mg, yield: 82%). <sup>1</sup>H NMR (600 MHz, DMSO) δ 7.52 (d, *J* = 8.1 Hz, 2H), 7.42 (d, *J* = 7.5 Hz, 1H), 7.40 (d, *J* = 8.1 Hz, 2H), 7.30 (brs, 1H), 7.28 – 7.21 (m, 3H), 7.14 (d, *J* = 6.8 Hz, 1H), 7.01 (d, *J* = 8.6 Hz, 2H), 6.90 – 6.79 (m, 2H), 5.33 (t, *J* = 5.7 Hz, 1H), 5.11 (s, 2H), 5.05 (t, *J* = 5.7 Hz, 1H), 4.56 (d, *J* = 5.6 Hz, 2H), 4.42 (d, *J* = 5.6 Hz, 2H), 4.30 – 4.19 (m, 2H), 3.98 – 3.77 (m, 2H), 2.10 (s, 3H). <sup>13</sup>C NMR (151 MHz, DMSO) δ 168.7, 157.4, 145.2, 143.2, 138.4, 135.1, 135.1, 134.9, 133.8, 130.0, 129.8, 128.1, 128.0, 127.8, 126.4, 126.2, 126.1, 125.2, 123.5, 119.2, 114.4, 68.4, 66.0, 62.6, 62.4, 39.5, 15.5.

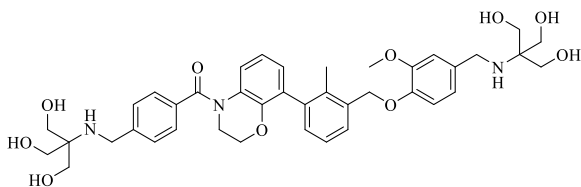
**(8-(3-((4-(hydroxymethyl)-2-methylphenoxy)methyl)-2-methylphenyl)-2,3-dihydro-4H-benzo[b][1,4]oxazin-4-yl)(4-(hydroxymethyl)phenyl)methanone (6.12)**



The compound **6.12** was prepared according to the procedure used for **6.10**. **6.9** (420 mg, 0.830 mmol), sodium borohydride (189 mg,

4.98 mmol) and mixture of anhydrous THF/MeOH (12:6 mL, v:v) were used to obtain compound **6.12** as a colorless foam (219 mg, yield: 52%). <sup>1</sup>H NMR (600 MHz, CDCl<sub>3</sub>) δ 7.54 – 7.48 (m, 3H), 7.37 (d, *J* = 7.9 Hz, 2H), 7.28 (t, *J* = 7.6 Hz, 1H), 7.22 (d, *J* = 7.5 Hz, 1H), 7.20 – 7.14 (m, 2H), 6.94 (d, *J* = 8.2 Hz, 1H), 6.92 (dd, *J* = 7.4, 1.3 Hz, 1H), 6.79 – 6.72 (m, 1H), 5.17 – 5.05 (m, 2H), 4.70 (s, 2H), 4.58 (s, 2H), 4.28 (s, 2H), 4.03 – 3.91 (m, 2H), 2.29 (s, 3H), 2.18 (s, 3H). <sup>13</sup>C NMR (151 MHz, CDCl<sub>3</sub>) δ 169.2, 156.7, 144.2, 143.6, 138.5, 135.4, 135.1, 134.2, 133.1, 130.8, 130.1, 129.9, 128.8, 127.6, 127.5, 127.4, 126.7, 126.1, 125.9, 125.6, 123.9, 119.6, 111.4, 69.0, 66.6, 65.1, 64.5, 16.5, 15.9.

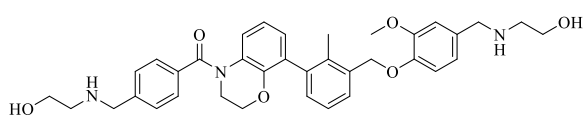
**(8-(3-((4-(((1,3-dihydroxy-2-(hydroxymethyl)propan-2-yl)amino)methyl)-2-methoxyphenoxy)methyl)-2-methylphenyl)-2,3-dihydro-4H-benzo[b][1,4]oxazin-4-yl)(4-(((1,3-dihydroxy-2-(hydroxymethyl)propan-2-yl)amino)methyl)phenyl)methanone (6.13)**



**6.10** (250 mg, 0.48 mmol) was dissolved in anhydrous DCM (7 mL) with catalytic amount of dry DMF (0.1 mL). The resulted solution was cooled to 0 °C and then, thionyl chloride (0.40 mL, 5.51 mmol) was added dropwise. The reaction mixture was stirred at room temperature for 2 h. Afterwards, the resulted solution was poured to the separation funnel with the 50 mL of sodium carbonate solution. Phases were separated and water phase was washed with dichloromethane (2 x 50 mL). The organic layers were combined, dried over anhydrous MgSO<sub>4</sub>, filtered, and the solvent was removed under reduced pressure. As a result yellow oil was obtained. In the second step of reaction, to the flask with resulted chloride TIRS (577 mg, 4.77 mmol), anhydrous DMF (9 mL) and DIPEA (0.70 mL, 3.80 mmol) were added respectively. Resulted mixture was heated overnight at 50 °C. Afterwards, solvent was removed under reduced pressure and the mixture of water and ethyl acetate (40 mL, 1:1, v:v) was added to separate the phases. The aqueous phase was further extracted with ethyl acetate: methanol (20:5 mL), and then washed with the mixture of chloroform: methanol (20:5 mL). The organic layers were combined, dried over anhydrous MgSO<sub>4</sub>, filtered, and then concentrated under reduced pressure. The crude product was purified by column chromatography (silica gel, chloroform: methanol, 4:1 + 1% solution of ammonia in methanol). A colorless solid **6.13** (197 mg, yield: 56%) was obtained as the product. <sup>1</sup>H NMR (600 MHz, MeOD) δ 7.53 – 7.47 (m, 4H), 7.44 (d, *J* = 6.8 Hz, 1H), 7.21 (t, *J* = 7.6 Hz, 1H), 7.11 (dd, *J* = 7.6, 1.0 Hz, 1H), 7.08 (t, *J* = 7.9 Hz, 1H), 7.00 (dd, *J* = 8.2, 1.2 Hz, 1H), 6.96 (dd, *J* = 7.6, 1.2 Hz, 1H), 6.83 (dd, *J* = 7.4, 1.3 Hz, 1H), 6.75 – 6.67 (m, 1H), 5.15 (q, *J* = 14.2 Hz, 2H), 4.31 – 4.18 (m, 2H), 3.98 – 3.91

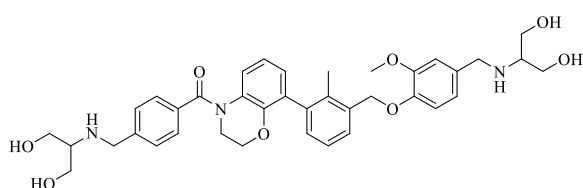
(m, 2H), 3.88 (s, 2H), 3.77 – 3.70 (m, 2H), 3.63 (s, 6H), 3.56 (s, 6H), 3.33 (s, 3H), 2.12 (s, 3H). <sup>13</sup>C NMR (151 MHz, MeOD) δ 171.2, 154.2, 147.0, 145.2, 140.0, 137.2, 136.8, 135.4, 132.4, 131.3, 130.6, 129.8, 129.7, 128.4, 127.3, 126.4, 125.8, 125.1, 123.0, 120.4, 113.5, 74.6, 67.6, 65.2, 62.8, 62.1, 56.4, 49.9, 49.0, 46.7, 42.1, 16.2. UPLC–MS (DAD/ESI): t<sub>R</sub> = 3.79 min, for C<sub>40</sub>H<sub>49</sub>N<sub>3</sub>O<sub>10</sub> [M + H]<sup>+</sup> found: 732.34 *m/z*; calc. mass: 732.35. HRMS ESI-MS-q-TOF for C<sub>40</sub>H<sub>49</sub>N<sub>3</sub>O<sub>10</sub> [M+H]<sup>+</sup> found: 732.3491 *m/z*; calc. mass: 732.3496.

**(8-(3-((4-(((2-hydroxyethyl)amino)methyl)-2-methoxyphenoxy)methyl)-2-methylphenyl)-2,3-dihydro-4H-benzo[b][1,4]oxazin-4-yl)(4-(((2-hydroxyethyl)amino)methyl)phenyl)methanone (6.14)**



The compound **6.14** was prepared according to the procedure used for **6.13**. In the first step, **6.10** (225 mg, 0.43 mmol), anhydrous DCM (7 mL) with addition of anhydrous DMF (0.1 mL), and thionyl chloride (0.31 mL, 4.28 mmol) were used. The product from the first step was treated with ethanolamine (0.26 mL, 4.28 mmol), DIPEA (0.60 mL, 3.42 mmol) and anhydrous DMF (9 mL). A colorless precipitate **6.14** (165 mg, yield: 55%) was obtained as the product. <sup>1</sup>H NMR (600 MHz, DMSO) δ 7.67 (d, *J* = 8.1 Hz, 2H), 7.60 (d, *J* = 8.1 Hz, 2H), 7.44 (d, *J* = 7.3 Hz, 1H), 7.28 – 7.19 (m, 2H), 7.18 – 7.12 (m, 3H), 6.92 – 6.79 (m, 2H), 5.21 (s, 2H), 5.09 (q, *J* = 11.3 Hz, 2H), 4.34 – 4.22 (m, *J* = 4.7 Hz, 2H), 4.17 (s, 2H), 4.01 (s, *J* = 9.9 Hz, 2H), 3.87 (s, 3H), 3.86 – 3.83 (m, 2H), 3.69 (t, *J* = 5.4 Hz, 2H), 3.64 (t, *J* = 5.4 Hz, 2H), 2.91 (t, *J* = 5.4 Hz, 2H), 2.87 – 2.78 (m, 2H), 2.16 (s, 3H). <sup>13</sup>C NMR (151 MHz, DMSO) δ 168.3, 152.5, 145.8, 143.3, 138.4, 135.8, 135.5, 135.2, 135.1, 130.2, 130.0, 129.9, 128.6, 128.2, 126.5, 125.9, 125.3, 124.4, 123.4, 122.2, 119.2, 113.5, 72.7, 65.9, 56.7, 56.6, 55.9, 49.7, 48.9, 48.8, 44.5, 39.5, 15.5. UPLC–MS (DAD/ESI): t<sub>R</sub> = 4.19 min, for C<sub>36</sub>H<sub>41</sub>N<sub>3</sub>O<sub>6</sub> [M + H]<sup>+</sup> found: 612.44 *m/z*; calc. mass: 612.31. HRMS ESI-MS-q-TOF for C<sub>36</sub>H<sub>41</sub>N<sub>3</sub>O<sub>6</sub> [M+H]<sup>+</sup> found: 612.3068 *m/z*; calc. mass: 612.3074.

**(8-(3-((4-(((1,3-dihydroxypropan-2-yl)amino)methyl)-2-methoxyphenoxy)methyl)-2-methylphenyl)-2,3-dihydro-4H-benzo[b][1,4]oxazin-4-yl)(4-(((1,3-dihydroxypropan-2-yl)amino)methyl)phenyl)methanone (6.15)**

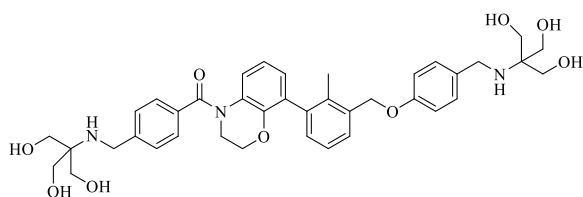


The compound **6.15** was prepared according to the procedure used for **6.13**. In the first step, **6.10** (250 mg, 0.48 mmol), anhydrous DCM (6 mL) with addition of anhydrous DMF (0.1 mL),



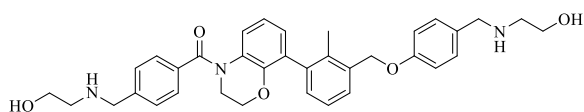
and thionyl chloride (0.34 mL, 4.75 mmol) were used. The product from the first step was treated with 2-amino-1,3-propanediol (432 mL, 4.75 mmol), DIPEA (0.66 mL, 3.23 mmol) and anhydrous DMF (7 mL). A colorless precipitate **6.15** (194 mg, yield: 61%) was obtained as the product. <sup>1</sup>H NMR (600 MHz, DMSO) δ 7.51 (d, *J* = 8.1 Hz, 2H), 7.44 (d, *J* = 8.2 Hz, 2H), 7.42 (d, *J* = 7.8 Hz, 1H), 7.33 (s, 1H), 7.24 (t, *J* = 7.6 Hz, 1H), 7.17 – 7.13 (m, 1H), 7.03 (d, *J* = 8.2 Hz, 1H), 7.01 (d, *J* = 1.7 Hz, 1H), 6.88 – 6.78 (m, 3H), 5.07 (s, 2H), 4.45 (brs, 4H), 4.29 – 4.19 (m, 2H), 3.90 – 3.85 (m, 2H), 3.83 (s, 2H), 3.76 (s, 3H), 3.72 (s, 2H), 3.45 – 3.25 (m, 8H), 2.59 – 2.53 (m, 2H), 2.11 (s, 3H). <sup>13</sup>C NMR (151 MHz, DMSO) δ 168.7, 149.1, 146.7, 144.1, 143.3, 138.4, 135.3, 133.9, 133.7, 130.0, 129.8, 128.1, 127.8, 126.4, 126.1, 125.2, 123.5, 120.0, 119.2, 113.6, 112.1, 69.24, 65.91, 61.06, 60.90, 60.36, 60.15, 55.51, 50.40, 39.52, 15.45. UPLC–MS (DAD/ESI): *t*<sub>R</sub> = 3.83 min, for C<sub>38</sub>H<sub>45</sub>N<sub>3</sub>O<sub>8</sub> [M - H]<sup>+</sup> found: 670.46 *m/z*; calc. mass: 670.31. HRMS ESI-MS-q-TOF for C<sub>38</sub>H<sub>45</sub>N<sub>3</sub>O<sub>8</sub> [M + H]<sup>+</sup> found: 672.3278 *m/z*; calc. mass: 672.3285.

**(8-(3-(((4-(((1,3-dihydroxy-2-(hydroxymethyl)propan-2-yl)amino)methyl)phenoxy)methyl)-2-methylphenyl)-2,3-dihydro-4H-benzo[b][1,4]oxazin-4-yl)(4-(((1,3-dihydroxy-2-(hydroxymethyl)propan-2-yl)amino)methyl)phenyl)methanone (6.16)**



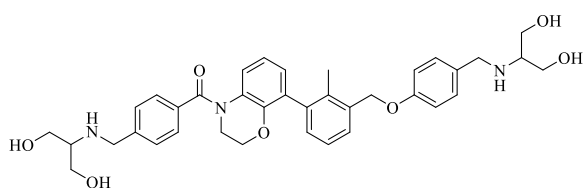
The compound **6.16** was prepared according to the procedure used for **6.13**. In the first step, **6.11** (250 mg, 0.50 mmol), anhydrous DCM (7 mL) with addition of anhydrous DMF (0.1 mL), and thionyl chloride (0.40 mL, 5.51 mmol) were used. The product from the first step was treated with TRIS (612 mg, 5.06 mmol), DIPEA (0.70 mL, 3.80 mmol) and anhydrous DMF (9 mL). A colorless precipitate **6.16** (88.5 mg, yield: 25%) was obtained as the product. <sup>1</sup>H NMR (600 MHz, DMSO) δ 7.53 (d, *J* = 8.1 Hz, 2H), 7.50 (d, *J* = 8.1 Hz, 2H), 7.43 (d, *J* = 7.3 Hz, 1H), 7.40 (d, *J* = 8.3 Hz, 2H), 7.25 (t, *J* = 7.6 Hz, 1H), 7.15 (d, *J* = 7.0 Hz, 1H), 7.06 (d, *J* = 8.6 Hz, 2H), 6.91 – 6.80 (m, 2H), 5.14 (s, 2H), 4.25 (s, 2H), 4.03 – 3.91 (m, 4H), 3.86 (s, 2H), 3.55 (s, 6H), 3.47 (s, 6H), 2.11 (s, 3H). <sup>13</sup>C NMR (151 MHz, DMSO) δ 168.6, 158.2, 143.2, 138.5, 135.2, 135.0, 134.1, 130.9, 130.0, 129.9, 128.5, 128.0, 127.9, 126.4, 126.1, 125.2, 123.5, 119.2, 114.5, 68.4, 65.9, 60.3, 59.3, 58.9, 45.2, 44.9, 39.5, 15.5. UPLC–MS (DAD/ESI): *t*<sub>R</sub> = 3.80 min, for C<sub>39</sub>H<sub>47</sub>N<sub>3</sub>O<sub>9</sub> [M - H]<sup>+</sup> found: 700.17 *m/z*; calc. mass: 700.32. HRMS ESI-MS-q-TOF for C<sub>39</sub>H<sub>47</sub>N<sub>3</sub>O<sub>9</sub> [M+H]<sup>+</sup> found: 702.3385 *m/z*; calc. mass: 702.3391.

**(8-(3-((4-(((2-hydroxyethyl)amino)methyl)phenoxy)methyl)-2-methylphenyl)-2,3-dihydro-4H-benzo[b][1,4]oxazin-4-yl)(4-(((2-hydroxyethyl)amino)methyl)phenyl)methanone (6.17)**



The compound **6.17** was prepared according to the procedure used for **6.13**. In the first step, **6.11** (200 mg, 0.40 mmol), anhydrous DCM (6 mL) with addition of anhydrous DMF (0.1 mL), and thionyl chloride (0.29 mL, 4.04 mmol) were used. The product from the first step was treated with ethanolamine (0.24 mL, 4.04 mmol), DIPEA (0.56 mL, 3.23 mmol) and anhydrous DMF (7 mL). A colorless precipitate **6.17** (86 mg, yield: 37%) was obtained as the product. <sup>1</sup>H NMR (600 MHz, DMSO) δ 7.61 (d, *J* = 7.5 Hz, 2H), 7.58 (d, *J* = 7.6 Hz, 2H), 7.50 (d, *J* = 8.1 Hz, 2H), 7.43 (d, *J* = 7.3 Hz, 1H), 7.24 (t, *J* = 7.4 Hz, 1H), 7.15 (d, *J* = 7.4 Hz, 1H), 7.09 (d, *J* = 8.2 Hz, 2H), 6.90 – 6.71 (m, 2H), 5.15 (s, 2H), 4.25 (s, 2H), 4.09 (s, 2H), 4.05 (s, 2H), 3.90 – 3.79 (m, 2H), 3.74 – 3.58 (m, 4H), 2.95 – 2.76 (m, 4H), 2.10 (s, 3H). <sup>13</sup>C NMR (151 MHz, DMSO) δ 168.4, 158.8, 143.3, 138.5, 136.7, 135.4, 135.3, 134.9, 131.7, 130.0, 130.0, 129.6, 128.2, 128.0, 126.6, 125.9, 125.3, 124.7, 123.5, 119.3, 114.8, 68.5, 65.9, 57.4, 56.7, 50.2, 49.5, 49.2, 48.3, 39.5, 15.6. UPLC–MS (DAD/ESI): *t*<sub>R</sub> = 4.13 min, for C<sub>35</sub>H<sub>39</sub>N<sub>3</sub>O<sub>5</sub> [M + H]<sup>+</sup> found: 582.33 *m/z*; calc. mass: 582.30. HRMS ESI-MS-q-TOF for C<sub>35</sub>H<sub>39</sub>N<sub>3</sub>O<sub>5</sub> [M+H]<sup>+</sup> found: 582.2962 *m/z*; calc. mass: 582.2968.

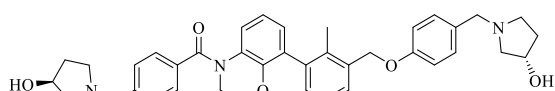
**(8-(3-((4-(((1,3-dihydroxypropan-2-yl)amino)methyl)phenoxy)methyl)-2-methylphenyl)-2,3-dihydro-4H-benzo[b][1,4]oxazin-4-yl)(4-(((1,3-dihydroxypropan-2-yl)amino)methyl)phenyl)methanone (6.18)**



The compound **6.18** was prepared according to the procedure used for **6.13**. In the first step, **6.11** (250 mg, 0.50 mmol), anhydrous DCM (7 mL) with addition of anhydrous DMF (0.1 mL), and thionyl chloride (0.32 mL, 5.04 mmol) were used. The product from the first step was treated with 2-amino-1,3-propanediol (458 mL, 5.04 mmol), DIPEA (0.74 mL, 4.03 mmol) and anhydrous DMF (9 mL). A colorless precipitate **6.18** (182 mg, yield: 56%) was obtained as the product. <sup>1</sup>H NMR (600 MHz, DMSO) δ 7.51 (d, *J* = 8.1 Hz, 2H), 7.45 (d, *J* = 8.1 Hz, 2H), 7.42 (d, *J* = 7.7 Hz, 1H), 7.31 (d, *J* = 8.5 Hz, 2H), 7.24 (t, *J* = 7.6 Hz, 1H), 7.14 (d, *J* = 6.9 Hz, 1H), 7.02 (d, *J* = 8.6 Hz, 2H), 6.88 – 6.80 (m, 2H), 5.11 (s, 2H), 4.48 (brs, 4H), 4.26 – 4.19 (m, 2H), 3.86 (s, 2H), 3.84 (s, 2H), 3.78 (s, 2H), 3.52 – 3.35 (m, 8H), 2.63 (p, *J* = 5.5 Hz, 1H), 2.57 (p, *J* = 5.5 Hz, 1H), 2.10 (s, *J* = 11.6 Hz, 3H). <sup>13</sup>C NMR (151 MHz, DMSO) δ 168.7, 157.6, 143.8

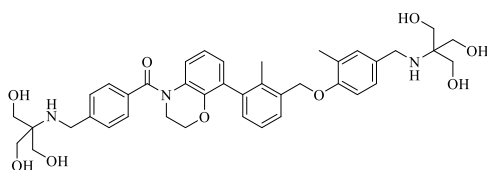
143.24 138.4, 135.2, 135.1, 133.8, 130.0, 129.8, 129.6, 128.1, 127.9, 126.4, 126.1, 125.2, 123.5, 119.2, 114.5, 68.4, 65.9, 60.9, 60.3, 60.0, 50.3, 49.7, 39.5, 15.5. UPLC–MS (DAD/ESI):  $t_R$  = 3.86 min, for  $C_{37}H_{43}N_3O_7$   $[M - H]^+$  found: 640.49  $m/z$ ; calc. mass: 640.30. HRMS ESI-MS-q-TOF for  $C_{37}H_{43}N_3O_7$   $[M + H]^+$  found: 642.3174  $m/z$ ; calc. mass: 642.3179.

**(8-(3-((4-(((S)-3-hydroxypyrrolidin-1-yl)methyl)phenoxy)methyl)-2-methylphenyl)-2,3-dihydro-4H-benzo[b][1,4]oxazin-4-yl)(4-(((S)-3-hydroxypyrrolidin-1-yl)methyl)phenyl)methanone (6.19)**



The compound **6.19** was prepared according to the procedure used for **6.13**. In the first step, **6.11** (183 mg, 0.37 mmol), anhydrous DCM (6 mL) with addition of anhydrous DMF (0.1 mL), and thionyl chloride (0.27 mL, 3.69 mmol) were used. The product from the first step was treated with (S)-pyrrolidin-3-ol (0.52 mL, 3.69 mmol), DIPEA (0.52 mL, 2.97 mmol) and anhydrous DMF (8 mL). A colorless precipitate **6.19** (86 mg, yield: 37%) was obtained as the product.  $^1H$  NMR (600 MHz, DMSO)  $\delta$  7.51 (d,  $J$  = 8.1 Hz, 2H), 7.42 (d,  $J$  = 7.0 Hz, 1H), 7.39 (d,  $J$  = 8.1 Hz, 2H), 7.34 (brs, 1H), 7.29 – 7.21 (m, 3H), 7.14 (dd,  $J$  = 7.5, 0.9 Hz, 1H), 7.01 (d,  $J$  = 8.6 Hz, 2H), 6.88 – 6.78 (m, 2H), 5.11 (s, 2H), 4.80 – 4.67 (m, 2H), 4.29 – 4.15 (m, 4H), 3.93 – 3.82 (m, 2H), 3.73 – 3.51 (m, 4H), 2.76 – 2.66 (m, 2H), 2.63 – 2.55 (m, 2H), 2.48 – 2.38 (m, 2H), 2.38 – 2.30 (m, 2H), 2.10 (s, 3H), 2.02 – 1.94 (m, 2H), 1.59 – 1.46 (m, 2H).  $^{13}C$  NMR (151 MHz, DMSO)  $\delta$  168.6, 157.6, 143.2, 141.8, 138.4, 135.1, 135.0, 134.0, 130.0, 129.9, 129.8, 128.4, 128.1, 127.9, 126.4, 126.0, 125.2, 123.4, 119.1, 114.4, 69.4, 69.2, 68.4, 65.9, 62.5, 62.2, 59.3, 58.9, 52.4, 52.2, 39.5, 34.4, 34.2, 15.5. UPLC–MS (DAD/ESI):  $t_R$  = 4.17 min, for  $C_{39}H_{43}N_3O_5$   $[M + H]^+$  found: 634.58  $m/z$ ; calc. mass: 634.33. HRMS ESI-MS-q-TOF for  $C_{39}H_{43}N_3O_5$   $[M+H]^+$  found: 634.3275  $m/z$ ; calc. mass: 634.3281.

**(8-(3-((4-(((1,3-dihydroxy-2-(hydroxymethyl)propan-2-yl)amino)methyl)-2-methylphenoxy)methyl)-2-methylphenyl)-2,3-dihydro-4H-benzo[b][1,4]oxazin-4-yl)(4-(((1,3-dihydroxy-2-(hydroxymethyl)propan-2-yl)amino)methyl)phenyl)methanone (6.20)**

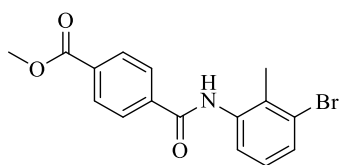


The compound **6.20** was prepared according to the procedure used for **6.13**. In the first step, **6.12** (200 mg, 0.39 mmol), anhydrous DCM (19 mL) with addition of anhydrous DMF (0.1 mL), and thionyl chloride (0.29 mL, 3.92 mmol) were used. The product from the first step was treated with TRIS (475 mg, 3.92 mmol), DIPEA (0.58 mL, 3.14 mmol) and anhydrous DMF (19 mL). A colorless

precipitate **6.20** (105 mg, yield: 38%) was obtained as the product.  $^1\text{H}$  NMR (400 MHz, DMSO- $d_6$ )  $\delta$  7.50 (d,  $J = 8.2$  Hz, 2H), 7.48 – 7.42 (m, 3H), 7.32 (brs, 1H), 7.25 (t,  $J = 7.6$  Hz, 1H), 7.20 – 7.11 (m, 3H), 7.05 (d,  $J = 8.1$  Hz, 1H), 6.88 – 6.79 (m, 2H), 5.13 (s, 2H), 4.42 (brs, 3H), 4.27 – 4.17 (m, 2H), 3.90 – 3.84 (m, 2H), 3.83 (s, 2H), 3.75 (s, 2H), 3.46 (s, 6H), 3.42 (s, 6H), 3.37 (brs, 3H), 2.19 (s, 3H), 2.12 (s, 3H).  $^{13}\text{C}$  NMR (101 MHz, DMSO- $d_6$ )  $\delta$  168.7, 155.6, 143.2, 138.4, 135.4, 135.0, 133.7, 131.1, 130.0, 129.7, 128.1, 127.4, 127.3, 126.4, 126.1, 125.6, 125.2, 123.5, 119.2, 111.5, 68.4, 65.9, 61.0, 60.4, 60.2, 45.2, 44.9, 43.6, 16.2, 15.5. UPLC–MS (DAD/ESI):  $t_{\text{R}} = 4.06$  min, for  $\text{C}_{40}\text{H}_{49}\text{N}_3\text{O}_9$   $[\text{M} - \text{H}]^+$  found: 714.27  $m/z$ ; calc. mass: 714.33. HRMS ESI-MS-q-TOF for  $\text{C}_{40}\text{H}_{49}\text{N}_3\text{O}_9$   $[\text{M} + \text{H}]^+$  found: 716.3540  $m/z$ ; calc. mass: 716.3547.

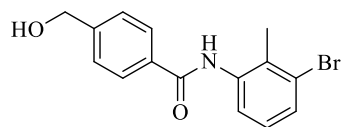
#### 4.2.7. Elongated Pseudo $\text{C}_2$ -symmetric PD-1/PD-L1 Inhibitors

##### methyl 4-((3-bromo-2-methylphenyl)carbamoyl)benzoate (7.1)



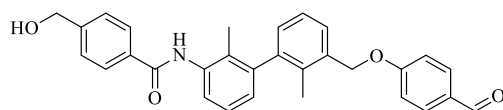
4- (methoxycarbonyl) benzoic acid (3.60 g, 19.87 mmol) was placed in the dried, one- neck round bottom flask under argon. Then,  $\text{SOCl}_2$  (14.51 mL) was added and resulted suspension was stirred for 4 hours at 80 ° C under a cooling condenser fitted with a tube with calcium chloride. Heating was continued for 1 hour until a clear solution was obtained. The solvent was removed under reduced pressure to get the corresponding acid chloride. To the resulted solid, toluene (15 mL x 2) was added and it was concentrated again under reduced pressure to remove the residues of thionyl chloride. In the second step, to the acid chloride solubilized in anhydrous THF (40 mL), 3-bromo-2-methylaniline (3.7 mL, 30 mmol) solution in anhydrous THF (40 mL) and triethylamine (14 mL, 100 mmol) were added respectively and portionwise. Resulted suspension was stirred overnight at 50 °C and then it was concentrated under reduced pressure. Water (100 mL) was added and the mixture was washed with DCM (2 x 100 mL). The organic layers were combined, dried over anhydrous  $\text{MgSO}_4$ , filtered, and concentrated under reduced pressure. The product was obtained as a colorless solid (6.92 g, 100%).  $^1\text{H}$  NMR (600 MHz,  $\text{CDCl}_3$ )  $\delta$  8.15 (d,  $J = 8.4$  Hz, 2H), 7.93 (d,  $J = 8.1$  Hz, 2H), 7.80 (s, 1H), 7.73 (d,  $J = 7.5$  Hz, 1H), 7.47 (d,  $J = 8.0$  Hz, 1H), 7.12 (t,  $J = 8.0$  Hz, 1H), 3.96 (s, 3H), 2.41 (s, 3H).  $^{13}\text{C}$  NMR (151 MHz,  $\text{CDCl}_3$ )  $\delta$  166.3, 165.2, 138.4, 136.4, 133.4, 131.0, 130.5, 130.3, 127.7, 127.3, 125.8, 123.7, 52.7, 18.1.

### N-(3-bromo-2-methylphenyl)-4-(hydroxymethyl)benzamide (7.2)



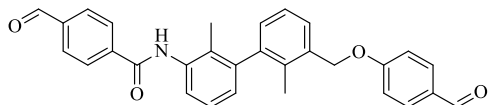
**7.1** (2.00 g, 5.75 mmol) was placed in the dry, two-neck, round bottom flask under argon. Then, anhydrous THF (80 mL) and MeOH (16 mL) were added, and followingly LiBH<sub>4</sub> (624 mg, 28.65 mmol) was added portionwise. Reaction mixture was stirred for 2 hours at room temperature. After, that time reaction was quenched, water (80 mL) was added and the mixture was extracted with AcOEt (2 x 80 mL). The organic layers were combined, dried over anhydrous MgSO<sub>4</sub>, filtered, and concentrated under reduced pressure. The crude product was purified by flash chromatography (silica gel, 0-100% AcOEt in hexane) to give **7.2** as a colorless solid (1.84 g, 100%). <sup>1</sup>H NMR (600 MHz, MeOD) δ 7.97 (d, *J* = 8.2 Hz, 2H), 7.54 (dd, *J* = 8.1, 1.0 Hz, 1H), 7.52 (d, *J* = 8.5 Hz, 2H), 7.33 (d, *J* = 7.3 Hz, 1H), 7.19 – 7.11 (m, 1H), 4.71 (s, 2H), 2.37 (s, 3H). <sup>13</sup>C NMR (151 MHz, MeOD) δ 169.1, 147.4, 138.5, 136.1, 134.1, 132.2, 128.8, 128.4, 127.8, 127.7, 126.5, 64.6, 18.7.

### N-(3'-((4-formylphenoxy)methyl)-2,2'-dimethyl-[1,1'-biphenyl]-3-yl)-4-(hydroxymethyl)benzamide (7.3)



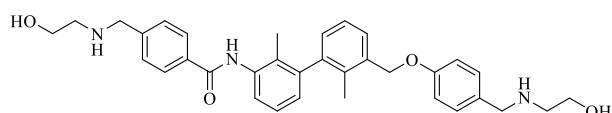
**7.2** (840 mg, 2.61 mmol), **6.5** (1.20 g, 3.39 mmol) and K<sub>2</sub>CO<sub>3</sub> (1.08 g, 7.83 mmol) were placed in the two-neck round bottom flask under argon. Then, dioxane (24 mL) and water (12 mL) were added and the resulted mixture was deoxygenated for 15 minutes. Afterwards, the mixture was heated to 85 °C and Pd(PPh<sub>3</sub>)<sub>4</sub> (152 mg, 0.13 mmol) was added. Reaction mixture was stirred for 3 h at 85 °C and then it was cooled to the room temperature. Then, water (80 mL) was added and extraction with AcOEt (2 x 80 mL) was carried out. The organic layers were combined, dried over anhydrous MgSO<sub>4</sub>, filtered, and concentrated under reduced pressure. The crude product was purified by flash chromatography (silica gel, 0-100% ethyl acetate in hexane) to give a colorless solid (1.10 g, 85%) as the product. <sup>1</sup>H NMR (600 MHz, DMSO) δ 9.94 (s, 1H), 9.89 (s, 1H), 7.98 (d, *J* = 8.2 Hz, 2H), 7.93 – 7.88 (m, 2H), 7.50 (d, *J* = 7.1 Hz, 1H), 7.47 (d, *J* = 8.3 Hz, 2H), 7.39 (d, *J* = 7.6 Hz, 1H), 7.35 – 7.25 (m, 4H), 7.16 – 7.11 (m, 1H), 7.05 – 7.00 (m, 1H), 5.35 (t, *J* = 5.7 Hz, 1H), 5.33 – 5.28 (m, 2H), 4.60 (d, *J* = 5.7 Hz, 2H), 2.05 (s, 3H), 1.92 (s, 3H). <sup>13</sup>C NMR (151 MHz, DMSO) δ 191.4, 165.2, 163.5, 146.4, 142.0, 141.8, 136.8, 134.7, 134.5, 132.8, 132.0, 131.9, 129.9, 129.3, 127.9, 127.5, 127.0, 126.1, 126.0, 125.6, 115.3, 68.8, 62.5, 15.3, 15.1.

**4-formyl-N-(3'-((4-formylphenoxy)methyl)-2,2'-dimethyl-[1,1'-biphenyl]-3-yl)benzamide (7.4)**



**7.3** (690 mg, 1.48 mmol) was placed in round bottom flask and it was dissolved in anhydrous DCM (14 mL). Then Dess-Martin's reagent (756 mg, 1.78 mmol) and  $\text{NaHCO}_3$  (311 mg, 3.70 mmol) were added. Reaction mixture was stirred for 2 hours at room temperature. After 2 hours, water (80 mL) was added and it was washed with DCM (2 x 80 mL). The organic layers were combined, dried over anhydrous  $\text{MgSO}_4$ , filtered, and concentrated under reduced pressure. The product was purified by flash chromatography (silica gel, 0-100% AcOEt in hexane) to give an orange solid as the product (325 mg, 51%).  $^1\text{H}$  NMR (600 MHz,  $\text{CDCl}_3$ )  $\delta$  10.11 (s, 1H), 9.89 (s, 1H), 8.07 (d,  $J = 7.9$  Hz, 2H), 8.01 (d,  $J = 8.2$  Hz, 2H), 7.89 (brs, 2H), 7.88 – 7.82 (m, 2H), 7.48 – 7.44 (m, 1H), 7.33 (t,  $J = 7.8$  Hz, 1H), 7.29 (t,  $J = 7.6$  Hz, 1H), 7.16 (dd,  $J = 7.5, 0.9$  Hz, 1H), 7.14 – 7.10 (m, 2H), 7.06 (dd,  $J = 7.5, 1.0$  Hz, 1H), 5.18 (s, 2H), 2.08 (s, 3H), 2.05 (s, 3H).  $^{13}\text{C}$  NMR (151 MHz,  $\text{CDCl}_3$ )  $\delta$  191.5, 190.9, 164.0, 142.7, 142.2, 140.2, 138.6, 135.7, 134.9, 134.4, 132.2, 130.4, 130.2, 130.1, 128.5, 128.2, 128.0, 127.5, 126.5, 125.9, 123.0, 115.2, 69.4, 15.8, 14.9.

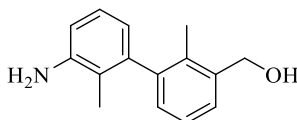
**4-(((2-hydroxyethyl)amino)methyl)-N-(3'-((4-(((2-hydroxyethyl)amino)methyl)phenoxy)methyl)-2,2'-dimethyl-[1,1'-biphenyl]-3-yl)benzamide (7.5)**



**7.4** (250 mg, 0.54 mmol) was dissolved in anhydrous DMF (11 mL) and ethanolamine (0.30 mL, 4.91 mmol) and AcOH (8 droplets) were added. The resulted mixture was stirred for 2 hours at room temperature. After that time,  $\text{NaBH}_3\text{CN}$  (340 mg, 5.39 mmol) was added and reaction mixture was stirred overnight at room temperature. Solvent was removed under reduced pressure. The crude product was purified by column chromatography (silica gel, 4:1 DCM: MeOH + 2%  $\text{NH}_3$  in MeOH) to give the product **7.5** as a colorless solid (91mg, 31%).  $^1\text{H}$  NMR (600 MHz, DMSO)  $\delta$  9.92 (s, 1H), 7.96 (d,  $J = 8.1$  Hz, 2H), 7.51 – 7.44 (m, 3H), 7.38 (d,  $J = 7.7$  Hz, 1H), 7.34 – 7.23 (m, 4H), 7.14 – 7.08 (m, 1H), 7.06 – 6.97 (m, 3H), 5.17 – 5.10 (m, 2H), 3.79 (s, 2H), 3.65 (s, 2H), 3.52 – 3.44 (m, 4H), 2.64 – 2.54 (m, 4H), 2.04 (s, 3H), 1.91 (s, 3H).  $^{13}\text{C}$  NMR (151 MHz, DMSO)  $\delta$  165.2, 161.2, 157.3, 144.9, 142.1, 141.6, 136.7, 135.6, 134.3, 133.0, 132.7, 132.0, 129.2, 129.0, 127.8, 127.5, 127.0, 125.9, 125.6, 125.5, 114.4, 68.3, 60.4, 60.3, 52.5, 52.3, 51.0, 50.9, 15.2, 15.1. UPLC-MS (DAD/ESI):  $t_R = 3.91$  min, for  $\text{C}_{34}\text{H}_{39}\text{N}_3\text{O}_4$   $[\text{M} - \text{H}]^+$  found:

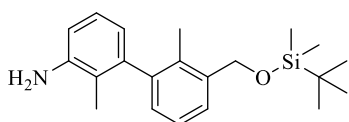
552.16 *m/z*; calc. mass: 552.29. HRMS ESI-MS-q-TOF for C<sub>34</sub>H<sub>39</sub>N<sub>3</sub>O<sub>4</sub> [M + H]<sup>+</sup> found: 554.3013 *m/z*; calc. mass: 554.3018.

### (3'-amino-2,2'-dimethyl-[1,1'-biphenyl]-3-yl)methanol (7.6)



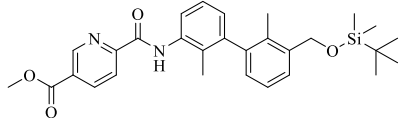
**7.6** (800 mg, 3.43 mmol), (3-bromo-2-methylphenyl)methanol (575 mg, 2.86 mmol) and potassium carbonate (1180 g, 8.58 mmol) were placed in the two-neck, round bottom flask under argon and mixture of dioxane and water (20:10 mL, v:v) was added. The mixture was deoxygenated by rinsing with argon for 15 min. Then, resulting mixture was heated up to 85 °C and Pd(dppf)Cl<sub>2</sub>·DCM complex (117 mg, 0.14 mmol) was added. The mixture was stirred at 85 °C for 3 hours. Afterwards, water (100 mL) was added to the reaction mixture and it was extracted with ethyl acetate (2x100 mL). The organic layers were combined, dried over anhydrous MgSO<sub>4</sub>, filtered, and the solvent was removed under reduced pressure. The crude product was purified by flash chromatography (silica gel, 0-60% ethyl acetate in hexane) to give a white solid (668 mg, yield: 100%). <sup>1</sup>H NMR (600 MHz, CDCl<sub>3</sub>) δ 7.37 (d, *J* = 6.9 Hz, 1H), 7.23 (t, *J* = 7.6 Hz, 1H), 7.10 – 7.05 (m, 2H), 6.78 (d, *J* = 7.8 Hz, 1H), 6.62 (d, *J* = 7.5 Hz, 1H), 4.76 (s, 2H), 2.06 (s, 3H), 1.88 (s, 3H). <sup>13</sup>C NMR (101 MHz, CDCl<sub>3</sub>) δ 144.7, 142.8, 142.6, 138.9, 134.3, 129.3, 126.5, 126.2, 125.5, 120.7, 120.3, 114.0, 64.1, 15.4, 14.0.

### 3'-(((tert-butyldimethylsilyl)oxy)methyl)-2,2'-dimethyl-[1,1'-biphenyl]-3-amine (7.7)



**7.6** (650 mg, 2.86 mmol), TBDMSCl (647 mg, 4.29 mmol) and imidazole (287 mg, 4.29 mmol) were placed in the round bottom flask under argon. Then, anhydrous DCM (44 mL) was added and resulted mixture was stirred overnight at room temperature. After that time, water was added to separate the phases. Followingly, water was washed with DCM (2 x 50 mL). The organic layers were combined, dried over anhydrous MgSO<sub>4</sub>, filtered, and the solvent was removed under reduced pressure. The crude product was purified by flash chromatography (silica gel, 0-40% ethyl acetate in hexane) to give a white solid (775 mg, yield: 79%). <sup>1</sup>H NMR (600 MHz, CDCl<sub>3</sub>) δ 7.44 (d, *J* = 7.5 Hz, 1H), 7.22 (t, *J* = 7.6 Hz, 1H), 7.09 – 7.02 (m, 2H), 6.73 (dd, *J* = 7.8, 0.6 Hz, 1H), 6.59 (dd, *J* = 7.5, 0.7 Hz, 1H), 4.76 (q, *J* = 13.4 Hz, 2H), 1.96 (s, 3H), 1.85 (s, 3H), 0.96 (s, 9H), 0.12 (d, *J* = 5.3 Hz, 6H). <sup>13</sup>C NMR (151 MHz, CDCl<sub>3</sub>) δ 144.4, 142.9, 142.2, 139.4, 133.2, 128.4, 126.2, 125.3, 125.3, 120.9, 120.6, 114.1, 63.8, 26.1, 18.5, 15.2, 14.0, -5.1, -5.1.

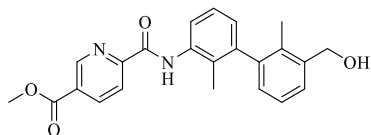
**methyl 6-((3'-(((tert-butyl dimethylsilyl)oxy)methyl)-2,2'-dimethyl-[1,1'-biphenyl]-3-yl)carbamoyl)nicotinate (7.8)**



5-(methoxycarbonyl)picolinic acid (398 mg, 2.19 mmol)

was placed in the dried, one-neck round bottom flask under argon. Then,  $\text{SOCl}_2$  (7.20 mL) and anhydrous toluene (7 mL) was added and resulted suspension was stirred for 4 hours at  $80^\circ\text{C}$  under a cooling condenser fitted with a tube with calcium chloride. The solvent was removed under reduced pressure to get the corresponding acid chloride. To the resulted solid, toluene (15 mL x 2) was added and it was concentrated again under reduced pressure to remove the residues of thionyl chloride. In the second step, to the acid chloride solubilized in anhydrous THF (15 mL), **7.7** (750 mg, 2.19 mmol) solution in anhydrous THF (15 mL) and triethylamine (1.4 mL, 10.88 mmol) were added respectively and portionwise. Resulted suspension was stirred overnight at room temperature and then it was concentrated under reduced pressure. Water (50 mL) was added and the mixture was washed with DCM (2 x 50 mL). The organic layers were combined, dried over anhydrous  $\text{MgSO}_4$ , filtered, and concentrated under reduced pressure. The product **7.8** was obtained as a colorless solid (827 mg, 75%).  $^1\text{H}$  NMR (600 MHz,  $\text{CDCl}_3$ )  $\delta$  10.14 (s, 1H), 9.22 (dd,  $J = 2.0, 0.7$  Hz, 1H), 8.52 (dd,  $J = 8.1, 2.0$  Hz, 1H), 8.41 (dd,  $J = 8.1, 0.6$  Hz, 1H), 8.26 (dd,  $J = 8.2, 0.9$  Hz, 1H), 7.48 (d,  $J = 7.5$  Hz, 1H), 7.32 (t,  $J = 7.8$  Hz, 1H), 7.25 (t,  $J = 7.6$  Hz, 1H), 7.05 (d,  $J = 6.8$  Hz, 1H), 6.99 (dd,  $J = 7.5, 1.0$  Hz, 1H), 4.77 (q,  $J = 13.4$  Hz, 2H), 4.00 (s, 3H), 2.10 (s, 3H), 1.97 (s, 3H), 0.96 (s, 9H), 0.13 (d,  $J = 5.7$  Hz, 6H).  $^{13}\text{C}$  NMR (151 MHz,  $\text{CDCl}_3$ )  $\delta$  165.2, 161.1, 153.3, 149.5, 143.0, 141.5, 139.7, 139.1, 135.8, 133.2, 128.4, 126.9, 126.6, 126.3, 125.7, 125.5, 122.2, 120.7, 63.8, 52.9, 26.1, 26.1, 18.6, 15.3, 14.5, -5.1, -5.1.

**methyl 6-((3'-(hydroxymethyl)-2,2'-dimethyl-[1,1'-biphenyl]-3-yl)carbamoyl)nicotinate (7.9)**



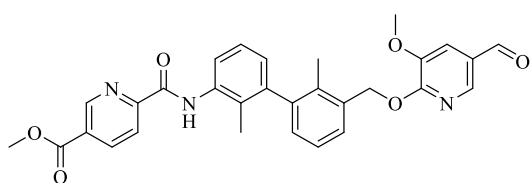
**7.8** (540 mg, 1.07 mmol) was placed in the round bottom flask and it was dissolved in anhydrous DCM (17 mL). Then, HCl (4 M solution in dioxane) was added dropwise and resulted mixture

was stirred at room temperature. The progress of reaction was monitored by TLC. After 1 hour reaction was completed and NaOH (1M solution) was added portionwise to neutralized the solution to neutral pH. Followingly, water (50 mL) was added and the mixture was washed with DCM (2 x 50 mL). The organic layers were combined, dried over anhydrous  $\text{MgSO}_4$ , filtered, and concentrated under reduced pressure. The product **7.9** was obtained as a colorless solid (430 mg, 100%) without additional purification.  $^1\text{H}$  NMR (600 MHz,  $\text{CDCl}_3$ )  $\delta$  10.14 (s, 1H),



9.23 (d,  $J = 1.4$  Hz, 1H), 8.52 (dd,  $J = 8.1, 2.0$  Hz, 1H), 8.41 (d,  $J = 8.2$  Hz, 1H), 8.26 (d,  $J = 8.1$  Hz, 1H), 7.41 (d,  $J = 7.4$  Hz, 1H), 7.32 (t,  $J = 7.8$  Hz, 1H), 7.26 (t,  $J = 7.6$  Hz, 1H), 7.10 (d,  $J = 6.9$  Hz, 1H), 6.98 (d,  $J = 7.0$  Hz, 1H), 4.78 (s, 2H), 4.00 (s, 3H), 2.10 (s, 3H), 2.07 (s, 3H).  $^{13}\text{C}$  NMR (151 MHz,  $\text{CDCl}_3$ )  $\delta$  165.1, 161.2, 153.2, 149.5, 142.8, 142.0, 139.2, 139.1, 135.8, 134.2, 129.2, 128.4, 126.8, 126.8, 126.5, 126.4, 125.7, 122.2, 120.8, 64.0, 52.9, 15.5, 14.5.

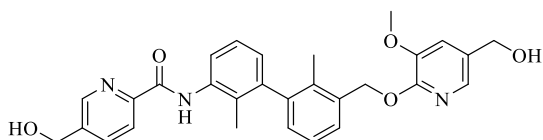
**methyl 6-((3'-(((5-formyl-3-methoxypyridin-2-yl)oxy)methyl)-2,2'-dimethyl-[1,1'-biphenyl]-3-yl)carbamoyl)nicotinate (7.10)**



**7.9** (300 mg, 0.77 mmol), 6-chloro-2-methoxynicotinaldehyde (78 mg, 0.59 mmol), cesium carbonate (300 mg, 1.18 mmol), *tert*-Bu-XPhoS (39 mg, 0.12 mmol) and XPhoS (57 mg,

0.12 mmol) were placed in the round-bottom flask under argon. Then, anhydrous toluene (12 mL) was added and the reaction mixture was heated to 80 °C. Followingly,  $\text{Pd}(\text{OAc})_2$  and  $\text{Pd}(\text{dppf})\text{Cl}_2 \cdot \text{DCM}$  were added and reaction mixture was reflux for 5 hours. Afterwards, reaction mixture was concentrated under reduced pressure, and the mixture of dichloromethane and water (100 mL, 1:1, v:v) was added to the residue. The mixture was extracted one more time with  $\text{AcOEt}$  (50 mL), organic layers were combined and dried over  $\text{MgSO}_4$ . Filtrate was concentrated under reduced pressure. The product was purified by flash chromatography on silica gel using 0–60%  $\text{EtOAc}$  in hexane to give pure product (243 mg, 78%).  $^1\text{H}$  NMR (600 MHz,  $\text{CDCl}_3$ )  $\delta$  10.21 (s,  $J = 0.6$  Hz, 1H), 10.14 (s, 1H), 9.22 (dd,  $J = 1.9, 0.6$  Hz, 1H), 8.52 (dd,  $J = 8.1, 2.0$  Hz, 1H), 8.41 (dd,  $J = 8.1, 0.6$  Hz, 1H), 8.27 (dd,  $J = 8.1, 0.7$  Hz, 1H), 8.06 (d,  $J = 8.3$  Hz, 1H), 7.45 (dd,  $J = 7.5, 0.8$  Hz, 1H), 7.33 (t,  $J = 7.8$  Hz, 1H), 7.27 (t,  $J = 7.6$  Hz, 1H), 7.15 (dd,  $J = 7.5, 1.0$  Hz, 1H), 7.00 (dd,  $J = 7.6, 0.8$  Hz, 1H), 6.46 (dd,  $J = 8.3, 0.7$  Hz, 1H), 5.52 (s, 2H), 4.07 (s, 3H), 4.00 (s, 3H), 2.11 (s, 3H), 2.11 (s,  $J = 7.0$  Hz, 3H).  $^{13}\text{C}$  NMR (151 MHz,  $\text{CDCl}_3$ )  $\delta$  187.7, 166.5, 165.1, 165.1, 161.2, 153.2, 149.5, 142.5, 142.3, 140.5, 139.1, 135.8, 135.2, 134.8, 130.0, 128.5, 128.4, 126.8, 126.5, 126.4, 125.7, 122.2, 120.9, 112.5, 103.9, 67.60, 54.02, 52.86, 15.88, 14.52.

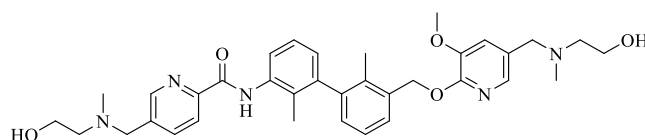
**5-(hydroxymethyl)-N-(3'-(((5-(hydroxymethyl)-3-methoxypyridin-2-yl)oxy)methyl)-2,2'-dimethyl-[1,1'-biphenyl]-3-yl)picolinamide (7.11)**



Compound **7.11** was prepared following the procedure for **7.21**. **7.10** (340 mg, 0.65 mmol),  $\text{LiBH}_4$  2M solution in THF (3.25 mL, 6.47 mmol)

and mixture of anhydrous THF/MeOH (29:15 mL, v:v) were used to obtain compound **7.11** as a yellow foam (62 mg, yield: 19%). <sup>1</sup>H NMR (400 MHz, CDCl<sub>3</sub>) δ 10.12 (s, 1H), 8.58 (d, *J* = 1.4 Hz, 1H), 8.27 – 8.20 (m, 2H), 7.89 (dd, *J* = 8.0, 2.0 Hz, 1H), 7.48 (d, *J* = 7.9 Hz, 1H), 7.45 (d, *J* = 6.7 Hz, 1H), 7.31 (t, *J* = 7.8 Hz, 1H), 7.24 (t, *J* = 7.6 Hz, 1H), 7.12 (dd, *J* = 7.5, 1.1 Hz, 1H), 6.98 (dd, *J* = 7.5, 0.9 Hz, 1H), 6.36 (d, *J* = 7.9 Hz, 1H), 5.42 (s, 2H), 4.80 (s, 2H), 4.57 (s, 2H), 3.97 (s, 3H), 2.10 (2d, 6H). <sup>13</sup>C NMR (101 MHz, CDCl<sub>3</sub> + MeOD (20:1)) δ 162.4, 162.0, 160.2, 148.9, 146.9, 142.6, 142.0, 140.4, 140.2, 136.1, 135.7, 134.9, 129.5, 128.2, 126.9, 126.3, 126.2, 125.5, 122.2, 120.9, 120.8, 114.3, 101.2, 66.7, 61.8, 60.0, 53.4, 15.7, 14.4.

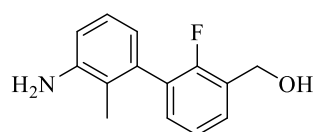
**5-(((2-hydroxyethyl)(methyl)amino)methyl)-N-(3'-(((5-(((2-hydroxyethyl)(methyl)amino)methyl)-3-methoxypyridin-2-yl)oxy)methyl)-2,2'-dimethyl-[1,1'-biphenyl]-3-yl)picolinamide (7.12)**



The compound **7.12** was prepared according to the procedure used for **7.35**.

In the first step, **7.11** (90 mg, 0.18 mmol), anhydrous DCM (5 mL) with addition of anhydrous DMF (0.1 mL), and thionyl chloride (0.11 mL, 1.93 mmol) were used. The product from the first step was treated with 2-(methylamino)ethan-1-ol (144 μL, 1.80 mmol), DIPEA (0.27 mL, 1.44 mmol) and anhydrous DMF (5 mL). A brown oil **7.12** (61 mg, yield: 55%) was obtained as the product. <sup>1</sup>H NMR (400 MHz, CDCl<sub>3</sub>) δ 10.13 (s, 1H), 8.56 (d, *J* = 1.5 Hz, 1H), 8.28 (t, *J* = 7.3 Hz, 2H), 7.86 (dd, *J* = 8.0, 1.9 Hz, 1H), 7.45 (d, *J* = 7.8 Hz, 2H), 7.31 (t, *J* = 7.9 Hz, 1H), 7.23 (d, *J* = 7.6 Hz, 1H), 7.12 (d, *J* = 6.8 Hz, 1H), 6.98 (d, *J* = 6.9 Hz, 1H), 6.36 (d, *J* = 7.9 Hz, 1H), 5.42 (s, 2H), 3.95 (s, 3H), 3.73 – 3.61 (m, 6H), 3.50 (s, 2H), 2.72 – 2.59 (m, 4H), 2.26 (s, 3H), 2.24 (s, 3H), 2.14 – 2.06 (2s, 6H). <sup>13</sup>C NMR (101 MHz, CDCl<sub>3</sub>) δ 162.1, 161.9, 160.9, 149.4, 148.8, 142.6, 142.5, 142.2, 138.2, 137.5, 136.1, 135.8, 135.1, 129.6, 128.3, 126.6, 126.3, 126.2, 125.6, 122.3, 120.7, 111.2, 101.3, 66.7, 59.5, 58.8, 58.7, 58.5, 58.5, 55.0, 53.5, 41.8, 41.7, 15.8, 14.5. UPLC–MS (DAD/ESI): *t*<sub>R</sub> = 5.70 min, for C<sub>35</sub>H<sub>43</sub>N<sub>5</sub>O<sub>5</sub> [M + H]<sup>+</sup> found: 614.45, *m/z*; calc. mass: 614.33. HRMS ESI-MS-q-TOF for C<sub>35</sub>H<sub>43</sub>N<sub>5</sub>O<sub>5</sub> [M + H]<sup>+</sup> found: 614.3336 *m/z*; calc. mass: 614.3342.

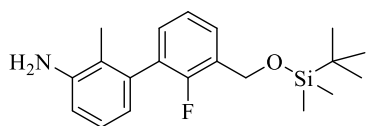
**(3'-amino-2-fluoro-2'-methyl-[1,1'-biphenyl]-3-yl)methanol (7.13)**



Compound **7.13** was prepared following the procedure for **7.6**. Preparation involved the use of **5.1** (1200 mg, 5.15 mmol), (3-bromo-2-fluorophenyl)methanol (880 mg, 4.29 mmol), potassium carbonate (1777 mg, 12.88 mmol), which were stirred in mixture of deoxygenated dioxane and water

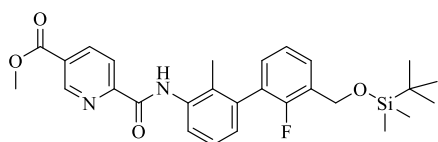
(40:20 mL, v:v) at 85°C after addition of Pd(dppf)Cl<sub>2</sub>·DCM complex (175 mg, 0.21 mmol). The crude product was purified by column chromatography (silica gel, 0–100% AcOEt in hexane) and yielded **7.13** (729 mg, 74%) as a colorless solid. <sup>1</sup>H NMR (600 MHz, CDCl<sub>3</sub>) δ 7.44 – 7.40 (m, 1H), 7.22 – 7.18 (m, 2H), 7.09 (t, *J* = 7.7 Hz, 1H), 6.74 (d, *J* = 7.9 Hz, 1H), 6.68 (d, *J* = 7.5 Hz, 1H), 4.81 (s, 2H), 1.99 (d, *J* = 1.4 Hz, 3H). <sup>13</sup>C NMR (101 MHz, CDCl<sub>3</sub>) δ 157.5 (d, <sup>1</sup>*J*<sub>C-F</sub> = 246.0 Hz), 144.8, 136.5, 131.2 (d, *J*<sub>C-F</sub> = 4.2 Hz), 129.7 (d, <sup>2</sup>*J*<sub>C-F</sub> = 17.0 Hz), 128.3 (d, *J*<sub>C-F</sub> = 4.7 Hz), 128.0 (d, <sup>2</sup>*J*<sub>C-F</sub> = 15.9 Hz), 126.3, 124.0 (d, *J*<sub>C-F</sub> = 4.4 Hz), 121.2, 120.9, 114.9, 59.7 (d, <sup>2</sup>*J*<sub>C-F</sub> = 5.2 Hz), 14.4 (d, <sup>4</sup>*J*<sub>C-F</sub> = 2.7 Hz).

**3'-(((tert-butyldimethylsilyloxy)methyl)-2'-fluoro-2-methyl-[1,1'-biphenyl]-3-amine (7.14)**



Compound **7.14** was prepared following the procedure for **7.7**. Preparation involved the use of **7.6** (700 mg, 3.03 mmol), TBDMSCl (685 mg, 4.55 mmol) and imidazole (304 mg, 4.55 mmol), which were stirred overnight in anhydrous DCM (46 mL). The crude product was purified by column chromatography (silica gel, 0–100% AcOEt in hexane) and yielded **7.14** (987 mg, 92%) as a colorless solid. <sup>1</sup>H NMR (600 MHz, CDCl<sub>3</sub>) δ 7.50 (td, *J* = 7.5, 1.9 Hz, 1H), 7.19 (t, *J* = 7.5 Hz, 1H), 7.15 (td, *J* = 7.3, 1.9 Hz, 1H), 7.09 (t, *J* = 7.7 Hz, 1H), 6.76 (dd, *J* = 7.9, 0.9 Hz, 1H), 6.70 (dd, *J* = 7.5, 0.8 Hz, 1H), 4.85 (d, *J* = 17.1 Hz, 2H), 3.96 (brs, 2H), 2.00 (d, *J* = 1.4 Hz, 3H), 0.97 (s, 9H), 0.14 (s, 6H). <sup>13</sup>C NMR (151 MHz, CDCl<sub>3</sub>) δ 156.7 (d, <sup>1</sup>*J*<sub>C-F</sub> = 245.3 Hz), 144.4, 136.8, 130.3 (d, *J*<sub>C-F</sub> = 3.4 Hz), 129.1 (d, *J*<sub>C-F</sub> = 16.7 Hz), 128.7 (d, *J*<sub>C-F</sub> = 15.4 Hz), 127.4 (d, *J*<sub>C-F</sub> = 4.4 Hz), 126.3, 123.8 (d, *J*<sub>C-F</sub> = 3.8 Hz), 121.6, 121.2, 115.0, 59.3 (d, *J*<sub>C-F</sub> = 5.5 Hz), 26.1, 18.6, 14.4, -5.2.

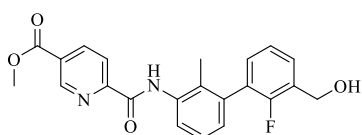
**methyl 6-((3'-(((tert-butyldimethylsilyloxy)methyl)-2'-fluoro-2-methyl-[1,1'-biphenyl]-3-yl)carbamoyl)nicotinate (7.15)**



Compound **7.15** was prepared following the procedure for **7.8**. In the first step 5-(methoxycarbonyl)picolinic acid (506 mg, 2.80 mmol) was refluxed in the mixture of SOCl<sub>2</sub> (9.40 mL) and anhydrous toluene (9.40 mL). After isolation of acid chloride, **7.14** (968 mg, 2.80 mmol) dissolved in anhydrous THF (33 mL) and TEA (1.85 mL, 14.38 mmol) were added dropwise. The crude product was purified by column chromatography (silica gel, 0–100% AcOEt in hexane) and yielded **7.15** (1207 mg, 85%) as a colorless solid. <sup>1</sup>H NMR (600 MHz, CDCl<sub>3</sub>) δ 10.15 (s, 1H), 9.23 (d, *J* = 1.3 Hz, 1H), 8.51 (dd, *J* = 8.1, 2.0 Hz, 1H), 8.41 (d, *J* = 8.1

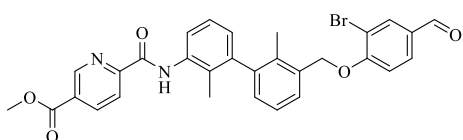
Hz, 1H), 8.30 (d,  $J = 8.1$  Hz, 1H), 7.53 (t,  $J = 6.5$  Hz, 1H), 7.34 (t,  $J = 7.9$  Hz, 1H), 7.22 (t,  $J = 7.5$  Hz, 1H), 7.20 – 7.13 (m, 1H), 7.09 (d,  $J = 7.5$  Hz, 1H), 4.86 (d,  $J = 16.8$  Hz, 2H), 4.00 (s, 3H), 2.23 (s,  $J = 39.2$  Hz, 3H), 0.97 (s, 9H), 0.14 (s, 6H).  $^{13}\text{C}$  NMR (151 MHz,  $\text{CDCl}_3$ )  $\delta$  165.1, 161.2, 156.6 (d,  $J_{\text{C-F}} = 245.8$  Hz), 153.2, 149.6, 139.0, 136.9, 135.9, 130.2 (d,  $J_{\text{C-F}} = 2.7$  Hz), 128.9 (d,  $J_{\text{C-F}} = 15.1$  Hz), 128.5 (d,  $J_{\text{C-F}} = 16.4$  Hz), 128.4, 127.8 (d,  $J_{\text{C-F}} = 4.3$  Hz), 127.5, 127.1, 126.4, 124.0 (d,  $J_{\text{C-F}} = 3.4$  Hz), 122.2, 121.5, 59.3 (d,  $J_{\text{C-F}} = 5.3$  Hz), 52.8, 26.1, 18.6, 14.8, -5.2.

**methyl 6-((2'-fluoro-3'-(hydroxymethyl)-2-methyl-[1,1'-biphenyl]-3-yl)carbamoyl)nicotinate (7.16)**



Compound **7.16** was prepared following the procedure for **7.9**. Preparation involved the use of **7.15** (1207 mg, 2.37 mmol) dissolved in anhydrous DCM (38 mL) and addition of HCl in dioxane (4 M, 3.96 mL). The crude product was purified by column chromatography (silica gel, 0–100% AcOEt in hexane) and yielded **7.16** (758 mg, 81%) as a colorless solid.  $^1\text{H}$  NMR (600 MHz,  $\text{CDCl}_3$ )  $\delta$  10.14 (s, 1H), 9.22 (s, 1H), 8.51 (d,  $J = 7.2$  Hz, 1H), 8.39 (d,  $J = 7.7$  Hz, 1H), 8.28 (d,  $J = 8.0$  Hz, 1H), 7.53 – 7.44 (m, 1H), 7.33 (t,  $J = 7.8$  Hz, 1H), 7.24 – 7.18 (m, 2H), 7.08 (d,  $J = 7.5$  Hz, 1H), 4.82 (s, 2H), 3.99 (s, 3H), 2.23 (s, 3H).  $^{13}\text{C}$  NMR (151 MHz,  $\text{CDCl}_3$ )  $\delta$  165.1, 161.2, 157.4 (d,  $J_{\text{C-F}} = 246.2$  Hz), 153.1, 149.5, 139.1, 136.7, 135.9, 131.1 (d,  $J_{\text{C-F}} = 2.6$  Hz), 129.0 (d,  $J_{\text{C-F}} = 16.8$  Hz), 128.7 (d,  $J_{\text{C-F}} = 3.8$  Hz), 128.3 (d,  $J_{\text{C-F}} = 15.3$  Hz), 128.5, 127.5, 127.1, 126.4, 124.2 (d,  $J_{\text{C-F}} = 3.4$  Hz), 122.2, 121.7, 59.6 (d,  $J_{\text{C-F}} = 4.3$  Hz), 52.9, 14.9.

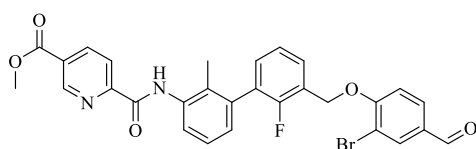
**methyl 6-((3'-((2-bromo-4-formylphenoxy)methyl)-2,2'-dimethyl-[1,1'-biphenyl]-3-yl)carbamoyl)nicotinate (7.17)**



**7.9** (430 mg, 1.10 mmol) was dissolved in dry DCM (11 mL) with catalytic amount of anhydrous DMF (0.3 mL) and it was cooled to 0 °C. Then  $\text{SOCl}_2$  (1.26 mL, 17.36 mmol) was added portionwise. After 2 hours,  $\text{NaHCO}_3$  (40 mL) was added and it was washed with DCM (2 x 40 mL). Organic layers were extracted with water (50 mL), combined, dried over anhydrous  $\text{MgSO}_4$ , filtered, and concentrated under reduced pressure. After drying of the product,  $\text{K}_2\text{CO}_3$  (455 g, 3.41 mmol), 3-bromo-4-hydroxybenzaldehyde (334 g, 1.66 mmol) and anhydrous DMF (11 mL) were added and resulted mixture was stirred overnight at room temperature. Afterwards, mixture was concentrated under reduced pressure, water was added (50 mL) and it was extracted with ethyl acetate (2 x 50 mL). The organic layers were combined,

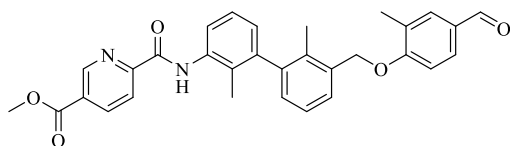
dried over anhydrous MgSO<sub>4</sub>, filtered, and concentrated. The crude product was purified by flash chromatography (silica gel, 0-100% AcOEt in hexane). The product was obtained as a colorless solid (486 mg, 77%). <sup>1</sup>H NMR (400 MHz, CDCl<sub>3</sub>) δ 10.14 (s, 1H), 9.85 (s, 1H), 9.22 (d, *J* = 1.4 Hz, 1H), 8.51 (dd, *J* = 8.1, 2.0 Hz, 1H), 8.40 (dd, *J* = 8.2, 0.5 Hz, 1H), 8.28 (d, *J* = 7.4 Hz, 1H), 8.11 (d, *J* = 2.0 Hz, 1H), 7.83 (dd, *J* = 8.5, 2.0 Hz, 1H), 7.54 (d, *J* = 7.1 Hz, 1H), 7.37 – 7.27 (m, 2H), 7.17 (dd, *J* = 7.5, 0.9 Hz, 1H), 7.14 (d, *J* = 8.5 Hz, 1H), 7.01 (dd, *J* = 7.5, 0.9 Hz, 1H), 5.27 (d, *J* = 3.3 Hz, 2H), 3.99 (s, 3H), 2.11 (s, 3H), 2.10 (s, 3H). <sup>13</sup>C NMR (101 MHz, CDCl<sub>3</sub>) δ 189.7, 165.1, 161.1, 159.9, 153.1, 149.5, 142.3, 142.3, 139.0, 135.8, 134.8, 134.6, 133.8, 131.2, 131.0, 130.0, 128.4, 127.5, 126.7, 126.4, 125.9, 122.2, 120.8, 113.3, 112.9, 70.2, 52.9, 15.8, 14.4.

**methyl 6-((3'-((2-bromo-4-formylphenoxy)methyl)-2'-fluoro-2-methyl-[1,1'-biphenyl]-3-yl)carbamoyl)nicotinate (7.18)**



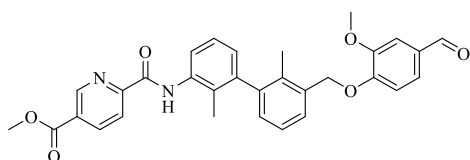
Compound **7.18** was prepared following the procedure for **7.17**. In the first step **7.9** (430 mg, 1.09 mmol), anhydrous DCM (11 mL) with addition of anhydrous DMF (0.1 mL), and thionyl chloride (1.32 mL, 17.22 mmol) were used. The product from the first step was treated with 4-hydroxy-3-methoxybenzaldehyde (331 mg, 2.17 mmol), and potassium carbonate (506 mg, 3.67 mmol), which were stirred in anhydrous DMF (11 mL) at room temperature overnight. The crude product was precipitated from AcOEt and yielded **7.18** (476 mg, 76%) as a colorless solid. <sup>1</sup>H NMR (600 MHz, CDCl<sub>3</sub>) δ 10.16 (s, 1H), 9.85 (s, 1H), 9.23 (dd, *J* = 2.0, 0.7 Hz, 1H), 8.52 (dd, *J* = 8.1, 2.0 Hz, 1H), 8.40 (dd, *J* = 8.1, 0.7 Hz, 1H), 8.33 – 8.29 (m, 1H), 8.12 (d, *J* = 2.0 Hz, 1H), 7.82 (dd, *J* = 8.5, 2.0 Hz, 1H), 7.69 – 7.63 (m, 1H), 7.36 (t, *J* = 7.9 Hz, 1H), 7.31 – 7.27 (m, 2H), 7.13 (d, *J* = 8.5 Hz, 1H), 7.10 (dd, *J* = 7.5, 0.8 Hz, 1H), 5.37 (d, *J* = 19.4 Hz, 2H), 4.00 (s, 3H), 2.25 (s, 3H). <sup>13</sup>C NMR (151 MHz, CDCl<sub>3</sub>) δ 189.7, 165.1, 161.2, 159.6, 157.0 (d, *J*<sub>C-F</sub> = 247.1 Hz), 153.1, 149.6, 139.1, 136.3, 135.97, 134.8, 131.8 (d, *J*<sub>C-F</sub> = 2.6 Hz), 131.2, 131.2, 129.2 (d, *J*<sub>C-F</sub> = 16.6 Hz), 128.6 (d, *J*<sub>C-F</sub> = 2.2 Hz), 128.5, 127.5, 127.0, 126.6, 124.6 (d, *J*<sub>C-F</sub> = 3.2 Hz), 123.1 (d, *J*<sub>C-F</sub> = 14.9 Hz), 122.2, 121.8, 113.4, 113.0, 65.1 (d, *J*<sub>C-F</sub> = 5.0 Hz), 52.9, 14.9.

**methyl 6-((3'-((4-formyl-2-methylphenoxy)methyl)-2,2'-dimethyl-[1,1'-biphenyl]-3-yl) carbamoyl)nicotinate (7.19)**



Compound **7.19** was prepared following the procedure for **7.17**. In the first step **7.9** (300 mg, 0.77 mmol), anhydrous DCM (8 mL) with addition of anhydrous DMF (0.1 mL), and thionyl chloride (0.99 mL, 13.64 mmol) were used. The product from the first step was treated with 4-hydroxy-3-methylbenzaldehyde (209 mg, 1.54 mmol), and potassium carbonate (318 mg, 2.31 mmol), which were stirred in anhydrous DMF (8 mL) at room temperature overnight. The crude product was purified by column chromatography (silica gel, 0–100% AcOEt in hexane) and yielded **7.19** (279 mg, 71%) as a colorless solid. <sup>1</sup>H NMR (600 MHz, CDCl<sub>3</sub>) δ 10.14 (s, 1H), 9.87 (s, 1H), 9.22 (dd, *J* = 2.0, 0.7 Hz, 1H), 8.52 (dd, *J* = 8.1, 2.0 Hz, 1H), 8.41 (dd, *J* = 8.1, 0.7 Hz, 1H), 8.28 (dd, *J* = 8.1, 0.8 Hz, 1H), 7.75 – 7.70 (m, 2H), 7.48 (d, *J* = 7.1 Hz, 1H), 7.34 (t, *J* = 7.8 Hz, 1H), 7.30 (t, *J* = 7.6 Hz, 1H), 7.17 (dd, *J* = 7.5, 0.9 Hz, 1H), 7.07 (d, *J* = 8.1 Hz, 1H), 7.02 (dd, *J* = 7.5, 1.0 Hz, 1H), 5.25 – 5.17 (m, 2H), 4.00 (s, 3H), 2.33 (s, 3H), 2.12 (s, 3H), 2.09 (s, 3H). <sup>13</sup>C NMR (151 MHz, CDCl<sub>3</sub>) δ 191.2, 165.1, 162.1, 161.2, 153.1, 149.5, 142.5, 142.3, 139.1, 135.9, 134.7, 134.6, 131.8, 130.7, 129.9, 129.8, 128.4, 128.1, 127.5, 126.8, 126.5, 125.8, 122.2, 120.9, 111.0, 69.2, 52.9, 16.5, 15.7, 14.5.

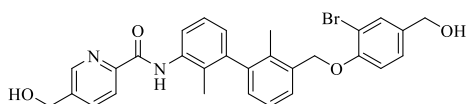
**methyl 6-((3'-((4-formyl-2-methoxyphenoxy)methyl)-2,2'-dimethyl-[1,1'-biphenyl]-3-yl) carbamoyl)nicotinate (7.20)**



Compound **7.20** was prepared following the procedure for **7.17**. In the first step **7.9** (400 mg, 1.03 mmol), anhydrous DCM (11 mL) with addition of anhydrous DMF (0.1 mL), and thionyl chloride (1.32 mL, 18.18 mmol) were used. The product from the first step was treated with 4-hydroxy-3-methoxybenzaldehyde (312 mg, 2.05 mmol), and potassium carbonate (425 mg, 3.08 mmol), which were stirred in anhydrous DMF (11 mL) at room temperature overnight. The crude product was purified by column chromatography (silica gel, 0–100% AcOEt in hexane) and yielded **7.20** (472 mg, 88%) as a colorless solid. <sup>1</sup>H NMR (600 MHz, CDCl<sub>3</sub>) δ 10.14 (s, 1H), 9.86 (s, 1H), 9.22 (d, *J* = 1.3 Hz, 1H), 8.51 (dd, *J* = 8.1, 2.0 Hz, 1H), 8.41 (d, *J* = 8.1 Hz, 1H), 8.27 (d, *J* = 7.7 Hz, 1H), 7.49 – 7.41 (m, 3H), 7.33 (t, *J* = 7.8 Hz, 1H), 7.26 (t, *J* = 7.6 Hz, 1H), 7.14 (d, *J* = 6.9 Hz, 1H), 7.07 (d, *J* = 8.6 Hz, 1H), 7.01 (d, *J* = 6.8 Hz, 1H), 5.26 (s, 2H), 4.00 (s, 3H), 3.94 (s, 3H), 2.11 (s, 3H), 2.09 (s, 3H). <sup>13</sup>C NMR (151 MHz, CDCl<sub>3</sub>) δ 191.0, 165.1, 161.2, 153.9, 153.2, 150.4, 149.5, 142.5, 142.2, 139.1, 135.8,

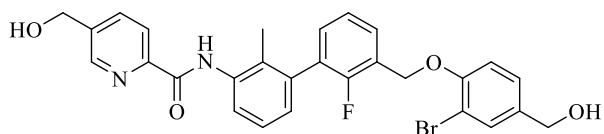
134.6, 134.4, 130.5, 129.9, 128.4, 127.7, 126.8, 126.7, 126.5, 126.4, 125.8, 122.2, 120.9, 112.6, 109.6, 70.0, 56.2, 52.9, 15.7, 14.5.

**N-(3'-((2-bromo-4-(hydroxymethyl)phenoxy)methyl)-2,2'-dimethyl-[1,1'-biphenyl]-3-yl)-5-(hydroxymethyl)picolinamide (7.21)**



**7.17** (486 mg, 0.85 mmol) was placed in the dry, two-neck, round bottom flask under argon. Then, anhydrous THF (38 mL) and MeOH (19 mL) were added, and followingly LiBH<sub>4</sub> 2M solution in THF (4.26 mL, 8.48 mmol) was added dropwise. Reaction mixture was stirred for 2 hours at room temperature. After, that time reaction was quenched, water (50 mL) was added and the mixture was extracted with AcOEt (2 x 50 mL). The organic layers were combined, dried over anhydrous MgSO<sub>4</sub>, filtered, and concentrated under reduced pressure. The crude product was purified by flash chromatography (silica gel, 0-100% AcOEt in hexane) to give **7.21** as a colorless solid (330 mg, 71%). <sup>1</sup>H NMR (400 MHz, DMSO) δ 10.34 (s, 1H), 8.66 (s, 1H), 8.16 (d, *J* = 7.9 Hz, 1H), 8.00 (d, *J* = 8.0 Hz, 1H), 7.92 – 7.82 (m, 1H), 7.58 – 7.49 (m, 2H), 7.36 – 7.23 (m, 4H), 7.11 (d, *J* = 7.6 Hz, 1H), 6.97 (d, *J* = 7.5 Hz, 1H), 5.54 (t, *J* = 4.7 Hz, 1H), 5.24 (m, 3H), 4.67 (d, *J* = 5.2 Hz, 2H), 4.44 (d, *J* = 5.3 Hz, 2H), 2.07 (s, 3H), 2.00 (s, 3H). <sup>13</sup>C NMR (101 MHz, DMSO) δ 162.1, 153.2, 148.3, 146.9, 142.0, 141.6, 141.4, 136.7, 136.2, 136.0, 135.1, 134.4, 131.2, 129.1, 128.7, 127.4, 127.1, 126.1, 125.8, 125.5, 122.5, 121.9, 113.9, 110.9, 69.2, 61.8, 60.4, 15.3, 14.5.

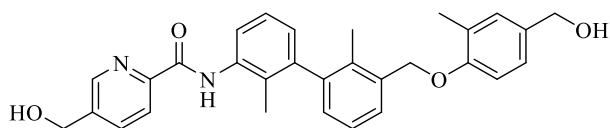
**N-(3'-((2-bromo-4-(hydroxymethyl)phenoxy)methyl)-2'-fluoro-2-methyl-[1,1'-biphenyl]-3-yl)-5-(hydroxymethyl)picolinamide (7.22)**



Compound **7.22** was prepared following the procedure for **7.21**. **7.18** (334 mg, 0.58 mmol), LiBH<sub>4</sub> 2M solution in THF (2.90 mL, 5.79 mmol) and mixture of anhydrous THF/MeOH (26:13 mL, v:v) were used to obtain compound **7.22** as a colorless foam (147 mg, yield: 46%). <sup>1</sup>H NMR (600 MHz, DMSO) δ 10.39 (s, 1H), 8.68 (d, *J* = 1.3 Hz, 1H), 8.16 (d, *J* = 8.0 Hz, 1H), 8.00 (dd, *J* = 8.0, 2.0 Hz, 1H), 7.86 (d, *J* = 7.8 Hz, 1H), 7.65 (td, *J* = 6.8, 2.6 Hz, 1H), 7.54 (d, *J* = 1.9 Hz, 1H), 7.41 – 7.32 (m, 3H), 7.29 (dd, *J* = 8.4, 1.9 Hz, 1H), 7.24 (d, *J* = 8.5 Hz, 1H), 7.13 (d, *J* = 7.0 Hz, 1H), 5.53 (t, *J* = 5.7 Hz, 1H), 5.30 (s, 2H), 5.22 (t, *J* = 5.8 Hz, 1H), 4.67 (d, *J* = 5.6 Hz, 2H), 4.43 (d, *J* = 5.8 Hz, 2H), 2.11 (s, 3H). <sup>13</sup>C NMR (151 MHz, DMSO) δ 162.3, 156.9 (d, <sup>1</sup>*J*<sub>C-F</sub> = 247.0 Hz), 153.0, 148.3, 146.9, 141.4, 137.1, 136.4, 135.9, 135.8, 131.6, 131.1, 129.6, 129.5, 128.5 (d, <sup>2</sup>*J*<sub>C-F</sub> = 16.3 Hz),

127.0, 127.0, 125.9, 124.5 (d,  $^3J_{C-F} = 2.9$  Hz), 124.0 (d,  $^2J_{C-F} = 15.4$  Hz), 123.8, 121.9, 114.1, 111.1, 64.7 (d,  $^3J_{C-F} = 3.0$  Hz), 61.8, 60.4, 14.8.

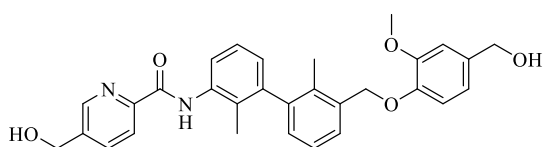
**5-(hydroxymethyl)-N-(3'-((4-(hydroxymethyl)-2-methylphenoxy)methyl)-2,2'-dimethyl-[1,1'-biphenyl]-3-yl)picolinamide (7.23)**



Compound **7.23** was prepared following the procedure for **7.21**. **7.19** (250 mg, 0.49 mmol), LiBH<sub>4</sub> 2M solution in THF (2.47 mL,

4.91 mmol) and mixture of anhydrous THF/MeOH (22:11 mL, v:v) were used to obtain compound **7.23** as a colorless foam (236 mg, yield: 99%). <sup>1</sup>H NMR (600 MHz, DMSO) δ 10.34 (s, 1H), 8.66 (d,  $J = 1.3$  Hz, 1H), 8.15 (d,  $J = 8.0$  Hz, 1H), 7.99 (dd,  $J = 8.0, 1.9$  Hz, 1H), 7.87 (d,  $J = 7.9$  Hz, 1H), 7.50 (d,  $J = 7.5$  Hz, 1H), 7.33 – 7.26 (m, 2H), 7.14 – 7.07 (m, 3H), 7.04 (d,  $J = 9.0$  Hz, 1H), 6.98 (d,  $J = 7.4$  Hz, 1H), 5.14 (s, 2H), 4.66 (d,  $J = 2.8$  Hz, 2H), 4.39 (s, 2H), 2.19 (s, 3H), 2.04 (s, 3H), 1.99 (s, 3H). <sup>13</sup>C NMR (151 MHz, DMSO) δ 162.1, 155.3, 148.4, 146.9, 142.0, 141.5, 141.4, 136.2, 136.0, 135.8, 134.4, 134.2, 129.2, 128.9, 128.7, 127.3, 126.1, 125.8, 125.5, 125.5, 125.2, 122.5, 121.9, 111.4, 68.27, 62.65, 60.37, 16.13, 15.22, 14.49.

**5-(hydroxymethyl)-N-(3'-((4-(hydroxymethyl)-2-methoxyphenoxy)methyl)-2,2'-dimethyl-[1,1'-biphenyl]-3-yl)picolinamide (7.24)**

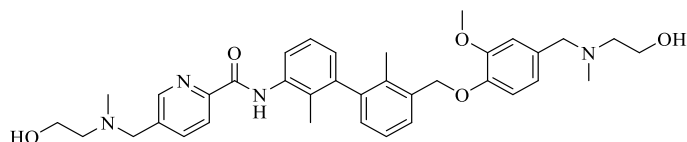


Compound **7.24** was prepared following the procedure for **7.21**. **7.20** (440 mg, 0.84 mmol), LiBH<sub>4</sub> 2M solution in THF (4.21 mL, 8.38 mmol)

and mixture of anhydrous THF/MeOH (38:19 mL, v:v) were used to obtain compound **7.24** as a colorless foam (344 mg, yield: 82%). <sup>1</sup>H NMR (600 MHz, CDCl<sub>3</sub>) δ 10.13 (s, 1H), 8.57 (d,  $J = 1.4$  Hz, 1H), 8.23 (t,  $J = 7.4$  Hz, 2H), 7.88 (dd,  $J = 8.0, 1.9$  Hz, 1H), 7.46 (d,  $J = 7.1$  Hz, 1H), 7.31 (t,  $J = 7.8$  Hz, 1H), 7.23 (t,  $J = 7.6$  Hz, 1H), 7.11 (dd,  $J = 7.5, 0.9$  Hz, 1H), 6.99 (dd,  $J = 7.5, 0.9$  Hz, 1H), 6.96 (d,  $J = 1.8$  Hz, 1H), 6.91 (d,  $J = 8.1$  Hz, 1H), 6.85 (dd,  $J = 8.1, 1.9$  Hz, 1H), 5.14 (s, 2H), 4.79 (s, 2H), 4.62 (s, 2H), 3.88 (s, 3H), 2.09 (s, 3H), 2.08 (s, 3H). <sup>13</sup>C NMR (151 MHz, CDCl<sub>3</sub>) δ 162.2, 150.2, 149.2, 147.9, 146.8, 142.7, 142.0, 139.7, 136.2, 135.9, 135.4, 134.6, 134.6, 129.6, 127.8, 126.9, 126.4, 126.3, 125.7, 122.4, 120.8, 119.5, 114.5, 111.2, 70.35, 65.36, 62.38, 56.08, 15.67, 14.54.



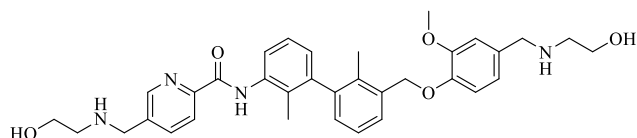
**5-(((2-hydroxyethyl)(methyl)amino)methyl)-N-(3'-((4-(((2-hydroxyethyl)(methyl)amino)methyl)-2-methoxyphenoxy)methyl)-2,2'-dimethyl-[1,1'-biphenyl]-3-yl)picolinamide (7.25)**



The compound **7.25** was prepared according to the procedure used for **7.35**. In the first step, **7.24** (93 mg,

0.19 mmol), anhydrous DCM (5 mL) with addition of anhydrous DMF (0.1 mL), and thionyl chloride (0.12 mL, 2.43 mmol) were used. The product from the first step was treated with 2-(methylamino)ethan-1-ol (92  $\mu$ L, 1.14 mmol), DIPEA (0.17 mL, 0.91 mmol) and anhydrous DMF (5 mL). A colorless precipitate **7.25** (71.8 mg, yield: 61%) was obtained as the product.  $^1\text{H}$  NMR (400 MHz,  $\text{CDCl}_3$ )  $\delta$  10.13 (s, 1H), 8.56 (d,  $J = 1.3$  Hz, 1H), 8.28 (t,  $J = 6.9$  Hz, 2H), 7.86 (dd,  $J = 8.0, 1.9$  Hz, 1H), 7.46 (d,  $J = 7.6$  Hz, 1H), 7.31 (t,  $J = 7.9$  Hz, 1H), 7.23 (t,  $J = 7.6$  Hz, 1H), 7.11 (d,  $J = 7.6$  Hz, 1H), 6.98 (d,  $J = 7.7$  Hz, 2H), 6.90 (d,  $J = 8.1$  Hz, 1H), 6.82 (dd,  $J = 8.1, 1.7$  Hz, 1H), 5.15 (s, 2H), 3.89 (s, 3H), 3.75 – 3.60 (m, 8H), 2.71 (t,  $J = 5.2$  Hz, 2H), 2.64 (t,  $J = 5.3$  Hz, 2H), 2.36 (s, 3H), 2.26 (s, 3H), 2.10 (s, 3H), 2.08 (s, 3H).  $^{13}\text{C}$  NMR (101 MHz,  $\text{CDCl}_3$ )  $\delta$  162.1, 150.1, 149.4, 148.8, 148.1, 142.6, 142.1, 138.2, 137.5, 136.1, 135.3, 134.6, 129.6, 127.7, 126.7, 126.3, 126.2, 125.6, 122.3, 121.7, 120.6, 114.2, 113.1, 70.3, 62.1, 59.5, 58.8, 58.7, 58.3, 58.1, 56.2, 41.7, 41.5, 15.7, 14.5. UPLC–MS (DAD/ESI):  $t_{\text{R}} = 8.0$  min, for  $\text{C}_{36}\text{H}_{44}\text{N}_4\text{O}_5$   $[\text{M} + \text{H}]^+$  found: 613.50,  $m/z$ ; calc. mass: 613.34. HRMS ESI-MS-q-TOF for  $\text{C}_{36}\text{H}_{44}\text{N}_4\text{O}_5$   $[\text{M} + \text{H}]^+$  found: 613.3383  $m/z$ ; calc. mass: 613.3390.

**5-(((2-hydroxyethyl)amino)methyl)-N-(3'-((4-(((2-hydroxyethyl)amino)methyl)-2-methoxyphenoxy)methyl)-2,2'-dimethyl-[1,1'-biphenyl]-3-yl)picolinamide (7.26)**

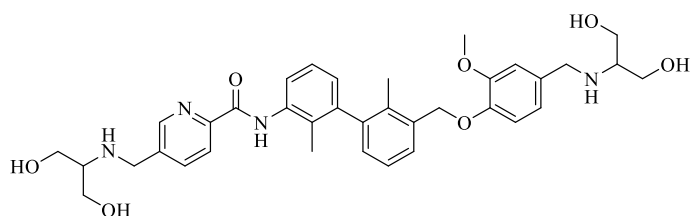


The compound **7.26** was prepared according to the procedure used for **7.35**. In the first step, **7.24** (100 mg, 0.20 mmol),

anhydrous DCM (5 mL) with addition of anhydrous DMF (0.1 mL), and thionyl chloride (0.10 mL, 2.08 mmol) were used. The product from the first step was treated with ethanolamine (122  $\mu$ L, 2.00 mmol), DIPEA (0.30 mL, 1.60 mmol) and anhydrous DMF (5 mL). A colorless precipitate **7.26** (51.9 mg, yield: 44%) was obtained as the product.  $^1\text{H}$  NMR (400 MHz, DMSO)  $\delta$  10.34 (s, 1H), 8.69 (d,  $J = 1.3$  Hz, 1H), 8.14 (d,  $J = 8.0$  Hz, 1H), 8.03 (dd,  $J = 8.0, 1.8$  Hz, 1H), 7.86 (d,  $J = 7.8$  Hz, 1H), 7.46 (d,  $J = 7.3$  Hz, 1H), 7.34 – 7.25 (m, 2H), 7.17 (d,  $J = 1.6$  Hz, 1H), 7.13 – 7.05 (m, 2H), 7.00 – 6.90 (m, 2H), 5.12 (d,  $J = 2.5$  Hz, 2H), 3.88 (s, 4H),

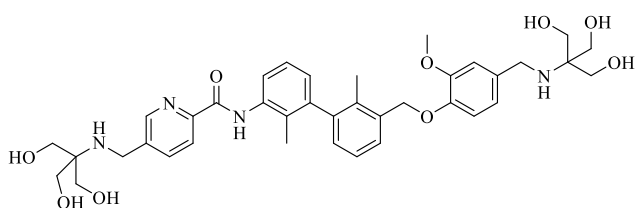
3.78 (s, 3H), 3.58 (t,  $J = 5.5$  Hz, 2H), 3.49 (t,  $J = 5.7$  Hz, 2H), 2.76 (t,  $J = 5.5$  Hz, 2H), 2.61 (t,  $J = 5.7$  Hz, 2H), 2.04 (s, 3H), 1.99 (s, 3H).  $^{13}\text{C}$  NMR (101 MHz, DMSO)  $\delta$  162.2, 149.1, 148.4, 148.3, 147.5, 142.0, 141.5, 139.6, 137.6, 136.3, 135.5, 134.5, 129.2, 128.8, 128.7, 127.9, 126.2, 125.8, 125.5, 122.6, 121.8, 121.5, 113.6, 113.2, 69.1, 60.1, 58.2, 55.6, 51.1, 50.9, 49.7, 49.5, 15.2, 14.6. UPLC–MS (DAD/ESI):  $t_{\text{R}} = 7.8$  min, for  $\text{C}_{34}\text{H}_{40}\text{N}_4\text{O}_5$   $[\text{M} + \text{H}]^+$  found: 585.45,  $m/z$ ; calc. mass: 585.31. HRMS ESI-MS-q-TOF for  $\text{C}_{34}\text{H}_{40}\text{N}_4\text{O}_5$   $[\text{M} + \text{H}]^+$  found: 585.3074  $m/z$ ; calc. mass: 585.3077.

**5-(((1,3-dihydroxypropan-2-yl)amino)methyl)-N-(3'-((4-(((1,3-dihydroxypropan-2-yl)amino)methyl)-2-methoxyphenoxy)methyl)-2,2'-dimethyl-[1,1'-biphenyl]-3-yl)picolinamide (7.27)**



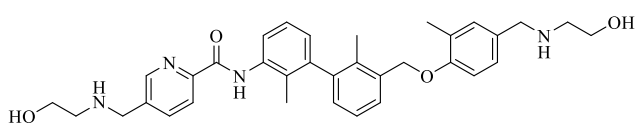
The compound **7.27** was prepared according to the procedure used for **7.35**. In the first step, **7.24** (93 mg, 0.19 mmol), anhydrous DCM (5 mL) with addition of anhydrous DMF (0.1 mL), and thionyl chloride (0.10 mL, 1.92 mmol) were used. The product from the first step was treated with 2-amino-1,3-propanediol (170 mg, 1.86 mmol), DIPEA (0.28 mL, 1.49 mmol) and anhydrous DMF (5 mL). A colorless precipitate **7.27** (30.6 mg, yield: 26%) was obtained as the product.  $^1\text{H}$  NMR (400 MHz, DMSO- $d_6$ )  $\delta$  10.36 (s, 1H), 8.79 (s, 1H), 8.20 – 8.10 (m, 2H), 7.84 (d,  $J = 8.0$  Hz, 1H), 7.47 (d,  $J = 7.5$  Hz, 1H), 7.36 – 7.25 (m, 3H), 7.18 – 7.10 (m, 2H), 7.06 (d,  $J = 8.2$  Hz, 1H), 6.98 (d,  $J = 7.4$  Hz, 1H), 5.25 (brs, 2H), 5.20 – 5.06 (m, 2H), 4.87 (brs, 2H), 4.26 – 4.02 (m, 4H), 3.79 (s, 3H), 3.65 (2s, 4H), 3.60 – 3.48 (m, 4H), 2.97 (t,  $J = 5.0$  Hz, 1H), 2.78 (brs, 1H), 2.04 (s, 3H), 1.99 (s, 3H).  $^{13}\text{C}$  NMR (101 MHz, DMSO- $d_6$ )  $\delta$  162.1, 149.1, 148.8, 148.1, 142.0, 141.5, 138.5, 136.2, 135.4, 134.5, 129.2, 128.9, 127.9, 126.3, 125.8, 125.5, 122.8, 122.6, 121.8, 113.9, 113.4, 79.2, 69.0, 60.2, 59.6, 59.3, 57.6, 55.7, 48.6, 48.2, 46.8, 15.2, 14.6. UPLC–MS (DAD/ESI):  $t_{\text{R}} = 5.59$  min, for  $\text{C}_{36}\text{H}_{44}\text{N}_4\text{O}_7$   $[\text{M} + \text{H}]^+$  found: 645.45  $m/z$ ; calc. mass: 645.33. HRMS ESI-MS-q-TOF for  $\text{C}_{36}\text{H}_{44}\text{N}_4\text{O}_7$   $[\text{M} + \text{H}]^+$  found: 645.3279  $m/z$ ; calc. mass: 645.3288.

**5-(((1,3-dihydroxy-2-(hydroxymethyl)propan-2-yl)amino)methyl)-N-(3'-((4-(((1,3-dihydroxy-2-(hydroxymethyl)propan-2-yl)amino)methyl)-2-methoxyphenoxy)methyl)-2,2'-dimethyl-[1,1'-biphenyl]-3-yl)picolinamide (7.28)**



The compound **7.28** was prepared according to the procedure used for **7.35**. In the first step, **7.24** (80 mg, 0.16 mmol), anhydrous DCM (5 mL) with addition of anhydrous DMF (0.1 mL), and thionyl chloride (0.10 mL, 1.60 mmol) were used. The product from the first step was treated with TRIS (194 mg, 1.60 mmol), DIPEA (0.24 mL, 1.28 mmol) and anhydrous DMF (5 mL). A colorless precipitate **7.28** (39.8 mg, yield: 35%) was obtained as the product. <sup>1</sup>H NMR (400 MHz, DMSO) δ 10.36 (s, 1H), 8.75 (s, 1H), 8.17 – 8.09 (m, 2H), 7.86 (d, *J* = 8.0 Hz, 1H), 7.46 (d, *J* = 7.6 Hz, 1H), 7.39 – 7.27 (m, 2H), 7.24 (d, *J* = 1.5 Hz, 1H), 7.11 (t, *J* = 6.7 Hz, 2H), 7.01 (dd, *J* = 8.3, 1.6 Hz, 1H), 6.97 (d, *J* = 7.6 Hz, 1H), 5.20 – 5.10 (m, 2H), 4.16 – 4.05 (m, 4H), 3.80 (s, 3H), 3.61 (s, 6H), 3.50 (s, 6H), 2.04 (s, 3H), 1.99 (s, 3H). <sup>13</sup>C NMR (101 MHz, DMSO) δ 162.1, 149.1, 148.9, 148.6, 148.0, 142.0, 141.5, 138.5, 136.2, 135.5, 134.5, 129.2, 128.8, 127.9, 126.2, 125.8, 125.5, 122.7, 122.6, 121.7, 114.2, 113.4, 69.0, 65.5, 59.9, 57.9, 55.7, 45.3, 42.8, 29.0, 15.2, 14.6. UPLC–MS (DAD/ESI): *t<sub>R</sub>* = 4.82 min, for C<sub>38</sub>H<sub>48</sub>N<sub>4</sub>O<sub>9</sub> [M - H]<sup>+</sup> found: 703.26 *m/z*; calc. mass: 703.33. HRMS ESI-MS-q-TOF for C<sub>38</sub>H<sub>48</sub>N<sub>4</sub>O<sub>9</sub> [M + H]<sup>+</sup> found: 705.3495 *m/z*; calc. mass: 705.3499.

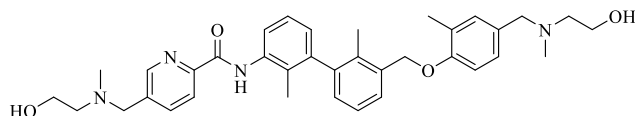
**5-(((2-hydroxyethyl)amino)methyl)-N-(3'-((4-(((2-hydroxyethyl)amino)methyl)-2-methylphenoxy)methyl)-2,2'-dimethyl-[1,1'-biphenyl]-3-yl)picolinamide (7.29)**



The compound **7.29** was prepared according to the procedure used for **7.35**. In the first step, **7.23** (100 mg, 0.21 mmol), anhydrous DCM (5 mL) with addition of anhydrous DMF (0.1 mL), and thionyl chloride (0.12 mL, 2.28 mmol) were used. The product from the first step was treated with ethanolamine (127 μL, 2.07 mmol), DIPEA (0.31 mL, 1.66 mmol) and anhydrous DMF (5 mL). A colorless precipitate **7.29** (68.9 mg, yield: 58%) was obtained as the product. <sup>1</sup>H NMR (400 MHz, DMSO) δ 10.34 (s, 1H), 8.67 (d, *J* = 1.4 Hz, 1H), 8.13 (d, *J* = 8.0 Hz, 1H), 8.01 (dd, *J* = 8.0, 2.0 Hz, 1H), 7.87 (d, *J* = 7.2 Hz, 1H), 7.50 (d, *J* = 6.9 Hz, 1H), 7.36 – 7.26 (m, 2H), 7.19 – 7.13 (m, 2H), 7.13 – 7.03 (m, 2H), 6.98 (dd, *J* = 7.6, 1.0 Hz, 1H), 5.15 (s, 2H), 4.64 (brs, 1H), 4.52 (brs, 1H), 3.85 (s, 2H), 3.71 (s, 2H), 3.52 – 3.44 (m, 4H), 2.64 (t, *J* = 5.7 Hz, 2H), 2.58 (t, *J* = 5.8 Hz, 2H), 2.19 (s, 3H), 2.04 (s, 3H), 1.99 (s, 3H). <sup>13</sup>C NMR (101 MHz, DMSO-*d*<sub>6</sub>) δ 162.1,

156.3, 148.5, 148.3, 142.0, 141.6, 139.4, 137.7, 136.3, 135.7, 134.3, 131.8, 129.0, 128.7, 128.3, 127.3, 126.9, 126.1, 125.8, 125.6, 122.5, 121.8, 111.6, 68.3, 60.0, 57.8, 50.8, 50.6, 49.7, 49.2, 16.1, 15.3, 14.5. UPLC–MS (DAD/ESI):  $t_R = 5.70$  min, for  $C_{34}H_{40}N_4O_4$   $[M + H]^+$  found: 569.40  $m/z$ ; calc. mass: 569.31. HRMS ESI-MS-q-TOF for  $C_{34}H_{40}N_4O_4$   $[M + H]^+$  found: 569.3121  $m/z$ ; calc. mass: 569.3128.

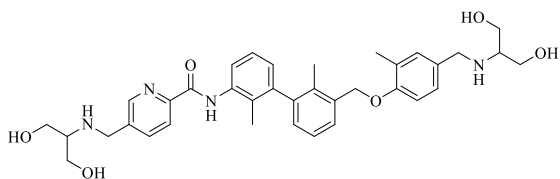
**5-(((2-hydroxyethyl)(methyl)amino)methyl)-N-(3'-((4-(((2-hydroxyethyl)(methyl)amino)methyl)-2-methylphenoxy)methyl)-2,2'-dimethyl-[1,1'-biphenyl]-3-yl)picolinamide (7.30)**



The compound **7.30** was prepared according to the procedure used for **7.35**.

In the first step, **7.23** (80 mg, 0.17 mmol), anhydrous DCM (5 mL) with addition of anhydrous DMF (0.1 mL), and thionyl chloride (0.12 mL, 2.11 mmol) were used. The product from the first step was treated with 2-(methylamino)ethan-1-ol (132  $\mu$ L, 1.64 mmol), DIPEA (0.25 mL, 1.34 mmol) and anhydrous DMF (5 mL). A colorless precipitate **7.30** (45.6 mg, yield: 46%) was obtained as the product.  $^1H$  NMR (400 MHz,  $CDCl_3$ )  $\delta$  10.29 (s, 1H), 8.71 (s, 1H), 8.51 – 8.37 (m, 2H), 8.01 (d,  $J = 7.6$  Hz, 1H), 7.65 (d,  $J = 7.4$  Hz, 1H), 7.54 – 7.38 (m, 2H), 7.34 – 7.20 (m, 3H), 7.15 (d,  $J = 7.4$  Hz, 1H), 7.06 (d,  $J = 8.4$  Hz, 1H), 5.24 (s, 2H), 3.92 – 3.73 (m, 6H), 3.67 (s, 2H), 2.85 – 2.71 (m, 4H), 2.52 – 2.33 (3s, 9H), 2.27 (s, 3H), 2.23 (s, 3H).  $^{13}C$  NMR (101 MHz,  $CDCl_3$ )  $\delta$  162.1, 156.4, 149.4, 148.8, 142.5, 142.1, 138.2, 137.5, 136.1, 135.7, 134.5, 131.8, 123.0, 129.5, 127.6, 127.4, 127.1, 126.6, 126.3, 126.1, 125.7, 122.3, 120.7, 111.2, 69.0, 61.7, 59.5, 58.8, 58.7, 58.4, 58.3, 41.7, 41.5, 16.5, 15.7, 14.5. UPLC–MS (DAD/ESI):  $t_R = 5.73$  min, for  $C_{36}H_{44}N_4O_4$   $[M + H]^+$  found: 597.45  $m/z$ ; calc. mass: 597.34. HRMS ESI-MS-q-TOF for  $C_{36}H_{44}N_4O_4$   $[M + H]^+$  found: 597.3438  $m/z$ ; calc. mass: 597.3441.

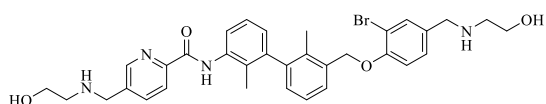
**5-(((1,3-dihydroxypropan-2-yl)amino)methyl)-N-(3'-((4-(((1,3-dihydroxypropan-2-yl)amino)methyl)-2-methylphenoxy)methyl)-2,2'-dimethyl-[1,1'-biphenyl]-3-yl)picolinamide (7.31)**



The compound **7.31** was prepared according to the procedure used for **7.35**. In the first step, **7.23** (100 mg, 0.21 mmol), anhydrous DCM (5 mL) with addition of anhydrous DMF (0.1 mL), and thionyl chloride (0.12 mL, 2.28 mmol) were used. The product from the first step was treated with 2-amino-1,3-propanediol (189 mg, 2.07 mmol), DIPEA (0.31 mL, 1.66 mmol) and anhydrous DMF (5 mL). A colorless precipitate **7.31**

(50.3 mg, yield: 38%) was obtained as the product.  $^1\text{H}$  NMR (400 MHz, DMSO- $d_6$ )  $\delta$  10.36 (s, 1H), 8.77 (s, 1H), 8.21 – 8.08 (m, 2H), 7.84 (d,  $J = 7.9$  Hz, 1H), 7.50 (d,  $J = 7.4$  Hz, 1H), 7.40 – 7.25 (m, 4H), 7.19 – 7.10 (m, 2H), 6.99 (d,  $J = 7.4$  Hz, 1H), 5.20 (brs, 2H), 5.19 (s, 2H), 4.80 (brs, 2H), 4.09 (2s, 4H), 3.59–3.69 (m, 4H), 3.57 – 3.45 (m, 4H), 3.03 – 2.93 (m, 1H), 2.80 – 2.70 (m, 1H), 2.20 (s, 3H), 2.04 (s, 3H), 1.99 (s, 3H).  $^{13}\text{C}$  NMR (101 MHz, DMSO- $d_6$ )  $\delta$  162.1, 156.7, 149.0, 148.7, 142.0, 141.6, 138.3, 136.2, 135.5, 134.3, 132.3, 129.0, 128.9, 127.3, 126.2, 125.9, 125.8, 125.5, 122.8, 121.8, 111.6, 68.3, 60.2, 59.8, 59.2, 57.6, 47.8, 46.9, 16.1, 15.3, 14.5. UPLC–MS (DAD/ESI):  $t_{\text{R}} = 5.69$  min, for  $\text{C}_{36}\text{H}_{44}\text{N}_4\text{O}_6$   $[\text{M} + \text{H}]^+$  found: 629.40  $m/z$ ; calc. mass: 629.33. HRMS ESI-MS-q-TOF for  $\text{C}_{36}\text{H}_{44}\text{N}_4\text{O}_6$   $[\text{M} + \text{H}]^+$  found: 629.3332  $m/z$ ; calc. mass: 629.3339.

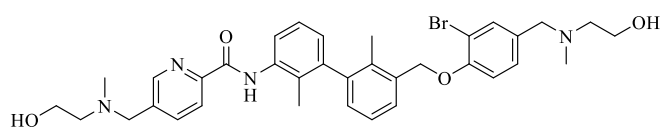
**5-(((2-hydroxyethyl)(methyl)amino)methyl)-N-(3'-(((5-(((2-hydroxyethyl)N-(3'-((2-bromo-4-(((2-hydroxyethyl)amino)methyl)phenoxy)methyl)-2,2'-dimethyl-[1,1'-biphenyl]-3-yl)-5-(((2-hydroxyethyl)amino)methyl)picolinamide (7.32)**



The compound **7.32** was prepared according to the procedure used for **7.35**. In the first step, **7.21** (100 mg, 0.18 mmol), anhydrous DCM (4 mL)

with addition of anhydrous DMF (0.1 mL), and thionyl chloride (0.12 mL, 1.83 mmol) were used. The product from the first step was treated with ethanolamine (111  $\mu\text{L}$ , 112 mg, 1.83 mmol), DIPEA (0.27 mL, 1.46 mmol) and anhydrous DMF (4 mL). A brown precipitate **7.32** (37.1 mg, yield: 32%) was obtained as the product.  $^1\text{H}$  NMR (400 MHz, DMSO)  $\delta$  10.36 (s, 1H), 8.73 (s, 1H), 8.15 (d,  $J = 8.0$  Hz, 1H), 8.08 (dd,  $J = 8.0, 1.2$  Hz, 1H), 7.84 (d,  $J = 7.9$  Hz, 1H), 7.77 (d,  $J = 1.4$  Hz, 1H), 7.55 (d,  $J = 7.5$  Hz, 1H), 7.49 (d,  $J = 8.5$  Hz, 1H), 7.35 – 7.27 (m, 3H), 7.12 (d,  $J = 7.4$  Hz, 1H), 6.98 (d,  $J = 7.5$  Hz, 1H), 5.27 (s, 2H), 3.97 (2s, 4H), 3.61 (t,  $J = 5.4$  Hz, 2H), 3.54 (t,  $J = 5.6$  Hz, 2H), 2.81 (t,  $J = 5.4$  Hz, 2H), 2.69 (t,  $J = 5.6$  Hz, 2H), 2.06 (s, 3H), 1.98 (s, 3H).  $^{13}\text{C}$  NMR (101 MHz, DMSO)  $\delta$  162.1, 154.3, 148.8, 148.6, 141.9, 141.6, 138.1, 136.2, 135.0, 134.5, 134.2, 130.4, 129.2, 128.9, 128.7, 127.5, 126.2, 125.8, 125.6, 122.8, 121.9, 113.9, 110.9, 69.3, 59.4, 57.6, 50.5, 49.6, 49.2, 49.1, 15.4, 14.6. UPLC–MS (DAD/ESI):  $t_{\text{R}} = 5.18$  min, for  $\text{C}_{33}\text{H}_{37}\text{BrN}_4\text{O}_4$   $[\text{M} - \text{H}]^+$  found: 631.04  $m/z$ ; calc. mass: 631.19. HRMS ESI-MS-q-TOF for  $\text{C}_{33}\text{H}_{37}\text{BrN}_4\text{O}_4$   $[\text{M} + \text{H}]^+$  found: 633.2073  $m/z$ ; calc. mass: 633.2076.

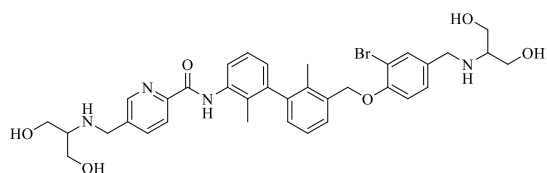
**N-(3'-((2-bromo-4-(((2-hydroxyethyl)(methyl)amino)methyl)phenoxy)methyl)-2,2'-dimethyl-[1,1'-biphenyl]-3-yl)-5-(((2-hydroxyethyl)(methyl)amino)methyl)picolinamide (7.33)**



The compound **7.33** was prepared according to the procedure used for **7.35**.

In the first step, **7.21** (95 mg, 0.17 mmol), anhydrous DCM (5 mL) with addition of anhydrous DMF (0.1 mL), and thionyl chloride (0.11 mL, 1.74 mmol) were used. The product from the first step was treated with 2-(methylamino)ethanol (130 mg, 1.74 mmol), DIPEA (0.26 mL, 1.39 mmol) and anhydrous DMF (5 mL). A colorless precipitate **7.33** (58 mg, yield: 50%) was obtained as the product.  $^1\text{H}$  NMR (400 MHz,  $\text{CDCl}_3$ )  $\delta$  10.06 (s, 1H), 8.48 (d,  $J = 1.3$  Hz, 1H), 8.21 (d,  $J = 8.0$  Hz, 2H), 7.78 (dd,  $J = 8.0, 1.8$  Hz, 1H), 7.47 (d,  $J = 7.5$  Hz, 1H), 7.43 (d,  $J = 1.9$  Hz, 1H), 7.21 (dd,  $J = 15.3, 7.6$  Hz, 2H), 7.12 (dd,  $J = 8.3, 1.8$  Hz, 1H), 7.07 (d,  $J = 7.3$  Hz, 1H), 6.90 (t,  $J = 7.5$  Hz, 2H), 5.12 – 4.98 (m, 2H), 3.64 – 3.52 (m, 6H), 3.41 (s, 2H), 2.56 (t,  $J = 5.3$  Hz, 2H), 2.51 (t,  $J = 5.3$  Hz, 2H), 2.18 (s, 3H), 2.14 (s, 3H), 2.02 (2s, 6H).  $^{13}\text{C}$  NMR (101 MHz,  $\text{CDCl}_3$ )  $\delta$  162.1, 154.4, 149.4, 148.8, 142.4, 142.1, 138.2, 137.5, 136.1, 134.8, 134.5, 134.0, 132.6, 129.6, 129.1, 127.4, 126.6, 126.3, 126.1, 125.7, 122.3, 120.7, 113.6, 112.4, 70.0, 61.3, 59.5, 58.8, 58.7, 58.5, 58.4, 41.7, 41.5, 15.8, 14.5. UPLC–MS (DAD/ESI):  $t_{\text{R}} = 5.75$  min, for  $\text{C}_{35}\text{H}_{41}\text{BrN}_4\text{O}_4$   $[\text{M} + \text{H}]^+$  found: 661.30  $m/z$ ; calc. mass: 661.24. HRMS ESI-MS-q-TOF for  $\text{C}_{35}\text{H}_{41}\text{BrN}_4\text{O}_4$   $[\text{M} + \text{H}]^+$  found: 661.2387  $m/z$ ; calc. mass: 661.2389.

**N-(3'-((2-bromo-4-(((1,3-dihydroxypropan-2-yl)amino)methyl)phenoxy)methyl)-2,2'-dimethyl-[1,1'-biphenyl]-3-yl)-5-(((1,3-dihydroxypropan-2-yl)amino)methyl)picolinamide (7.34)**

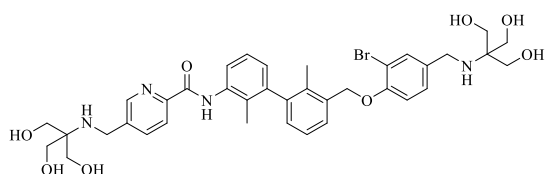


The compound **7.34** was prepared according to the procedure used for **7.35**. In the first step, **7.21** (100 mg, 0.18 mmol), anhydrous DCM (4 mL) with addition of anhydrous DMF (0.1 mL), and thionyl

chloride (0.12 mL, 1.83 mmol) were used. The product from the first step was treated with 2-aminopropane-1,3-diol (166 mg, 1.83 mmol), DIPEA (0.27 mL, 1.46 mmol) and anhydrous DMF (4 mL). A colorless precipitate **7.34** (40.4 mg, yield: 32%) was obtained as the product.  $^1\text{H}$  NMR (600 MHz, DMSO)  $\delta$  10.35 (s, 1H), 8.70 (d,  $J = 1.4$  Hz, 1H), 8.13 (d,  $J = 8.1$  Hz, 1H), 8.05 (dd,  $J = 8.0, 2.0$  Hz, 1H), 7.88 (d,  $J = 7.7$  Hz, 1H), 7.62 (d,  $J = 1.9$  Hz, 1H), 7.55 (d,  $J = 7.2$  Hz, 1H), 7.38 – 7.29 (m, 3H), 7.26 (d,  $J = 8.5$  Hz, 1H), 7.12 (d,  $J = 7.5$  Hz, 1H), 7.01 – 6.94

(m, 1H), 5.24 (s, 2H), 4.51 (s, 4H), 3.94 (s, 2H), 3.76 (s, 2H), 3.44 (dd,  $J = 10.7, 5.6$  Hz, 4H), 3.39 (dd,  $J = 10.1, 5.0$  Hz, 4H), 2.61 – 2.57 (m, 1H), 2.57 – 2.52 (m, 1H), 2.07 (s, 3H), 2.00 (s, 3H).  $^{13}\text{C}$  NMR (151 MHz, DMSO)  $\delta$  162.2, 153.3, 148.3, 148.3, 148.2, 142.0, 141.6, 140.6, 137.5, 136.3, 135.1, 134.5, 132.7, 129.2, 128.7, 127.5, 126.1, 125.8, 125.5, 122.6, 121.8, 113.9, 110.9, 69.3, 61.1, 60.7, 60.3, 60.3, 60.1, 60.1, 49.2, 47.8, 15.4, 14.6. UPLC–MS (DAD/ESI):  $t_{\text{R}} = 5.10$  min, for  $\text{C}_{35}\text{H}_{41}\text{BrN}_4\text{O}_6$   $[\text{M} - \text{H}]^+$  found: 691.16  $m/z$ ; calc. mass: 691.21. HRMS ESI-MS-q-TOF for  $\text{C}_{35}\text{H}_{41}\text{BrN}_4\text{O}_6$   $[\text{M} + \text{H}]^+$  found: 693.2285  $m/z$ ; calc. mass: 693.2287.

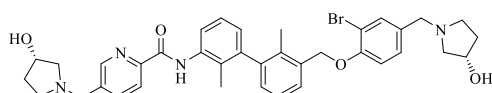
**N-(3'-((2-bromo-4-(((1,3-dihydroxy-2-(hydroxymethyl)propan-2-yl)amino)methyl)phenoxy)methyl)-2,2'-dimethyl-[1,1'-biphenyl]-3-yl)-5-(((1,3-dihydroxy-2-(hydroxymethyl)propan-2-yl)amino)methyl)picolinamide (7.35)**



**7.21** (66 mg, 0.12 mmol) was dissolved in anhydrous DCM (4 mL) with catalytic amount of dry DMF (0.01 mL). The resulted solution was cooled to 0 °C and then, thionyl chloride (76  $\mu\text{L}$ , 1.21 mmol) was added dropwise. The reaction mixture was stirred at room temperature for 2 h. Afterwards, the resulted solution was poured to the separation funnel with the 50 mL of sodium carbonate solution. Phases were separated and water phase was washed with dichloromethane (2 x 30 mL). The organic layers were combined, dried over anhydrous  $\text{MgSO}_4$ , filtered, and the solvent was removed under reduced pressure. As a result colorless precipitate was obtained. In the second step of reaction, to the flask with resulted chloride TIRS (146 mg, 1.21 mmol), anhydrous DMF (4 mL) and DIPEA (0.18 mL, 0.97 mmol) were added respectively. Resulted mixture was heated overnight at 50 °C. Afterwards, solvent was removed under reduced pressure and the mixture of water, dichloromethane and methanol (40 mL, 4:4:1, v:v:v) was added to separate the phases. The aqueous phase was further extracted with dichloromethane: methanol (2 x 20 mL, 4:1, v:v) mixture. The organic layers were combined, dried over anhydrous  $\text{MgSO}_4$ , filtered, and then concentrated under reduced pressure. The crude product was purified by column chromatography (silica gel, chloroform: methanol, 4:1 + 1% solution of ammonia in methanol). A colorless solid **7.35** (33 mg, yield: 36%) was obtained as the product.  $^1\text{H}$  NMR (600 MHz, DMSO)  $\delta$  10.33 (s, 1H), 8.69 (d,  $J = 1.4$  Hz, 1H), 8.11 (d,  $J = 8.1$  Hz, 1H), 8.05 (dd,  $J = 8.0, 1.9$  Hz, 1H), 7.89 (d,  $J = 7.5$  Hz, 1H), 7.61 (d,  $J = 1.4$  Hz, 1H), 7.54 (d,  $J = 7.2$  Hz, 1H), 7.37 – 7.27 (m, 3H), 7.23 (d,  $J = 8.5$  Hz, 1H), 7.11 (d,  $J = 6.8$  Hz, 1H), 6.97 (d,  $J = 6.7$  Hz, 1H), 5.23 (s, 2H), 4.35 (brs, 6H), 3.91 (s, 2H), 3.70 (s, 2H), 3.45 – 3.37 (m, 12H), 2.06 (s, 3H), 1.99 (s, 3H).  $^{13}\text{C}$  NMR (151 MHz, DMSO)  $\delta$  162.2, 153.2, 148.4, 148.0, 142.0,

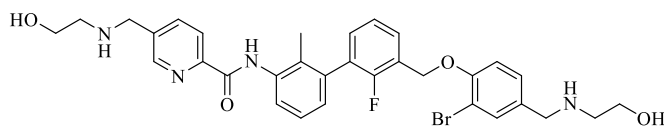
141.6, 141.4, 137.4, 136.3, 135.1, 134.5, 132.7, 129.2, 128.7, 128.5, 127.5, 126.1, 125.8, 125.5, 122.4, 121.7, 113.9, 110.9, 69.3, 61.3, 61.0, 60.3, 44.3, 42.9, 15.3, 14.5. UPLC–MS (DAD/ESI):  $t_R = 5.09$  min, for  $C_{37}H_{45}BrN_4O_8$   $[M - H]^+$  found: 751.21  $m/z$ ; calc. mass: 751.23. HRMS ESI-MS-q-TOF for  $C_{37}H_{45}BrN_4O_8$   $[M + H]^+$  found: 753.2491  $m/z$ ; calc. mass: 753.2499.

**N-(3'-((2-bromo-4-(((S)-3-hydroxypyrrolidin-1-yl)methyl)phenoxy)methyl)-2,2'-dimethyl-[1,1'-biphenyl]-3-yl)-5-(((S)-3-hydroxypyrrolidin-1-yl)methyl)picolinamide (7.36)**



The compound **7.36** was prepared according to the procedure used for **7.35**. In the first step, **7.21** (100 mg, 0.18 mmol), anhydrous DCM (4 mL) with addition of anhydrous DMF (0.1 mL), and thionyl chloride (0.12 mL, 1.83 mmol) were used. The product from the first step was treated with (S)-pyrrolidin-3-ol (159 mg, 1.83 mmol), DIPEA (0.27 mL, 1.46 mmol) and anhydrous DMF (4 mL). A beige precipitate **7.36** (67.4 mg, yield: 54%) was obtained as the product.  $^1H$  NMR (400 MHz, )  $\delta$  10.14 (s, 1H), 8.59 (d,  $J = 1.4$  Hz, 1H), 8.33 – 8.23 (m, 2H), 7.89 (dd,  $J = 8.0, 2.1$  Hz, 1H), 7.57 (d,  $J = 2.0$  Hz, 1H), 7.55 (dd,  $J = 7.6, 0.8$  Hz, 1H), 7.36 – 7.27 (m, 3H), 7.17 – 7.13 (m, 1H), 7.03 – 6.96 (m, 2H), 5.17 (d,  $J = 3.1$  Hz, 2H), 4.46 – 4.34 (m, 2H), 3.73 – 3.60 (m, 2H), 3.05 – 2.97 (m, 1H), 2.94 – 2.80 (m, 2H), 2.76 – 2.67 (m, 2H), 2.62 – 2.54 (m, 1H), 2.42 – 2.33 (m, 1H), 2.29 – 2.14 (m, 3H), 2.10 (s, 3H), 2.09 (s, 3H), 1.94 – 1.83 (m, 2H), 1.83 – 1.70 (m, 2H). UPLC–MS (DAD/ESI):  $t_R = 5.25$  min, for  $C_{37}H_{41}BrN_4O_4$   $[M + H]^+$  found: 685.23  $m/z$ ; calc. mass, 685.24. HRMS ESI-MS-q-TOF for  $C_{37}H_{41}BrN_4O_4$   $[M + H]^+$  found: 685.2384  $m/z$ ; calc. mass: 685.2389.

**N-(3'-((2-bromo-4-(((2-hydroxyethyl)amino)methyl)phenoxy)methyl)-2'-fluoro-2-methyl-[1,1'-biphenyl]-3-yl)-5-(((2-hydroxyethyl)amino)methyl)picolinamide (7.37)**

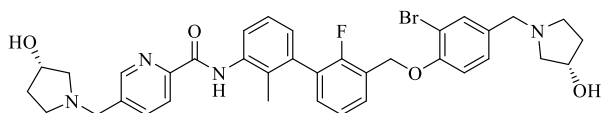


The compound **7.37** was prepared according to the procedure used for **7.35**. In the first step, **7.22** (100 mg, 0.18 mmol), anhydrous DCM (5 mL) with addition of anhydrous DMF (0.1 mL), and thionyl chloride (0.11 mL, 1.95 mmol) were used. The product from the first step was treated with ethanolamine (111  $\mu$ g, 1.82 mmol), DIPEA (0.27 mL, 1.45 mmol) and anhydrous DMF (5 mL). A colorless precipitate **7.37** (39 mg, yield: 34%) was obtained as the product.  $^1H$  NMR (400 MHz,  $CDCl_3$ )  $\delta$  10.37 (s, 1H), 8.68 (s, 1H), 8.13 (d,  $J = 8.0$  Hz, 1H), 8.01 (dd,  $J = 8.0, 1.4$  Hz, 1H), 7.86 (d,  $J = 8.0$  Hz, 1H), 7.70 – 7.61 (m, 1H), 7.59 (d,  $J = 1.4$  Hz, 1H), 7.40 – 7.28 (m,



4H), 7.22 (d,  $J = 8.5$  Hz, 1H), 7.11 (d,  $J = 7.5$  Hz, 1H), 5.29 (s, 2H), 3.86 (s, 2H), 3.68 (s, 2H), 3.53 – 3.44 (m, 4H), 2.65 – 2.54 (m, 4H), 2.11 (s, 3H).  $^{13}\text{C}$  NMR (101 MHz,  $\text{DMSO-}d_6$ )  $\delta$  162.3, 159.6 (d,  $^1J_{\text{C-F}} = 294.9$  Hz), 155.7, 153.1, 148.3, 148.2, 140.1, 137.4, 136.4, 135.9, 134.7, 132.6, 131.6, 129.6, 128.6 (d,  $^3J_{\text{C-F}} = 8.2$  Hz), 128.5 (d,  $^2J_{\text{C-F}} = 16.5$  Hz), 127.0, 125.9, 124.5 (d,  $J_{\text{C-F}} = 3.7$  Hz), 124.0 (d,  $^2J_{\text{C-F}} = 15.4$  Hz), 123.8, 121.9, 114.1, 111.1, 64.8 (d,  $^3J_{\text{C-F}} = 3.9$  Hz), 60.4, 60.0, 51.3, 51.0, 50.7, 49.9, 14.9 (d,  $^4J_{\text{C-F}} = 1.9$  Hz). UPLC–MS (DAD/ESI):  $t_{\text{R}} = 5.68$  min, for  $\text{C}_{32}\text{H}_{34}\text{BrFN}_4\text{O}_4$   $[\text{M} + \text{H}]^+$  found: 637.25  $m/z$ ; calc. mass: 637.18. HRMS ESI-MS-q-TOF for  $\text{C}_{32}\text{H}_{34}\text{BrFN}_4\text{O}_4$   $[\text{M} + \text{H}]^+$  found: 637.1821  $m/z$ ; calc. mass: 637.1826.

**N-(3'-((2-bromo-4-(((S)-3-hydroxypyrrolidin-1-yl)methyl)phenoxy)methyl)-2'-fluoro-2-methyl-[1,1'-biphenyl]-3-yl)-5-(((S)-3-hydroxypyrrolidin-1-yl)methyl)picolinamide (7.38)**



The compound **7.38** was prepared according to the procedure used for **7.35**. In the first step, **7.22** (85 mg, 0.15 mmol), anhydrous DCM (5 mL) with addition of anhydrous DMF (0.1 mL), and thionyl chloride (0.94 mL, 1.65 mmol) were used. The product from the first step was treated with (S)-pyrrolidin-3-ol (134 mg, 1.54 mmol), DIPEA (0.23 mL, 1.23 mmol) and anhydrous DMF (5 mL). A colorless precipitate **7.38** (50 mg, yield: 47%) was obtained as the product.  $^1\text{H}$  NMR (400 MHz,  $\text{CDCl}_3$ )  $\delta$  10.15 (s, 1H), 8.58 (d,  $J = 1.4$  Hz, 1H), 8.30 (d,  $J = 7.6$  Hz, 1H), 8.26 (d,  $J = 8.0$  Hz, 1H), 7.87 (dd,  $J = 8.0, 2.0$  Hz, 1H), 7.71 – 7.64 (m, 1H), 7.55 (d,  $J = 2.0$  Hz, 1H), 7.34 (t,  $J = 7.9$  Hz, 1H), 7.26 (s, 3H), 7.07 (d,  $J = 7.0$  Hz, 1H), 6.95 (d,  $J = 8.4$  Hz, 1H), 5.25 (d,  $J = 11.4$  Hz, 2H), 4.42 – 4.28 (m, 2H), 3.73 (s, 2H), 3.55 (s, 2H), 2.93 – 2.79 (m, 2H), 2.68 (dd,  $J = 16.7, 7.0$  Hz, 2H), 2.63 – 2.50 (m, 2H), 2.39 – 2.27 (m, 2H), 2.25 – 2.14 (m, 5H), 1.84 – 1.65 (m, 2H).  $^{13}\text{C}$  NMR (101 MHz,  $\text{CDCl}_3$ )  $\delta$  162.2, 156.9 (d,  $^1J_{\text{C-F}} = 246.6$  Hz), 154.0, 149.1, 148.6, 138.0, 137.9, 136.4, 136.2, 133.9, 133.0, 131.4 (d,  $J_{\text{C-F}} = 3.5$  Hz), 129.0 (m, 2C), 128.7 (d,  $J_{\text{C-F}} = 3.7$  Hz), 127.4, 126.7, 126.4, 124.4 (d,  $J_{\text{C-F}} = 4.0$  Hz), 124.1 (d,  $^2J_{\text{C-F}} = 15.0$  Hz), 122.3, 121.6, 113.7, 112.5, 71.3 (2C), 65.0 (d,  $^3J_{\text{C-F}} = 5.2$  Hz), 63.0, 62.9, 59.1, 57.3, 52.6, 52.4, 35.1, 35.0, 14.9 (d,  $J_{\text{C-F}} = 2.3$  Hz). UPLC–MS (DAD/ESI):  $t_{\text{R}} = 5.74$  min, for  $\text{C}_{36}\text{H}_{38}\text{BrFN}_4\text{O}_4$   $[\text{M} + \text{H}]^+$  found: 689.30  $m/z$ ; calc. mass, 689.21. HRMS ESI-MS-q-TOF for  $\text{C}_{36}\text{H}_{38}\text{BrFN}_4\text{O}_4$   $[\text{M} + \text{H}]^+$  found: 689.2134  $m/z$ ; calc. mass: 689.2139.

### 4.3. Protein Expression and Purification

All chemicals used for protein expression and purification were received from BioShop Sigma-Aldrich. The preparation of proteins including IgV domains of human and mouse PD-L1 protein (hPD-L1 residues, 18–134, C-terminal His-tag; mPD-L1 residues, 19–134) and the extracellular domain of human PD-1 (hPD-1 residues 34–150, C93S) were expressed and purified as described in the following paper (Zak *et al.*, 2016).

Additionally, to obtain  $^{15}\text{N}$  labelling bacterial cells were cultured at 37 °C in LB or M9 minimal medium containing  $^{15}\text{NH}_4\text{Cl}$  as the sole nitrogen source. 1 mM isopropyl  $\beta$ -D-1-thiogalactopyranosid (IPTG) at an  $\text{OD}_{600}$  of 0.8 was used for induction of protein expression. After overnight culture of cells (temperature decreased to 28 °C for hPD-1), purification of inclusion bodies was carried out as described previously (Zak *et al.*, 2015). Followingly, proteins were refolded by dropwise dilution into a solution containing 0.1 M Tris pH 8.0, 0.4 M L-arginine hydrochloride, 2 mM EDTA, 5 mM cystamine, and 0.5 mM cysteamine for hPD-1, and 0.1 M Tris pH 8.0, 1 M L-arginine hydrochloride, 0.25 mM oxidized glutathione, and 0.25 mM reduced glutathione for hPD-L1. After refolding process, proteins were subjected to dialyses, and there were dialyzed three times against 10 mM Tris pH 8.0 and 20 mM NaCl solution. Purification involved size-exclusion chromatography (SEC) on an HiLoad 26/600 Superdex 75 column in 25 mM sodium phosphate pH 6.4 with 100 mM NaCl for hPD-1 and for N66A hPD-1 mutant. PBS pH 7.4 was applied for hPD-L1, hPD-L1(18–239) (Konieczny *et al.*, 2020).

### 4.4. *weak*-Antagonist-Induced Dissociation Assay (*w*-AIDA-NMR)

All spectra were recorded at 300 K on a Bruker Avance III 600 MHz spectrometer equipped with the nitrogen cryoprobe. Sample preparation involved the addition of 10% (v/v) of  $\text{D}_2\text{O}$  to provide the signal lock. In the experiment  $^{15}\text{N}$ -labeled wt- and N66A PD-1 (0.15 mM) were slightly over titrated with the unlabelled PD-L1. The compounds were added into the resulting mixture. During the (*weak*) antagonist-induced dissociation assay (*w*-AIDA-NMR), the  $^1\text{H}$ - $^{15}\text{N}$  signals were monitored by SOFAST HMQC to check the competence of small molecules towards PD-L1/(wt or N66A)PD-1 dissociation.

### 4.5. Homogeneous Time-Resolved Fluorescence (HTRF)

The certified Cis-Bio assay kit was used to determine the ability of small molecule to interrupt PD-1/PD-L1 pathway. Following the standard protocol, the measurement was carried

out at 20  $\mu$ L final volume with 5 nM concentration of hPD-L1 and 50 nM concentration of hPD-1 in the final formulation. Separate dilution series were performed to calculate the half maximal inhibitory concentration ( $IC_{50}$ ) of the most potent compounds. Analyte and detection reagents (anti-analyte conjugated donor and acceptor conjugated antibody) were placed in the proper wells on microplate as suggested in the Cis-Bio protocol. The plate was left for 2 h of incubation and it was read on an HTRF certified microplate reader Tecan Spark 20M. Output data were subjected to background subtraction on negative control, normalization in correlation to positive control and they were averaged. Half maximal inhibitory concentrations were calculated using Mathematica 12 by fitting with normalized Hill's equation to get the final values.

#### **4.6. Cell Culture**

CHO-K1 cells overexpressing hPD-L1 and the recombinant TCR ligand (CHO/TCRAct/PD-L1) and Jurkat T cells overexpressing hPD-1 and bearing a luciferase reporter gene under the control of Nuclear Factor of Activated T-cells Response Element (NFAT-RE) (hPD-1 Effector Cells, hPD-1 ECs, Promega) were cultured in RPMI-1640 medium (Biowest, Billerica, MA) supplemented with 10% Fetal Bovine Serum (FBS, Biowest) and 200 mM L-glutamine (Biowest) in the presence of G418 (250  $\mu$ g/ml, InvivoGen, San Diego, CA) and Hygromycin B Gold (50  $\mu$ g/ml, InvivoGen) as selection antibiotics. To check the overexpression of hPD-L1 and TCR ligand in aAPCs and PD-1 in ECs, flow cytometry and Western blot analysis were performed respectively.

#### **4.7. hPD-1/hPD-L1 Immune Checkpoint Blockade Assay**

The examination of the functional effects of the blockade of PD-1/PD-L1 immune checkpoint was performed according to the manufacturer's instructions included in the protocol for PD-1/PD-L1 Blockade Bioassay (Promega). CHO/TCRAct/PD-L1 cells or CHO/TCRAct or CHO-K1 cells were seeded on 96-well plates at the density 10 000 cells/well 17 h prior to the experiment. The 2.5-fold dilution of the small molecules was prepared in DMSO, and then the compounds were diluted 1000-fold in the assay buffer (99% RPMI 1640, 1% FBS) to form the solutions with 0.1% of DMSO in total volume. On the day of the assay the 2.5-fold dilutions of durvalumab, a positive control anti-hPD-L1 monoclonal antibody (Imfinzi, Medimmune/AstraZeneca), were prepared in the assay buffer. The culture medium was discarded from the wells, and serial dilutions of either the small molecule or the antibody were added. Then, Jurkat-ECs cells were seeded at the density of 20 000 cells/well onto the assay plates. Activation of the Jurkat T cells, reflected by luciferase activity, was monitored by

luminescence measurements after 6 h of incubation (37 °C, 5% CO<sub>2</sub>), and 20 min of additional incubation with the Bio-Glo assay reagent (Promega) at room temperature. Spark microplate reader (Tecan) allow the luminescence signal detection. Half-maximal effective concentrations (EC50 values) were calculated from the dose–response curve using OriginPro 2020 (OriginLab) software.

#### **4.8. Cytotoxicity Assay**

Since Jurkat-ECs afford the read-out in the ICB assay and could possess vulnerability to compounds' toxicity, the cytotoxicity of small molecules towards Jurkat-ECs was verified. For this purpose, Jurkat-ECs were seeded on 96-well transparent plates in the presence of increasing concentrations of the compounds, keeping constant (0.1%) concentration of DMSO. After 48 h of incubation, a tetrazolium reagent, Biolog redox dye MIX MB (Biolog), was added according to the manufacturer's protocol, and the culture plates were incubated for an additional 2 h (37 °C, 5% CO<sub>2</sub>). Afterwards, Spark microplate reader (Tecan) allow the measurement of absorbance at 590 nm with 750 nm as a reference. The data are presented as Jurkat-EC survival relative to DMSO-treated control cells.

#### **4.9. Crystallization and the Crystal Structure Determination**

##### Protein expression and purification

The hPD-L1 protein was expressed and purified as previously described in (Zak et al., 2016 PMID 27083005). The construct containing the amino acids 18-134 was cloned into pET21b and expressed in the form of Inclusion Bodies (IB) in LB medium containing the corresponding antibiotic at 37 °C until an OD of 0.6 was reached; the temperature then was reduced to 30 °C and the culture was left shaking overnight. The IBs were then washed, and the refolding of the protein was performed in a drop-wise fashion in buffer containing 0.1 M Tris pH 8.0, 1 M L-Arg hydrochloride, 0.25 mM oxidized glutathione and 0.25 mM reduced glutathione. The refolded solution was then dialyzed against buffer containing 20 mM NaCl and 10 mM Tris-HCl pH 8.0. The final purification step consisted of a size exclusion chromatography on Superdex 75 (GE Healthcare). Protein purity and folded status were checked by SDS-Page and NMR, respectively.

## Literature

- Ahmed, F. *et al.* (1996). Reductive Amination of Aldehydes and Ketones with Sodium Triacetoxyborohydride. Studies on Direct and Indirect Reductive Amination Procedures, *J. Org. Chem.*, 61, 3849-3862. doi: 10.1021/jo960057x.
- Aktoudianakis, E. *et al.* (2018). PD-1/PD-L1 INHIBITORS. US 2018/0305315 A1.
- Amatore, *et al.* (2011). Kinetic Data for the Transmetalation/Reductive Elimination in Palladium-Catalyzed Suzuki-Miyaura Reactions: Unexpected Triple Role of Hydroxide Ions Used as Base, *Chem. Eur. J.*, 17, 2492–2503. doi:10.1002/chem.201001911.
- Balar, A.V. *et al.* (2017). Atezolizumab as first-line treatment in cisplatin-ineligible patients with locally advanced and metastatic urothelial carcinoma: a single-arm, multicentre, phase 2 trial, *Lancet*, 389, 67–76. doi: 10.1016/S0140-6736(16)32455-2.
- Baldo, B.A. (2013). Adverse events to monoclonal antibodies used for cancer therapy: Focus on hypersensitivity responses, *Oncoimmunology*, 2, e26333-1-15. doi: 10.4161/onci.26333.
- Luca, B. *et al.* (2001). Lithium Borohydride, e-EROS Encyclopedia of Reagents for Organic Synthesis, John Wiley & Sons. doi:10.1002/047084289X.rl061.pub2.
- Basu, S. *et al.* (2019). Design, Synthesis, Evaluation, and Structural Studies of C2-Symmetric Small Molecule Inhibitors of Programmed Cell Death- 1/Programmed Death-Ligand 1 Protein–Protein Interaction, *J. Med. Chem.*, 62, 7250–7263. doi: 10.1021/acs.jmedchem.9b00795.
- Baumeister, S.H. *et al.* (2016). Coinhibitory Pathways in Immunotherapy for Cancer, *Annu. Rev. Immunol.*, 34, 539–573. doi: 10.1146/annurev-immunol-032414-112049.
- Baxter, E.W. and Reitz A.B. (2004). Reductive Aminations of Carbonyl Compounds with Borohydride and Borane Reducing Agents, *Org. React.*, 59, 1–714. doi:10.1002/0471264180.or059.01.
- Carpino, L.A. (1993). 1-Hydroxy-7-azabenzotriazole. An efficient peptide coupling additive, *J. Am. Chem. Soc.*, 115, 4397–4398. doi:10.1021/ja00063a082.
- Carpino, L.A. *et al.*, (2000). Comparison of the Effects of 5- and 6-HOat on Model Peptide Coupling Reactions Relative to the Cases for the 4- and 7-Isomers, *Org. Lett.*, 2, 2253–2256. doi:10.1021/ol006013.
- Chen, F.F., Li, Z., Ma, D. and Yu, Q. (2020). Small-molecule PD-L1 inhibitor BMS1166 abrogates the function of PD-L1 by blocking its ER export, *Oncoimmunology*, 9, e1831153. doi: 10.1080/2162402X.2020.1831153.

- Cheng, B. *et al.* (2020). Discovery of Novel Resorcinol Dibenzyl Ethers Targeting the Programmed Cell Death-1/Programmed Cell Death – Ligand 1 Interaction as Potential Anticancer Agents, *J. Med. Chem.*, 63, 8338-8358. doi: 10.1021/acs.jmedchem.0c00574.
- Chupak, L.S.; Zheng, X. (2015a). Compounds Useful as Immunomodulators. WO2015034820 A1.
- Chupak, L.S. *et al.* (2015b). Compounds Useful as Immunomodulators. WO2015160641.
- Couzin-Frankel J. (2013). Cancer Immunotherapy, *Science*, 342, 1432–1433. doi: 10.1093/glycob/cwy069.
- Degorce, F. *et al.* (2009). HTRF: A technology tailored for drug discovery - a review of theoretical aspects and recent applications, *Curr Chem Genomics.*, 3, 22-32. doi:10.2174/1875397300903010022.
- Dess, D.B. and Martin, J.C. (1983). Readily accessible 12-I-5 oxidant for the conversion of primary and secondary alcohols to aldehydes and ketones, *J. Org. Chem.*, 48, 4155–4156. doi:10.1021/jo00170a070.
- Dong, H. *et al.* (2002) Tumor-associated B7-H1 promotes T-cell apoptosis: A potential mechanism of immune evasion, *Nat. Med.*, 8, 793–800. doi: 10.1038/nm730.
- Dunn, G.P. *et al.* (2002). Cancer immunoediting: From immunosurveillance to tumor escape, *Nat. Immunol.*, 3, 991–998. doi: 10.1038/ni1102-991.
- Farkona, S., Diamandis, E.P. and Blasutig, I.M. (2016). Cancer immunotherapy: The beginning of the end of cancer?, *BMC Med.*, 14, 73. doi: 10.1186/s12916-016-0623-5.
- Feng, Z. *et al.* (2017a). Benzyl Phenyl Ether Derivative, Preparation Method Therefor, and Pharmaceutical Composition and Uses Thereof. WO2017202273.
- Feng, Z. *et al.* (2017b). Bromo Benzyl Ether Derivative, Preparation Method Therefor, and Pharmaceutical Composition and Uses Thereof. WO2017202275.
- Feng, Z. *et al.* (2017c). Phenylate Derivative, Preparation Method Therefor, and Pharmaceutical Composition and Uses Thereof. WO2017202276.
- Forero-Cortés, P.A. and Haydl, A.M. (2019). The 25th Anniversary of the Buchwald–Hartwig Amination: Development, Applications, and Outlook. *Org Process Res Dev.* 23, 1478–1483. doi:10.1021/acs.oprd.9b00161. S2CID 198366762.
- Freeman, G.J. *et al.* (2000). Engagement of the PD-1 Immunoinhibitory Receptor by a Novel B7 Family Member Leads to Negative Regulation of Lymphocyte Activation, *J. Exp. Med.*, 192, 1028–1034. doi: 10.1084/jem.192.7.1027.
- Garon, E.B. *et al.* (2015). Pembrolizumab for the Treatment of Non–Small-Cell Lung Cancer, *N. Engl. J. Med.*, 372, 2018–2028. doi: 10.1056/NEJMoa1501824.

- Guzik, K. *et al.* (2017). Small-Molecule Inhibitors of the Programmed Cell Death-1/Programmed Death-Ligand 1 (PD-1/PD-L1) Interaction via Transiently Induced Protein States and Dimerization of PD-L1, *J. Med. Chem.*, 60, 5857–5867. doi: 10.1021/acs.jmedchem.7b00293.
- Guzik, K. *et al.* (2019). Development of the Inhibitors That Target the PD-1/PD-L1 Interaction—A Brief Look at Progress on Small Molecules, Peptides and Macrocycles, *Molecules*, 24, 2071–2100. doi:10.3390/molecules24112071.
- Hoos, A. (2016). Development of immuno-oncology drugs - from CTLA4 to PD1 to the next generations, *Nat. Rev. Drug Discov.*, 15, 235–247. doi: 10.1038/nrd.2015.35.
- Ishida, Y. *et al.* (1992). Induced expression of PD-1, a novel member of the immunoglobulin gene superfamily, upon programmed cell death, *EMBO J*, 11, 3887–3895. doi: 10.1002/j.1460-2075.1992.tb05481.x.
- Jiang, J. *et al.* (2021). Simultaneous Determination of a Novel PD-L1 Inhibitor, IMM-010, and Its Active Metabolite, YPD-29B, in Rat Biological Matrices by Polarity-Switching Liquid Chromatography-Tandem Mass Spectrometry: Application to ADME Studies, *Front. Pharmacol.*, 12, 677120. doi: 10.3389/fphar.2021.677120.
- Kawashita, S. *et al.* (2019). Symmetry-based ligand design and evaluation of small molecule inhibitors of programmed cell death-1/programmed death-ligand 1 interaction, *Bioorg. Med. Chem. Lett.*, 29, 2464–2467. doi: 10.1016/j.bmcl.2019.07.027.
- Kazemi, T. *et al.* (2016). Immunotherapeutic approaches for cancer therapy: An updated review, *Artif Cells Nanomed Biotechnol*, 44, 769–779. doi: 10.3109/21691401.2015.1019669.
- Khalil, D.N., Smith, E.L., Brentjens, R.J. and Wolchok, J.D. (2016). The future of cancer treatment: immunomodulation, CARs and combination immunotherapy, *Nat. Rev. Clin. Oncol.*, 13, 273–290. doi: 10.1038/nrclinonc.2016.25.
- Kim, J.M. and Chen, D.S. (2016). Immune escape to PD-L1/PD-1 blockade: Seven steps to success (or failure), *Ann. Oncol.*, 27, 1492–1504. doi: 10.1093/annonc/mdw217.
- Kitel, R. *et al.* (2022). Exploring the Surface of the Ectodomain of the PD-L1 Immune Checkpoint with Small-Molecule Fragments, *ACS Chem. Biol.*, 17, 2655–2663. doi: 10.1021/acscchembio.2c00583.
- Konieczny, M. *et al.* (2020). Di-bromo-Based Small-Molecule Inhibitors of the PD-1/PD-L1 Immune Checkpoint, *J. Med. Chem.*, 63, 11271–11285. doi: 10.1021/acs.jmedchem.0c01260.

- Lajkiewicz, N., Wu, L., Yao, W. (2017). Heterocyclic compounds as immunomodulators. US 20170174679 A1.
- Lange, C. *et al.* (2018). Immunomodulator Compounds. WO2018005374A1.
- Lange, C. *et al.* (2019). Immunomodulator Compounds. WO2019023575A1.
- Lazorchak, A.S. *et al.* (2016). CA-170, an oral small molecule PD-L1 and VISTA immune checkpoint antagonist, promotes T cell immune activation and inhibits tumor growth in pre-clinical models of cancer. In Proceedings of the AACR Special Conference on Tumor Immunology and Immunotherapy, Boston, MA, USA, 20–23 October 2016; p. A36. doi: 10.1158/2326-6074.TUMIMM16-A36.
- Leach, D.R., Krummel, M.F. and Allison, J.P. (1996). Enhancement of Antitumor Immunity by CTLA-4 Blockade, *Science*, 271, 1734–1736. doi: 10.1126/science.271.5256.1734.
- Ledford, H., Else, H. and Warren, M. (2018). Cancer immunologists scoop medicine Nobel prize, *Nature*, 562, 20–21. doi: 10.1038/d41586-018-06751-0.
- Lee, J.Y. *et al.* (2016). Structural basis of checkpoint blockade by monoclonal antibodies in cancer immunotherapy, *Nat. Commun.*, 7, 13354. doi: 10.1038/ncomms13354.
- Li, J., Wu, L., Yao, W. (2017a). Heterocyclic Compounds as Immunomodulators. WO2017087777 A1.
- Li, Z., Wu, L., Yao, W. (2017b). Heterocyclic Compounds as Immunomodulators. WO2017192961 A1.
- Lin, D.Y.W. *et al.* (2008). The PD-1/PD-L1 complex resembles the antigen-binding Fv domains of antibodies and T cell receptors, *Proc. Natl. Acad. Sci. U. S. A.*, 105, 3011–3016. doi: 10.1073/pnas.0712278105.
- Liu, C. *et al.* (2021). Discovery of a novel , potent and selective small-molecule inhibitor of PD-1 / PD-L1 interaction with robust in vivo anti- tumor efficacy, *Br. J. Pharmacol.*, 178, 2651–2670. doi: 10.1111/bph.15457.
- Liu, H. *et al.* (2019). Discovery of low-molecular weight anti-PD-L1 peptides for cancer immunotherapy, *J. ImmunoTher. Cancer*, 7, 1–14. doi: 10.1186/s40425-019-0705-y.
- Liu, K. *et al.* (2016). Structural basis of anti-PD-L1 monoclonal antibody avelumab for tumor therapy, *Cell Research*, 1–3. doi: 10.1038/cr.2016.102.
- Llosa, N.S. *et al.* (2014). Immune checkpoints expression in MSI versus MSS colorectal cancers and their potential therapeutic implications, *J. Clin. Oncol.*, 32, 3620. doi: 10.1200/jco.2014.32.15\_suppl.3620.
- Lu, L., Qian, D.Q., Wu, L., Yao, W. (2017). Heterocyclic Compounds as Immunomodulators. WO2017205464 A1.



- Magiera K., *et al.* (2017). Bioactive macrocyclic inhibitors of the PD-1/PD-L1 immune checkpoint, *Angew Chem Int Ed Engl.*, 56, 13732–13735. doi:10.1002/anie.201707707.
- Mahoney, K.M., Rennert, P.D. and Freeman, G.J. (2015). Combination cancer immunotherapy and new immunomodulatory targets, *Nat. Rev. Drug Discov.*, 14, 561–584. doi: 10.1038/nrd4591.
- Mann, G. *et al.* (1999). Palladium-Catalyzed C-O Coupling Involving Unactivated Aryl Halides. Sterically Induced Reductive Elimination To Form the C-O Bond in Diaryl Ethers, *J. Am. Chem. Soc.*, 121, 3224–3225, doi:10.1021/ja984321a.
- Miyaura, N. *et al.* (1979a). A new stereospecific cross-coupling by the palladium-catalyzed reaction of 1-alkenylboranes with 1-alkenyl or 1-alkynyl halides, *Tetrahedron Lett.*, 20, 3437–3440. doi: 10.1016/S0040-4039(01)95429-2.
- Miyaura, N. *et al.* (1979b). Stereoselective synthesis of arylated (E)-alkenes by the reaction of alk-1-enylboranes with aryl halides in the presence of palladium catalyst, *J. Chem. Soc., Chem. Commun.*, 866–867. doi: 10.1039/C39790000866.
- Miyaura, N. *et al.* (1995). Palladium-Catalyzed Cross-Coupling Reactions of Organoboron Compounds, *Chem. Rev.*, 95, 2457–2483. doi:10.1021/cr00039a007. S2CID 53050782.
- Musielak, B. *et al.* (2019). CA-170 – a potent small-molecule PD-L1 inhibitor or not?, *Molecules*, 24, 2804-2817. doi: 10.3390/molecules24152804.
- Muszak, D. *et al.* (2021). Terphenyl-Based Small-Molecule Inhibitors of Programmed Cell Death-1/Programmed Death-Ligand 1 Protein-Protein Interaction, *J. Med. Chem.*, 64, 11614–11636. doi: 10.1021/acs.jmedchem.1c00957.
- Musielak, B. *et al.* (2020). Competition NMR for Detection of Hit/Lead Inhibitors of Protein–Protein Interactions, *Molecules*, 25, 3017. doi: 10.3390/molecules25133017.
- Ohaegbulam, K.C. *et al.* (2015). Human cancer immunotherapy with antibodies to the PD-1 and PD-L1 pathway, *Trends Mol. Med.*, 21, 24–33. doi: 10.1016/j.molmed.2014.10.009.
- Okazaki, T. and Honjo, T. (2006). The PD-1-PD-L pathway in immunological tolerance, *Trends Immunol.*, 27, 195–201. doi: 10.1016/j.it.2006.02.001.
- Okazaki, T., Iwai, Y. and Honjo, T. (2002). New regulatory co-receptors: inducible co-stimulator and PD-1, *Curr. Opin. Immunol.*, 14, 779–782. doi: 10.1016/S0952-7915(02)00398-9.
- Overhauser, A.W. (1953). Polarization of Nuclei in Metals, *Phys. Rev.*, 92, 411–5. doi:10.1103/PhysRev.92.411.
- Pan, C. *et al.* (2021). Recent advance of peptide-based molecules and nonpeptidic small-molecules modulating PD-1 / PD-L1 protein-protein interaction or targeting PD-L1

- protein degradation, *Eur. J. Med. Chem.*, 213, 113170. doi: 10.1016/j.ejmech.2021.113170.
- Papaioannou, N.E. *et al.* (2016). Harnessing the immune system to improve cancer therapy, *Ann. Transl. Med.*, 4, 261–275. doi: 10.21037/atm.2016.04.01.
- Pardoll, D.M. (2012) The blockade of immune checkpoints in cancer immunotherapy, *Nat. Rev. Cancer*, 12, 252–264. doi: 10.1038/nrc3239.
- Park, J. J. *et al.* (2021). Checkpoint inhibition through small molecule-induced internalization of programmed death-ligand 1, *Nat. Commun.*, 12, 1222. doi: 10.1038/s41467-021-21410-1.
- Parsa, A.T. *et al.* (2007). Loss of tumor suppressor PTEN function increases B7-H1 expression and immunoresistance in glioma, *Nat. Med.*, 13, 84–88. doi: 10.1038/nm1517.
- Piha-Paul, S. *et al.* (2020). Pharmacodynamic Biomarkers Demonstrate T- Cell Activation in Patients Treated with the Oral PD-L1 Inhibitor INCB086550 in a Phase 1 Clinical Trial, *J. Immunother. Cancer*, 8, A255. doi: 10.1136/jitc-2020-SITC2020.0419.
- Qin, M. *et al.* (2019). Discovery of [1,2,4]Triazolo[4,3-a]pyridines as Potent Inhibitors Targeting the Programmed Cell Death-1/Programmed Cell Death-Ligand 1 Interaction, *J. Med. Chem.*, 62, 4703–4715. doi: 10.1021/acs.jmedchem.9b00312.
- Qin, M. *et al.* (2020). Discovery of the programmed cell death-1/programmed cell death-ligand 1 interaction inhibitors bearing an indoline scaffold, *Eur. J. Med. Chem.*, 186, 111856. doi: 10.1016/j.ejmech.2019.111856.
- Ramesh, C. *et al.* (2011). A Simple and Facile Route for the Synthesis of 2H-1,4-Benzoxazin-3-(4H)- Ones via Reductive Cyclization of 2-(2- Nitrophenoxy)Acetonitrile Adducts in the Presence of Fe/Acetic Acid, *Tetrahedron*, 67, 1187-1192. doi: 10.1016/j.tet.2010.11.095.
- Ramsay, A.G. (2013). Immune checkpoint blockade immunotherapy to activate anti-tumor T-cell immunity, *Br. J. Haematol.*, 162, 313–325. doi: 10.1111/bjh.12380.
- Sasikumar, P.G.N., Ramachandra, M., and Naremaddepalli, S.S.S. (2013). Peptidomimetic compounds as immunomodulators, US20130237580 A1.
- Sasikumar, P.G.N., Ramachandra, M., Naremaddepalli, S.S.S. (2015). 1,2,4- Oxadiazole Derivatives as Immunomodulators. Aurigene Discovery Technologies Limited, US20150073024 A1.
- Sasikumar, P.G.N. *et al.* (2016). Oral immune checkpoint antagonists targeting PD-L1/VISTA or PD-L1/Tim3 for cancer therapy. In Proceedings of the AACR 107th Annual Meeting

- 2016, New Orleans, LA, USA, 16–20 April 2016; p. 4861. doi: 10.1158/1538-7445.AM2016-4861.
- Sasikumar, P.G.N., Ramachandra, M., and Naremaddepalli, S.S.S. (2018a). 1,3,4-Oxadiazole and 1,3,4-Thiadiazole Derivatives as Immunomodulators. US10160736 B2.
- Sasikumar, P.G.N., Ramachandra, M., Naremaddepalli, S.S.S. and Prasad, A. (2018b). 3-Substituted-1,2,4-Oxadiazole and Thiadiazole Compounds as Immunomodulators. US20180044329A1.
- Sasikumar, P.G.N., Ramachandra, M., Naremaddepalli, S.S.S. (2019). 1,2,4-Oxadiazole Derivatives as Immunomodulators. US10173989B2.
- Sasikumar, P.G. *et al.* (2021). PD-1 derived CA-170 is an oral immune checkpoint inhibitor that exhibits preclinical anti-tumor efficacy, *Commun. Biol.*, 4, 699. doi: 10.1038/s42003-021-02191-1.
- Sasikumar, P.G. and Ramachandra, M. (2022). Small Molecule Agents Targeting PD-1 Checkpoint Pathway for Cancer Immunotherapy: Mechanisms of Action and Other Considerations for Their Advanced Development, *Front. Immunol.*, 13, 752065. doi: 10.3389/fimmu.2022.752065.
- Shaabani, S. *et al.* (2018). A patent review on PD-1/PD-L1 antagonists: small molecules, peptides and macrocycles (2015-2018), *Expert Opin. Ther. Pat.*, 28, 665-678. doi: 10.1080/13543776.2018.1512706.
- Sharpe, A.H.; Butte, M.J.; Oyama, S. (2011). Modulators of Immuno-inhibitory Receptor PD-1, and Methods of Use Thereof. WO2011082400 A2.
- Skalniak, L., Zak, K.M. *et al.* (2017). Small-molecule inhibitors of PD-1/PD-L1 immune checkpoint alleviate the PD-L1-induced exhaustion of T-cells, *Oncotarget*, 8, 72167–72181. doi: 10.18632/oncotarget.20050.
- Smith, G. *et al.* (1994). Mechanistic Studies of the Suzuki Cross-Coupling Reaction, *J. Org. Chem.*, 59, 8151–8156. doi:10.1021/jo00105a036.
- Tan, S., Li, D. and Zhu, X. (2020). Cancer immunotherapy: Pros, cons and beyond, *Biomed. Pharmacother.*, 124, 109821–109831. doi.org/10.1016/j.biopha.2020.109821.
- Taube, J.M. *et al.* (2013). Colocalization of Inflammatory Response with B7-H1 Expression in Human Melanocytic Lesions Supports an Adaptive Resistance Mechanism of Immune Escape, *Sci. Transl. Med.*, 4, 127ra37. doi: 10.1126/scitranslmed.3003689.
- Topalian, S.L. *et al.* (2012). Safety, activity, and immune correlates of anti-PD-1 antibody in cancer, *N Engl J Med*, 366, 2443–2454. doi: 10.1016/j.eururo.2014.12.052.

- Topalian, S.L., Drake, C.G. and Pardoll, D.M. (2015). Immune checkpoint blockade: a common denominator approach to cancer therapy, *Cancer Cell*, 27, 450–461. doi: 10.1016/j.ccell.2015.03.001.
- Trott, O. and Olson, A.J. (2009). AutoDock Vina: Improving the Speed and Accuracy of Docking with a New Scoring Function, Efficient Optimization, and Multithreading. *J. Comput. Chem.*, 31, 455–461. doi: 10.1002/jcc.21334.
- Vilalta Colomer, M. *et al.* (2018). A small molecule human PD-1/PD-L1 inhibitor promotes T cell immune activation and reduces tumor growth in a preclinical model. *Ann. Oncol.*, 29, X24. doi: 10.1093/annonc/mdy487.001.
- Wang, M. (2019). Symmetric or Semi-symmetric Compounds Useful as Immunomodulators. WO2018/026971.
- Wang, T. *et al.* (2019). Development of Inhibitors of the Programmed Cell Death-1/Programmed Cell Death-Ligand 1 Signaling Pathway, *J. Med. Chem.*, 62, 1715–1730. doi: 10.1021/acs.jmedchem.8b00990.
- Wang, T. *et al.* (2022). Discovery of Small-Molecule Inhibitors of the PD-1/PD-L1 Axis That Promote PD-L1 Internalization and Degradation, *J. Med. Chem.*, 65, 3879–3893. doi: 10.1021/acs.jmedchem.1c01682.
- Wang, Y., Xu, Z., Wu, T., He, M., Zhang, N. (2018a). Aromatic Acetylene or Aromatic Ethylene Compound, Intermediate, Preparation Method, Pharmaceutical Composition and Use Thereof. WO2018006795.
- Wang, Y. *et al.* (2018b). Novel small-molecule inhibitor of PD1/PDL1 pathway demonstrated single agent and drug combo effectiveness in cancer immunotherapy. In Proceedings of the American Association for Cancer Research Annual Meeting, Chicago, IL, USA, 14–18 April 2018; AACR Cancer Research: Philadelphia, PA, USA, 2018; Volume 78. Abstract 3851: doi: 10.1158/1538-7445.AM2018-3851.
- Wang, Y. *et al.* (2021). Metabolism and Interspecies Variation of IMM-010, a Programmed Cell Death Ligand 1 Inhibitor Prodrug, *Pharmaceutics*, 13, 598. doi: 10.3390/pharmaceutics13050598
- Wang, Y. *et al.* (2022). Discovery of quinazoline derivatives as novel small-molecule inhibitors targeting the programmed cell death-1/programmed cell death-ligand 1 (PD-1/PD-L1) interaction, *Eur. J. Med. Chem.*, 229, 113998. doi: 10.1016/j.ejmech.2021.113998.
- Webber, S., Almassy, R.J. (2018). Immune Checkpoint Inhibitors Compositions and Methods Thereof. WO2018/045142 A1.

- Williamson, A. (1850). Theory of *Ætherification*, *Lond. Edinb. Dublin philos. mag. j. sci.*, 37, 350–356. doi:10.1080/14786445008646627.
- Wolchok, J.D. *et al.* (2013). Nivolumab plus Ipilimumab in Advanced Melanoma, *N. Engl. J. Med.*, 369, 122–133. doi: 10.1056/NEJMoa1302369.
- Wu, L., Shen, B., Li, J., Li, Z., Liu, K., Zhang, F., Yao, W. (2017a). Heterocyclic Compounds as Immunomodulators. US20170107216 A1.
- Wu, L., Yu, Z., Zhang, F., Yao, W. (2017b). N-Phenyl-Pyridine-2-Carboxamide Derivatives and Their Use as PD-1/PD-L1 Protein/Protein Interaction Modulators. WO2017106634 A1.
- Wu, L., Zhang, F., Yao, W. (2018a). Heterocyclic Compounds as Immunomodulators. WO2018044783 A1.
- Wu, L. *et al.* (2018b). Heterocyclic Compounds as Immunomodulators. US 20180177784 A1.
- Xiao, K., Zhang, F., Wu, L., Yao, W. (2017). Heterocyclic compounds as immunomodulators. US20170362253 A1.
- Yamazaki, T. *et al.* (2005). Blockade of B7-H1 on Macrophages Suppresses CD4<sup>+</sup> T Cell Proliferation by Augmenting IFN- $\gamma$ -Induced Nitric Oxide Production, *J. Immun.*, 175, 1586–1592. doi: 10.4049/jimmunol.175.3.1586.
- Yeung, K.S. *et al.* (2017). Compounds Useful as Immunomodulators. WO2017066227.
- Yeung, K.S. *et al.* (2018a). 1,3-dihydroxy-phenyl derivatives useful as immunomodulators. WO2018009505 A1.
- Yeung, K.S. *et al.* (2018b). Biaryl Compounds Useful as Immunomodulators. WO2018044963A1.
- Yu, Z., Wu, L., Yao, W. (2018). Heterocyclic Compounds as Immunomodulators. WO2018013789 A1.
- Zak, K.M. *et al.* (2015). Structure of the Complex of Human Programmed Death 1, PD-1, and Its Ligand PD-L1, *Structure*, 23, 2341–2348. doi: 10.1016/j.str.2015.09.010.
- Zak, K.M. *et al.* (2016). Structural basis for small molecule targeting of the programmed death ligand 1 (PD-L1), *Oncotarget*, 7, 30323–30335. doi: 10.18632/oncotarget.8730.

## List of Abbreviations

- AcOEt – ethyl acetate  
ACN – acetonitrile  
AcOH – acetic acid  
ALPHA - Amplified Luminescent Proximity Homogeneous Assay  
APCs – antigen presenting cells  
ATR - attenuated total reflection  
B<sub>2</sub>Pin<sub>2</sub> – bis (pinacolato) diborane  
CD4 - cluster of differentiation 4  
CD8 - cluster of differentiation 8  
CD28 - cluster of differentiation 28  
CDCl<sub>3</sub>- deuterated chloroform  
CES1- Carboxylesterase 1  
CHO-K1 - Chinese hamster ovary cells, subclone K1  
CSF1 - colony stimulating factor 1  
CTLA-4 - cytotoxic T-lymphocyte antigen  
DBU – 1,8-diazabicyclo [5.4.0] undec-7-ene  
DCs - dendritic cells  
DCM – dichloromethane  
DIPEA - N, N-diisopropylethylamine  
DMF - N, N-dimethylformamide  
DMSO - dimethyl sulfoxide  
dppf - 1,1'-bis (diphenylphosphino) ferrocene  
EC – effector cells  
EC<sub>50</sub> – half-maximal effective concentration  
ELISA - enzyme-linked immunosorbent assay  
ER - endoplasmic reticulum  
ESI – electrospray ionisation  
FDA – Food and Drug Administration  
HATU – 1-[bis(dimethylamino)methylene]-1H-1,2,3-triazolo[4,5-b]pyridinium 3-oxide hexafluorophosphate  
HCOOH – formic acid  
HEK 293 - Human embryonic kidney 293  
HRMS - high resolution mass spectrometry  
HSQC NMR - Heteronuclear Single Quantum Coherence Nuclear Magnetic Resonance  
HTRF - Homogenous Time Resolved Fluorescence  
ICP - immune checkpoint  
ICIs - immunecheckpoint inhibitors  
IC<sub>50</sub> – half-maximal inhibitory concentration  
IFN- $\gamma$  – interferon  $\gamma$   
irAE – immune-related adverse effects  
ITIM - immunoreceptor tyrosine-based inhibitory motif  
ITSM - immunoreceptor tyrosine-based switch motif  
KT- killer T cells  
mAb – monoclonal antibody  
MCPs - macrocyclic peptides  
MeOH - methanol  
MLR - mixed lymphocyte reaction  
MSI - microsatellite instability  
MSPA - murine splenocyte proliferation assay  
NBS - N-bromosuccinimide  
NFAT - Nuclear factor of activated T-cells  
NKT- natural killer T cells  
NMR - Nuclear Magnetic Resonance  
NOESY - Nuclear Overhauser Effect Spectroscopy  
NSCLC - non-small cell lung cancer  
OS- overall survival  
PBMC - peripheral blood mononuclear cell  
PD-1 - Programmed Death 1  
PD-L1 - Programmed Death Ligand 1  
PD-L2 - Programmed Death Ligand 2  
PFS - progression-free survival  
SAR - structure-activity relationship  
SEC - size-exclusion chromatography  
SPR - Surface plasmon resonance  
STAT 3 - signal transducer and activator of transcription 3  
TCR - T-cell receptor  
TEA - triethylamine  
TGF- $\beta$  -Transforming growth factor beta  
TGI - tumor growth inhibition  
TLC - Thin-layer chromatography  
TME – tumor microenvironment  
THF - tetrahydrofuran  
TR-FRET- Time-Resolved Förster's Resonance Energy Transfer  
UPLC-MS - ultra-performance liquid chromatography-mass spectrometry  
w-AIDA - weak-Antagonist Induced Dissociation Assay  
VISTA - V-domain Ig suppressor of T cell activation